AN EPIGENETIC BASIS TO THE ETIOLOGY OF FETAL ALCOHOL SPECTRUM DISORDERS

A Dissertation

by

KYLEE JORDAN VEAZEY

Submitted to the Office of Graduate and Professional Studies of
Texas A&M University
in partial fulfillment of the requirements for the degree of

DOCTOR OF PHILOSOPHY

Chair of Committee,	Michael Golding
Co-Chair of Committee,	Charles Long
Committee Members,	Rajesh Miranda
	Beiyan Zhou
Interdisciplinary Faculty Chair,	Craig Coates

December 2015

Major Subject: Genetics

ABSTRACT

Observations from a number of independent laboratories indicate that ethanol has the capacity to act as a powerful epigenetic disruptor and potentially derail the process of cellular differentiation. The aim of this dissertation was to determine the epigenetic effects of alcohol on chromatin structure, the heritability of these effects *in vitro* and *in vivo*, and whether the severity of these alterations is tied to the differentiation state of the cell.

First, we investigated the epigenetic impact of ethanol exposure in a murine neural stem cell model using chromatin immunoprecipitation, quantitative polymerase chain reaction (ChIP-qPCR) and RNA analysis. We found that two widely-studied histone modifications, trimethylated histone 3 lysine 4 (H3K4me3) and trimethylated histone 3 lysine 27 (H3K27me3), were disrupted at promoters of a panel of homeobox genes involved in neural development in the presence of alcohol, and that these disruptions do not correlate with changes in the expression of the examined genes.

Second, we determined whether the disruption of chromatin structure caused by alcohol is heritable through cell division after an acute exposure *in vitro*. We monitored changes in H3K27me3, H3K4me3, and acetylation/demethylation of histone 3 lysine 9 (H3K9ac and H3K9me2, respectively) at the promoters of our candidate homeobox genes using ChIP-qPCR. We found that alterations in these marks persist beyond the window of exposure, and do not retain the same levels compared to controls after a recovery period in which ethanol is withdrawn. Furthermore, changes in the expression of these genes often occurred after recovery and again do not correlate with histone modifications present at their respective promoters. These alterations occur despite no indication of cell stress, but are associated with increased expression of genes involved in cell proliferation and neural lineage markers after recovery. A decrease in many oxidative stress pathway genes was also observed upon exposure that was rectified after recovery.

Importantly, changes in the gene expression of histone methyltransferases and DNA methyltransferases were observed, with a concurrent change in DNA methylation.

We next chose to determine if the observed alterations in chromatin structure also appear *in vivo* using a mouse model of early acute ethanol exposure. Pregnant dams injected with 2.9 g/kg ethanol at gestational day (GD) 7 were sacrificed at GD17, and the fetuses scored for ocular and forebrain defects. Levels of H3K27me3 were low at the promoters of many of the candidate genes in affected mice, and high levels of H3K9me2 specifically identified ethanol-affected mice, suggesting its potential as a marker for FASD phenotypes.

Finally, we determined whether the epigenetic effects of ethanol are dependent on the differentiation state of the cell using a murine embryonic stem cell (ESC) model. Acute ethanol exposure resulted in oscillating changes in levels of histone modifications for a long as 10 days post-exposure. Despite these changes in chromatin structure, no lasting changes in expression of our candidate genes or chromatin modifiers was detected. Acute ethanol exposure also did not impact the capacity of the ESCs to differentiate along a neural lineage.

While alcohol has the capacity to act as an epigenetic disruptor, its effects differ depending on the differentiation state of the cell and whether it is encountered in conditions maintaining stemness or during the execution of the developmental program. Furthermore, the alcohol-induced alterations in histone marks seem to be more of a byproduct of teratogenic insult rather than associated with a functional role in the transcriptional regulation of the cell. This study highlights the complexity of ethanol's teratogenic effects and suggest the histone code may not be a direct regulator of transcriptional control, at least in the context of an environmental exposure. None-the-less, alcohol-induced alterations in chromatin structure persist beyond the window of exposure and strongly correlate with the development of FAS birth defects. This study provides a platform for new hypotheses in fetal alcohol epigenetics and possibly the establishment of a mechanism of alcohol's effects on chromatin structure.

ACKNOWLEDGEMENTS

I would like to thank my committee chair, Dr. Golding for his patience, support, guidance, and motivation to excel as a graduate student. I would also like to thank my committee members, Dr. Long, Dr. Miranda, and Dr. Zhou for their guidance and support throughout the course of this research.

Thanks also go to my friends and colleagues and the department faculty and staff for making my time at Texas A&M University a great experience. I also want to extend my gratitude to the National Institute on Alcohol Abuse and Alcoholism, which provided the majority of the funding for this project.

Finally, thanks to my mother and stepfather for their encouragement, patience, and love.

TABLE OF CONTENTS

Page

LIST OF FIGURES

Page

Page

LIST OF TABLES

Page

CHAPTER I
INTRODUCTION*

Epigenetics - Developmental Programming and Fetal Alcohol Spectrum Disorders

Mammalian development consists of a series of carefully orchestrated changes in gene expression that occur as stem or progenitor cells differentiate to form the tissues and organs making up the growing fetus. Once established by lineage-specific transcription factors, the identity of each new cell type is maintained through unique alterations in the way in which the DNA encoding each gene becomes packaged within the nucleus (Hemberger et al., 2009). Much like a closed book cannot be read while an open book can, genes can either be tightly wound up and silent or in a relaxed, open, active state. As development proceeds, the DNA of each cell becomes packaged in a way that is unique to that cell type and thus "programmed" to express a specific cohort of genes, which confer its individual identity and physiological function (Barrero et al., 2010). Three enzymatic mechanisms control the assembly and regulation of chromatin structure: DNA methylation, post-translational histone modification, and ATP-dependent chromatin remodeling (Barrero et al., 2010). These fundamental processes, which control gene packaging, are heritable through cell division and referred to as epigenetic as they impart a level of regulation that is above or "*epi*" to genetics (Hemberger et al., 2009).

From studies using a diverse range of model organisms we now acknowledge that epigenetic modifications to chromatin structure provide a plausible link between environmental teratogens and lasting alterations in gene expression leading to disease phenotypes. Work from a number of independent laboratories have demonstrated exposure to ethanol is associated with genome-wide / gene specific

---

*Reprinted with permission from "Prenatal alcohol exposure and cellular differentiation: a role for Polycomb and Trithorax group proteins in FAS phenotypes?" by Veazey et al. 2013. *Alcohol Research: Current Reviews*, 35, 77-85, Copyright [2013] by Veazey et al.

changes in DNA methylation (Garro et al., 1991; Bielawski et al., 2002; Haycock, 2009; Ouko et al., 2009; Liu et al., 2009; Hicks et al., 2010; Zhou et al., 2011; Downing et al., 2011), alterations in post-translational histone modifications (Kim, 2005; Park, 2005; Pal-Bhadra et al., 2007), and a profound shift in epigenetically sensitive phenotypes (Kaminen-Ahola et al., 2010). Collectively, each of these observations indicates ethanol has the capacity to act as a powerful epigenetic disruptor and alter chromatin structure.

Although the mechanisms by which alcohol impacts chromatin structure are not completely understood, recent work suggests that some epigenetic changes are the downstream consequence of altered cellular metabolism. For example, Choudhury and colleagues recently observed an increase in reactive oxygen species (ROS) within primary rat hepatocytes treated with alcohol. This increase in ROS was correlated with an increase in acetylated histone 3 lysine 9 and when treated with cellular antioxidants, these alcohol-induced chromatin modifications were abated (Choudhury et al., 2010). Additionally, exposure to alcohol has well documented effects upon one-carbon metabolism and the bioavailability of the crucial methyl-donor s-adenosylmethionine. Impaired levels of this key substrate disrupt the ability of cells to methylate DNA and histones, resulting in compromised epigenetic programming (Zeisel, 2011). Interestingly, many of the patterning defects observed in FAS are phenocopied in studies examining deficiencies in one carbon metabolism (summarized in Zeisel, 2011).

Despite the fact that alcohol exerts several global changes in chromatin structure, many of the associated developmental defects appear to be rooted in gene-specific alterations. A recent study by Hashimoto-Torii and colleagues examining global changes in gene transcription within ethanol-exposed cerebral cortices reported that only 636 transcripts out of 39,000 candidate mRNAs were differentially expressed (Hashimoto-Torii et al., 2011). In further support of this assertion, several laboratories have identified alcohol-induced alterations in the expression of only a small number of key developmental regulators, including several HOX gene transcription factors, which play crucial roles in directing organ

patterning and morphogenesis (Godin et al., 2011; Mo et al., 2012; Rifas et al., 1997; Vangipuram and Lyman, 2012). In rodent models, these alterations have been associated with neural patterning defects and the development of cranial facial dysmorphogenesis reminiscent of those observed in clinical studies of FAS (Parnell et al., 2009; Rifas et al., 1997). However, these alcohol-induced alterations in expression are often limited to a specific tissue type and arise only during select developmental windows of exposure (Godin et al., 2011; KIM, 2005; Mo et al., 2012; Parnell et al., 2009). These observations suggest that the molecular machinery involved in epigenetic programming may also be disrupted by ethanol exposure and as a consequence, key epigenetic cues regulating development are not properly established.

Differentiation - Epigenetic Control and Developmental Programming

Of the three classes of epigenetic modifications, post-translational modification of histone proteins is undoubtedly the most complex. Post-translational, enzymatic modifications including acetylation, methylation, phosphorylation, and ubiquitination (to name the best studied subset) work together to produce a combinatorial "histone code" that serves to regulate cell-lineage-specific patterns of chromatin structure throughout development (Fisher and Fisher, 2011). Within the unique transcriptional environment of embryonic stem cells, several developmentally crucial genes are co-marked with both activating and repressive histone modifications (Bernstein et al., 2006; Jiang et al., 2011; Lim et al., 2009). Specifically, histone 3 lysine 4 trimethylation, which is typically associated with gene activation, co-exists with the repressive trimethyl state of histone 3 lysine 27. These uniquely marked loci are termed bivalent domains and generally encode transcription factors directing tissue-specific programs of differentiation (Fisher and Fisher, 2011). This same unique signature is found, albeit less frequently, in placental, neuronal and other tissue specific progenitor cell types (Lim et al., 2009; Rugg-Gunn et al., 2010). While these bivalently marked genes are generally not expressed, they are thought to be "primed" for either rapid activation or silencing during differentiation. Once established by lineage-specific transcription factor

networks, the transcriptional memory of each differentiating cell is maintained through the resolution of these co-existing epigenetic marks towards either the active or silent state. Importantly, many of these bivalently marked genes are disrupted in prenatal models of alcohol exposure and potentially explain the constellation of effects observed in FAS. Recent work from our laboratory using a neural stem cell model has revealed both histone 3 lysine 4 and lysine 27 trimethylation are altered by ethanol exposure (Veazey et al., 2013). Understanding the mechanistic basis of these epigenetic defects is crucial to deciphering the developmental origins of FAS.

Seminal studies using the fruit fly *Drosophila melanogaster* in the late 1970s - early 1980s revealed the existence of two large multi-protein complexes with diametrically opposite roles in the regulation of gene expression: the Polycomb group (PcG) and Trithorax group (TrxG) (Lewis, 1978; Poux et al., 2002; Schuettengruber et al., 2007). These two developmentally crucial enzyme complexes function at the hub of mammalian development, regulating the intricate balance between self-renewal and the execution of cellular differentiation. As differentiation progresses, the regulatory regions of bivalent genes “commit” to one of these two protein complexes and become exclusively occupied by either the PcG or TrxG proteins. This commitment occurs in a cell-lineage dependent manor and resolves the chromatin structure of these bivalent genes towards either an active or silent chromatin structure. Any defects in this delicate balancing act, particularly along the differentiation steps progressing towards the neural lineage, result in the acquisition of developmental defects and cause disease. Despite their fundamental importance to the processes of epigenetic programming and mammalian development, to date, the role of PcG and TrxG proteins in the etiology of FASD has not been examined.

Polycomb Group Proteins

The Polycomb group genes were originally discovered as key regulators of anterior / posterior axis specification in *Drosophila* over 30 years ago (Lewis, 1978). Since then, these gene families have been identified as essential regulators governing mammalian processes of cellular determination and lineage specific patterns of differentiation. In mammals, two major PcG chromatin-modifying complexes, Polycomb Repressive Complexes 1 and 2 (PRC1 and PRC2) have been characterized. Each complex is composed of proteins with different biochemical functions, many of which are not well understood. Ring finger protein 1A and 1B (RING1A and RING1B) are the catalytic engines of PRC1 and function to ubiquitinate the 119th lysine residue of histone H2A (Wang et al., 2004). This post-translational modification pushes local chromatin structure towards a transcriptionally repressive state and its proper establishment is essential to the coordinated silencing of genes throughout mammalian development (Boyer et al., 2006; Wang et al., 2004). Importantly, within embryonic stem cells, this mark stabilizes the presence of "poised" RNA polymerase II at bivalent chromatin domains and is crucial for maintenance of the pluripotent state (Ku et al., 2008).

PRC2 has similar repressive properties to PRC1 and is also an essential regulator of cellular differentiation. PRC2 facilitates the silencing of developmentally crucial genes through mono-, di-, and tri-methylation of the 27th lysine residue on histone H3 and tri-methylation of the 9th lysine residue on histone H3 (Cao et al., 2002; Czermin et al., 2002). Together, the repressive methyl marks on H3K27 and H3K9 promote the generation of facultative heterochromatin and mediate a transcriptionally silent state.

Adding a further layer of complexity, PRC2 associates with the mammalian DNA methyltransferase complexes, which aids in their ability to repress PRC2 target loci (Viré et al., 2006). This physical interaction suggests that the PcG complexes and the DNA methyltransferases function together to maintain the epigenetic memory of chromatin states through differentiation. Proper function of this gene

family and their interacting proteins is essential for the execution of cell specific differentiation programs and proper lineage specification (Pasini et al., 2007).

Trithorax Group Proteins

In flies, domains of gene expression within the early embryo are shaped by gradients of maternally deposited transcription factors that gradually diminish over time. After these initial transcriptional regulators disappear from the developing embryo, the memory of the active transcriptional state is propagated through the action of the Trithorax (TrxG) proteins (Lewis, 1978; Poux et al., 2002). Mammalian TrxG proteins have been implicated in fundamental epigenetic and cellular processes including: X-chromosome activation, genomic imprinting, stress response, apoptosis, tumorigenesis, cell proliferation, and embryonic stem cell renewal. However, compared to the PRC1 and PRC2 complexes, very little information exists regarding individual TrxG - associated members or their biochemical functions (Schuettengruber et al., 2007). TrxG proteins function as conserved, multi-protein complexes that catalyze the tri-methylation of histone 3 lysine 4 (H3K4me3) (Jiang et al., 2011). In mammalian cells the TrxG complex is formed from a core group of structural components that combine with at least one of six interchangeable histone methyltransferases. Together, these multi-subunit ensembles form the mammalian SET1/MLL family of complexes.

The main core of this complex is composed of four proteins including: WD40 repeat domain 5 (WDR5), retinoblastoma binding protein 5 (RbBP5), dosage compensation-related protein 30 (Dpy30), and absent, small, or homeotic-like (Ash2L). WDR5 recognizes the H3K4 methylated tail, which serves as the preferred binding substrate for the methyltransferase complex. WDR5 assists the binding of the methyltransferase complex to the dimethylated H3K4 tail and is an essential regulator of global K4 trimethylation (Wysocka et al., 2005). RbB5 is necessary for proper ES cell differentiation into neural progenitor cells and together with Dpy30 is essential to regulating global levels of H3K4 trimethylation (Jiang et al., 2011).

This TrxG core interacts with a group of interchangeable H3K4 methyltransferases including the Mixed Lineage Leukemia (MLL) proteins: MLL1, MLL2, MLL3, MLL4, SET1A, and SET domain containing 1B (SET1B) (Jiang et al., 2011; Steward et al., 2006). MLL1, initially discovered in human lymphoid and myeloid acute leukemias, has been implicated in promoting cell-specific patterns of gene expression by regulating global and gene specific H3K4 methylation during early embryogenesis (Yu et al., 1995). In contrast to Mll1, knockout of Mll2 in mouse ESCs leads to skewed differentiation, but exhibits no concrete alterations to H3K4 methylation (Lubitz et al., 2007). Despite their irrefutable involvement in H3K4 methylation, much remains unknown regarding the remaining catalytic subunits MLL3, MLL4, and SET1a/b. Deletion of any one of these remaining MLL members may have minimal effects on global levels of H3K4 methylation, very likely due to functional redundancy among the MLL family members (Jiang et al., 2011). Despite progress in clarifying the roles of TrxG proteins, much remains to be resolved regarding the temporal and tissue specific regulatory events these proteins promote.

Polycomb & Trithorax in the Etiology of FAS

Fetal alcohol syndrome is broadly characterized by low birth weight, distinctive craniofacial malformations, microcephaly, and central nervous system dysfunction (Riley et al., 2011). Postmortem studies of children that succumbed to fetal alcohol syndrome revealed ectopic, nodular accumulations of poorly differentiated neuronal and glial cells within the brain; suggesting large-scale problems with cellular proliferation and differentiation (Swayze et al., 1997). Similarly, studies using animal models have demonstrated reduced brain size and abnormal neural migration in mice exposed to ethanol *in utero* (Godin et al., 2010; Parnell et al., 2009). Collectively, these observations indicate alcohol impairs the cellular processes of neuronal differentiation and migration during fetal development. In support of this conclusion, *in vitro* studies using human and rodent neurosphere cultures demonstrate treatment with ethanol increases neurosphere size, skews the developmental potential of neural progenitor cells, and fundamentally alters the

neuronal differentiation program (Roitbak et al., 2011; Vangipuram and Lyman, 2012). However, the specific molecular mechanisms by which alcohol disrupts the cellular processes governing differentiation remain poorly defined. Recent studies examining the consequences of ethanol exposure during embryonic stem cell differentiation demonstrate a delay in the ability of exposed cells to silence the pluripotency factors OCT4, NANOG and SOX2 (Arzumnayan et al., 2009). These studies are highly suggestive that ethanol interferes with the ability of differentiating cells to recruit epigenetic modifiers to key developmental loci and execute the molecular programs governing cellular differentiation.

During early mammalian development, some 2000 genes are bivalently marked and progressively resolve towards the lineage-specific patterns of chromatin organization characterizing each unique cell type (Rugg-Gunn et al., 2010). As development proceeds, many precursor cell types both maintain a subset of developmentally critical genes in this conformation and push new groups of cellular factors into a bivalent state. For example, in embryonic stem cells the neural precursor genes Dlx2, Hand1, Msx2, Nestin, Nkx2.1, Nkx2.2, Olig2, Pax6, and Sox1 are all bivalently marked whereas in neural precursor cells only Dlx2 and Pax6 maintain this conformation. Interestingly the astrocyte markers myelin basic protein (*MBP*) and glial fibrillary acidic protein (*GFAP*) establish novel bivalent domains in preparation for progression towards either the neural or astrocyte cell fates respectively (Golebiewska et al., 2009). Proper function of the TrxG complexes are absolutely essential to resolving these bivalent loci into the actively transcribed state required for the induction of neurogenesis (Huang et al., 2007; Jiang et al., 2011; Lim et al., 2009). Similarly, PcG complexes are necessary to silence the myriad of developmental regulators specifying other cell types and ensure that lineage specific patterns of gene expression arise (Pereira et al., 2010). By propagating the transcriptional memory established by lineage-specific transcription factor networks, these two complexes cooperatively regulate the balance between stem cell renewal and lineage differentiation.

Importantly, the expression of many of these bivalently marked PcG / TrxG regulated factors are disrupted in various models of prenatal alcohol exposure and have been associated with profound errors in neuronal patterning. For example, alcohol suppresses the activation of the Hox genes Msx2 and Pax6 leading to cranio-facial abnormalities and hyper-differentiation of glutamatergic neurons respectively (KIM, 2005; Mo et al., 2012; Rifas et al., 1997). Similarly, both the expression and localization of Nkx2.1 and Olig2 are diminished by alcohol, potentially disrupting the balance between excitation and inhibition in the postnatal cerebral cortex (Godin et al., 2011). Recent studies by Taléns-Visconti and colleagues demonstrated that ethanol both affects proliferation of neural progenitor cells and markedly reduces their potential to differentiate into mature neurons, astrocytes, and oligodendrocytes (Taléns-Visconti et al., 2011). Given this broad-spectrum impediment to nearly every neuronal developmental fate, it is possible that the observed impact of ethanol on overall architecture and size of the brain in FAS children stems from some aspect of PcG / TrxG regulation of neural precursor differentiation. Importantly, using an *in vitro* neurosphere model of differentiation, Mo and colleagues recently demonstrated that ectopic expression of Pax6 was able to ameliorate the impacts of ethanol on cell proliferation and neurogenesis (Mo et al., 2012). These results suggest that within a limited scope, rescue of the developmental program is possible.

Histone 3 Lysine 9 Acetylation and Methylation

Select residues on histone tails can be monomethylated, dimethylated, or trimethylated by histone methyltransferases. The level of methylation on certain residues can often correlate with changes in gene expression. For example, H3K4 mono-, di-, and trimethylation are associated with gene activation (Koch et al., 2007). However, H3K27 monomethylation is associated with gene activation, while H3K27 dimethylation and trimethylation are associated with gene repression (Barski et al., 2007; Rosenfeld et al., 2009). Similar to H3K27 methylation, H3K9 dimethylation and trimethylation correlate with gene repression, and H3K9 monomethylation correlates with gene activation. Adding a further layer of

complexity, H3K9 trimethylation may be activating if it is present within the gene body, or it may be silencing if it is present within the gene promoter (Vakoc et al., 2005). Out of the three residues discussed here, only H3K9 can be acetylated as well as methylated. Histone acetylation results in gene activation and is mediated by histone acetyl tranferases (HATs) (Roh, 2005). HP1 (Heterochromatin Protein 1) contains a chromodomain that allows it to bind to H3K9me, which facilitates histone deacetylase and methyltransferase activity (Bannister et al., 2001; Lachner et al., 2001). There are various proteins that methylate and demethylate H3K9. Histone methyltransferases that deliver methyl groups to H3K9 include Suv39H1, Suv39H2, G9a, and SetDB1 (Rea et al., 2000; O'Carroll et al., 2000; Strahl et al., 1999). H3K9 can be demethylated by members of the JMJD and LSD1 complexes. Together, these epigenetic marks are integral to the ability of stem cells to dynamically regulate the balance between self-renewal and differentiation. Any abnormalities in this process have the capacity to compromise differentiation and cause disease.

Conclusions

One of the most frustrating aspects in the study of fetal alcohol spectrum disorders has been trying to explain the wide range of severity and enormous variation in FASD associated birth defects. During fetal gastrulation, the process of organogenesis is initiated and different rudimentary organ systems are formed and grow during unique developmental windows (Zorn and Wells, 2009). Each organ system cycles between periods of intense growth and steady state maintenance. Importantly, periods of growth are characterized by carefully orchestrated changes in DNA methylation and chromatin structure as differentiating cells are programmed with their epigenetic identity (Zhou et al., 2011). In studies using animal models, correlation of ethanol exposure at varying developmental time-points with major periods of tissue growth strongly indicate that different tissues are largely susceptible to ethanol-induced teratogenesis during specific developmental windows (Becker et al., 1996). Given the demonstrated ability of alcohol to alter DNA methylation and chromatin structure, it is likely that as each organ system enters a period of active epigenetic programming, ethanol exposure induces lasting

epigenetic lesions that persist throughout organogenesis, while non-developing systems remain largely refractory. Accounting for differences in the timing and dose of alcohol received, epigenetic errors resulting from even minor exposures to this single teratogen could lead to the wide variance in severity and range of birth defects that characterize FASD (Becker et al., 1996).

Since their discovery, the PcG and TrxG protein complexes have been identified in numerous disease contexts, ranging from cellular transformation to structural defects and mental illness (Huang et al., 2007; Varambally et al., 2002; Yu et al., 1995). From these studies, we now know that a molecular event or teratogen that alters PcG/ TrxG programming within even a few neural progenitor stem cells during fetal growth is likely to disproportionately influence subsequent brain development, and has the potential to impart severe neurological birth defects (Boyer et al., 2006; Hirabayashi and Gotoh, 2010). A complete characterization of the involvement of Polycomb and Trithorax group complexes in the etiology of FASD will undoubtedly aid in our efforts to understand the role of epigenetic programming in this complex disorder.

The question of whether histone marks themselves are the true epigenetic mark is an area of much controversy. Histone marks correlate with differential regulation of a single sequence of DNA, however it is unclear as to whether they are heritable through cell division. Two opposing models exist that attempt to explain the maintenance of histone post-translational modifications through cell division. One model suggests that some nucleosomes that contain a certain repertoire of marks are maintained through the replication fork (Hansen et al., 2008; Margueron et al., 2009). These marks facilitate recruitment of their respective chromatin remodeling machinery to propagate the mark to newly incorporated nucleosomes. On the other hand, the second model states that the chromatin remodeling complexes remain associated with DNA through the replication fork, and re-establish histone marks on newly incorporated nucleosomes (Petruk et al., 2012). Therefore, the true ‘epigenetic mark’ is the chromatin modifying complex itself. Although there is opposing evidence supporting each model, it is still unclear whether histone marks

are heritable through cell division. It is also unclear if cells can re-establish histone marks that were disturbed by an obstructive agent after it is removed. This study attempts to provide insight to the question of the epigenetic basis of the etiology of FASD as well as shed light on the epigenetic importance of the histone code.

CHAPTER II
SELECTION OF STABLE REFERENCE GENES FOR QUANTITATIVE RT-PCR COMPARISONS OF MOUSE EMBRYONIC AND EXTRA-EMBRYONIC STEM CELLS*

Introduction

During mammalian pre-implantation development a series of asynchronous divisions result in the formation of the blastocyst. At this stage of development three distinct cell types have emerged: the epiblast, trophectoderm and primitive endoderm, which give rise to the fetus, placenta and extraembryonic endoderm respectively (Rossant, 1975; Rossant and Tam, 2004; Rossant and Tam, 2009). To better define the developmental and transcriptional processes unique to each of these distinct lineages, *in vitro* cultured progenitor stem cells have been derived (Martin, 1981; Nagy et al., 1993; Tanaka, 1998; Kunath, 2005). Analysis of ES, TS and XEN stem cell lines have revealed much about the cellular processes controlling mammalian development and demonstrated surprising differences in the epigenetic regulation of gene expression between these three lineages (Kunath, 2005; Cherry et al., 2000; Mann et al., 2004; Fortier et al., 2008; Golding et al., 2010; Macfarlan et al., 2011). Identifying the biochemical factors underlying these differences remains an essential step to understanding the molecular processes driving development and better defining crucial aspects of mammalian stem cell biology.

Quantitative reverse transcription-polymerase chain reaction (qPCR) has emerged as a powerful technique to rapidly assess transcriptional differences between cell types and differing experimental conditions. However, accurate quantitative analysis is dependent upon proper, empirical selection of a suitable reference. Using published microarray data, and a novel statistical algorithm, (geNORM) Vandesompele and colleagues demonstrated that the geometric mean of

---

*Reprinted with permission from "Selection of stable reference genes for quantitative rt-PCR comparisons of mouse embryonic and extra-embryonic stem cells" by Veazey and Golding, 2011, *PLOS ONE*, 6, e27592, Copyright [2011] by Veazey, Golding.

three reference genes provided the most accurate and reliable means of normalizing qPCR expression data (Vandesompele et al., 2002). Subsequently, this experimental strategy has been validated and additional algorithms written and utilized to identify the most suitable reference genes for a variety of experimental conditions (Andersen et al., 2004; Pfaffl et al., 2004; Goossens et al., 2005; Gilsbach et al., 2006; Willems et al., 2006; Mamo et al., 2007; Gutierrez et al., 2008; Tatsumi et al., 2008; Boda et al., 2008; Suter and Aagaard-Tillery, 2009; van den Bergen et al., 2009; Galiveti et al., 2009).

In this study we sought to identify a list of genes most suitable for use as normalization controls in qPCR-based comparisons between ES, TS and XEN stem cells or their *in vitro* differentiated progeny. In order to help identify candidate genes we set two main criteria that the mRNAs would have to fulfill: 1) the transcripts needed to be expressed above background and easily detectable, and 2) candidate mRNAs needed to be stably expressed between each of the three stem cell lineages under investigation. To this end we surveyed the recent literature and compiled a short list of fourteen candidate genes, including *Actb*, *B2m*, *Hsp70*, *Gapdh*, *Gusb*, *H2afz*, *Hk2*, *Hprt*, *Pgk1*, *Ppia*, Rn*7sK*, *Sdha*, *Tbp* and *Ywhaz* *(Andersen et al., 2004; Pfaffl et al., 2004; Goossens et al., 2005; Gilsbach et al., 2006; Willems et al., 2006; Mamo et al., 2007; Gutierrez et al., 2008; Tatsumi et al., 2008; Boda et al., 2008; Suter and Aagaard-Tillery, 2009; van den Bergen et al., 2009; Galiveti et al., 2009; Allen et al., 2004; Hwang et al., 2007; Espinoza et al., 2004)*. These genes belong to diverse functional classes and should not be co-regulated, thus providing a non-biased method of normalizing qPCR expression data.

To evaluate the stability of our candidate genes we isolated RNA from three independent lines of varying genotypes for each of the three stem cell types. This RNA was quantified and seeded into five independent qPCR reactions measuring each of the candidate genes. Using the geNORM, NormFinder and BestKeeper algorithms, we identify the *Pgk1*, *Sdha* and *Tbp* transcripts as the most stably expressed reference genes between each of these stem cell types. To determine which of these candidates was most suitable for use during *in vitro* differentiation

studies, we cultured ES and TS cells in the absence of crucial growth factors LIF and FGF4 respectively. Using three independent RNA samples isolated on Day 0 and Day 8, we identify *Sdha*, *Tbp* and *Ywhaz* as well as *Ywhaz*, *Pgk1* and *Hk2* as the three most stable reference genes through the *in vitro* differentiation of ES and TS cells. Our results suggest that normalization of qPCR data using the geometric means of the transcripts listed above will yield the most accurate quantification of gene expression between these three unique stem cell types.

Results

After a survey of the recent literature we curated a short list of fourteen commonly used reference genes and either designed new primers or pulled existing ones from references cited in the materials and methods. These genes are listed in Table 1 and represent several distinct functional classes so as to minimize the possibility of co-regulation. For each gene, a minimum of two independent primer sets were tested and of these, the primer set exhibiting the greatest efficiency was selected. To conduct an accurate survey of candidate gene expression levels between ES, TS and XEN stem cells we isolated RNA from at least three independent stem cell lines, representing at least two different genotypes. We postulate that utilizing lines derived from diverse genotypes will more accurately identify stable reference genes to be used in future studies contrasting patterns of gene expression.

Previous studies in our laboratory have utilized stem cell lines derived from *Mus musculus castaneus x mus musculus (*C57Black6) F1 embryos. Polymorphisms between these genetic strains allow the examination of mono-allelic patterns of epigenetic marks and gene expression within loci regulated by genomic imprinting (Golding and Mann, 2011). For ES, TS and XEN stem cell analysis we utilized lines derived from F1 embryos of reciprocal crosses between these strains (C57Black6 x Castaneous and Cast7 x Black6) (Golding et al., 2010; Golding and Mann, 2011; Market-Velker et al., 2009). For analysis of ES and TS cells we also utilized the previously described R1 ES and TS3.5 lines derived from 129 stain mice (Nagy et al., 1990; Tanaka, 1998). Each of these different lines demonstrated cellular

Table 1: Descriptions of the fourteen candidate reference genes studied.

Symbol	Name	Accession	Brief Description
Rn7sk	7SK, small nuclear RNA	NR_030687	Small nuclear RNA that binds elongation factor P-TEFb and negatively regulates transcription.
Actb	Beta-Actin	NM_007393	A highly conserved protein found in all eukaryotic cells involved in various cellular processes such as cell motility and cytokinesis.
B2m	beta-2 microglobulin	NM_009735	Gene that codes for Beta-2-microglobulin, a component of the MHC
Gapdh	glyceraldehyde-3-phosphate dehydrogenase	NM_008084	Enzyme involved in metabolic and non-metabolic processes such as glycolysis, transcription activation, and apoptosis.
Gusb	glucuronidase, beta	NM_010368	Gene that codes for Beta-glucuronidase, which catalyzes the hydrolysis of B-D-glucuronic acid.
H2afz	H2A histone family, member Z	NM_016750	Member of the H2A histone family that is required for embryonic development.
Hk2	hexokinase 2	NM_013820	Enzyme that phosphorylates hexoses, including glucose to produce glucose-6-phosphate.
Hprt	hypoxanthine-phosphoribosyl transferase	NM_013556	Transferase that aids in the generation of new purine nucleotides from degraded DNA.
Hsp70	heat shock 70kD protein	NM_010478	Heat shock protein that aids in protein folding and cellular stress response.
Pgk1	phosphoglycerate kinase 1	NM_008828	A highly conserved transferase involved in glycolysis that catalyzes the formation of ATP.
Ppia	peptidylprolyl isomerase A	NM_008907	Gene that codes for peptidylprolyl isomerase A, a protein that catalyzes the folding of proteins.
Sdha	Succinate dehydrogenase complex, subunit A	BC011301	Gene that codes for a subunit of succinate dehydrogenase and is important in cellular respiration.
Tbp	TATA box binding protein	NM_013684	Protein that binds to the TATA box sequence and aids in transcription initiation.
Ywhaz	Tyrosine 3-monooxygenase /tryptophan 5-monooxygenase activation protein, zeta polypeptide	NM_011740	Codes for a highly conserved protein that helps mediate signal transduction.

morphology consistent with their cell type and expressed unique cohorts of transcription factors characteristic of their lineage (Kunath, 2005; Strumpf, 2005) (Figure 1). Cell lines were cultured to 80% confluence, RNA isolated and seeded into five independent qRT-PCR reactions measuring our fourteen candidate genes. Results presented below are the combined analysis of all genetic backgrounds tested.

Of the candidate genes tested *Rn7sk* demonstrated the most robust expression averaging expression levels 125 fold higher than the remaining candidates; which were all readily detectable in each of the cell lines tested. To measure the relative stability of each of the candidate genes between the ES, TS and XEN lines, the CT values for the measured transcripts were compiled and run through the NormFinder, GENorm, and BestKeeper software packages (Vandesompele et al., 2002; Andersen et al., 2004; Pfaffl et al., 2004). Each of these algorithms utilize slightly different methods of estimating both the intra- and the intergroup expression variation, and allow the ranking of candidate genes based on the calculation of a "stability value". While there was variation amongst the mid-range to least stable genes, all three software packages identified *Pgk1*, *Sdha*, *Tbp* and *H2afz* as the most consistently stable reference genes between ES, TS and XEN stem cells (Table 2). Similar to previous studies by Mamo et al., we observed the classic "housekeeping genes" *Actb*, *Hprt* and to a lesser extent *Gapdh* were comparatively unstable and by our analysis would not be the best choice to normalize qPCR expression levels (Mamo et al., 2007).

We next chose to make pair-wise comparisons between ES and TS, ES and XEN as well as TS and XEN to see which candidates emerged as the most stable in contrasts between any two cell types. A consensus of all three software packages can be seen in table 3. As with the comparisons between all three lines, *Pgk1*, *Sdha*, *Tbp* and *H2afz* remained in the top five most stable genes indicating no one cell type was biasing our analysis and that these five reference genes represent the best normalization controls for qPCR-based analysis of gene expression. Utilizing the geometric mean of *Pgk1*, *Sdha*, and *Tbp* we normalized the CT values

for each of the fourteen candidates and graphed their relative expression levels as described previously (Vandesompele et al., 2002; Livak and Schmittgen, 2001; Schmittgen and Livak, 2008). As can be seen in Figure 2, *Rn7sk* is expressed at a drastically higher level than any of the other candidates tested and therefore does not represent a viable reference gene. Similarly, analysis of *Actb*, *B2m*, *Gapdh* and *Ywhaz* all yielded significant differences in measurements of TS cell expression as compared to both ES and XEN cells eliminating their candidacy. Our results indicate normalizing quantitative RT-PCR measurements using the geometric mean CT values obtained for the Pgk1, Sdha and Tbp mRNAs, offers the most reliable method to assess differing patterns of gene expression between the three founding stem cell lineages present within the mammalian preimplantation embryo.

We next sought to determine which of the candidate genes remained the most stable throughout the process of differentiation. Therefore we chose to differentiate our ES and TS cell lines by removal of the key growth factors LIF and FGF4 respectively (Tanaka, 1998; Niwa et al., 1998; Williams et al., 1988). To this end ES cells were cultured in LIF $^{-}$ ES cell medium, allowed to form embryoid bodies on untreated plastic dishes and then plated on regular tissue culture plastic to differentiate into fibroblast like cells. Similarly, TS cells were plated on tissue culture treated plastic at low density in FGF4- medium which promoted the formation of TS giant-like cells. We chose not to investigate the process of XEN cell differentiation as reliable protocols for the induction of differentiation have not yet been established. In contrast to both ES and TS cell lines, when XEN cells are plated on plastic many cells simply senesce, while the remainder do not uniformly differentiate into one cell type, thus complicating our analysis. RNA samples were collected from ES cells on Day 0, Day 4 (embryoid body) and Day 8 and RNA seeded into five independent qPCR reactions measuring each of the fourteen candidate genes. Using a similar experimental design as described above, we identify Sdha, Tbp and Ywhaz as the three most stable transcripts (Table 4). To examine relative changes in gene expression, we utilized the geometric mean of these three most stable candidates to normalize CT values and graphed the relative expression of all fourteen candidate genes though ES cell differentiation (Figure 3a). We then chose

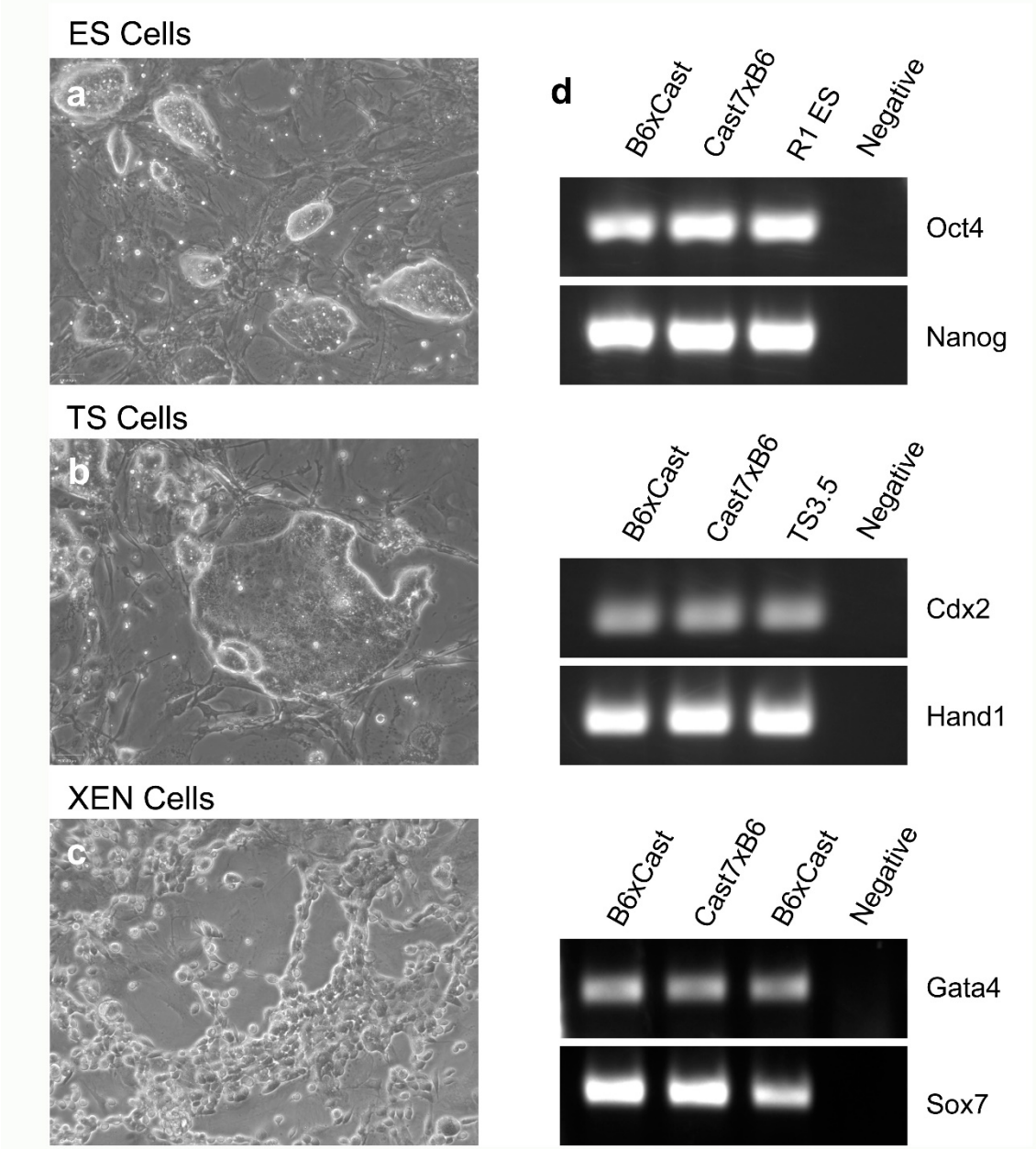

Figure 1: Characteristic cellular morphology and marker gene expression for ES, TS and XEN Stem Cells. a-c Light micrographs of representative ES (a) TS (b) and XEN (c) stem cell lines used in this study. d) Expression of transcription factors characteristic of each of the stem cell lineages

Table 2: Candidate reference genes ranked in order of their stability. Stability of the candidate genes between ES, TS and XEN stem cells ranked using the NormFinder, GENorm and BestKeepr software tools.

NormFinder			**geNORM**			**BestKeeper**	
Rank	**Gene Name**	**Stability Value**	**Rank**	**Gene Name**	**Stability Value**	**Rank**	**Gene Name**
1	Pgk1	0.012	1	Pgk1	0.121	1	Pgk1
2	Sdha	0.047	2	Sdha	0.132	2	Sdha
3	Tbp	0.054	3	Tbp	0.138	3	H2afz
4	H2afz	0.057	4	H2afz	0.139	4	Tbp
5	Gapdh	0.061	5	Gusb	0.142	5	Gusb
6	Ppia	0.062	6	Gapdh	0.145	6	Ppia
7	Gusb	0.062	7	Ppia	0.145	7	Gapdh
8	Hsp70	0.088	8	Hsp70	0.168	8	Ywhaz
9	Ywhaz	0.088	9	Ywhaz	0.168	9	Hsp70
10	Actb	0.099	10	Actb	0.182	10	Actb
11	B2m	0.107	11	Hprt	0.192	11	Hprt
12	Hk2	0.109	12	B2m	0.192	12	Hk2
13	Hprt	0.109	13	Hk2	0.193	13	B2m
14	Rn7sk	0.128	14	Rn7sk	0.212	14	Rn7sk

Table 3: Consensus of the stability rankings for pair-wise comparisons between the stem cell types.

ES vs. TS		ES vs. XEN		TS vs. XEN	
Rank	**Gene Name**	**Rank**	**Gene Name**	**Rank**	**Gene Name**
1	Pgk1	1	Pgk1	1	Pgk1
2	Sdha	2	Gapdh	2	Sdha
3	Tbp	3	H2afz	3	H2afz
4	Gusb	4	Tbp	4	Tbp
5	H2afz	5	Sdha	5	Ppia
6	Ppia	6	Gusb	6	Gusb
7	Gapdh	7	Ppia	7	Gapdh
8	Ywhaz	8	Hsp70	8	Ywhaz
9	Hsp70	9	Ywhaz	9	Hsp70
10	Actb	10	Actb	10	Actb
11	Hprt	11	B2m	11	B2m
12	Hk2	12	Rn7sk	12	Hprt
13	B2m	13	Hk2	13	Hk2
14	Rn7sk	14	Hprt	14	Rn7sk

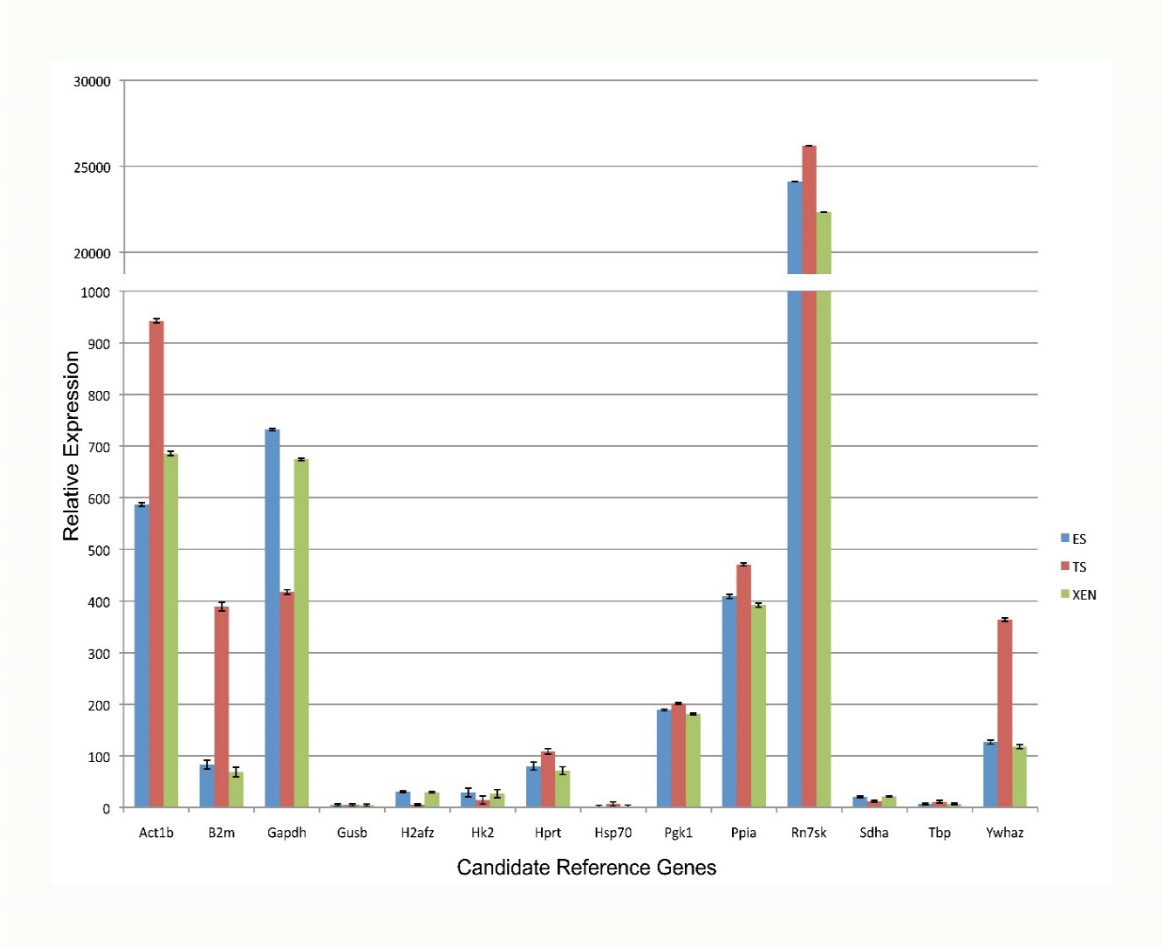

Figure 2: Relative expression of the fourteen candidate genes between all three genetic backgrounds of ES, TS and XEN stem cells. CT values for each measured transcript were normalized to the geometric mean of *Pgk1*, *Sdha* and *Tbp*, and then graphed as relative values using methods described (Vandesompele et al., 2002; Livak and Schmittgen, 2001; Schmittgen and Livak, 2008). Error bars represent the standard error of the mean.

to examine the expression of the cell lineage marker fibroblast-specific protein-1 (FSP-1) which is active in fibroblasts but not inepithelium, mesangial cells or embryonic endoderm (Strutz et al., 1995). In accordance with previous studies this marker demonstrated increasing expression in differentiating cell cultures, indicating our three candidate genes provided a valid reference point (Figure 3b) (Lee et al., 2010; Hernandez et al., 2003). In contrast, transcripts encoding *Pgk1*, *H2afz*, *Ppia* (*Cyclophillin*) and *Gapdh* all demonstrate a significant down-regulation and therefore are not suitable reference genes for this experimental time course. Similar to results reported by Willems et al., examining ES cell differentiation induced by both DMSO and Retinoic acid, we also identify *B2m* and *Hprt* as among the most unstable transcripts (Willems et al., 2006). Using similar methodologies, we identified the *Ywhaz*, *Pgk1* and *Hk2* transcripts as the most stable during TS cell differentiation (Table 5). After applying the geometric mean of these three candidates to normalize CT values we observed massive changes in transcripts encoding *Actb*, *B2m* and *Rn7sk* (Figure 4). Previous studies have identified increased actin mobilization as a key feature of trophectoderm stem cell differentiation, validating our identified reference genes (Vong et al., 2010). Taken together our data indicate *Sdha*, *Tbp* and *Ywhaz* and *Ywhaz*, *Pgk1* and *Hk2* represent the most stable of our fourteen candidate reference genes for use as qPCR normalization controls during ES and TS cell differentiation respectively.

Discussion

Analysis of gene expression using qPCR has become the corner stone to nearly every facet of the biological sciences. However, despite numerous studies demonstrating the importance of careful selection and validation of appropriate reference genes, several studies continue to emerge utilizing inappropriate methods of qPCR normalization (Vandesompele et al., 2002; Andersen et al., 2004; Pfaffl et al., 2004; Willems et al., 2006; Gutierrez et al., 2008; Tatsumi et al., 2008; Bustin et al., 2009). A recent survey of the literature identified the single use of either Actb or Gapdh to normalize expression data in the vast majority of qPCR based studies

without any form of validation to ensure their experimental stability (Vandesompele et al., 2002). In this study we sought to identify the most stable and appropriate reference genes for studies contrasting patterns of gene expression between the three founding stem cell lineages present within the mammalian preimplantation embryo. From a list of fourteen commonly utilized reference genes we identify *Pgk1, Sdha* and *Tbp* as the most suitable reference genes and further find compelling evidence to suggest that both *Actb* and *Gapdh* are not suitable normalization controls for these experiments. Of the top three candidates to emerge from our analysis two are components of pathways controlling cellular respiration. *Pgk1* - *phosphoglycerate kinase 1* is the seventh step of glycolysis and *Sdha* - *Succinate dehydrogenase* or *succinate-coenzyme Q reductase* is an enzyme complex that binds to the inner mitochondrial membrane and is an essential component of both the citric acid cycle and electron transport chain (Yoshida and Tani, 1983; Oyedotun and Lemire, 2003). One potential weakness of our top three candidates is that although *Pgk1* and *Sdha* are components of distinct pathways, they are both components of cellular respiration leaving the possibility that an experimental condition that impacts metabolicprocesses would significantly alter these normalization controls. The third and fourth candidates to emerge from our analysis were *Tbp* and *H2afz* respectively. *Tbp* is a central component of the RNA polymerase II pre-initiation complex and *H2afz* is an essential component of chromatin structure which is hypothesized to play a role in chromosome organization and stability (Kornberg, 2007; Rangasamy et al., 2004; Fan et al., 2004; Greaves et al., 2007). The third and fourth candidates are truly functionally distinct from both each-other and from pathways controlling cellular respiration. As such, where experimental design permits we would recommend normalizing CT values to the geometric mean of all four of these reference genes to improve experimental rigor. However, when we incorporated this strategy we did not observe any meaningful changes in relative gene expression (data not shown).

The first differentiation event during mammalian embryogenesis is the formation of the epiblast, trophectoderm and primitive endoderm which go on to give rise to the three founding embryonic lineages. Stem cells derived from each of

Table 4: Candidate reference genes ranked in order of their stability throughout ES cell differentiation using the NormFinder, GENorm and BestKeepr software tools.

NormFinder			geNORM			BestKeeper	
Rank	Gene Name	Stability Value	Rank	Gene Name	Stability Value	Rank	Gene Name
1	Sdha	0.033	1	Sdha	0.005	1	Sdha
2	Tbp	0.033	2	Tbp	0.005	2	Tbp
3	Ywhaz	0.038	3	Ywhaz	0.015	3	Ywhaz
4	H2afz	0.039	4	Gusb	0.017	4	Gusb
5	Gusb	0.039	5	Actb	0.017	5	H2afz
6	Actb	0.04	6	H2afz	0.017	6	Hsp70
7	Hsp70	0.04	7	Hsp70	0.018	7	Actb
8	Gapdh	0.045	8	Gapdh	0.024	8	Gapdh
9	Ppia	0.047	9	Ppia	0.026	9	Ppia
10	Hk2	0.05	10	Hk2	0.027	10	Hk2
11	Pgk1	0.051	11	Pgk1	0.028	11	Hprt
12	Hprt	0.054	12	Hprt	0.033	12	Pgk1
13	Rn7sk	0.057	13	Rn7sk	0.034	13	Rn7sk
14	B2m	0.058	14	B2m	0.036	14	B2m

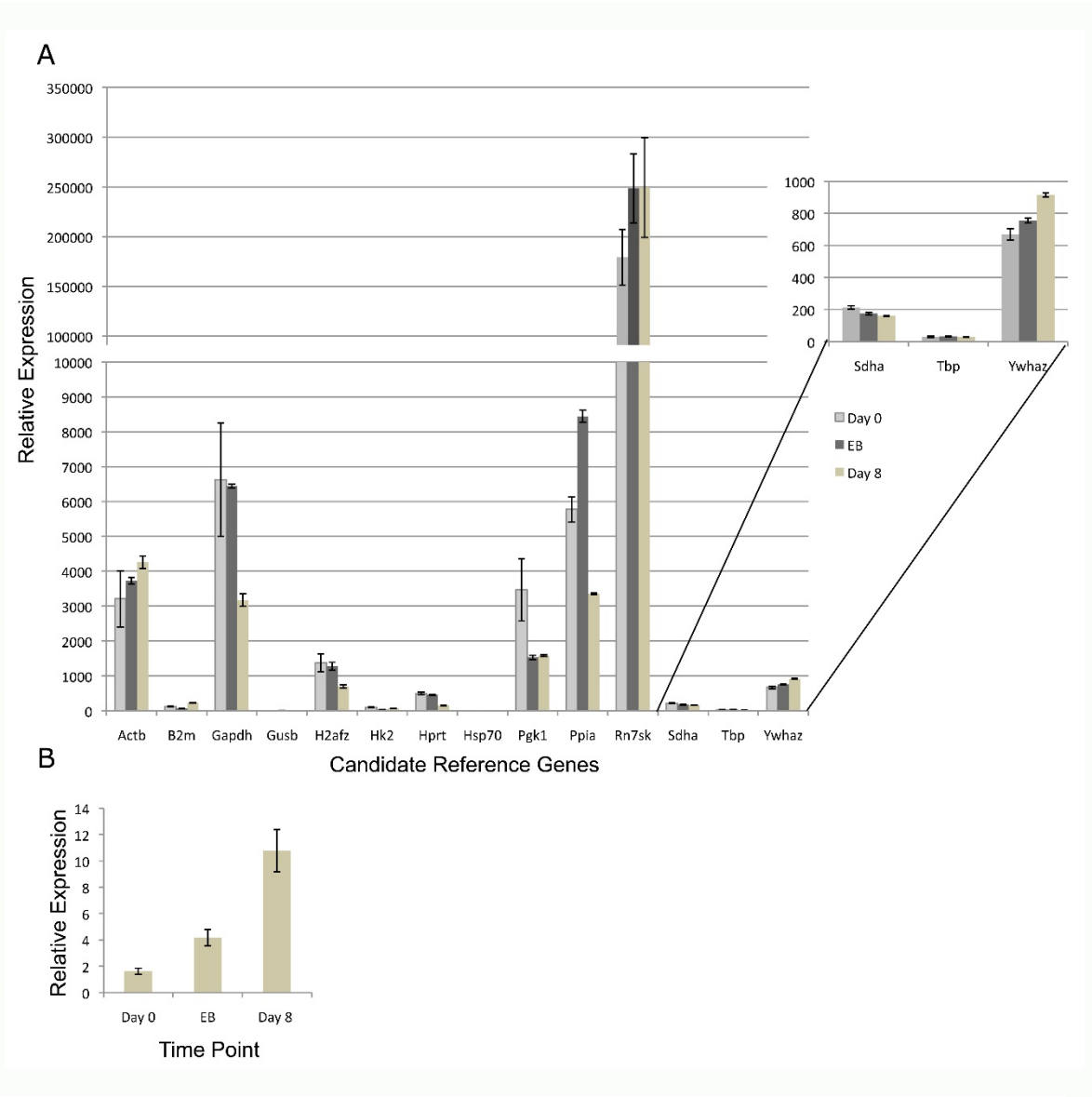

Figure 3: 3a. Relative expression of the fourteen candidate genes throughout differentiation of all three genetic backgrounds of ES cells examined. CT values for each transcript were measure on Day 0, Day 4 (embryoid body) and Day 8 and were then normalized to the geometric mean of *Sdha Tbp and Ywhaz.* Relative values were determined using methods described previously [13,34,35] and graphed. Error bars represent the standard error of the mean. 3b. Increased expression of fibroblast specific protein 1 throughout ES cell differentiation. Error bars represent the standard error of the mean for three independent replicates.

Table 5: Candidate reference genes ranked in order of their stability throughout TS cell differentiation using the NormFinder, GENorm and BestKeepr software tools.

NormFinder			geNORM			BestKeeper	
Rank	Gene Name	Stability Value	Rank	Gene Name	Stability Value	Rank	Gene Name
1	Ywhaz	0.095	1	Ywhaz	0.018	1	Ywhaz
2	Pgk1	0.096	2	Pgk1	0.029	2	Pgk1
3	H2afz	0.102	3	Hk2	0.036	3	Hk2
4	Hk2	0.104	4	H2afz	0.04	4	H2afz
5	Hprt	0.11	5	Hprt	0.042	5	Hprt
6	Tbp	0.111	6	Tbp	0.044	6	Tbp
7	Actb	0.112	7	Actb	0.044	7	Sdha
8	Sdha	0.122	8	Ppia	0.048	8	Actb
9	Hsp70	0.127	9	Sdha	0.06	9	Ppia
10	Ppia	0.128	10	Hsp70	0.061	10	Hsp70
11	Gusb	0.133	11	Gusb	0.065	11	Gusb
12	Gapdh	0.153	12	Gapdh	0.093	12	Gapdh
13	B2m	0.183	13	B2m	0.12	13	B2m
14	Rn7sk	0.202	14	Rn7sk	0.24	14	Rn7sk

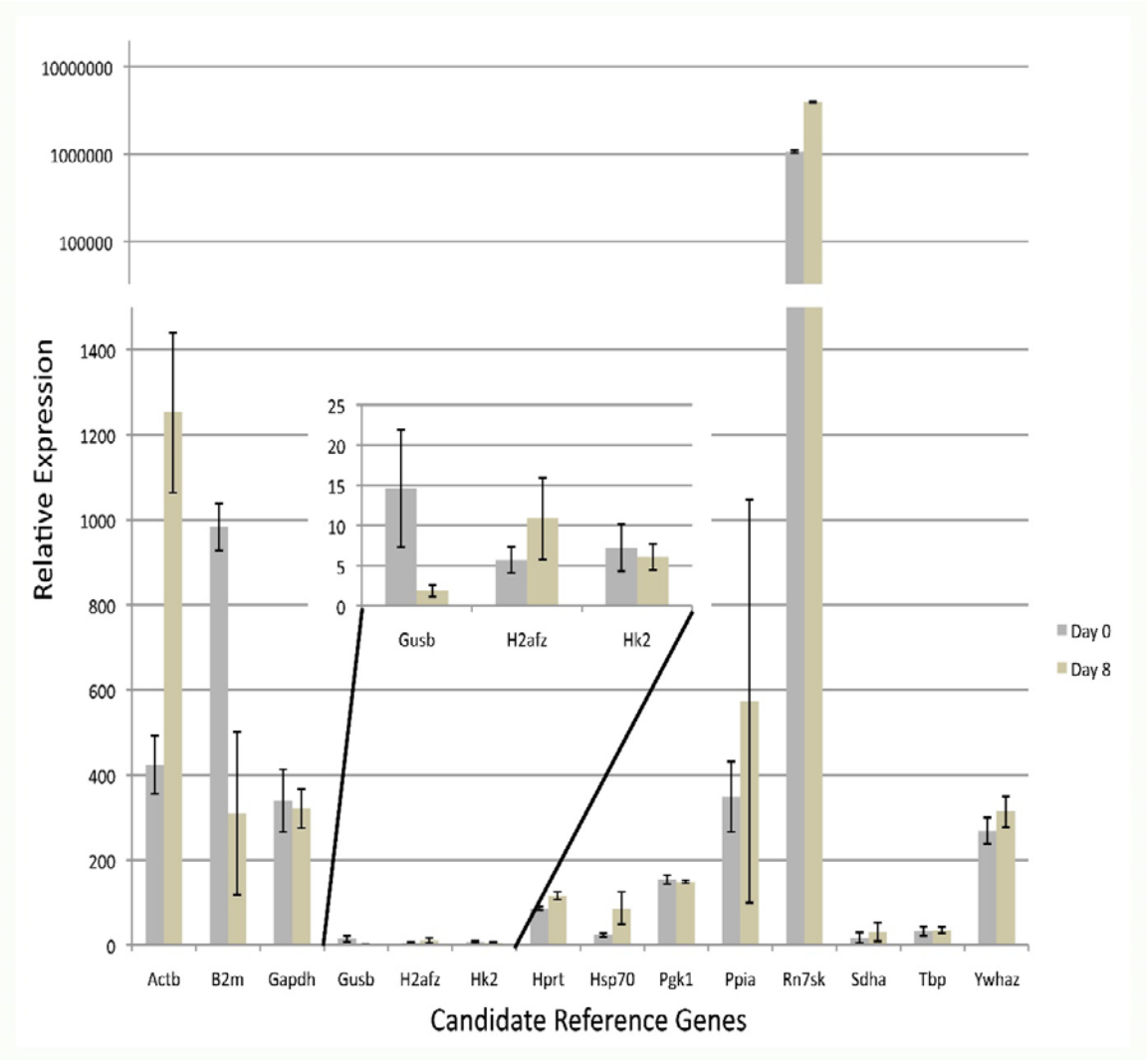

Figure 4: Relative expression of the fourteen candidate genes throughout differentiation of all three genetic backgrounds of TS cells. CT values for each transcript were measured on Day 0 and Day 8 and were then normalized to the geometric mean of *Ywhaz, Pgk1* and *Hk2.* Relative values were determined using methods described previously [13,34,35] and graphed. Error bars represent the standard error of the mean. Note that the top third of the graph is in an exponential scale.

these lineages represent an excellent model system to study mammalian development and understand crucial aspects of stem cell biology necessary in developing regenerative therapies. Analysis of gene expression using qPCR will undoubtedly play a pivotal role in deciphering the cellular and molecular propertiesthat define these different cell types. In these analysis, the identification of stable reference genes is an essential prerequisite to accurately interpreting experimental data. Using three independent, highly referenced and validated statistical methods, our analysis of fourteen potential candidate reference genes identify *Pgk1, Sdha* and *Tbp* as the most stable reference genes with which to normalize qPCR data. We believe these three genes will serve as excellent reference controls examining the basis for the differing developmental and epigenetic properties unique to embryonic, trophectoderm and extraembryonic endoderm stem cells.

Materials and Methods

Stem Cell Culture

Primary ES cells, TS cells, and XEN cells were derived from either 129 strain (R1 ES cells, (Nagy et al., 1990) TS 3.5) (Tanaka, 1998) B6 x CAST or CAST7 x B6 F_1 embryos (Golding et al., 2010) as previously described (Nagy et al., 1993; Tanaka, 1998; Kunath, 2005; Golding et al., 2010). Briefly, ES cultures were maintained in DMEM (Sigma, St. Lousi MO. Cat# D5671) supplemented with 50 µg/ml Penicillin/Streptomycin (Invitrogen, Carlsbad CA.), 100 µm β-mercaptoethanol, 1X LIF, (Sigma, St. Lousi MO.) 2 mM L-Glutamine, 1X MEM non-essential amino acids (Invitrogen, Carlsbad CA.) and 15% Hyclone ES grade fetal bovine serum (Fisher Scientific, Pittsburgh PA.). TS and XEN cell cultures were maintained as described (Kunath, 2005; Tanaka, 1998) using RPMI (Sigma, St. Lousi MI. Cat# R0883) supplemented with 50 µg/ml Penicillin/Streptomycin, 1 mM Sodium Pyruvate (Invitrogen, Carlsbad CA.), 100 µm β -mercaptoethanol, 1 µg/ml Heparin (Sigma, St. Lousi MO), 2 mM L-Glutamine, 1X FGF basic, 1X FGF4 (R&D Systems) and 20% Hyclone ES grade FBS. Cells were grown on a Mytomycin C (Sigma) treated feeder mouse fibroblast layer. For studies examining ES cell differentiation, sub-confluent

cultures were dissociated with 1X trypsin (Accutase - Millipore Billerica, MA) and plated on non-tissue culture treated petri dishes in ES cell medium lacking LIF for four days and subsequently plated on 10 cm tissue culture treated dishes to differentiate into fibroblast like cells. To differentiate TS cells we followed methods described previously (Tanaka, 1998).

RNA Isolation and Reverse Transcription

Cultured cells were grown to 80% confluence, washed twice in warm PBS, and dissociated with 1X trypsin (Accutase - Millipore Billerica, MA). Cells were spun down, washed once in cold PBS, then RNA isolated using Trizol (Invitrogen, Carlsbad CA.) according to the manufacturer's protocol. One µg of purified total RNA was treated with amplification grade DNaseI (Invitrogen) according to the manufacturer's protocol, and 250ng RNA seeded into a reverse transcription reaction using the SuperScriptII system (Invitrogen) by combining 1 µl random hexamer oligonucleotides (Invitrogen), 1 µl 10 mM dNTP (Invitrogen), 11 µl RNA plus water. This mixture was brought to 70°C for 5 minutes then cooled to room temperature. SuperScriptII reaction buffer, DTT (Invitrogen) and SuperScriptII were then added according to manufacturer's protocol and the mixture was brought to 25°C for 5 minutes, 42°C for 50 minutes, 45°C for 20 minutes, 50°C for 15 minutes then 70°C for five minutes.

Real-Time PCR Amplification

Real-time PCR analysis of mRNA levels was carried out using the DyNAmo Flash SYBR Green qPCR Mastermix (Fisher Scientific, Pittsburgh PA.) following the manufacturer's instructions. Reactions were performed on a StepOnePlus Real Time PCR system (Applied Biosystems, Foster City CA.). DNA primer information is available in Table S1.

Analysis of Real Time PCR Data

The measured CT (Cycle Threshold) values for each sample were compiled and the stability of each of the fourteen reference genes analyzed using the

GENorm, NORMFinder and BESTKeeper software tools; which have been described in detail elsewhere (Vandesompele et al., 2002; Andersen et al., 2004; Pfaffl et al., 2004). Once suitable reference genes were identified, the geometirc mean CT values of the best three candidate genes were calculated for each individual sample and used to normalize expression levels using the ΔΔCT method described previously (Vandesompele et al., 2002; Livak and Schmittgen, 2001; Schmittgen and Livak, 2008). These normalized values were averaged and the standard error of the mean calculated and graphed using Excel.

CHAPTER III

IDENTIFICATION OF CELL-SPECIFIC PATTERNS OF REFERENCE GENE STABILITY IN QUANTITATIVE REVERSE TRANSCRIPTION POLYMERASE CHAIN REACTION STUDIES OF EMBRYONIC, PLACENTAL AND NEURAL STEM MODELS OF PRENATAL ETHANOL EXPOSURE*

Introduction

The American College of Obstetricians and Gynecologists has indicated that three out of every one hundred babies born in the United States exhibit one type of major birth defect. Of these, nearly one third are due to the consumption of alcohol during pregnancy (Syndrome and Medicine, 1996; Floyd and Sidhu, 2004; Hoyme et al., 2005). As a result, 9.1 cases per 1000 live births exhibit some degree of fetal alcohol spectrum disorder, which can vary from barely detectable to severe functional and cognitive birth defects (Becker et al., 1996; Floyd et al., 2009). Despite years of intense study, both the biochemical mechanisms of alcohol induced teratogenesis and the developmental origins of fetal alcohol spectrum disorders remain poorly defined.

Identification of the transcriptional networks disrupted by prenatal ethanol exposure remains a core requirement to better understanding the molecular mechanisms of alcohol-induced teratogenesis. In this regard, the isolation and culture of both embryonic and tissue specific stem cells provide an enormous opportunity to model the molecular processes driving differentiation and study the developmental impact of teratogens. To gain insight into early embryonic development, pluripotent stem cells from both the embryonic and extraembryonic lineages present within the mammalian preimplantation blastocyst have been derived (Martin, 1981; Nagy et al., 1993; Tanaka, 1998). Embryonic (ES), and trophectoderm (TS) stem cells exhibit the developmental potential of these distinct

*Reprinted with permission from "Identification of cell-specific patterns of reference gene stability in quantitative reverse transcription polymerase chain reaction studies of embryonic, placental and neural stem models of prenatal ethanol exposure." By Carnahan et al. 2013. *Alcohol*, 47, 109-120, Copyright [2013] Elsevier Inc.

cellular lineages and offer the opportunity to model early differentiation of the embryo and placenta respectively. Similarly, fetal neuroepithelial stem cells cultured as neurospheres enable the examination of the molecular mechanisms governing neurogenesis *in vitro,* and aid in our understanding of why, above all others, the brain is so profoundly affected by the consumption of alcohol during pregnancy (Frederiksen et al., 1988; McKay, 1997; Miranda et al., 2008; Taléns-Visconti et al., 2011). Using these unique cell types, researchers are now examining the transcriptional consequences of ethanol exposure and monitoring the efficacy of potential therapeutic interventions.

Quantitative reverse transcription-polymerase chain reaction (qPCR) has emerged as an essential technique in our efforts to characterize alterations in gene expression brought on by exposure to alcohol. Many publications, however, continue to report the utilization of inappropriate methods of data normalization calling onto question the conclusions put forward (Bustin et al., 2009). In studies of stem or progenitor cell differentiation, it has been well documented that changes of as little as two-fold can significantly alter the developmental program and change cell fate (Niwa et al., 2000). Given the recent evidence that alcohol has the capacity to alter cellular differentiation within the developing central nervous system (Santillano et al., 2005; Taléns-Visconti et al., 2011), reliable methods to identify the underlying transcriptional changes are crucial to deciphering the developmental origins of fetal alcohol spectrum disorders. For this reason, identifying a cohort of stable reference genes for use as normalization controls is absolutely essential for both accurate data interpretation and reliable candidate gene discovery. Despite the widespread use of qPCR in the field of alcohol research, to the best of our knowledge, only two studies have currently been published which consider reference gene stability within the context of alcohol exposure (Johansson et al., 2007; Boujedidi et al., 2011). The retractions of the 2005 Science breakthrough of the year and studies linking childhood vaccinations to autism are two recent, widely-publicized examples, which highlight the importance of qPCR data normalization to the integrity of the overall study (Böhlenius et al., 2007; , 2010). Empirical selection and validation of a set of stable reference genes is absolutely essential to ensure

both the validity of the measurements being taken as well as their accurate interpretation. To address recurring errors in qPCR data interpretation, Bustin and colleagues recently established the Minimum Information for publication of Quantitative Real-Time PCR Experiments (MIQE) guidelines to ensure that studies utilizing qPCR are accurately interpreted and reproducible (Bustin et al., 2009). From these guidelines, the geometric mean of three carefully selected reference genes has become a validated requirement for normalizing qPCR data and the accurate assessment of quantitative changes in gene expression (Vandesompele et al., 2002; Andersen et al., 2004; Pfaffl et al., 2004; Gutierrez et al., 2008; Bustin et al., 2009; Lanoix et al., 2012).

Using these parameters, we sought to identify a list of candidate genes most suitable for use as normalization controls in qPCR-based comparisons between control and ethanol exposed ES, TS, and neurosphere stem cells. In addition, we initiated studies to examine the stability of reference genes throughout the process of *in vitro* differentiation, and to identify the best possible reference genes to examine the impact of alcohol upon these processes. In order to help identify candidate genes, we set three main criteria that potential reference genes would have to fulfill: 1) the transcripts needed to be expressed above background and easily detectable, 2) candidate mRNAs needed to be expressed within each of the three cellular lineages under investigation, and 3) the genes needed to be expressed throughout *in vitro* differentiation. We then surveyed the recent literature and compiled a short list of fourteen candidate genes, including: *Actb*, *B2m*, *Gapdh*, *Gusb*, *H2afz*, *Hk2*, *Hmbs*, *Hprt*, *Mrpl1*, *Pgk1*, *Ppia*, *Sdha*, *Tbp,* and *Ywhaz* (Allen et al., 2004; Andersen et al., 2004; Pfaffl et al., 2004; Goossens et al., 2005; Gilsbach et al., 2006; Willems et al., 2006; Hwang et al., 2007; Mamo et al., 2007; Espinoza et al., 2004; Gutierrez et al., 2008; Tatsumi et al., 2008; Golding et al., 2010; Suter and Aagaard-Tillery, 2009; van den Bergen et al., 2009; Galiveti et al., 2009; Rugg-Gunn et al., 2010; Veazey and Golding, 2011). These genes belong to diverse functional classes and should not be co-regulated in order to provide a non-biased method of normalizing qPCR expression data within ethanol-exposed cells (Supplemental Table S1). Results presented here identify the top three most stable reference

genes suitable for normalization of qPCR-based studies of alcohol induced teratogenesis within each of these three unique stem cell models, and highlight the importance of empirical reference gene selection.

Materials and Methods

Embryonic and Trophectoderm Stem Cell Culture

Previous studies in our laboratory have utilized stem cell lines derived from *Mus musculus castaneus x mus musculus (*C57Black6) F1 embryos (Golding et al., 2010; Golding and Mann, 2011). Polymorphisms between these genetic strains allow the examination of mono-allelic patterns of epigenetic marks and gene expression within loci regulated by genomic imprinting (Golding et al., 2010). ES cultures were maintained in DMEM (Sigma, St. Louis MO. Cat# D5671) supplemented with 50 µg/ml Penicillin/Streptomycin (Invitrogen, Carlsbad, CA. Cat# 15240096), 100 µm β-mercaptoethanol, 1X LIF (Sigma, St. Louis, MO. Cat# L5158), 2 mM L-Glutamine (Sigma, St. Louis, MO. Cat#G7513), 1X MEM non-essential amino acids (Invitrogen, Carlsbad, CA. Cat# 11140-050), and 15% Premium Select grade fetal bovine serum (Atlanta Biologicals Lawrenceville, GA Cat # S11550). TS cell cultures were maintained as described (Tanaka, 1998; Golding et al., 2010) using RPMI (Sigma, St. Louis, MO. Cat# R0883) supplemented with 50 µg/ml Penicillin/Streptomycin, 1 mM Sodium Pyruvate (Invitrogen, Carlsbad, CA. Cat# 11360070), 100 µm β -mercaptoethanol, 1 µg/ml Heparin (Sigma, St. Louis, MO. Cat# H3149), 2 mM L-Glutamine, 1X FGF basic, 1X FGF4 (R&D Systems, Minneapolis, MN. Cat# 233-FB and 235-F4 respectively), and 20% Premium Select FBS. Cells were initially grown on a Mytomycin C (Sigma, St. Louis, MO. Cat#M0503) treated feeder mouse fibroblast layer then moved to a feeder free system using conditioned medium as described previously (Tanaka, 1998).

For studies examining ES cell differentiation, a basic neuronal differentiation protocol was employed (Bain et al., 1995). Briefly, sub-confluent ES cell cultures were lightly dissociated with 1X trypsin (Accutase - Millipore, Billerica, MA. Cat#SF006). Colonies were released from the plate but maintained as “clumps”.

Dissociating colonies into individuals greatly reduced the number of cells surviving the differentiation procedure. Cellular clumps were plated in Corning ultra-low attachment flasks (VWR, Cat #89089-876) using ES cell medium lacking LIF and β -mercaptoethanol, and cultured for four days. Subsequently, cells were treated with 0.5M all-trans-retinoic acid (Sigma, St. Louis MO. Cat # R2625) and cultured for an additional 4 days. Finally, cells were plated on 10 cm tissue culture treated dishes to differentiate into neuronal like cells. For studies examining ES cell differentiation and ethanol treatment, cells were cultured in medium containing 320mg/dL ethanol and the lid was sealed with parafilm and placed in a standard incubator. Medium was changed every two days.

Neurosphere Stem Cell Culture

Culture and media preparations for neurospheres have been described previously (Miranda et al., 2008). Briefly, fetal cerebral cortical neuroepithelial stem cells isolated from C57Black6 mice were cultured as neurospheres in T25 flasks in media containing GlutaMAX™ DMEM F-12 (Invitrogen, Carlsbad, CA. Cat# 11330-032), 20ng/ml FGF basic, 20ng/ml EGF (Invitrogen, Carlsbad, CA Cat# 53003-018), 0.15ng/ml LIF, 1x ITS-X (Invitrogen, Carlsbad, CA. Cat# 51500-056), 0.85 units/ml heparin, and 20nM progesterone (Sigma, St. Louis, MO. Cat#P6149). Neurospheres were incubated for a total of 5 days at 37°C, 5% CO_2 in a humidified environment before passage. Medium was changed every 2-3 days depending on the level of confluence.

Differentiation of Neurospheres

Neurospheres were grown in complete medium containing FGF, EGF, and LIF. Differentiation was initiated as previously described (Miranda et al., 2008). Briefly, neurosphere cultures were seeded onto Laminin (Invitrogen, Carlsbad, CA. Cat# 23017015) coated dishes to initiate dis-aggregation and extracellular matrix attachment of sphere-derived progenitor cells. After 2 days, EGF and LIF were removed from the medium. Within approximately 24 hours early neuronal differentiation was visualized (“SVZ” stage). The final cortical progenitor stage was

achieved by removing FGF from the culture medium and culturing cells for an additional two days. At each stage, cells were collected and RNA extractions performed.

Ethanol Treatment

Cells were cultured in T25 flasks, with a parafilm (VWR) sealed lid to prevent ethanol evaporation. Dosing for ethanol followed previously published studies (Camarillo and Miranda, 2008), and utilized 60 mg/dL (13mM), 120 mg/dL (26mM), and 320 mg/dL (70mM) of ethanol (Sigma). Control samples for non-ethanol treated stem cells were concurrently cultured during the same experimental time course and in the same culture conditions. Neurospheres received fresh medium containing either ethanol every 2-3 days while ES and TS cells received fresh medium every 48 hours. On day 5 of treatment, cells were collected and RNA extraction was performed.

RNA Isolation and Reverse Transcription

Cultured cells were grown to 80% confluence, washed twice in warm PBS, and dissociated with 1X trypsin (Accutase). Cells were spun down, washed once in cold PBS, and RNA isolated using Trizol (Invitrogen, Carlsbad, CA. Cat # 15596026) according to the manufacturer's protocol. 1 µg of purified total RNA was treated with amplification grade DNaseI (Sigma, St. Louis, MO. Cat# AMPD1) according to the manufacturer's protocol, and 250ng of RNA was seeded into a reverse transcription reaction using the SuperScriptII kit (Invitrogen, Carlsbad, CA. Cat# 18064-071) by combining 1 µl random hexamer oligonucleotides (Invitrogen, Carlsbad, CA. Cat# 48190011), 1 µl 10 mM dNTP (Invitrogen, Carlsbad, CA. Cat# 18427-013), and 11 µl RNA plus water. This mixture was brought to 70°C for 5 minutes then cooled to room temperature. SuperScriptII reaction buffer, DTT, and SuperScriptII were then added according to manufacturer's protocol, and the mixture was brought to 25°C for 5 minutes, 42°C for 50 minutes, 45°C for 20 minutes, 50°C for 15 minutes, then 70°C for five minutes.

Real-Time PCR Amplification

Primers were designed using the NetPrimer software tool (www.premierbiosoft.com/netprimer) or identified from previously published research (Supplemental Table S2.). Real-time PCR analysis of mRNA levels was carried out using the DyNAmo Flash SYBR Green qPCR Mastermix (Fisher Scientific, Pittsburgh PA. Cat # F-415L) following the manufacturer's instructions. Reactions were performed on a StepOnePlus Real Time PCR system (Applied Biosystems, Foster City CA.).

Candidate Gene Ranking

Empirical selection and validation of a set of at least three stable reference genes has emerged as a core requirement for accurate interpretation of qPCR-based measurements of gene expression (Vandesompele et al., 2002; Andersen et al., 2004; Pfaffl et al., 2004; Gutierrez et al., 2008; Bustin et al., 2009). To facilitate the identification and selection of stable reference genes, three Microsoft Excel-based statistical programs have been produced and their predictive accuracy confirmed using published microarray data. GeNorm, NormFinder, and BestKeeper utilize slightly different methods of estimating both the intra- and the intergroup expression variation, and allow the ranking of candidate genes based on their overall stability across multiple experimental conditions and/or cell types. For example, GeNorm uses a measure of mean pair-wise variation between an individual candidate and the other reference genes measured to produce a stability value, and then ranks candidate genes according to this number (Vandesompele et al., 2002). NormFinder assigns a stability value based on statistical comparisons of inter- and intra-group stability and ranks candidate genes according to their expression variance across all samples measured (Andersen et al., 2004). Similarly, BestKeeper measures the geometric mean for each experiment, computes a pair-wise correlation coefficient for each candidate and then ranks candidate genes according to this index (Pfaffl et al., 2004). As BestKeeper has a maximal allowance of ten candidate genes, we elected to exclude this software package from

our analyses. In each of our experiments we have tabulated the rankings from both the GeNorm and Normfinder software tools. Candidate genes with GeNorm stability values greater than 0.5 are not acceptable for use as normalization controls, and have been demarcated with an * (Hellemans et al., 2007). A similar threshold for Normfinder has not been demonstrated, therefore only the rankings can be utilized as a guide for candidate gene suitability. Each of these programs is publicly available as a macro-program, which runs in older versions of Microsoft Excel.

Analysis of Real Time PCR Data and Statistical Analyses

The measured CT (Cycle Threshold) values for each sample were compiled and the stability of each of the fourteen reference genes analyzed using the GeNorm and NormFinder software tools (Vandesompele et al., 2002; Andersen et al., 2004; Pfaffl et al., 2004). Once suitable reference genes were identified, the geometric mean CT values of the best three candidate genes were calculated for each individual sample and used to normalize expression levels using the ΔΔCT method described previously (Livak and Schmittgen, 2001; Vandesompele et al., 2002; Schmittgen and Livak, 2008). Normalized CT values were averaged and the standard error of the mean calculated and graphed using Excel.

Using the JMP (SAS Institute, NC) software package, we conducted one- and two-way ANOVAs, as appropriate, and applied Tukey's HSD analysis for multiple comparisons. Main effects and first order interactions were considered in all models.

Results

Reference Gene Stability in Embryonic Stem Cells

We began by examining the stability of our candidate reference genes in mouse ES cells exposed to varying concentrations of ethanol (EtOH). Based on previous studies, we chose to examine 60 mg/dL, 120 mg/dL, and 320 mg/dL exposures of ethanol (Camarillo and Miranda, 2008). Unsurprisingly, cells cultured in the highest concentration of EtOH displayed slower growth and increased amounts of cellular debris suggesting a rise in the number of dead or dying cells.

However, cells cultured in 120mg/dL did display a modest increase in growth rate that trended towards statistical significance, but did not achieve a p-value less than .05 (data not shown). Cell lines were cultured to 80% confluence under both control and ethanol conditions, cellular extracts collected, and RNA isolated from four independent experimental replicates (N=4). RNA from each replicate was seeded into four independent reverse transcription reactions and used in three independent qPCR reactions measuring the fourteen candidate genes in duplicate. From these experiments, the CT values were compiled and analyzed using the GeNorm and NormFinder software packages (Vandesompele et al., 2002; Andersen et al., 2004). Results from these analyses consistently identified *Gapdh*, *Ppia*, and *Hprt* as the most stable reference genes across all experimental treatments examined. In contrast, *Pgk1* and *GusB* displayed GeNorm stability values in excess of 0.5, indicating they would not serve as acceptable normalization controls (Table 1a) (Hellemans et al., 2007). To visualize changes in candidate gene expression in response to our experimental treatments, we utilized the geometric mean of these three best candidates to normalize and graph our qPCR data using the comparative or $\Delta\Delta$ CT method (Livak and Schmittgen, 2001; Schmittgen and Livak, 2008). While treatment with EtOH increased variability, it did not dramatically alter the expression of any one gene (Fig 1a). While *Actb* did display a 1.5 to 2-fold change across all EtOH treatments, a one-way ANOVA revealed this change was not statistically significant. Moreover, this analysis revealed that exposure to alcohol did not significantly influence the expression of any of the candidate genes examined.

The *in vitro* differentiation of embryonic and tissue specific stem cells provide an enormous opportunity to model the cellular processes driving differentiation, and allow mechanistic studies into the molecular actions of teratogens. We next sought to determine the influence of EtOH upon reference gene stability throughout the process of *in vitro* differentiation. ES cells were differentiated using a standard embryoid-body-neuronal differentiation protocol (see Materials and Methods). ES cells were gently dissociated into large clumps, transferred to ultra-low adherence flasks and exposed to retinoic acid (see Materials and Methods). For these experiments, we focused on comparisons between control and 320mg/dL EtOH

Table 6: GeNorm and Normfinder rankings of candidate gene stability in experiments comparing ethanol and control treatments of embryonic stem cell cultures.

Table 6a. Cultures maintained as stem cells

	GeNorm		Normfinder	
		Stability		Stability
Rank	Gene name	value	Gene name	value
1	Gapdh	0.092	Gapdh	0.019
2	Ppia	0.104	Ppia	0.033
3	Hprt	0.107	Hprt	0.045
4	Ywhaz	0.107	Ywhaz	0.048
5	B2m	0.115	H2afz	0.05
6	Mrpl1	0.115	B2m	0.054
7	H2afz	0.116	Mrpl1	0.058
8	Actb	0.12	Actb	0.06
9	Sdha	0.122	Sdha	0.06
10	Tbp	0.341	Hmbs	0.074
11	Hmbs	0.373	Tbp	0.078
12	Hk2	0.424	Hk2	0.083
13	Pgk1 *	0.577	Pgk1	0.095
14	Gusb *	0.678	Gusb	0.102

Table 6b. Differentiating cultures

	GeNorm		Normfinder	
		Stability		Stability
Rank	Gene name	value	Gene name	value
1	Ppia	0.088	Ppia	0.027
2	Sdha	0.095	Mrpl1	0.037
3	Mrpl1	0.096	Sdha	0.04
4	Hk2	0.098	Hk2	0.043
5	Hprt	0.1	Ywhaz	0.044
6	Gusb	0.102	Gusb	0.045
7	Ywhaz	0.103	Hprt	0.045
8	Hmps	0.104	Hmps	0.047
9	B2m	0.105	Tbp	0.048
10	Tbp	0.106	B2m	0.051
11	H2afz	0.151	H2afz	0.059
12	Actb	0.187	Actb	0.064
13	Gapdh *	0.545	Gapdh	0.086
14	Pgk1 *	0.681	Pgk1	0.106

Candidate genes with GeNorm stability values greater than 0.5 are designated by a * and are not acceptable for use as normalization controls (Hellemans et al., 2007).

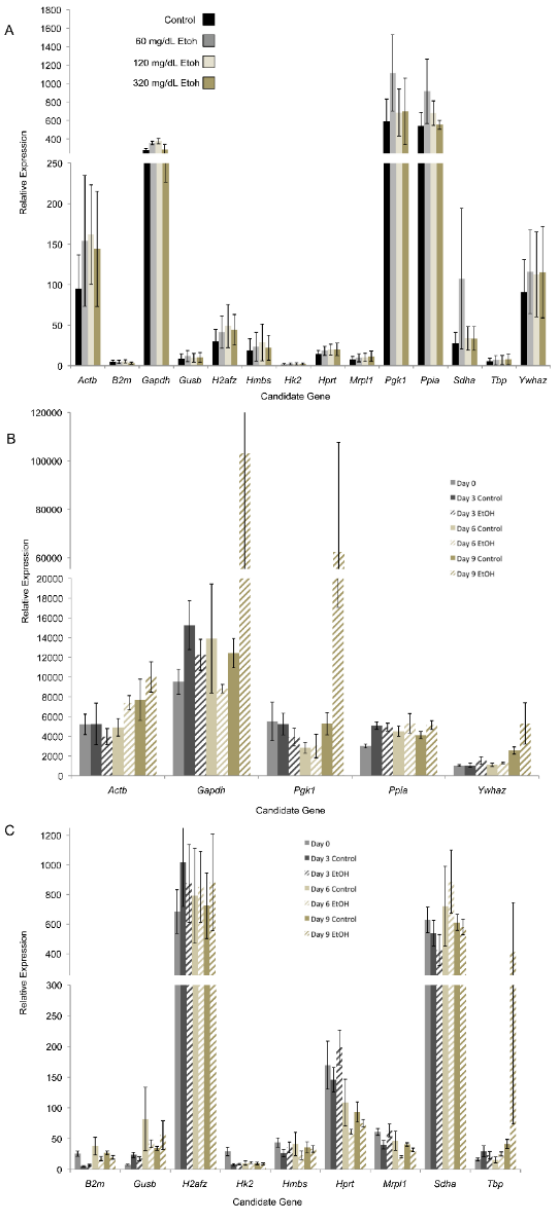

Figure 5: Analysis of reference genes in ethanol exposed embryonic stem cells. A) Experiments contrasting control samples with 60mg/dL, 120mg/dL, and 320mg/dL ethanol treatments under conditions maintaining ES cell stemness. Data was normalized to the geometric mean of *Gapdh, Ppia,* and *Hprt*. Using a one-way ANOVA, no statistically significant differences in candidate gene expression were observed ($p < .05$). Graphs are representative of four independent cell culture experiments (N = 4). B) & C) Relative expression of the fourteen candidate reference genes in differentiating embryonic stem cell cultures contrasting control samples with 320mg/dL ethanol treatments. Samples were collected on days 0, 3, 6, and 9 of a standard neuronal differentiation protocol. Data was normalized to the geometric mean of *Mrpl1*, *Ppia,* and *Sdha.* Figures 1b and 1c were grouped and separated due to differences in the scale of candidate gene expression level. A two-way ANOVA revealed exposure to alcohol did not influence the expression of any of the candidate genes examined ($p < .05$). Graphs are representative of three independent cell culture experiments (N = 3). All data presented in figure 1 were graphed as relative values using the $\Delta\Delta$ CT method (Livak and Schmittgen, 2001; Schmittgen and Livak, 2008). Error bars represent the standard error of the mean.

treatments. Cells from both groups readily formed embryoid bodies and neurons when plated under appropriate conditions. Cells within the 320mg/dL EtOH treated cultures exhibited a large increase in the amount of cellular debris, consistent with previous studies, (Arzumnayan et al., 2009) demonstrating increased apoptosis within differentiating ES cell cultures exposed to alcohol. Samples were collected on days 3, 6, and 9 of the differentiation protocol and RNA was analyzed as indicating this nearly ubiquitous reference gene is a poor choice for normalizing qPCR expression data when examining the consequences of ethanol exposure during ES cell differentiation. We then utilized the geometric mean of the three highest ranked candidate genes to normalize and graph the relative expression of our fourteen reference genes (Fig 1b and 1c). Analysis using a two-way ANOVA considering the two experimental treatments across days of the differentiation protocol revealed exposure to ethanol did not significantly impact the expression of any of our candidate genes. As a means to further validate our normalization controls, we utilized the top three reference genes as a base to monitor the expression of the well-established ES cell pluripotency markers *Oct4, Nanog,* and *Klf4* throughout ES cell differentiation. Changes in the expression of these transcription factors throughout *in vitro* differentiation are extremely well characterized, offering the opportunity to confirm the validity of our chosen references. As expected, each of these markers demonstrated coordinated down-regulation throughout the course of ES cell differentiation (Fig 2). We conducted a two-way ANOVA, including interactions, comparing ethanol treatments across the nine-day experimental course to determine if EtOH induced alterations in the expression of these transcription factors. Although significant differences were detected, Tukey's HSD analysis revealed that these were due to the differentiation that occurred across days in culture and that EtOH did not significantly influence the expression of our candidate pluripotency markers (Fig 2).

Reference Gene Stability in Trophectoderm Stem Cells

To model the impact of ethanol exposure on placentation, we examined the consequences of exposing trophectoderm stem (TS) cells *in vitro* to varying

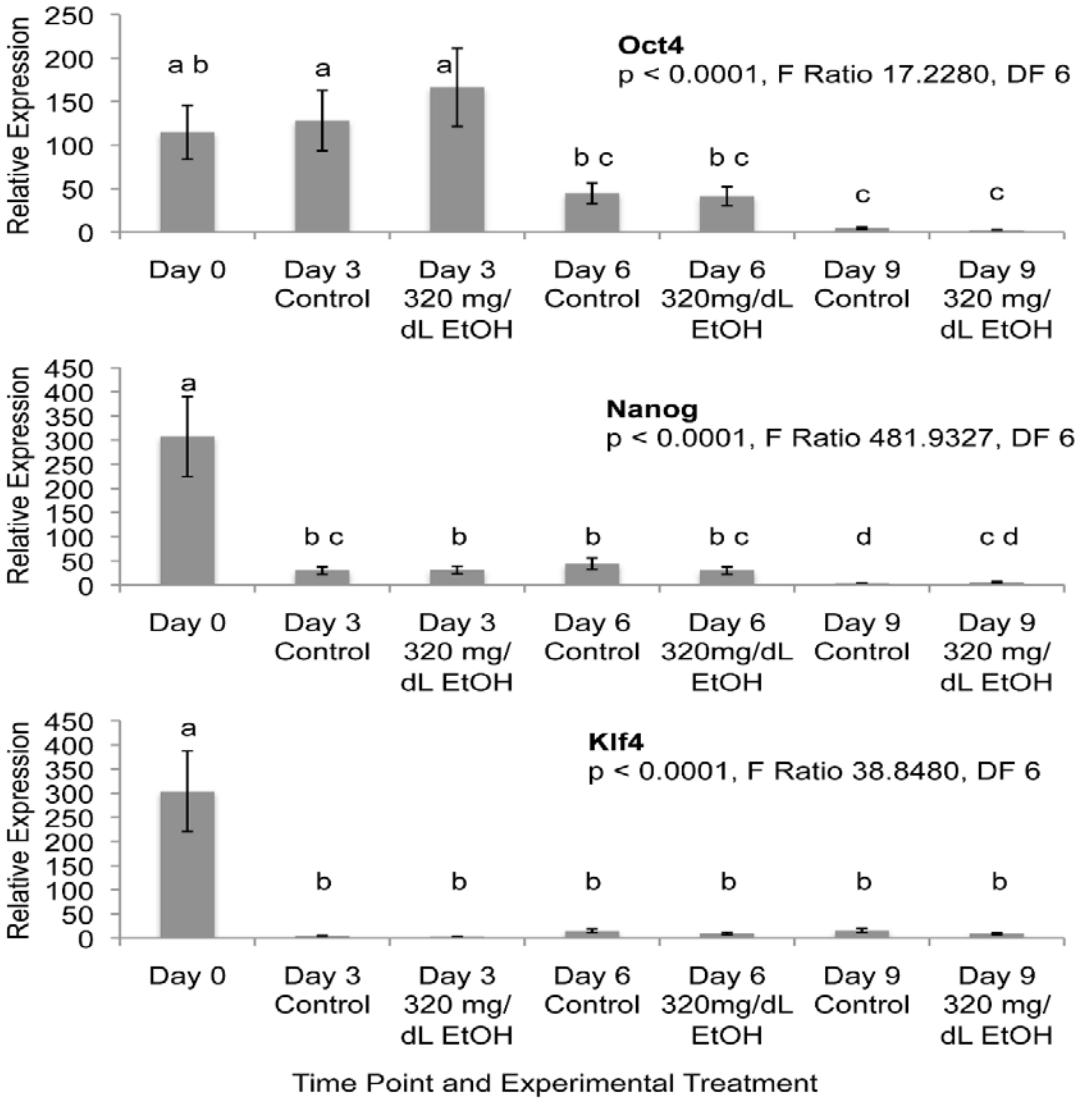

Figure 6: Validation of normalization controls in ES cell cultures. Relative expression of stem cell markers of pluripotency *Oct4*, *Nanog,* and *Klf4* in differentiating ES cells under either control conditions or exposure to 320mg/dL ethanol. Data was normalized to the geometric mean of *Mrpl1*, *Ppia,* and *Sdha.* Tukey's HSD analysis revealed the significant differences observed ($p < 0.0001$) were only across days in culture, and that EtOH did not significantly influence the expression of the candidate pluripotency markers. All data presented in figure 2 were graphed as relative values using the $\Delta\Delta$ CT method (Livak and Schmittgen, 2001; Schmittgen and Livak, 2008). Graphs are representative of three independent cell culture experiments (N = 3). Error bars represent the standard error of the mean.

concentrations of EtOH. For these experiments we utilized control, 120mg/dL and 320mg/dL EtOH treatments. Surprisingly, TS cells did not exhibit any noticeable changes in growth rate nor an increase in cell death, even when exposed to the higher range of EtOH concentrations tested. Cells were cultured to 80% confluence, RNA isolated and analyzed as above. From these analyses, all of the fourteen candidate genes examined would serve as suitable normalization controls (Table 2a). When we normalized gene expression levels using the geometric mean of the top three candidate genes (*Sdha*, *Hprt,* and *Mrpl1*), we found the expression levels of all candidate genes to be completely homogenous (Fig 3a). A one-way ANOVA comparing all experimental treatments for each gene confirmed no statistically significant changes in gene expression could be detected.

To examine the influence of EtOH on the stability of our candidate reference genes throughout TS cell differentiation, we followed a previously described differentiation protocol (Tanaka, 1998; Veazey and Golding, 2011). For these experiments, we focused on comparisons between 120mg/dL EtOH, 320mg/dL EtOH, and control treatments. Twenty-four hours after plating, alcohol was added to the newly seeded TS cell cultures. Twenty-four hours later, FGF4 and heparin were withdrawn from the culture medium, marking Day 0 of the differentiation protocol. Over the course of the next five days, TS cell cultures readily differentiated into placental giant cells. In contrast to our analysis of undifferentiated TS cells, however, the 320mg/dL treatments produced a modest increase in cell death as measured solely by increased cellular debris. RNA was then isolated and analyzed as described in the materials and methods. Interestingly, TS cells again showed a very narrow range of reference gene fluctuation, with *Sdha, Mrpl1* and *Ppia* being ranked as the three most stable genes (Table 2b). Using the geometric mean of *Sdha, Ppia*, and *Mrpl1*, we normalized and graphed the relative expression of our fourteen candidate genes (Fig 3b). Similar to previously published observations, *Actb* exhibited large fluctuations in expression inherent to TS cell differentiation (Vong et al., 2010; Veazey and Golding, 2011). Using a two-way ANOVA examining experimental treatments across days in culture, we did not find any significant alterations in gene expression arising as a consequence of EtOH exposure. To

Table 7: GeNorm and Normfinder rankings of candidate gene stability in experiments comparing ethanol and control treatments of trophectoderm stem cell cultures.

Table 7a. Cultures maintained as stem cells

	GeNorm		Normfinder	
		Stability		Stability
Rank	Gene	value	Gene name	value
1	Hprt	0.028	Sdha	0.002
2	Ppia	0.028	Hprt	0.003
3	Sdha	0.028	Mrpl1	0.003
4	Ywhaz	0.028	Ppia	0.003
5	Mrpl1	0.029	Ywhaz	0.006
6	Gapdh	0.03	Pgk1	0.007
7	Pgk1	0.03	Gapdh	0.008
8	Actb	0.031	Actb	0.01
9	Tbp	0.035	Tbp	0.014
10	B2m	0.037	B2m	0.015
11	H2afz	0.043	H2afz	0.023
12	Hk2	0.054	Hk2	0.031
13	Gusb	0.068	Gusb	0.043
14	Hmbs	0.101	Hmbs	0.068

Table 7b. Differentiating cultures

	GeNorm		Normfinder	
		Stability		Stability
Rank	Gene	value	Gene name	value
1	Sdha	0.048	Sdha	0.009
2	Mrpl1	0.049	Ppia	0.01
3	Gapdh	0.05	Mrpl1	0.013
4	Ppia	0.05	Gapdh	0.016
5	B2m	0.057	B2m	0.023
6	Ywhaz	0.061	H2afz	0.03
7	Hprt	0.062	Ywhaz	0.03
8	Pgk1	0.062	Hprt	0.031
9	H2afz	0.063	Pgk1	0.031
10	Gusb	0.07	Gusb	0.037
11	Hk2	0.072	Hk2	0.038
12	Hmbs	0.08	Hmbs	0.046
13	Tbp	0.081	Tbp	0.05
14	Actb	0.094	Actb	0.058

Candidate genes with GeNorm stability values greater than 0.5 are designated by a * and are not acceptable for use as normalization controls (Hellemans et al., 2007).

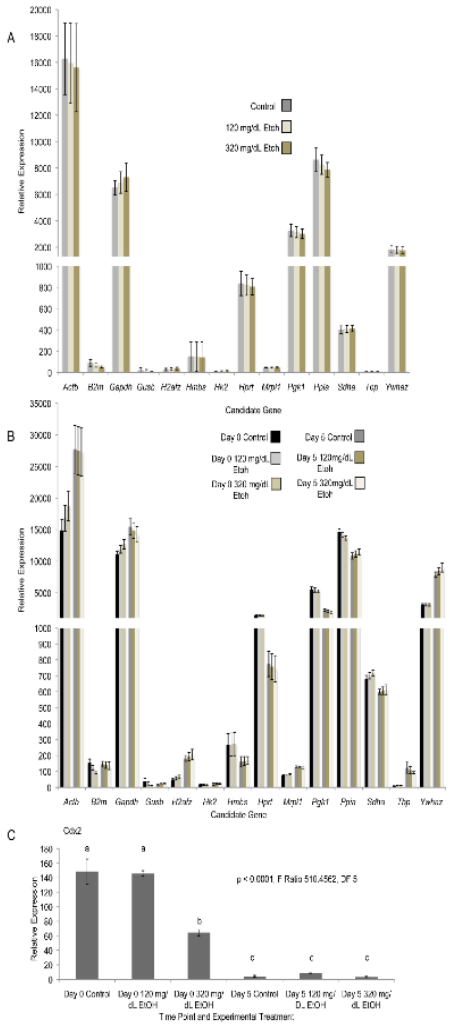

Figure 7: Analysis of reference genes in ethanol exposed trophectoderm stem cells. A) Relative expression of the fourteen candidate reference genes in trophectoderm stem cell cultures contrasting control samples with 120mg/dl and 320mg/dL ethanol treatments. Cells were cultured under conditions maintaining TS cell stemness. Data were normalized to the geometric mean of *Sdha*, *Hprt,* and *Mrpl1.* Using a one-way ANOVA, no statistically significant differences in candidate gene expression were observed ($p < .05$). Graphs are representative of four independent cell culture experiments (N = 4). B) Relative expression of the fourteen candidate reference genes in differentiating trophectoderm stem cell cultures contrasting control samples with 120mg/dL and 320mg/dL ethanol treatments. Samples were collected on days 0 and 5 of *in vitro* differentiation. Data was normalized to the geometric mean of *Mrpl1*, *Ppia*, and *Sdha.* Using a two-way ANOVA, no statistically significant differences in candidate gene expression could be detected ($p < .05$). Graphs are representative of four independent cell culture experiments (N = 4). C) Validation of normalization controls in differentiating TS cell cultures. Expression of the TS cell marker of pluripotency, *Cdx2*, in differentiating TS cells under either control conditions or exposure to 120mg/dL or 320mg/dL ethanol. *Cdx2* expression was normalized to the geometric mean of *Mrpl1*, *Ppia*, and *Sdha.* A two-way ANOVA and Tukey's HSD analysis comparing ethanol doses over time revealed *Cdx2* levels within the Day 0 320mg/dL EtOH treatments were significantly different than the Day 0 120mg/dL and control treatments ($p < 0.0001$). No significant differences were found for the Day 5 cultures. Graphs are representative of four independent cell culture experiments (N = 4). All data presented in figure 3 were graphed as relative values using the $\Delta\Delta$ CT method (Livak and Schmittgen, 2001; Schmittgen and Livak, 2008). Error bars represent the standard error of the mean.

validate our normalization controls, we utilized the geometric mean of *Sdha, Ppia*, and *Mrpl1* to graph the expression of the TS cell stemness marker *Cdx2*. Similar to our analyses of *Oct4*, *Nanog,* and *Klf4* in differentiating ES cells, we observed a large decrease in the expression of this cellular marker of trophectoderm stem cell potency throughout the course of *in vitro* differentiation (Fig 3c). To determine if EtOH induced alterations in the expression of *Cdx2*, we conducted a two-way ANOVA comparing ethanol doses over time. This analysis revealed that day 0 320mg/dL treatments significantly reduced *Cdx2* expression, whereas, Day 0 120mg/dL treatments were unaffected and remained identical to the controls ($p < 0.0001$).

Reference Gene Stability in Neurosphere Stem Cells

Fetal development is characterized by multiple region-specific periods of neurogenic growth, giving rise to millions of neuroblasts that migrate away from their germinal zones to populate the developing brain. To model this developmental process *in vitro*, cell cultures have been derived from the fetal neuroepithelium. These stem cells grow as free-floating, clonal aggregates termed “neurospheres” (Conti and Cattaneo, 2010). To determine the impact of EtOH exposure on our fourteen candidate reference genes within this model system, neurospheres were cultured under control conditions or 60 mg/dL, 120 mg/dL, or 320 mg/dL EtOH and analyzed as above. As can be seen in Table 3a, *Actb* stability is affected by exposure to EtOH, and would not serve as an acceptable normalization control. From these experiments, the top three candidate genes identified were *Pgk1, Gapdh*, and *Hprt*. Using the geometric mean of these three candidates as normalization controls, we graphed the relative expression levels of the fourteen candidate genes (Fig 4a). Using a one-way ANOVA comparing each experimental treatment, we were unable to discern any significant differences between the treatment groups, for any of the candidate genes examined.

Table 8: GeNorm and Normfinder rankings of candidate gene stability in experiments comparing ethanol and control treatments of neurosphere stem cell cultures.

Table 8a. Cultures maintained as stem cells

	GeNorm		Normfinder	
		Stability		Stability
Rank	Gene	value	Gene name	value
1	Gapdh	0.078	Pgk1	0.495
2	Pgk1	0.079	Gapdh	0.52
3	Tbp	0.079	Hprt	0.595
4	Hprt	0.081	Sdha	0.622
5	Sdha	0.081	Tbp	0.627
6	Gusb	0.084	Ywhaz	0.692
7	H2afz	0.086	H2afz	0.737
8	Mrpl1	0.086	Mrpl1	0.786
9	Ywhaz	0.088	Gusb	0.805
10	B2m	0.094	B2m	0.945
11	Ppia	0.111	Ppia	1.405
12	Hmbs	0.325	Actb	1.707
13	Hk2	0.434	Hmbs	1.859
14	Actb *	0.869	Hk2	2.397

Table 8b. Differentiating cultures

	GeNorm		Normfinder	
		Stability		Stability
Rank	Gene	value	Gene name	value
1	Hprt	0.063	Hprt	0.012
2	Sdha	0.064	Sdha	0.016
3	Gusb	0.065	Mrpl1	0.017
4	Mrpl1	0.065	Gusb	0.018
5	Gapdh	0.067	Gapdh	0.023
6	Pgk1	0.068	Pgk1	0.023
7	Hk2	0.107	Hk2	0.026
8	Ywhaz	0.479	Hmbs	0.038
9	Hmbs *	0.803	Ywhaz	0.038
10	Tbp *	0.833	Ppia	0.042
11	Ppia *	0.857	Tbp	0.042
12	H2afz *	0.901	H2afz	0.059
13	B2m *	0.921	B2m	0.075
14	Actb *	1.544	Actb	0.1

Candidate genes with GeNorm stability values greater than 0.5 are designated by a * and are not acceptable for use as normalization controls (Hellemans et al., 2007).

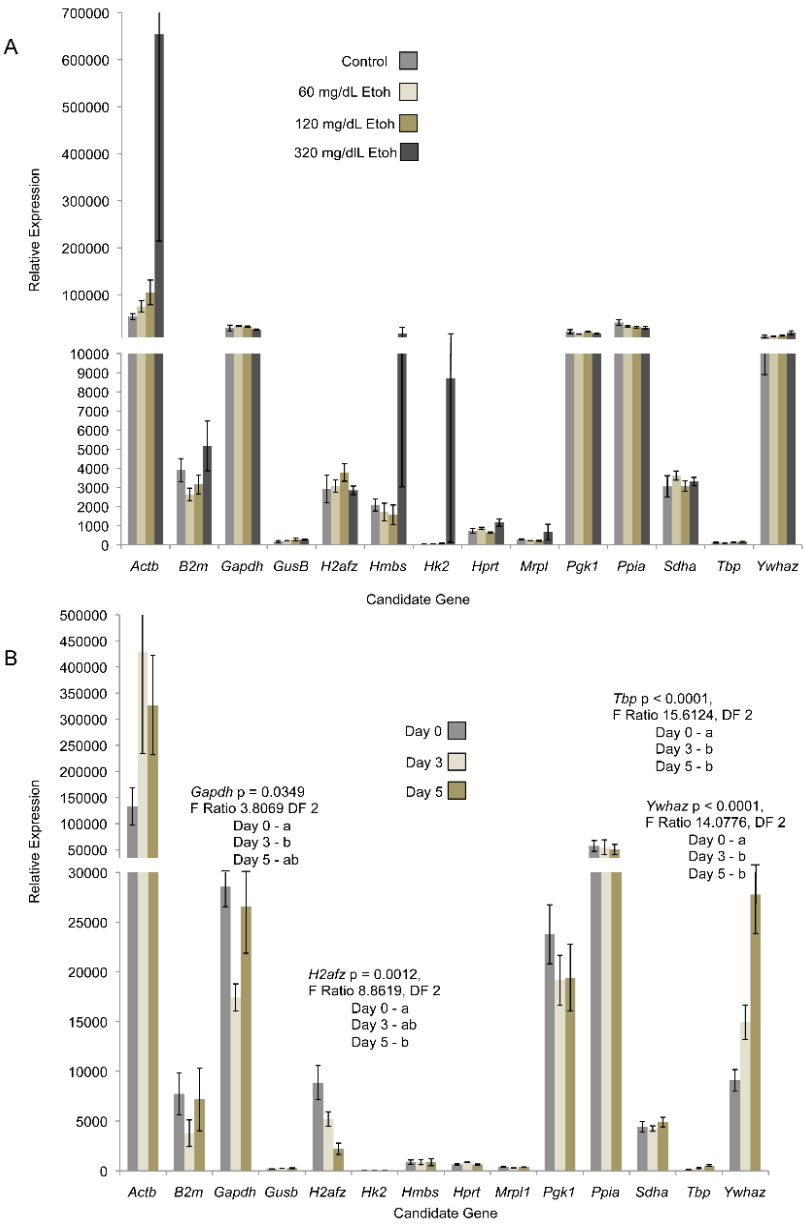

Figure 8: Analysis of candidate reference genes in neurosphere stem cells. A) Relative expression of the fourteen candidate reference genes in neurosphere stem cell cultures contrasting control samples with 60mg/dL, 120mg/dL, and 320mg/dL ethanol treatments. Data were normalized to the geometric mean of Pgk1, Hprt, and Gapdh. Using a one-way ANOVA, no statistically significant differences in candidate gene expression were observed ($p < .05$). Graphs are representative of four independent cell culture experiments (N = 4). B) Relative expression of the fourteen candidate reference genes in differentiating neurosphere cultures. Samples were collected on days 0, 3, and 5 of the in vitro differentiation protocol as previously described (Miranda et al., 2008). Data were normalized to the geometric mean of Hprt, Mrpl1, and Sdha. Statistically significant differences in the expression of Gapdh, H2afz, Tbp and Ywhaz were identified using a two-way ANOVA followed by Tukey's HSD analysis. Graphs are representative of three independent cell culture experiments (N = 3). All data presented in figure 4 were graphed as relative values using the $\Delta\Delta$ CT method (Livak and Schmittgen, 2001; Schmittgen and Livak, 2008). Error bars represent the standard error of the mean.

We next sought to examine the impact of ethanol exposure on neurosphere differentiation. We began by examining the expression of our candidate genes throughout a previously published, five-day neurosphere differentiation protocol (Miranda et al., 2008). Candidate gene expression was assayed during the early and late stages of differentiation. From these analyses, we observed that the expression of many of our reference genes were profoundly altered during the course of neurosphere differentiation, with six of the fourteen genes having GeNorm stability values in excess of 0.5. As can be seen in Table 3b, *Hprt*, *Sdha*, *Mrpl1,* and *GusB* were identified as the most consistently stable reference genes. Using the geometric mean of *Hprt*, *Mrpl1,* and *Sdha*, we normalized and graphed the relative expression of the fourteen candidate genes using methods previously discussed (Fig 4b). Using a two-way ANOVA comparing experimental treatments across days of the differentiation protocol, we observed statistically significant differences in the expression of *Gapdh*, *H2afz*, *Tbp*, and *Ywhaz*.

Unexpectedly, when we assayed the expression of mRNAs encoding markers of neurosphere stemness (*Sox2* and *Nestin*), we found that their expression significantly increased as differentiation progressed (Fig 5). Paradoxically, while these markers of stemness increased so did established makers of neuronal differentiation, including *Gfap* and *Dlx2*. *Gfap*, which was minimally detected on day 0, became undetectable on day 3 and strongly expressed on day 5. In contrast, *Dlx2* was undetectable on day 0 but progressively increased over the course of *in vitro* differentiation. Similar to previous reports, the relative ratios in which these transcription factors were expressed seemed to change through cellular passaging (Conti and Cattaneo, 2010). This suggests the complex population of cells present within neurospheres was constantly fluctuating. From previous studies (Campos, 2004), it has been suggested that the heterogeneity of the neurospheres is linked to their three-dimensional structure, where different cells within the spherical structure are exposed to varying and sometimes suboptimal conditions. For example, neurospheres display a tendency to generate differentiated cells within their core while cells on the surface are more stem-like (Campos, 2004). These results prompted us to question what proportion of thecellular population were differentiating

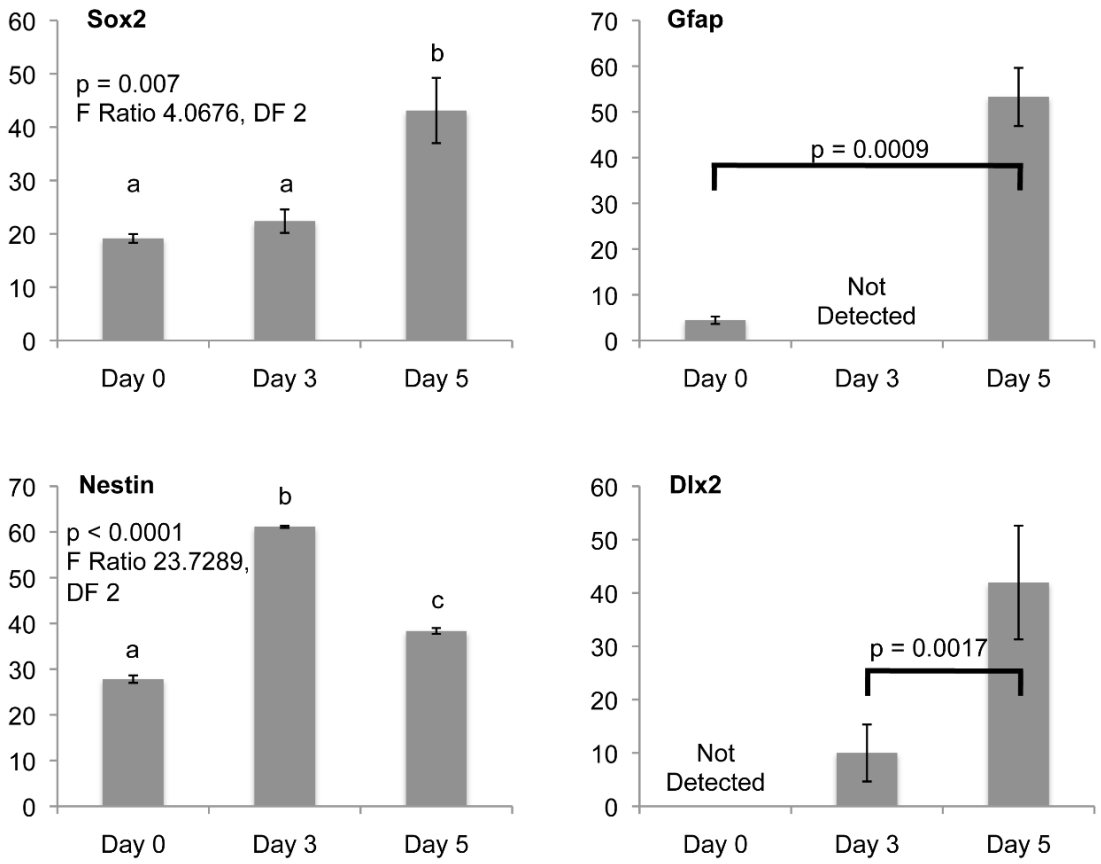

Figure 9: Analysis of lineage specific transcription factors in differentiating neurosphere stem cell cultures. Expression of neurosphere stem cell markers of stemness (*Sox2* and *Nestin*) as well as differentiation (*Gfap* and *Dlx2*) in differentiating neurosphere stem cells under control conditions. Expression was normalized to the geometric mean of *Hprt*, *Mrpl1,* and *Sdha.* Graphs are representative of three independent cell culture experiments (N = 3). Statistically significant differences were observed for all four candidate genes examined using either an ANOVA (*Sox2, Nestin*) or a students t-test (*Dlx2 Gfap*). All data presented in figure 5 were graphed as relative values using the ΔΔ CT method (Livak and Schmittgen, 2001; Schmittgen and Livak, 2008). Error bars represent the standard error of the mean.

versus those that were being maintained in a stem-like-state simply due to either exposure to local paracrine factors or cell–extracellular matrix interactions. Most studies of neurosphere differentiation predominately utilize immunocytochemistry to visually examine the expression of cellular markers within individual populations of cells. These studies tend to focus on individual colonies of cells rather than the total population of cells as in qPCR studies. Our results suggest a global survey of the transcriptome using qPCR may not be sensitive enough to finely monitor the intricacies of gene expression during neurosphere differentiation. Similar to previous studies (Santillano et al., 2005; Camarillo and Miranda, 2008), under conditions of alcohol exposure we observed an increase in differentiating neurosphere size, and many of the cultures exhibited drastic differences in cellular morphology or progression through the stages of differentiation. Due to the extreme variation in both cell type and the expression of molecular markers within these cultures, we did not feel we were able to definitively and reliably assay candidate gene stability through differentiation.

Discussion

Analysis of gene expression using quantitative reverse transcription-polymerase chain reaction (qPCR) has become a widely utilized core technique in nearly every area of biological research. However, many publications continue to report the implementation of inappropriate methods of qPCR normalization (Bustin et al., 2009). A recent study of 8-Oxoguanine DNA glycosylase expression in preeclamptic placental samples by Lanoix et al., elegantly demonstrates how normalization with an inappropriate reference gene can produce a statistically significant result, which is diametrically opposite to the one predicted of a characterized physiological response (Lanoix et al., 2012). Despite numerous publications demonstrating significant fluctuations in the expression of established reference genes such as *Actb* and *Gapdh*, the single use of either of these reference genes to normalize gene expression data remains the norm for the vast majority of published qPCR-based studies (Vandesompele et al., 2002; Radonić et al., 2004; Bustin and Nolan, 2004; Dheda et al., 2005; Goossens et al., 2005; Johansson et

al., 2007; Mamo et al., 2007). While many *in vitro* and *in vivo* studies modeling prenatal alcohol exposure employ qPCR-based measurements as a key analytic tool, very few studies have been published which consider the suitability / stability of their reference gene(s) (Johansson et al., 2007; Boujedidi et al., 2011).

Previous studies by Vandesompele and colleagues demonstrated that the geometric mean of three reference genes provided the most accurate and reliable means of normalizing qPCR expression data (Vandesompele et al., 2002). Subsequently, this experimental strategy was validated, and a series of statistical algorithms was written in order to identify the three most suitable reference genes for a variety of experimental conditions (Andersen et al., 2004; Pfaffl et al., 2004; Goossens et al., 2005; Gilsbach et al., 2006; Willems et al., 2006; Gutierrez et al., 2008; Tatsumi et al., 2008; Boda et al., 2008; Suter and Aagaard-Tillery, 2009; van den Bergen et al., 2009; Galiveti et al., 2009; Veazey and Golding, 2011). The GeNorm software tool ranks candidate genes according to a derived M-value (Vandesompele et al., 2002). An M-value describes the variation of a gene relative to all the other candidate genes examined. The GeNorm algorithm progressively assigns M-values by removing the gene with the highest M-value, and repeating the process until only the optimal set of reference genes remains (Vandesompele et al., 2002). In contrast, Normfinder was designed to independently account for the various sample or treatment groups (Andersen et al., 2004). This allows for the selection of an optimum reference gene pair rather than ranking genes individually from highest to lowest stability. Using this slightly different approach, the most stable pair of genes selected by Normfinder may have compensating expression levels. For instance, one reference gene may be highly expressed in one sample group while its paired gene is underexpressed in the same group. This difference between algorithms explains the slight differences in the assigned stability values and gene rankings observed in this study. Many of the gene rankings reported, however, were only different by a very small margin or were in fact the same but grouped differently due to alphabetical ordering of the gene names.

In the present study, we sought to assay the stability of fourteen commonly used reference genes within *in vitro* cultures of embryonic, placental, and neurosphere stem cells exposed to alcohol. Using these two independent software tools to assess gene stability, we find broad consensus in the identification of the three best normalization controls across cell types, alcohol exposures, and stages of *in vitro* differentiation. Based upon the framework provided by MIQE Guidelines, we propose utilizing the geometric mean of the top three genes identified for each experimental condition as normalization controls in studies examining the impact of alcohol upon the transcriptomes of the three stem cell types examined.

The overarching goal of this paper was to lay the groundwork for the use of embryonic, trophectoderm and neurosphere stem cells as models to examine the transcriptional consequences of prenatal ethanol exposure. While our study found no single reference to be entirely refractory to the influence of alcohol nor completely stable throughout *in vitro* differentiation, *Hprt*, *Mrpl1*, *Sdha*, *Ppia* (and to a lesser extent *Gapdh),* were identified as the most consistently stable transcripts across all cell types and experimental conditions examined. This core group of candidates should be considered as a starting point for future studies of reference gene stability within other models of alcohol exposure.

In contrast, our analyses identified transcripts encoding one of the most commonly used reference genes, *Actb*, as often amongst the least stable candidate genes tested, and in many cases, it would not serve as an acceptable normalization control. Importantly, a significant number of studies modeling prenatal alcohol exposure continue to utilize *Actb* as their sole normalization control. Given the observations reported here and elsewhere indicating alcohol can modulate expression of this gene (Romero et al., 2010), its candidacy as a valid reference should be reconsidered. Overall, these investigations highlight the importance of empirical reference gene selection and identify a core group of candidate genes for use as normalization controls in qPCR studies of ethanol induced teratogenesis.

CHAPTER IV

ALCOHOL-INDUCED EPIGENETIC ALTERATIONS TO DEVELOPMENTALLY CRUCIAL GENES REGULATING NEURAL STEMNESS AND DIFFERENTIATION*

Introduction

Studies using a broad range of model systems representing multiple tissue types reveal exposure to alcohol significantly alters the developmental trajectory of progenitor cells and fundamentally compromises histogenesis (Camarillo and Miranda, 2008; Crabb et al., 2011; Crews et al., 2006; Gong and Wezeman, 2004; Hipp et al., 2010; Ieraci and Herrera, 2007; Mo et al., 2012; Roitbak et al., 2011; Vangipuram and Lyman, 2010; Vangipuram and Lyman, 2012; Vemuri and Chetty 2005). These observations are highly suggestive that ethanol interferes with the ability of differentiating cells to properly engage the molecular systems necessary to execute cellular differentiation and patterning. Once established by lineage-specific transcription factors, the identity of each developing cell type is maintained through unique alterations in the way in which the DNA encoding each gene becomes packaged within the nucleus (Hemberger et al., 2009). From studies using a diverse range of model organisms, we now acknowledge that epigenetic changes to chromatin structure provide a plausible link between the environment and lasting alterations in gene expression leading to disease (Feil and Fraga, 2011).

The coordinated recruitment of activating and repressive chromatin modifying enzymes to developmentally crucial loci is absolutely essential for differentiating cells to exit the transcriptional networks promoting pluripotency and establish lineage-specific patterns of gene expression (Hemberger et al., 2009). Work from a number of independent laboratories have demonstrated exposure to ethanol is associated with genome-wide / gene specific changes in DNA methylation, (Downing et al., 2011; Garro et al., 1991; Haycock, 2009; Liu et al., 2009; Ouko et

*Reprinted with permission from "Alcohol-induced epigenetic alterations to developmentally crucial genes regulating neural stemness and differentiation." By Veazey et al. 2013. *Alcoholism Clinical and Experimental Research*, 37, 1111-1122, Copyright [2013] by the Research Society on Alcoholism.

al., 2009; Zhou et al., 2011) alterations of post-translational histone modifications (KIM, 2005; Pal-Bhadra et al., 2007; Park, 2005), and a profound shift in epigenetically sensitive phenotypes (Kaminen-Ahola et al., 2010). Collectively, each of these observations indicate ethanol has the capacity to act as a powerful epigenetic disruptor and derail the coordinated processes of cellular differentiation. Understanding how ethanol impacts the epigenetic processes by which stem or progenitor cells maintain potency and execute lineage-specific programs of differentiation is fundamental to determining both the molecular mechanisms of alcohol induced teratogenesis and the developmental origins of fetal alcohol spectrum disorders (FASDs).

While several models of prenatal alcohol exposure have examined epigenetic alterations within the context of stem cell differentiation, it remains unclear whether progenitor cells are themselves sensitive to alcohol-induced epigenetic alterations or if the processes of differentiation sensitize cells for brief developmental periods. In studies using animal models, correlation of acute ethanol exposures with major periods of organ growth strongly indicate that different tissues are largely susceptible to ethanol-induced teratogenesis during specific developmental windows (Becker et al., 1996). These results would suggest progenitor cells are able to faithfully maintain chromatin structure, while the reorganization that occurs as cells differentiate creates an epigenetically labile period, where ethanol can perturb the developmental program. To begin to address this question, we sought to examine static cultures of neural stem cells for changes in key post-translational histone modifications within the regulatory regions of developmentally crucial genes. We find that alcohol profoundly alters the epigenetic landscape of neural stem cells, imparting a lasting signature of exposure. These alcohol-induced alterations of the epigenetic programs regulating fetal stem cell maintenance and differentiation are likely to have persistent, organizational effects upon subsequent neuronal maturation and potentially explain some of the pattering defects observed with the central nervous systems of FASD children.

Materials and Methods

Neurosphere Stem Cell Culture

All animal procedures were approved and conducted in accordance with the Institutional Animal Care and Use Committee at TAMHSC. Culture and media preparations for neurospheres have been described previously (Camarillo and Miranda, 2008). Briefly, fetal cerebral cortical neuroepithelial stem cells isolated from gestational day 12.5 C57BL/6 mice were cultured as neurospheres in T25 flasks in media containing GlutaMAX™ DMEM F-12 (Invitrogen, Carlsbad, CA. Cat# 11330-032), 20ng/ml FGF basic, 20ng/ml EGF (Invitrogen, Carlsbad, CA Cat# 53003-018), 0.15ng/ml LIF, 1x ITS-X (Invitrogen, Carlsbad, CA. Cat# 51500-056), 0.85 units/ml heparin, and 20nM progesterone (Sigma, St. Louis, MO. Cat#P6149). Neurospheres were typically incubated for a total of 5 days at 37°C, 5% CO_2 in a humidified environment before passage. Medium was changed every 2-3 days depending on the level of confluence.

Ethanol Treatment

Neurospheres were cultured in T25 flasks, with a parafilm (VWR) sealed lid to prevent ethanol evaporation. Dosing for ethanol followed previously published studies (Camarillo and Miranda, 2008), and utilized 60 mg/dL (13mM), 120 mg/dL (26mM), and 320 mg/dL (70mM) of ethanol (Sigma). Control samples for non-ethanol treated stem cells were concurrently cultured during the same experimental time course and in the same culture conditions. Neurospheres received fresh medium containing either control or ethanol treatments every 2-3 days. On day 5 of treatment, cells were isolated and cellular extracts collected for either Chromatin Immunoprecipitation or RNA analysis.

Chromatin Immunoprecipitation (ChIP) Analysis

Cultured neurospheres were grown to 80% confluence, washed twice in warm PBS, trypsinized then resuspended in warm growth medium containing 0.1 volume of crosslinking solution (Kondo et al., 2004). Subsequently, Chromatin

Immunoprecipitation (ChIP) reactions were performed as described previously (Golding et al., 2010), which was followed by DNA purification using a Qiagen PCR Cleanup kit. Antibodies used in the immunoprecipitation of modified histones and Ezh2 were anti-Rabbit IGG (Santa Cruz SC-2027), anti-Trimethyl Histone H3 Lysine 4 (Millipore 04-745), anti-Trimethyl Histone H3 Lysine 27 (Millipore 17-622), and anti-Ezh2 (Millipore 17-662). Antibodies for modified histones were used at 1 µg/ChIP reaction while antibodies to Ezh2 were used at 2 µg/ChIP reaction. The concentration of IgG was adjusted from 1 µg to 2 µg as appropriate. For these experiments, a minimum of 3 independent experimental replicates were conducted. Cellular extracts from each of these replicates were subjected to 3 independent chromatin immunoprecipitations for each of the post-translational histone modifications examined. DNA precipitated from these ChIP reactions were analyzed by qPCR and results normalized to 1% of the total input. Analysis of candidate promoter regions was carried out using the DyNAmo Flash SYBR Green qPCR Mastermix (Fisher Scientific, Pittsburgh PA. Cat # F-415L) following the manufacturer's instructions. Primers used to examine the relative enrichment of candidate gene promoter regions are described in Supplementary Table 1. Reactions were performed on either a StepOnePlus Real Time PCR system (Applied Biosystems, Foster City CA.) or a CFX384 Real Time System (BioRad Hercules CA).

RNA Isolation and Reverse Transcription

Cultured cells were grown to 80% confluence, washed twice in warm PBS, and dissociated with 1X trypsin (Accutase Millipore Cat# SCR005). Cells were spun down, washed once in cold PBS, and RNA isolated using Trizol (Invitrogen, Carlsbad, CA. Cat # 15596026) according to the manufacturer's protocol. 1 µg of purified total RNA was treated with amplification grade DNaseI (Sigma, St. Louis, MO. Cat# AMPD1) according to the manufacturer's protocol, and 250ng RNA seeded into a reverse transcription reaction using the SuperScriptII kit (Invitrogen, Carlsbad, CA. Cat# 18064-071) by combining 1 µl random hexamer oligonucleotides (Invitrogen, Carlsbad, CA. Cat# 48190011), 1 µl 10 mM dNTP (Invitrogen, Carlsbad,

CA. Cat# 18427-013), and 11 µl RNA plus water. This mixture was brought to 70°C for 5 minutes then cooled to room temperature. SuperScriptII reaction buffer, DTT, and SuperScriptII were then added according to manufacturer's protocol and the mixture was brought to 25°C for 5 minutes, 42°C for 50 minutes, 45°C for 20 minutes, 50°C for 15 minutes, then 70°C for five minutes.

Real-Time PCR Amplification of cDNA

Primers were designed using the NetPrimer software tool (www.premierbiosoft.com/netprimer) or identified from previously published research references (Supplemental Table S2). Real-time PCR analysis of mRNA levels was carried out using the DyNAmo Flash SYBR Green qPCR Mastermix (Fisher Scientific, Pittsburgh PA. Cat # F-415L) following the manufacturer's instructions. Reactions were performed on a StepOnePlus Real Time PCR system (Applied Biosystems, Foster City CA.) or a CFX384 Real Time System (BioRad Hercules CA).

Statistical Analysis of Real Time PCR - Expression and ChIP Data

For analysis of gene expression, the measured CT (Cycle Threshold) experimental values for each transcript were compiled and normalized to the geometric mean of the reference genes Phosphoglycerate kinase 1 (*Pgk1* - NM_008828), Glyceraldehyde 3-phosphate dehydrogenase (*Gapdh* - NM_008084), and Hypoxanthine-phosphoribosyl transferase (*Hprt* - NM_013556). From our previous studies of fourteen candidate reference genes in ethanol-exposed neurosphere cultures, *Pgk1*, *Gapdh* and *Hprt* were identified as being the most stable across all alcohol treatments (Vandesompele et al., 2002). Normalized expression levels were calculated using the ΔΔCT method described previously (Schmittgen and Livak, 2008). Values from these calculations were transferred into the statistical analysis program Graph Pad and an Analysis of Variance (ANOVA) run to assay differences between experimental treatments. For samples with p values greater than 0.05 we applied Tukey's HSD analysis for multiple comparisons and have marked statistically significant differences with the lower case letters.

Samples not connected by the same letter are significantly different. For quantitative analysis of candidate gene regulatory region enrichment, ChIP samples were normalized to 1% input, and data analyzed using the formula previously described (Mukhopadhyay et al., 2008). The cumulative mean from each of the 3 independent experiments were calculated and the standard error of the mean derived. The statistical analysis package Graph Pad was used to measure statistical significance between the % input for the control and ethanol treated samples using a paired student's *t*-test.

Results

Ethanol Alters the Promoter Regions of Key Neurogenic Regulators

Within the unique transcriptional environment of embryonic stem cells, several developmentally crucial genes are co-marked with both activating and repressive histone modifications (Bernstein et al., 2006; Lim et al., 2009; Pan et al., 2007). Specifically, histone 3 lysine 4 trimethylation, which is typically associated with gene activation, co-exists with the repressive trimethyl state of histone 3 lysine 27. These uniquely marked loci are termed bivalent domains and generally encode transcription factors directing tissue-specific programs of differentiation (Fisher and Fisher, 2011). This same unique signature is found, albeit less frequently, in neuronal and other tissue specific progenitor stem cell types (Lim et al., 2009). While these bivalently marked genes are generally not expressed, they are thought to be "primed" for either rapid activation or silencing during differentiation. As differentiation progresses, the regulatory regions of bivalent genes commit to one of these two post-translational modifications in a cell-lineage dependent manner and resolve their chromatin structure towards either an active or silent conformation. The correct resolution of these chromatin marks, and their faithful maintenance during differentiation is a fundamental element of normal histogenesis (Hemberger et al., 2009).

Given the reported impact ethanol has upon cellular differentiation, both *in vitro* and *in vivo*, we hypothesized that exposure to alcohol would disrupt the

distribution of these two vital post-translational histone marks. To address this question, primary neurosphere cultures were maintained under conditions promoting the stem cell state and treated with 320 mg/dL (70mM) ethanol for five days. This concentration of alcohol is representative of the blood alcohol levels obtainable in episodic binge drinking and chronic alcoholics (Centers for Disease Control and Prevention (CDC), 2004; White et al., 2006). Control and ethanol treated cellular extracts were immunoprecipitated with antibodies recognizing the specific chromatin modifications trimethylated histone 3 lysine 4 (H3K4 Me3) and trimethylated histone 3 lysine 27 (H3K27 Me3) using methods previously utilized by our lab (Golding et al., 2010). To assess alcohol-induced changes in chromatin structure, DNA fragments isolated from these chromatin immunoprecipitations were examined by quantitative PCR. qPCR reactions were carried out measuring the relative enrichment of candidate gene promoter regions relative to 1% of the total input. We began by examining the promoter regions of eight genes with established roles regulating neural stem cell biology (Kuegler et al., 2010; Zhou et al., 2011). As can be seen in Fig. 1a, all of our candidate genes exhibited significant changes in at least one of the post-translational marks examined, while two (*Igf1* and *Smarca2*) displayed changes in both. It is worth noting that a recent study examining alterations in DNA methylation within a similar neural stem cell model also identified these two candidates (Zhou et al., 2011). We next sought to determine the impact of ethanol upon the chromatin state of key genes regulating neuronal patterning. *Homeobox* genes operate at the hub of multiple growth factor signaling pathways controlling neurogenesis and therefore represent excellent candidates to examine in relation to the patterning defects seen in FASD studies. As can be seen in Fig. 1b, *Dlx2*, *Dlx5*, *HoxA1*, *HoxA7*, *Msx1*, *Msx2*, *Nanog*, *Nkx2.1*, *Nkx2.2* and *Pax6* all displayed alterations in at least one of the post-translational marks examined while *Dlx1* and *Dlx3* did not display any statistically significant changes ($p < 0.05$).

Ethanol Disrupts the Bivalent State

Interestingly, within our neurosphere stem cells *Dlx2* and *Nkx2.2* were equally marked by both histone 3 lysine 4 and histone 3 lysine 27 trimethylation and thus

appeared to have retained an ES-cell like bivalent signature. Given the importance of this chromatin state to subsequent differentiation, and its alteration upon exposure to ethanol, we next set out to determine if other bivalent genes were present in neural stem cells and became modified upon exposure to alcohol. To this end, we examined ten other candidate bivalent genes identified in ES cells (Rugg-Gunn et al., 2010). Of these, the *Vdr* promoter was the only other region to retain a bivalent signature within our neurosphere cultures, and it too exhibited significant changes in chromatin structure, namely a loss in H3K4 Me3 ($p = 0.0057$) (Fig. 1c). The chromatin status of an intergenic region of chromosome six was utilized as a negative control.

The Effect of Ethanol on Gene Transcription

To determine if the observed alterations in chromatin structure were accompanied by changes in gene expression, we collected RNA from ethanol exposed neurosphere stem cells and examined the mRNA levels of our candidate genes relative to the geometric mean of *Gapdh*, *Hprt1,* and *Pgk1* transcript levels. For these experiments, ethanol dosing followed previously published studies (Camarillo and Miranda, 2008), and utilized 60 mg/dL (13mM), 120 mg/dL (26mM), and 320 mg/dL (70mM) of ethanol. We began by examining the relative mRNA levels of six established neural markers. *Fabp7*, *Nestin*, and *Tuj1* were abundantly expressed within our neurosphere cultures while transcripts encoding *Gfap*, *Gli3*, and *Olig2* were detected at residual levels. Of these six, mRNAs encoding *Fabp7*, *Gfap*, *Nestin*, and *Olig2* all demonstrated significant changes for at least one of the exposure levels tested (Fig. 2a). We next examined the relative mRNA levels of candidate genes identified in Fig. 1. Of the twenty-one candidate genes examined in figure 1, only six were expressed within our neurosphere stem cells. Interestingly, while *Nkx2.2*, *Smarca2*, *Sox2* and *Vdr* all exhibited significant changes in chromatin structure, none of these candidates demonstrated detectable alterations in mRNA transcript levels (Fig. 2b). In contrast, *Dlx2* and *Pax6* both displayed significant differences in mRNA levels relative to the control ($p = 0.015$ and $p = 0.02$). Of note,

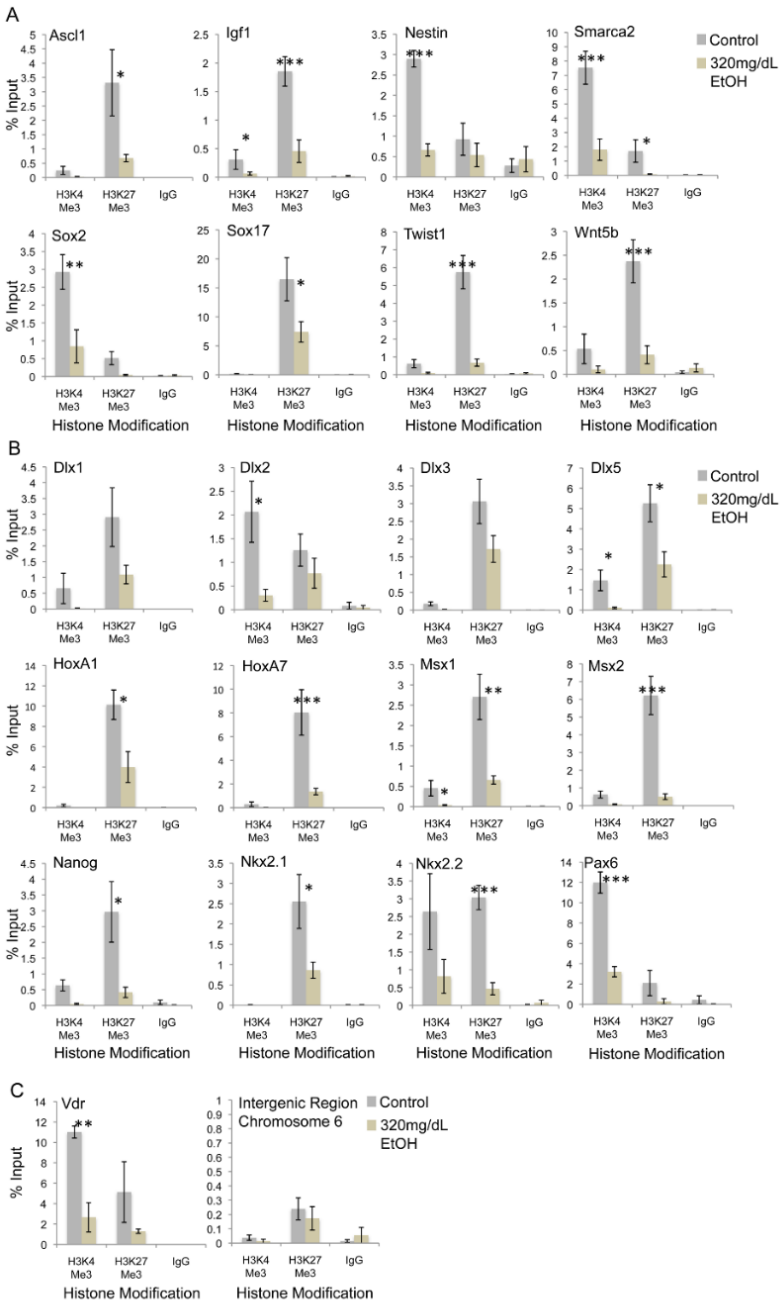

Figure 10: Alterations in Histone 3 Lysine 4 and Lysine 27 Trimethylation within ethanol exposed neurosphere stem cells. Levels in the relative enrichment of Histone 3 Lysine 4 Trimethylation (H3K4 Me3) and Histone 3 Lysine 27 Trimethylation (H3K27 Me3) were measure by ChIP for (A) eight candidates with established roles regulating neural stem cell biology (B) select homeobox genes with known roles regulating neural patterning and (C) a newly identified neurosphere stem cell bivalent domain. Neurosphere stem cells were treated with 320mg/dL ethanol for five days and extracts examined as outlined in the materials and methods. Statistical significance as measured using a paired students *t*-test at $p < 0.05$ is designated by a single *, $p < 0.01$ by two (**), and $p < 0.001$ by three (***). For these experiments, four independent cell culture experiments were conducted (N = 4). For each sample, background levels are represented by the IgG control. As a negative control, primers were used to examine the enrichment of an intergenic region of chromosome 6, which displayed minimal enrichment of H3K4 Me3 and H3K27 Me3.

a similar degree of *Pax6* mRNA repression was recently reported in a human radial glia progenitor cell model of ethanol exposure (Mo et al., 2012). Collectively, these results indicate that while select candidates display altered levels of gene expression, the transcriptional control of many genes remains unperturbed despite changes in the distribution of H3K4 Me3 and H3K27 Me3 within their regulatory regions.

Ethanol Alters Global Histone 3 Lysine 27 Trimethylation

To help determine if the chromatin alterations observed in Fig. 1 were gene specific or reflective of larger, genome-wide changes to the epigenome, we next sought to examine the chromatin status and expression of transposable elements. Mammalian genomes contain large amounts of parasitic nucleic acids that originate from retrotransposons and retroviruses that invaded the ancestral germline (Mandal and Kazazian, 2008). While protein coding genes represent a little less than 2% of our genetic information, as much as 45% of mammalian genomes are composed of endogenous retro-elements, making them excellent candidates to examine as an assessment of global alterations to the histone code. While transposable elements and protein coding genes are clearly regulated through distinct biochemical pathways, their overall abundance makes them suitable for use as an estimator of the genomic condition. Using control and 320mg/dL treatments outlined above, we immunoprecipitated cellular extracts with antibodies recognizing H3K4 Me3 and H3K27 Me3 and seeded precipitated DNA fragments into qPCR assays measuring enrichment of the *Long Interspersed Nuclear Element 1* (*LINE1*), *Intra-cisternal A particle* (*IAP*), *Mus D*, and *Etn* families of transposable elements. Each of these families have 660,000, 1300, 100 and 240 respective copies per haploid genome (, 1997; Mandal and Kazazian, 2008). These experiments revealed significant declines in the levels of H3K27 Me3 for all transposable element families examined, suggesting the global distribution of this mark had become altered as a consequence of *in vitro* ethanol exposure (Fig. 3a). Given the observed role of Polycomb group complexes and by proxy, H3K27 Me3 in maintaining the repressed state of transposable elements (Golding et al., 2010) we had anticipated a reduction

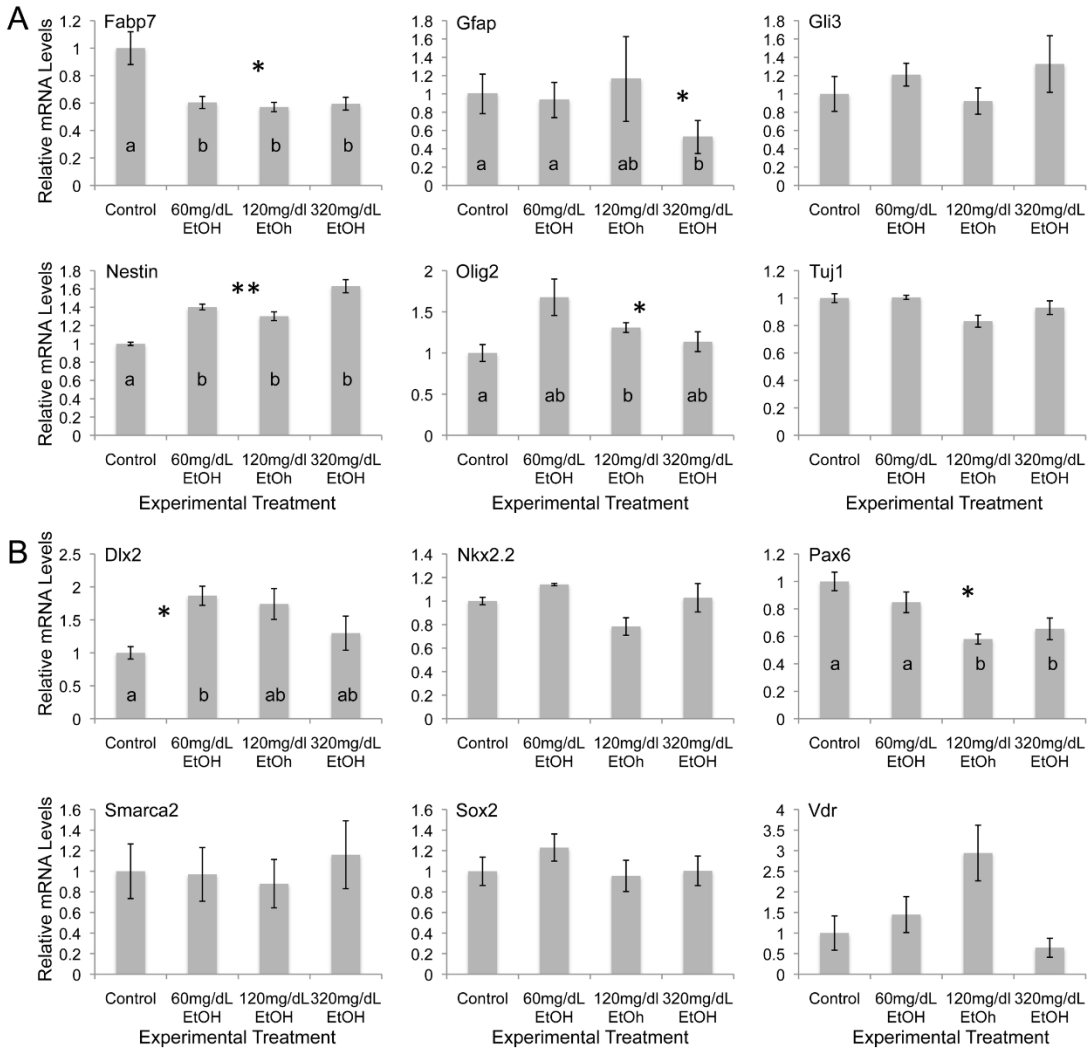

Figure 11: mRNA expression levels of candidate genes in ethanol exposed neurosphere stem cells exposed to control, 60mg/dL, 120mg/dL and 320mg/dL experimental treatments for five days. Quantitative RT-PCR measurements of mRNAs encoding (A) six candidate markers of various neural cell types and (B) six candidates from Fig. 1 were measured against the geometric mean of mean of *Gapdh*, *Hprt1* and *Pgk1* and graphed using the ΔΔCT method (Schmittgen, & Livak 2008). Although detectable, transcripts encoding *Vdr* were expressed at extremely low levels and exhibited wide variation. Graphs are representative of at least three independent cell culture experiments (N = 3). Statistical significance using ANOVA at $p < 0.05$ is designated by a single * and $p < 0.01$ by two (**). Results of Tukey's HSD analysis are represented by lower case letters. Samples not connected by the same letter are significantly different.

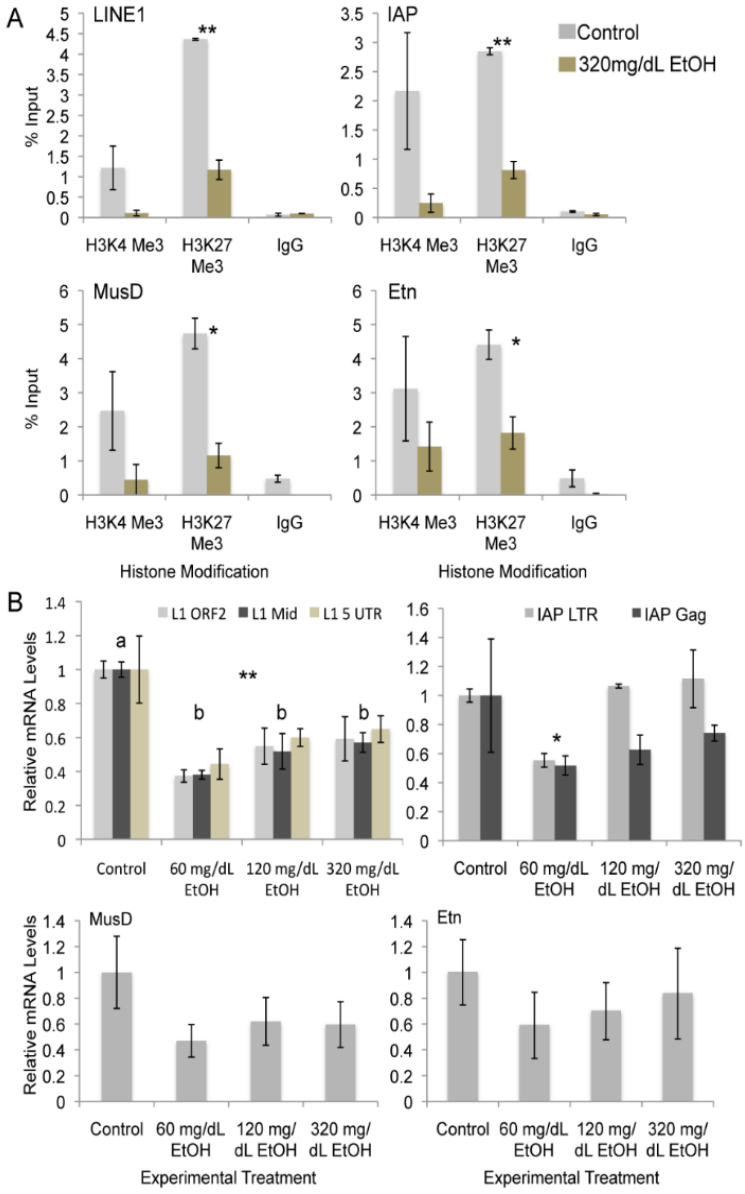

Figure 12: Analysis of the chromatin structure and transcriptional control of four families of transposable elements. (A) ChIP analysis of the *LINE1*, *IAP*, *MusD* and *EtN* families of transposable elements. Statistical significance as measured using a paired students *t*-test at $p < 0.05$ is designated by a single * and $p < 0.01$ by two (**). For these experiments, three independent cell culture experiments were conducted (N = 3). (B) Quantitative RT-PCR measurements of transcripts encoding the *LINE1*, *IAP*, *MusD* and *Etn* transposable elements in neurosphere stem cells exposed to control, 60mg/dL, 120mg/dL and 320mg/dL experimental treatments for five days. Measured CT values were normalized against the geometric mean of mean of *Gapdh*, *Hprt1* and *Pgk1.* Three independent primer sets measuring the second open reading frame (L1 ORF2), mid region (L1 Mid), and 5' untranslated region (L1 5 UTR) of the LINE1 transcript were used. For the IAP transposable element two independent primers measuring the viral long terminal repeat (IAP LTR) and Gag (IAP Gag) coding region were used. Graphs are representative of at least three independent cell culture experiments (N = 3) . Statistical significance using ANOVA at $p < 0.05$ is designated by a single * and $p < 0.01$ by two (**). Results of Tukey's HSD analysis are represented by lower case letters. Samples not connected by the same letter are significantly different.

in this mark would be correlated with a proportional increase in *LINE1*, *IAP*, *MusD* and *Etn* transcription. Surprisingly, only the *LINE1* family and 60mg/dL *IAP* group displayed statistically significant changes (*p = 0.001* and *p = 0.002* respectively) and transcript levels for both of these transposable elements were decreased (Fig 3b). For the *LINE1* family, we verified our observations using three independent primer sets measuring multiple regions of the *LINE1* transcript.

Expression of Epigenetic Modifying Enzymes in Alcohol Treated Neurospheres

To pursue a potential mechanistic basis for the observed epigenetic alterations, we again collected RNA from ethanol exposed neurosphere stem cells and examined the mRNA levels of transcripts encoding several of the most prominently studied epigenetic modifying enzymes. Cells were exposed to control, 60 mg/dL, 120 mg/dL, and 320 mg/dL experimental treatments and

mRNA levels normalized to the geometric mean of *Gapdh*, *Hprt1* and *Pgk1* as above. Of the thirty candidates evaluated (including Smarca2 in Fig 2b.) only *Dnmt1*, *Uhrf1*, *Ash2l*, *Wdr5*, *Ehmt1* and *Kdm1b* exhibited statistically significant changes (Fig. 4). *Dnmt1*, *Uhrf1* and *Ehmt1* are important components of the molecular machinery regulating genomic DNA methylation (*Dnmt1* and *Uhrf1*) and trimethylation of histone 3 lysine 9 (*Ehmt1)* (Sharif et al., 2007). Interestingly, all three demonstrate increased mRNA levels within ethanol-exposed cultures, consistent with the hyper-suppressed state of the *LINE1* transposable elements (Fig. 3b) (Meissner et al., 2008; Mikkelsen et al., 2007; Yoder et al., 1997). *Ash2l*, *Wdr5* and *Kdm1b* all serve to regulate H3K4 Me3 and display mixed changes in relative expression. Unexpectedly, our results indicate that the Polycomb Repressive Complex 2 (PRC2) members *Eed* and *Ezh2* did not demonstrate statistically significant changes in expression. This was surprising given the unique role of this enzyme complex in establishing and maintaining the repressive H3K27 Me3 mark.

Polycomb Complex Localization and Altered noncoding RNA Levels in Alcohol Treated Neurospheres

In an effort to help explain the dramatic alterations in H3K27 Me3 levels, we next set out to examine PRC2 localization within ethanol exposed neurosphere stem cells. As mammalian genomes are devoid of canonical *Polycomb* DNA binding elements, we began our investigations by looking at noncoding RNAs, which are hypothesized to regulate PRC2 recruitment. Work over the past decade has revealed the transcriptomes of eukaryotic cells are far more complex than was originally postulated. The noncoding compliment of the genome vastly outsizes the protein-coding and includes transcripts of well-defined function, as well as those to whose function we can only speculate (Guttman et al., 2011).Studies of long intergenic noncoding RNAs have indicated this class of transcripts plays a fundamental role in shaping the fetal epigenome by directing PRC2 localization during stem cell maintenance and differentiation (Guttman et al., 2011). Studies by Guttman and colleagues recently identified several noncoding RNAs in ES cells, which based upon the genes they regulate, were postulated to have roles in regulating neural stem cell differentiation (Guttman et al., 2011). We therefore sought to examine the impact of ethanol exposure upon these noncoding transcripts. Of the eight candidate neural stem cell differentiation-associated noncoding RNAs tested, only linc1354 was detected within our neurosphere stem cell model (Fig.5a). To examine the impact of ethanol exposure we again utilized control, 60 mg/dL, 120 mg/dL, and 320 mg/dL experimental treatments and normalized linc1354 RNA levels to the geometric mean of *Gapdh*, *Hprt1* and *Pgk1* measurements. As can be seen in Fig. 5b, ethanol induced a significant reduction in linc1354 levels across all ethanol concentrations tested ($p = 0.0022$). Given the previously characterized association between noncoding RNAs and PRC2 proteins, as well as the role dynamic changes in *PRC2* localization play during neural development, we next chose to examine *EZH2* occupancy within the regulatory regions of the candidate genes studied in Fig. 1 (Rinn et al., 2007). From these twenty-one candidate genes, only nine were bound by *EZH2* and with the exception of *Dlx1* ($p = 0.0256$), none demonstrated significant differences in enrichment relative to the untreated control

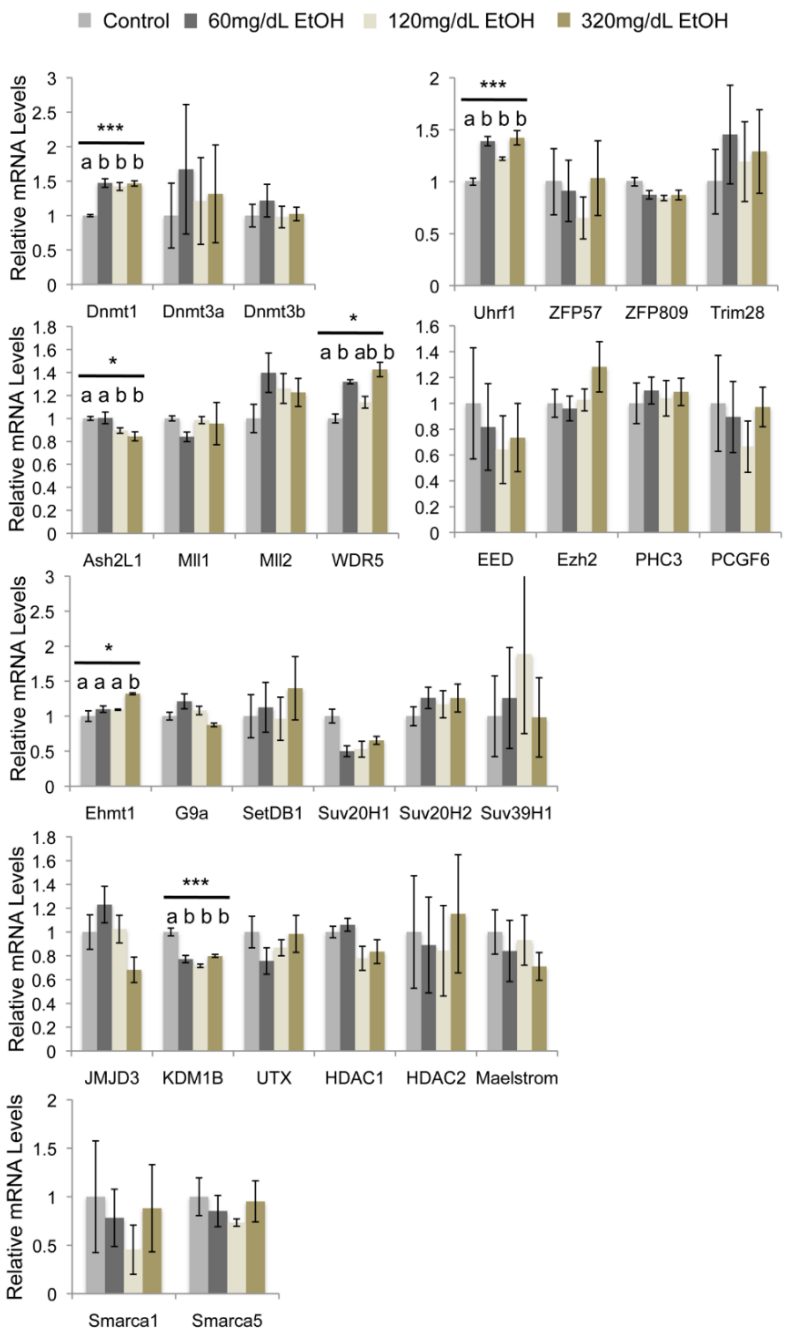

Figure 13: Expression of epigenetic modifying enzymes in alcohol treated neurospheres. Quantitative RT-PCR measurements of transcripts encoding several of the most prominently studied epigenetic modifying enzymes in neurosphere stem cells exposed to control, 60mg/dL, 120mg/dL and 320mg/dL experimental treatments for five days. Measured CT values were normalized against the geometric mean of mean of *Gapdh*, *Hprt1* and *Pgk1* and graphed using the ΔΔCT method (Schmittgen, & Livak 2008). Graphs are representative of at least three independent cell culture experiments (N = 3). Statistical significance using ANOVA at $p < 0.05$ is designated by a single * and $p < 0.01$ by two (**). Results of Tukey's HSD analysis are represented by lower case letters. Samples not connected by the same letter are significantly different.

(Fig. 5c). No enrichment of EZH2 was observed using primers amplifying the negative control, intergenic region of chromosome 6 (data not shown).

Discussion

In this study we sought to examine whether primary neurospheres cultured under conditions maintaining stemness were sensitive to alcohol induced alterations of the histone code. We focused on trimethylated histone 3 lysine 4 and trimethylated histone 3 lysine 27, as these are two of the most prominent post-translational histone modifications regulating stem cell maintenance and neural differentiation (Bernstein et al., 2006; Lim et al., 2009; Pan et al., 2007). We find that the regulatory regions of a number of genes controlling both precursor cell identity and neural differentiation exhibited significant alterations in the enrichment of these chromatin marks. Our results clearly indicate primary neurospheres maintained as stem cells *in vitro* are not refractory to alcohol induced perturbation of the histone code, and that maintained stem cells as well as differentiating neurospheres (Zhou et al., 2011) are susceptible to errors in the epigenetic program.

Alterations of Bivalent Genes

Within many tissue precursor cell types, bivalent genes are maintained in a poised confirmation and hypothesized to hold a maturation “tipping point” between formation of a specific cellular lineage and the closing off of a developmental pathway. Our studies identify three novel bivalent genes within cultured neurospheres and of these, two demonstrate significant loss of H3K4 Me3 (Fig. 1). Our studies also identified changes in H3K27 Me3 within the regulatory region of *Nkx2.2*, indicating the two marks examined are not uniformly affected. These results suggest that alcohol may impact cellular differentiation by disrupting the ability of precursor cells to activate and repress key genes in a developmentally appropriate manner. As a consequence, precursor cells would not be able to uniformly exit the stem cell state and initiate developmental patterning. Extending our *in vitro* observations into a clinical setting, postmortem and magnetic resonance imaging-

A

Non-coding RNA	Detected Neurosphere	Detected ES Cells
hotair	No	Yes
linc1471	No	Yes
linc1230	No	Yes
linc1354	Yes	Yes
linc1281	No	Yes
linc1418	No	Yes
linc1456	No	Yes
mistral	No	Yes

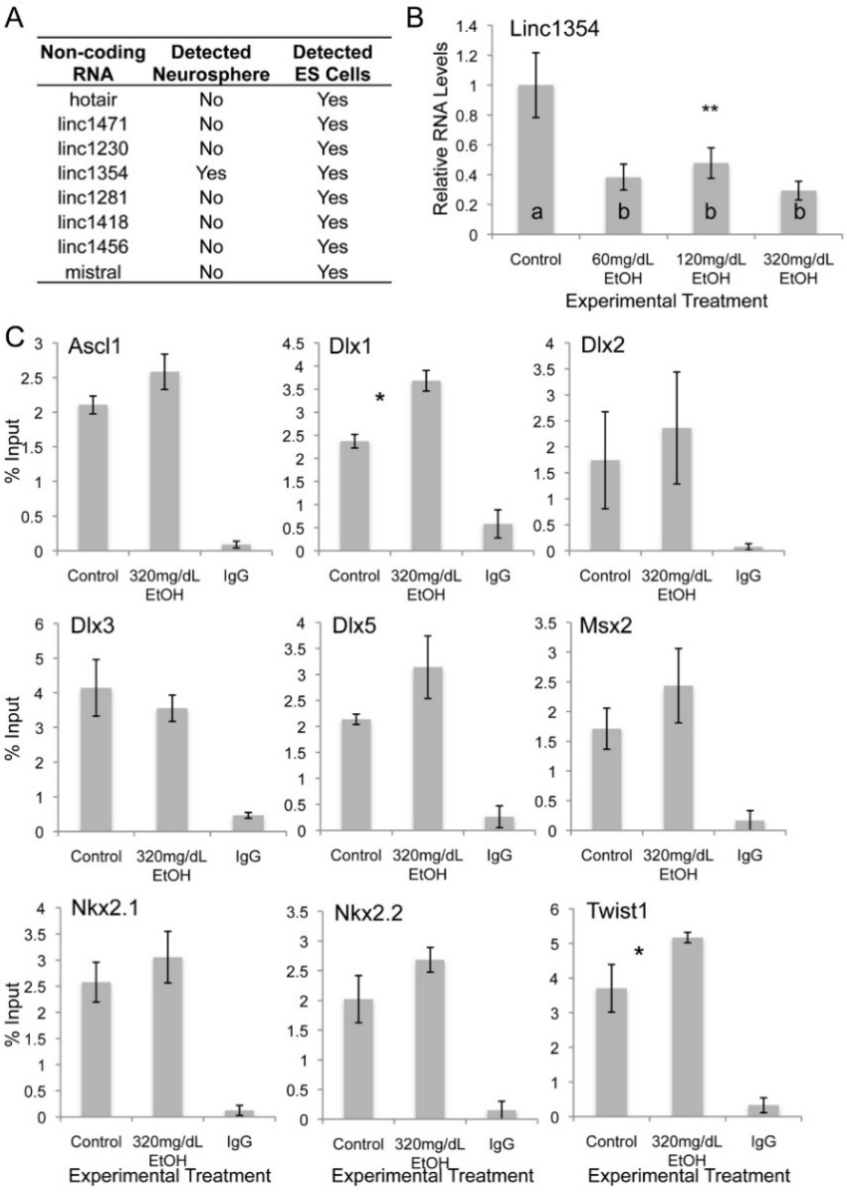

Figure 14: Polycomb complex localization and altered noncoding RNA levels in alcohol treated neurospheres. (A) Noncoding RNAs examined in our neural stem cell model. Using RT-PCR, all noncoding RNAs were detected within RNA extracts prepared from ES cells but only linc1354 was detected in primary neurospheres (N=3). (B) Quantitative RT-PCR measurements of linc1354 RNA levels in neurosphere stem cells exposed to control, 60mg/dL, 120mg/dL and 320mg/dL experimental treatments for five days. Measured CT values were normalized against the geometric mean of mean of *Gapdh*, *Hprt1* and *Pgk1* and graphed using the ΔΔCT method (Schmittgen, & Livak 2008). Using ANOVA the calculated P value was 0.0022. Results of Tukey's HSD analysis are represented by lower case letters. Samples not connected by the same letter are significantly different. Graphs are representative of at least three independent cell culture experiments (N = 3). (C) ChIP analysis of candidate promoters examining enrichment of the *Polycomb Repressive Complex 2* methyltransferase EZH2. Neurosphere stem cells were treated with 320mg/dL ethanol for five days and extracts examined as outlined in the materials and methods. For these experiments, three independent cell culture experiments were conducted (N = 3).. The statistical significance of Dlx1 measurements using a paired students *t*-test was *p = 0.0256.*

based studies examining the brains of Fetal Alcohol Syndrome children have revealed ectopic, nodular accumulations of poorly differentiated neuronal and glial cells called heterotopias (Jones and Smith, 1975; Swayze et al., 1997). These abnormal structures are consistent with cortical dysplasia and are suggestive that alcohol may induce a persistent destabilization of neuronal differentiation. Whether cortical dysplasia is associated with altered levels of H3K4 Me3 and H3K27 Me3 is currently under investigation.

Alcohol Induced Epigenetic Changes and Transcription

It is interesting to note that while the majority of candidate regulatory regions examined in this study displayed significant changes in levels of H3K4 Me3 and / or H3K27 Me3, the transcription of very few of the genes examined were altered upon exposure to ethanol. A recent study by Hashimoto-Torii and colleagues examining global changes in gene transcription within ethanol-exposed cerebral cortices reported a similar observation, in that only 636 transcripts out of 39,000 examined were differentially expressed (268 up regulated and 368 down) (Hashimoto-Torii et al., 2011). In our study, twelve of the twenty one candidate genes exhibited alcohol induced reductions in the repressive H3K27 Me3 mark, yet none of these candidates demonstrated an increase in expression or became activated *de novo* in exposed cells. Unexpectedly, this drop in H3K27 Me3 levels was not associated with any dramatic changes in EZH2 localization. Of the differentially expressed genes identified, both *Nestin* and *Dlx2* displayed significant declines in the activating H3K4 Me3 mark, yet transcripts encoding these genes went up. Of all the candidates studied, only *Pax6* demonstrated both reduced H3K4 Me3 levels within its regulatory region and a correlative drop in mRNA levels. These observations raise more questions as to the functional nature of the epigenetic changes resulting from ethanol exposure and suggest other post-translational histone modifications may have shifted to compensate for the loss of H3K4 and H3K27 trimethylation. While our data indicate the trimethyl state of H3K4 and H3K27 are affected, we have yet to address alterations in nucleosome positioning, polymerase II occupancy and changes to the mono and dimethylated states of these positions. Previous studies

examining alcohol-exposed primary rat hepatocytes demonstrated an increase in H3K4 dimethylation (Pal-Bhadra et al., 2007). These observations suggest the trimethyl mark may be preferentially lost in favor of increasing the dimethyl state. Each of these questions will be the subject of future investigations and will work towards determining if the observed epigenetic changes are a coordinated response to alcohol teratogenesis or the byproduct of a generalized cellular response to stress.

In an effort to distinguish gene-specific epigenetic alterations from global changes, we examined select aspects of transposable element biology within alcohol treated neurospheres. Our data reveal global levels of the repressive H3K27 Me3 mark were depressed, yet the expression of the largest family of transposable elements, the *LINE1* family, exhibited a ~50% decrease in measured transcripts as compared to the control. This was surprising given the established role of H3K27 Me3 in suppressing transposable elements (Leeb et al., 2010). It is possible that alcohol exposed cells compensate for the loss of H3K27 Me3 by up-regulating *Dnmt1* and *Uhrf1* expression and increasing genomic methylation levels, which has been observed previously (Kaminen-Ahola et al., 2010). Similar disruptions in the epigenetic regulation of *LINE1* elements have been observed in the brains of chronic alcoholics (Ponomarev et al., 2012). Given the hypothesized role of *LINE1* elements in promoting somatic mosaicism, suppressed *LINE1* transcription may have a detrimental impact upon neural diversification and higher brain function (Muotri et al., 2005). This large-scale alteration in the developmental program regulating neurogenesis will likely lead to a myriad of central nervous system developmental pathways being affected.

Altered Epigenetic Programming and FASDs

While this study focused on the impacts of alcohol within a neuronal stem cell model of exposure, it is likely that other precursor cell types and developmental programs, including those executing formation of the skeletal system will exhibit similar alterations in epigenetic programming. Of the candidate genes examined in

this study *Msx2*, and *Nkx2.1* have previously been associated with FASD birth defects (Godin et al., 2011; Rifas et al., 1997). Of note, *Ascl1* and *Twist1* regulate neural patterning and craniofacial development respectively and both of their promoter regions were altered by exposure to ethanol (Chen and Behringer, 1995; Guillemot et al., 1993). These data indicate that alcohol significantly impacts epigenetic processes regulating genes controlling neural patterning and facial development. Our observations indicate alterations to chromatin structure may represent a crucial component of alcohol teratogenesis and move towards better understanding the developmental origins of FASDs.

CHAPTER V
DOSE DEPENDENT ALCOHOL-INDUCED ALTERATIONS IN CHROMATIN STRUCTURE PERSIST BEYOND THE WINDOW OF EXPOSURE AND CORRELATE WITH FAS BIRTH DEFECTS*

Background

From studies using a diverse range of model organisms, we now acknowledge that epigenetic modifications to chromatin structure provide a plausible link between environmental exposures and alterations in cellular function leading to pathology (Feil and Fraga, 2011). These revelations create novel perspectives in our understanding of fetal development that must be investigated if we are to fully understand the molecular origins of birth defects. However, for many teratogens the link between exposure and altered epigenetic programming remains poorly defined.

Alcohol consumption during pregnancy is widespread in our society despite its proven association with the development of birth defects and severe mental impairment. Work from a number of independent research groups have demonstrated that ethanol (EtOH) has the capacity to alter chromatin structure, which suggests that epigenetic mechanisms may be relevant to the genesis of birth defects associated with fetal alcohol spectrum disorders (FASDs) (Mead and Sarkar, 2014; Resendiz et al., 2014; Ungerer et al., 2013). For example, studies examining tissue samples derived from both humans and rodents chronically exposed to alcohol have shown alterations in the levels of both the DNA methylating enzyme DNA methyltransferase 1 (Dnmt1) and DNA methylation within the regulatory regions of multiple genes, including those regulated though genomic imprinting (Garro et al., 1991; Bielawski et al., 2002; Kaminen-Ahola et al., 2010; Zhou et al., 2011; Knezovich and Ramsay, 2012). In addition, multiple *in vitro* studies have revealed alterations in post-translational histone modifications arising

*Reprinted with permission from "Dose dependent alcohol-induced alterations in chromatin structure persist beyond the window of exposure and correlate with FAS birth defects." By Veazey et al. 2015. *Epigenetics and Chromatin*, 8, Copyright [2015] by Veazey et al.

as a consequence of ethanol exposure (Veazey et al., 2013; Pal-Bhadra et al., 2007; Bekdash et al., 2013; Moonat et al., 2013; Pan et al., 2014). However, important questions as to the lasting heritability, the mechanism of induction, and the role these epigenetic errors have in the development of FASD-associated congenital malformations remain to be resolved.

In adults, alcohol is converted to acetaldehyde in an oxidation reaction that occurs primarily in the liver, and is driven by the enzymes alcohol dehydrogenase (ADH), cytochrome P450 (CYP2E1), and catalase. Even under normal physiologic conditions, this process produces excess acetaldehyde, reactive oxygen species (ROS) and other harmful adducts inducing oxidative stress (Brocardo et al., 2011). Due to the free passage of alcohol from mother to fetus, and the constant recycling of the amniotic fluid reservoir, fetal alcohol exposures achieve blood alcohol concentrations equivalent to the mother's, but of longer durations (Pikkarainen, 1971; Waltman and Iniquez, 1972; Brien et al., 1983). These longer exposures produce significant levels of ROS and free radicals, which have been hypothesized to be a significant factor in the teratogenic effects of alcohol (Brzezinski et al., 1999; Brocardo et al., 2011; Zakhari, 2013). Recently, a link between oxidative stress and the enzymes regulating chromatin structure has been identified (Chia et al., 2011). These observations would suggest that some of the epigenetic changes induced by alcohol may be linked to alterations in the activities of genes responding to ROS (Brocardo et al., 2011; Zakhari, 2013). However, no study has yet directly examined interactions between alcohol exposures, oxidative stress and chromatin structure.

To date, the large majority of studies examining epigenetic changes arising from fetal alcohol exposures have employed either chronic models of constant exposure or examinations of acute alterations in chromatin structure (Garro et al., 1991; Garro et al., 1992; Bielawski et al., 2002; Halsted et al., 2002; Haycock and Ramsay, 2009; Ouko et al., 2009; Liu et al., 2009; Zhou et al., 2011; Downing et al., 2011; KIM, 2005; Park, 2005; Pal-Bhadra et al., 2007; Kaminen-Ahola et al., 2010; Veazey et al., 2013; Bekdash et al., 2013). Very few of these studies have sought to investigate the lasting heritability of EtOH-induced changes in chromatin structure

arising from an acute encounter through development. This is significant as while there is ample evidence that chromatin structure can be perturbed by external factors, significant questions remain as to whether post-translational histone modifications are heritable, and can possibly contribute to environmentally induced phenotypes (Henikoff and Shilatifard, 2011). Are EtOH-induced alterations in histone modifications causal in FASD phenotypes, or are they merely transient differences between chromatin states induced by transcriptional / nucleosome remodeling responses to alcohol?

Using an ex vivo mouse model for fetal neural stem cells, our laboratory has shown dramatic reductions in Histone 3 lysine 27 trimethylation (H3K27me3) in response to acute EtOH exposure, but no correlative alterations in the localization of the histone methyltransferase EZH2 were observed (Veazey et al., 2013). Current models of epigenetic inheritance suggest that during S-phase, chromatin modifying enzymes re-establish the histone code on newly assembled unmethylated histones, and therefore enzyme complexes, like the *Polycomb* group, represent the true locus-specific epigenetic mark passed from one generation to the next (Petruk et al., 2012). These observations therefore call into question the heritability of alcohol-induced epigenetic alterations, and their capacity to contribute to fetal alcohol syndrome (FAS) phenotypes. This is especially significant as chromatin modifications induced by exposures to other drugs of abuse tend to be transient, and revert back to control states within hours or days after the toxicant is removed (Nestler, 2014).

In this study, we sought to examine two major questions: 1) are the epigenetic modifications induced by alcohol associated with a mobilization of epigenetic modifying genes downstream of the oxidative stress pathways, and 2) do alcohol-induced changes in chromatin structure persist beyond the window of exposure? We report multiple post-translational histone modifications display unique, dose-dependent responses to EtOH exposure, and in many cases, the epigenetic signatures arising after an acute exposure differ from those observed after a recovery period. These changes in chromatin structure are associated with

persistent alterations in transcripts encoding *Dnmt1*, *Ehmt2* (*G9a*), *Eed*, *Ezh2*, *Kdm1a*, *Kdm4c, Setdb1*, *Sod3, Tet1* and *Uhrf1*. Transitioning into an *in vivo* model, we observe that mice displaying craniofacial malformations and midline brain defects arising from an acute, early gestational exposure also display epigenetic errors, and that these signatures of change are consistent with those modeled *in vitro* after a recovery period. Our results indicate that the immediate and long-term impacts of EtOH exposure on chromatin structure are distinct and suggest the existence of a coordinated cellular response to exposure. Importantly, an epigenetic signature resulting from an acute gestational encounter persists beyond the window of exposure, and strongly correlates with the appearance of congenital malformations.

Results

Acute and Post-Recovery Epigenetic Signatures of EtOH Exposure Display Distinct, Dose-Dependent Profiles

We sought to model the capacity of primary fetal cerebral cortical neuroepithelial stem cells to restore alcohol-induced alterations in chromatin structure. To this end, we initiated a treatment protocol wherein cells were maintained in the stem cell state and exposed to varying concentrations of EtOH for three days; then allowed to progress through a four day recovery period representing at least three population doublings. The concentrations of alcohol utilized in this study were meant to mimic those obtained from a binge drinker. We utilized projected concentrations based on observations by White *et al*., which demonstrated that out of 7,356 college age females surveyed, 33.7% reported typical consumption rates at 1 x binge alcohol levels (four or more drinks at a time) and 8.2% reported consumption at 2 x binge levels (eight or more drinks at a time) (White et al., 2006). Based on average height and weight, these rates of consumption would yield blood alcohol levels in the range of 160mg/dL and 240 mg/dL respectively (Blood Alcohol Content - www.dot.wisconsin.gov).

To measure the impact of EtOH exposure and withdrawal on chromatin structure, control and alcohol-treated cellular extracts were immunoprecipitated with

antibodies recognizing the specific chromatin modifications trimethylated histone 3 lysine 4 (H3K4 me3), trimethylated histone 3 lysine 27 (H3K27 me3), acetylated histone 3 lysine 9 (H3K9 ac) and dimethylated histone 3 lysine 9 (H3K9 me2) using methods previously utilized by our laboratory (Golding et al., 2010). Alterations of these histone post-translational modifications have been observed in previous studies of acute alcohol exposure, but their capacity to restore over time has not been investigated (Veazey et al., 2013; Pal-Bhadra et al., 2007; Bekdash et al., 2013; Moonat et al., 2013; Pan et al., 2014). To examine gene-specific alcohol-induced changes in chromatin structure, DNA fragments isolated from these precipitations were examined by qPCR relative to 1% of the total input. Using primers homologous to sequences +/- 250 base pairs of the transcriptional start sites, we assessed alterations in chromatin structure occurring within the regulatory regions of 22 genes randomly distributed across the genome that are involved in controlling multiple growth factor signaling pathways directing neuronal patterning. Importantly, we and others have identified altered transcriptional control and aberrant localization of transcripts encoding many of these genes in FASD mouse models, thus making them suitable candidates for the current study (Rifas et al., 1997; Wentzel and Eriksson, 2009; Godin et al., 2011; Zhou et al., 2011).

The comprehensive results of these independent analyses are presented as a heat map in Figure 1, with the statistical significance demarcated in each cell. Analysis of individual candidate genes may be viewed in Additional file 1. For the post-translational marks examined, we observed a range of alterations on the order of 45% reductions to more than 200% increases. These scales of change are similar to those reported in experiments utilizing either over-expression or RNA interference mediated suppression of key epigenetic modifiers (EHMT1/G9a and *Polycomb Repressive Complex 2(PRC2))* (Mozzetta et al., 2014; Landeira et al., 2010; Li et al., 2010; Mejetta et al., 2011). Collectively, these experiments produced five novel observations. First, the examined histone post-translational modifications were not equally impacted by alcohol exposure. Broadly, the candidate genes examined displayed modest alterations in H3K4 me3, more pronounced changes in H3K27 me3 and H3K9 ac, and profound shifts in H3K9 me2 across all treatment

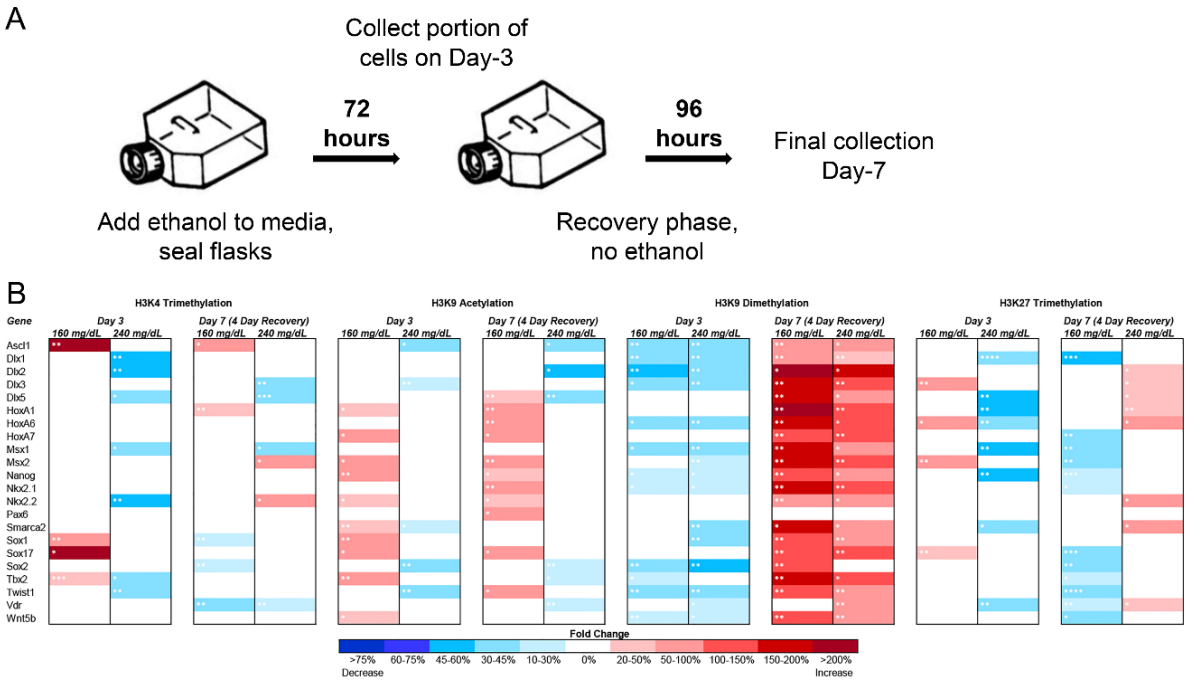

Figure 15: Dose-dependent epigenetic signatures of EtOH exposure persist past the period of exposure. A) Experimental paradigm. B) Alcohol-induced epigenetic alterations in H3K4 me3, H3K9 ac, H3K9 me2, and H3K27 me3. Primary fetal cerebral cortical neuroepithelial stem cells were cultured in the presence of 160 mg/dL or 240 mg/dL EtOH for 3 days, followed by a 4 day recovery in medium lacking EtOH. Samples were collected at days 3 and 7, and examined for changes in the indicated post-translational histone modifications using chromatin immunoprecipitation followed by quantitative PCR (ChIP-qPCR). Heat maps represent fold change in H3K4 me3, H3K9 ac, H3K9 me2, and H3K27 me3 within the regulatory regions of the genes listed. Primers were designed to fall within 250 base pairs of the transcriptional start site. Within the 3 separate biological replicates (N=3), 3 ChIPs were performed, and 2 qPCR replicates performed on each independent ChIP. Statistical measures were conducted using the Wilcoxon Signed Rank nonparametric test. *p<0.05; **p<0.01; ***p<0.001; ****p<0.0001.

groups and time points examined. It is interesting to note that epigenetic modifications associated with a condensed chromatin architecture displayed the largest and most frequent changes. Second, we observed that a loss of histone marks associated with repressive chromatin structure did not immediately correlate with gains in post-translational modifications associated with relaxed chromatin structure, and similarly, loci displaying decreases in marks associated with transcription did not see increases in post-translational modifications associated with gene repression. A number of studies have suggested an interdependent relationship between many of the marks examined here, yet even after a recovery period, this lack of correlation persists. Third, a clear dose dependent effect exists between the epigenetic changes observed in the 160mg/dL and the 240mg/dL treatment groups. While the 160mg/dL treatment elicited an enrichment of H3K4 me3, H3K9 ac, and H3K27 me3, depletion of these histone marks were observed in the 240mg/dL treatment groups. Only H3K9 me2 exhibited a uniform depletion across treatments at this time point.

Fourth, when extracts obtained after a 4-day recovery were examined (Day-7), we noticed a persisting signature of exposure that was unique to each post-translational modification examined. For example, gene promoters displaying alterations in chromatin modifications associated with relaxed chromatin (H3K9 ac and to a lesser extent H3K4 me3) on Day-3, maintained the observed altered profiles on Day-7. In contrast, loci that had become depleted for marks associated with compacted chromatin (H3K27 me3, and H3K9 me2) on Day-3 displayed a hypermethylated state on Day-7, suggesting these genes had been remodeled into a repressive chromatin state. The exception being the H3K27 me3 in the 160mg/dL treatments, which were hypermethylated on Day-3 and became depleted on Day-7. In addition, we observed that many genes displaying chromatin profiles identical to the control on Day-3 exhibited altered profiles on day-7 and several alterations present on day-3 resolved at the day-7 time point. As examples, the regulatory regions of *Dlx5* and *Nkx2.2* displayed H3K9 me2 and H3K27 me3 profiles identical to the control on Day-3, but became hypermethylated by Day-7. Finally, not all genes were uniformly affected in our system, and many only displayed alterations in

a subset of the post-translational modifications examined. The regulatory region of *Pax6* for instance only exhibited changes in H3K9ac at the Day-7 time point, while all other chromatin marks were identical to the controls, at the time-points examined. In contrast, *Ascl1*, *Msx2*, *Nkx2.2* and *Tbx2* all displayed significant changes in at least three of the four histone marks examined, and these changes varied across the range of concentrations tested and time points examined. Collectively, these results suggest that the epigenetic changes arising as a consequence of EtOH exposure are heavily dependent on the gene under investigation, the dose of alcohol encountered, the epigenetic mark under investigation, and that the profile of change arising acutely is not always consistent with ones measured after removal of the toxicant. These observations may have relevance to understanding the molecular basis underlying the enormous variation observed in clinical cases of FASDs.

EtOH Exposure *in vitro* is Associated with Alterations in Transcripts Encoding *Sod3* and *Tet1*, but No Alterations in Markers of Cell Death, Oxidative Stress, nor Significant Disruption of the Oxidative Stress Transcriptional Response

Given the observed increases in ROS following alcohol exposure, researchers have speculated that some of the teratogenicity associated with EtOH exposure is linked to oxidative stress (Dong et al., 2008; Brocardo et al., 2011). Recently, a link between components of the oxidative stress pathways and enzymes controlling chromatin structure has been identified (Chia et al., 2011; Bosch-Presegué et al., 2011). To examine a potential link between mobilization of the oxidative stress response, and the observed alterations in chromatin structure, we began by quantifying the transcript levels of 23 well characterized candidate genes involved in either the metabolic processing of alcohol or the oxidative stress response pathway (Dong et al., 2008). Of these 23 candidates, transcripts encoding *Cyp2e1*, *Gpx2* and *Gsta2* could not be detected in RNA samples isolated from our neurosphere cultures. Surprisingly, of the remaining 20 candidates, the majority of genes exhibited a down-regulation at the Day-3 time point and no significant alterations at Day-7 (Figure 2A.). The two notable exceptions to this trend

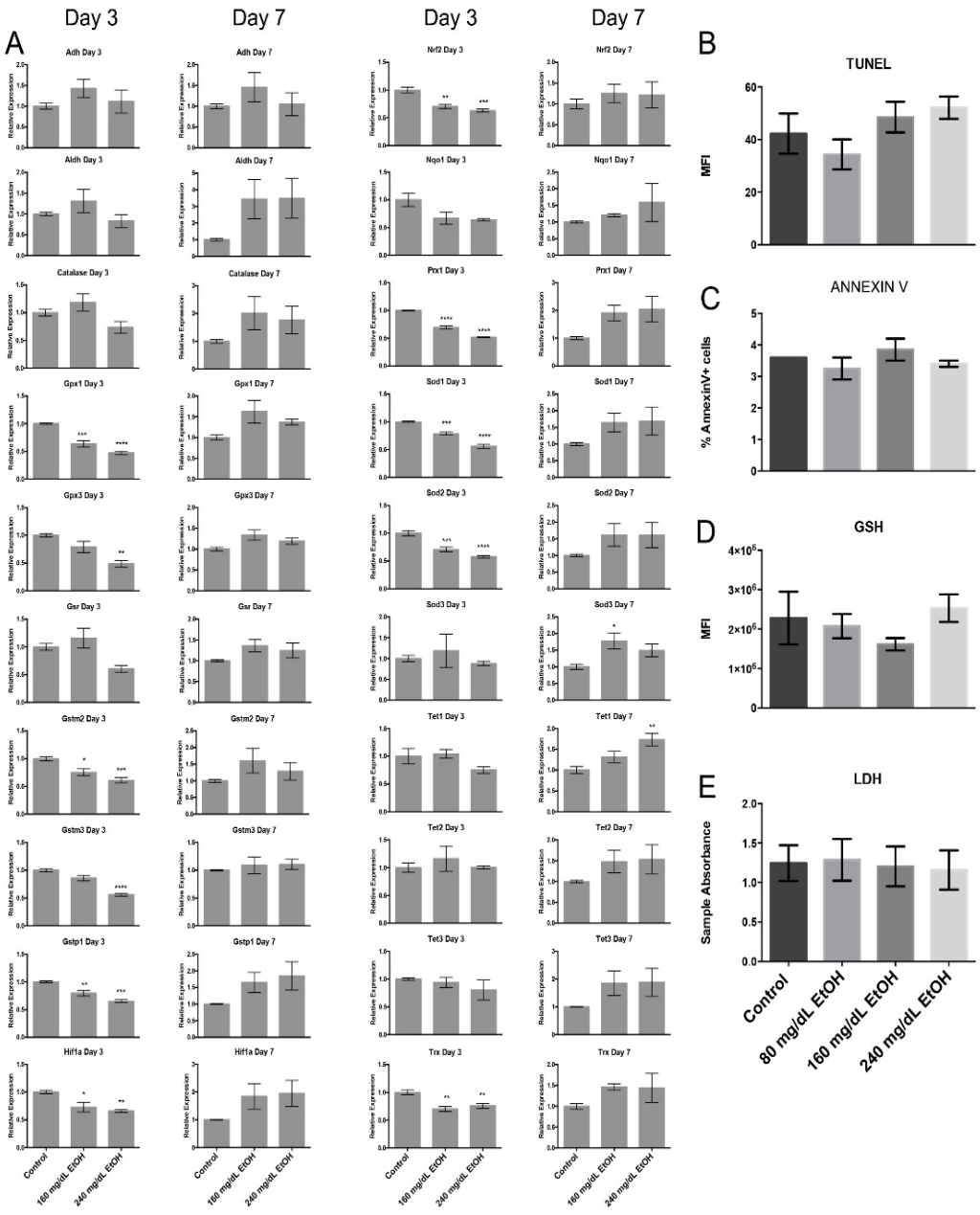

Figure 16: EtOH exposure *in vitro* alters levels of transcripts encoding *Sod3* and *Tet1*, but does not impact measures of cell death or oxidative stress. A) Measurements of transcripts encoding proteins involved in the metabolic processing of alcohol and oxidative stress response pathways. Primary neuroepithelial stem cells were cultured in the presence of 160 mg/dL or 240 mg/dL EtOH for 3 days, followed by a 4 day recovery in media lacking EtOH. Samples were harvested at days-3 and 7, and transcript levels determined by RT-qPCR. Graphs represent 3 independent biological replicates, (N = 3) with 2 independent RT reactions and 3 independent qPCR measurements for each RT. Significance was measured using a one-way ANOVA, error bars represent SEM. *p<0.05; **p<0.01; ***p<0.001; ****p<0.0001. B-E) Measures of cellular stress and apoptosis in primary neuroepithelial stem cells exposed to alcohol. Cells were cultured in the presence of 80 mg/dL- 240 mg/dL EtOH for 3 days, then assayed for markers of B & C) apoptosis, D) oxidative stress and E) cellular stress. Differences were measured using a one-way ANOVA, error bars represent SEM. Graphs represent 3 separate biological replicates (N=3)

were *Sod3*, and *Tet1*, which measured a 1.7 fold increase over the control at the Day-7 time point.

We next measured physiological parameters associated with apoptosis, oxidative stress and cytotoxicity. Neurosphere cultures were treated with 80mg/dL,160mg/dL, and 240 mg/dL EtOH for 72 hours, and subsequently examined using Annexin 5 and TUNEL assays (Figure 2B & C). Neither of these tests indicated a significant increase in levels of cellular apoptosis. When we examined our treatment groups for alterations in the levels of glutathione (GSH), decreases of which are associated with oxidative stress, no significant changes were observed (Figure 2D). We next examined cell cultures for increased levels of lactate dehydrogenase (LDH), a marker of generic cell stress. Again, this parameter did not show any significant changes across the range of EtOH concentrations examined (Figure 2E). These observations suggest that the oxidative stress pathways are not broadly engaged in our *in vitro* model of fetal alcohol exposure; at least not at the concentrations examined.

EtOH Exposure *in vitro* is Not Associated with an Inhibition of Histone Methyltransferase Enzymatic Activity but Does Induce Alterations in Transcriptional Regulation

Work by our group has demonstrated reductions in H3K27me3 arising due to acute EtOH exposure (Veazey et al., 2013). We therefore sought to determine if the acute losses of H3K9 me2 and H3K27 me3 observed in our cell culture model could possibly be linked to alcohol-induced inhibition of histone methyltransferase enzyme activity. To this end, cell cultures were treated with an EtOH dose response range from 80mg/dL to 240mg/dL, and both H3K9 and H3K27 methyltransferase activity quantified using a colorimetric assay. No significant differences in H3K9 nor H3K27 methyltransferase activity were observed across the range of concentrations tested (Figure 3A & B).

We then examined levels of transcripts encoding ten major proteins responsible for regulating DNA methylation as well as H3K9 and H3K27 methylation

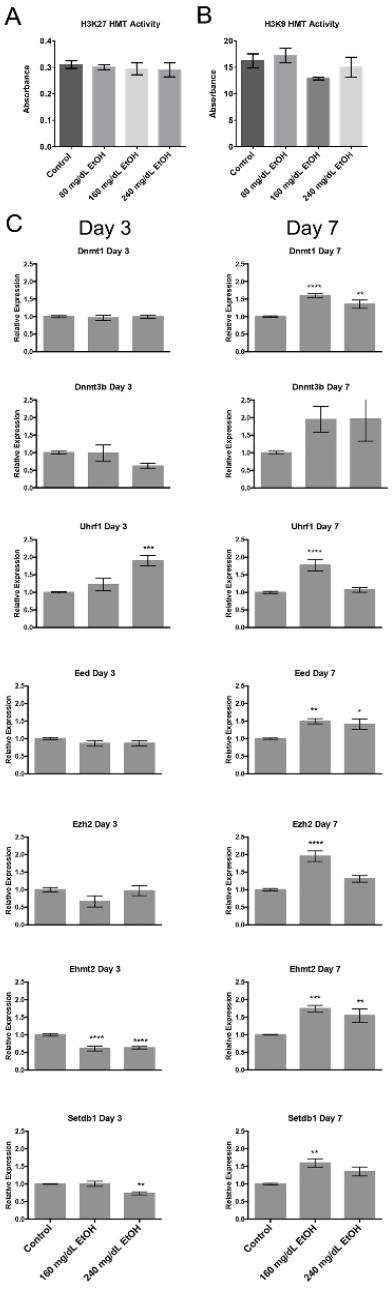

Figure 17: In vitro EtOH exposure does not inhibit methyltransferase enzymatic activity, but does induce alterations in the transcriptional control of DNA and Histone methyltransferase enzymes. A & B) Measures of Histone methyltransferase activity in EtOH exposed neuroepithelial stem cells. Cells were cultured in the presence of 80 mg/dL to 240 mg/dL EtOH for 3 days, and cellular extracts assayed for A) H3K27 and B) H3K9 histone methyltransferase activity using a colorimetric assay. Differences were measured using a one-way ANOVA. Error bars represent SEM. N = 3. C) Measurement of transcripts encoding enzymes governing DNA, H3K9, and H3K27 methylation. Primary neuroepithelial stem cells were cultured in the presence of 160 mg/dL or 240 mg/dL EtOH for 3 days, followed by a 4 day recovery in media lacking EtOH. Samples were harvested at days-3 and 7, and transcript levels determined by RT-qPCR. Graphs represent 3 independent biological replicates, (N = 3) with 2 independent RT reactions and 3 qPCR measurements for each RT. Significance was measured using a one-way ANOVA, error bars represent SEM. *p<0.05; **p<0.01; ***p<0.001; ****p<0.0001.

(Figure 3C) (Li et al., 1992; Okano et al., 1999; Cao et al., 2002; Schultz et al., 2002; Tachibana et al., 2002; Whetstine et al., 2006; Yamane et al., 2006; Bostick et al., 2007; Wissmann et al., 2007; Laurent et al., 2015). Interestingly, transcripts encoding *Ehmt2* (*G9a*) and *Setdb1*, the two enzymes responsible for methylating H3K9, display alcohol-induced suppression on Day-3 and an up-regulation on Day-7; which is consistent with the observations in Figure 1. However on Day-3, we also observed decreases in the abundance of transcripts encoding *Kdm1a*, and *Kdm4c*, as well as a modest increase in *Kdm1a* on Day-7. These two enzymes have established roles in demethylating H3K9 (Wissmann et al., 2007; Laurent et al., 2015). None of the other factors examined display altered transcript profiles on Day-3, with the exception of *Uhrf1* in the 240mg/dL treatments. In contrast, *Dnmt1*, *Uhrf1*, *Eed*, and *Ezh2* all exhibited alterations on Day-7. These observations suggest some of the alterations in chromatin structure may be tied to changes in the levels of enzymes regulating DNA / histone methylation.

EtOH-Induced Alterations in *Dnmt1*, *Tet1* and *Uhrf1* Transcript Levels are Associated with Measurable Alterations in DNA Methylation but not DNA Hydroxymethylation

Recently, it has been shown that the TET family of Fe(II) and α-KG-dependent dioxygenases rely upon oxygen to convert 5-methyl-Cytosine (5mC) into 5-hydroxy-methyl-cytosine (5hmC) (Tahiliani et al., 2009). This modified form of cytosine is abundant in the brain and is hypothesized to play a key role in the epigenetic control of neuronal function (Kriaucionis and Heintz, 2009). Importantly, the formation of 5hmC can lead to demethylation of DNA, which in turn can influence other aspects of chromatin structure; including H3K4 me3, H3K9 me2, and H3K27 me3 (Viré et al., 2006; Ciccone et al., 2009; Rothbart et al., 2012). Since our transcript profiles, as well as previous studies in other models (Zhou et al., 2011; Sakharkar et al., 2014) have identified alterations in gene family members regulating both 5mC and 5hmC, we set out to determine these alterations were associated with gene-specific changes in DNA methylation / hydroxy-methylation. To this end, we utilized glucosylation of genomic DNA followed by methylation-sensitive qPCR

(glucMS-qPCR) to examine alcohol-induced alterations in eight candidate genes. These candidates were identified in previous studies of 5hmC within the brain and embryonic stem cell-derived neural progenitor cells (Tan et al., 2013; Okashita et al., 2014; Irwin et al., 2014).

To first validate our methodologies, we examined levels of 5mC within the differentially methylated regions of two imprinted genes (*Peg3* and *Snrpn*) (Mann et al., 2004). Both candidates demonstrated 50% 5mC consistent with one allele being methylated and the other unmodified; but no detectable 5hmC (Figure 4A). At these two loci, no significant alterations in 5mC were induced by alcohol exposure across the range of concentrations tested and time points examined. We then evaluated expression of *Snrpn* in EtOH exposed cultures and did not observe any significant changes, consistent with the stable measures of 5mC at this locus (Figure 4B). We next assayed alterations in both 5mC and 5hmC within either the gene bodies or regulatory regions of eight candidate genes identified in previous studies of 5hmC. We observed increases in 5mC within the 5‘ UTR of *Gf* and the regulatory region of *Sycp3* (Figure 4C). While we were able to detect very low levels of 5hmC consistent with previous reports (Tan et al., 2013; Okashita et al., 2014; Irwin et al., 2014), none of these loci exhibited alcohol-induced changes as compared to the controls (Figure 4D). In our primary cultures, the 5‘ UTR of *Gf* did not exhibit any detectable 5hmc. Collectively, these results suggest that while the observed increase in DNA methyltransferase levels are correlated with modest increases in 5mC, increased *Tet1* transcript levels are not associated with any measurable changes in 5hmC across the candidate loci examined.

Alterations in *Homeobox* Gene Transcription Predominantly Manifest Beyond the Window of EtOH Exposure

Published reports examining acute EtOH exposure have been unable to demonstrate consistent correlations between alterations in H3K4 me3; a histone mark enriched at the promoter regions of actively transcribed genes (Liang et al., 2004), and changes in transcription (Veazey et al., 2013; Zhou et al., 2011;

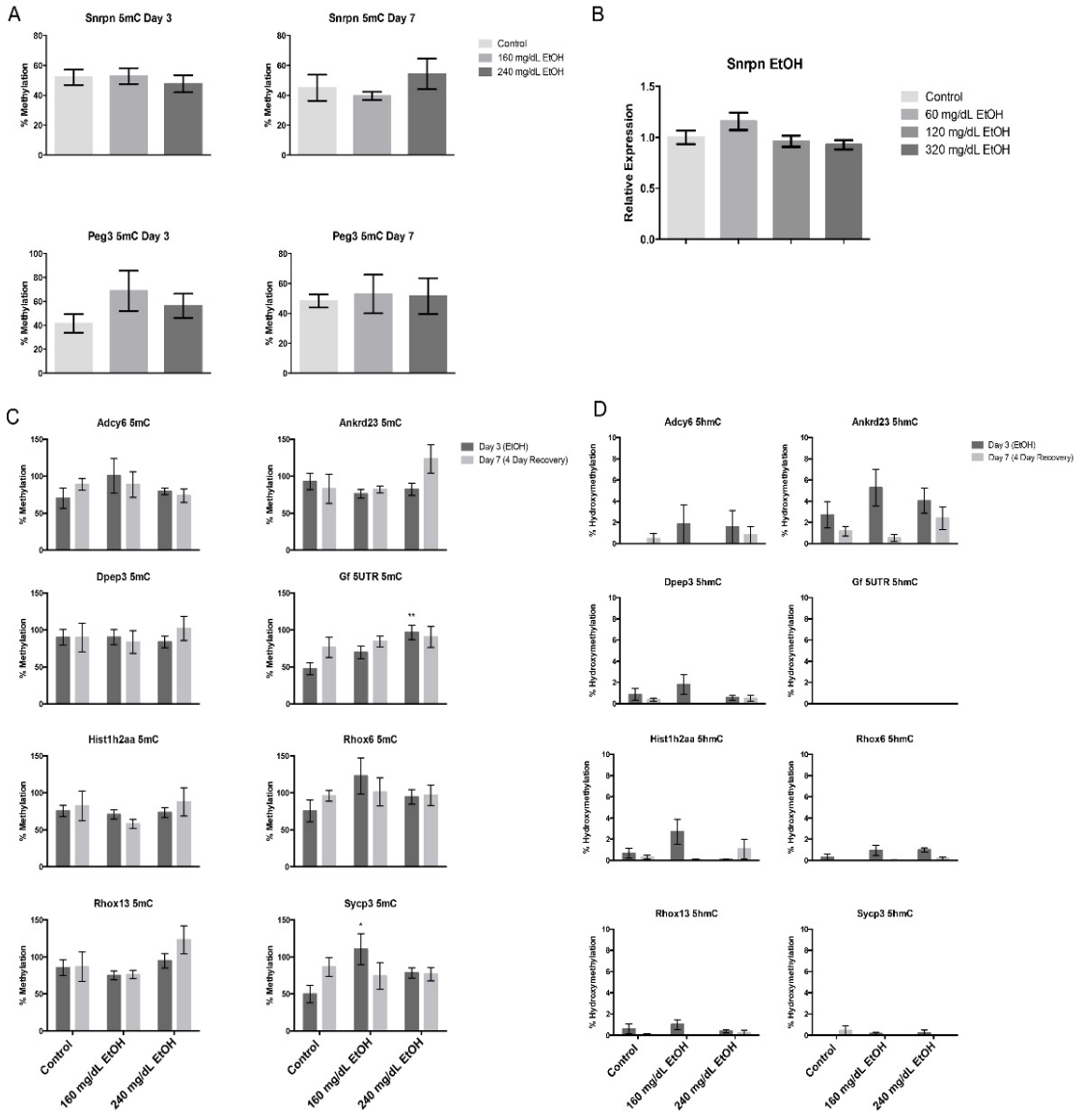

Figure 18: Alterations in DNA methylation but not hydroxymethylation in EtOH-exposed primary neuroepithelial stem cell cultures. A) Stable levels of DNA methylation within the differentially methylated regions of the imprinted genes Snrpn and Peg3. Stem cells were cultured in the presence of 160 mg/dL or 240 mg/dL EtOH for 3 days, followed by a 4 day recovery in media lacking EtOH. Genomic DNA was collected at days-3 and 7, and analyzed for alterations in DNA 5mC and 5hmC using glucMS-qPCR. Graphs represent 3 independent biological replicates, (N = 3) with 3 qPCR measurements each. B) Quantification of Snrpn transcript levels using RT-qPCR. Graphs represent 3 independent replicates, (N = 3) with 2 independent RT reactions and 3 qPCR measurements for each RT. Differences were measured using a one-way ANOVA, error bars represent SEM. C & D) Measurement of 5mC and 5hmC within the regulatory regions of 8 genes identified in previous studies of DNA hydroxymethylation. Cells were cultured in the presence of 160 mg/dL or 240 mg/dL EtOH for 3 days, followed by a 4 day recovery in media lacking EtOH. Genomic DNA was collected at days-3 and 7, and analyzed for alterations in DNA C) 5mC and D) 5hmC using glucMS-qPCR. Differences were measured using a one-way ANOVA, error bars represent SEM. Graphs represent 3 independent biological replicates, (N = 3) with 3 qPCR measurements each.

Ponomarev et al., 2012). We were therefore curious to determine if the candidate genes demonstrating changes in any of the measured chromatin marks either before or after the recovery period would display alterations in gene transcription. To this end, RNA was isolated from all treatment groups and gene expression measured using quantitative reverse transcriptase polymerase chain reaction (qRT-PCR). Of the 22 candidate genes examined in Figure 1, transcripts encoding *Ascl1*, *Dlx2*, *Dlx3*, *Pax6*, *Nkx2.2*, *Sox1*, *Sox2*, *Sox17*, and *Tbx2* could be detected in our cultures (Figure 5). Similar to our previous studies (Veazey et al., 2013), only a very small number (20%) of candidate genes (*Ascl1* and *Sox2*) displayed altered expression profiles arising as a consequence of EtOH exposure at Day-3. In contrast, eight of the nine detected candidates (~88%) displayed significant alterations in transcript levels on Day-7, across both concentrations of EtOH tested. These candidate homeobox genes sit at the hub of multiple transcriptional pathways controlling cellular identity and proliferation. We therefore assayed RNA samples for alterations in the expression of known markers of both cellular growth (Ki67, *cMyc*, and *Rb1*) and neural stem cell proliferation / identity (*Fabp7*, *Gfap*, *Gli3*, *Nestin*, *Olig2* and *Tuj1*). These analyses revealed changes in a small number of candidates within the 240mg/dL treatments on Day-3 (*Ki67*, *Fabp7*, and *Tuj1*), while the larger impact was again observed on Day-7, with eight of the nine candidates demonstrating alterations in transcription (Figure 6). These observations indicate the larger impact of EtOH exposure on the developmental program may arise beyond the initial period of exposure.

<u>An Epigenetic Signature of EtOH Exposure Arising from an Acute Gestational Encounter Persists Beyond the Window of Exposure</u>

Abnormalities in the cortex of the brain are often associated with alcohol-induced impairments in high-level sensory and motor processing, as well as with some FASD cognitive-behavioral phenotypes. As our stem cell cultures are derived from mouse cerebral cortex precursors, we sought to assess the relevance of our *in vitro* observations on the development of FASD associated birth defects. The C57Bl/6J mouse has been critical in defining some of the stage-dependent dysmorphologies

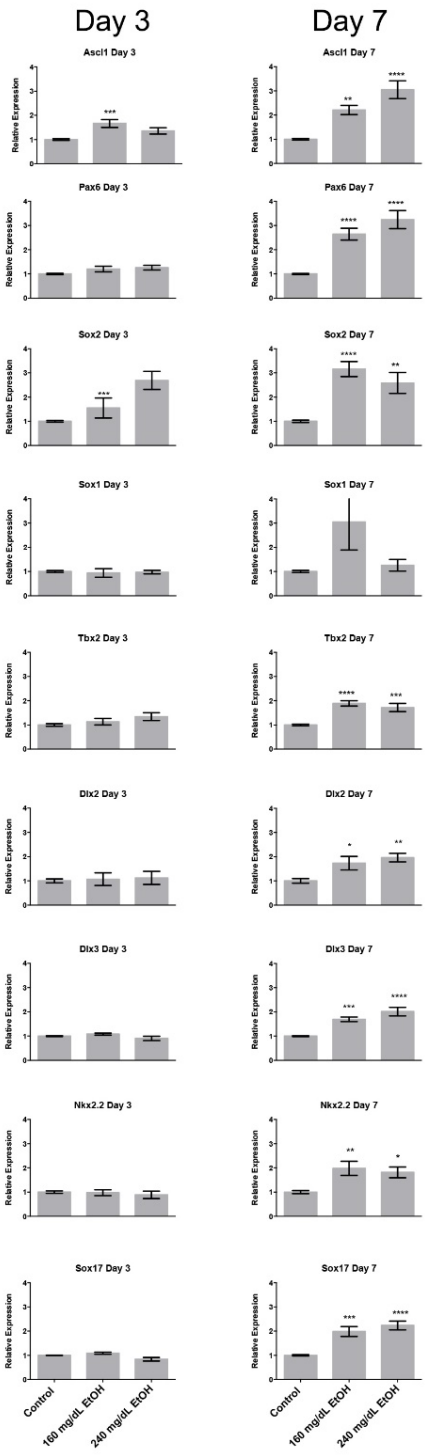

Figure 19: Distinct alterations in homeobox gene transcription arising during and after the window of EtOH exposure. Neural stem cells were cultured in the presence of 160 mg/dL or 240 mg/dL EtOH for 3 days, followed by a 4 day recovery in media lacking EtOH. Cells were harvested at days-3 and 7, and transcript levels measured using RT-qPCR. Graphs represent 3 independent replicates, (N = 3) with 2 independent RT reactions and 3 qPCR measurements for each RT. Differences were measured using a one-way ANOVA, error bars represent SEM. *p<0.05; **p<0.01; ***p<0.001; ****p<0.0001.

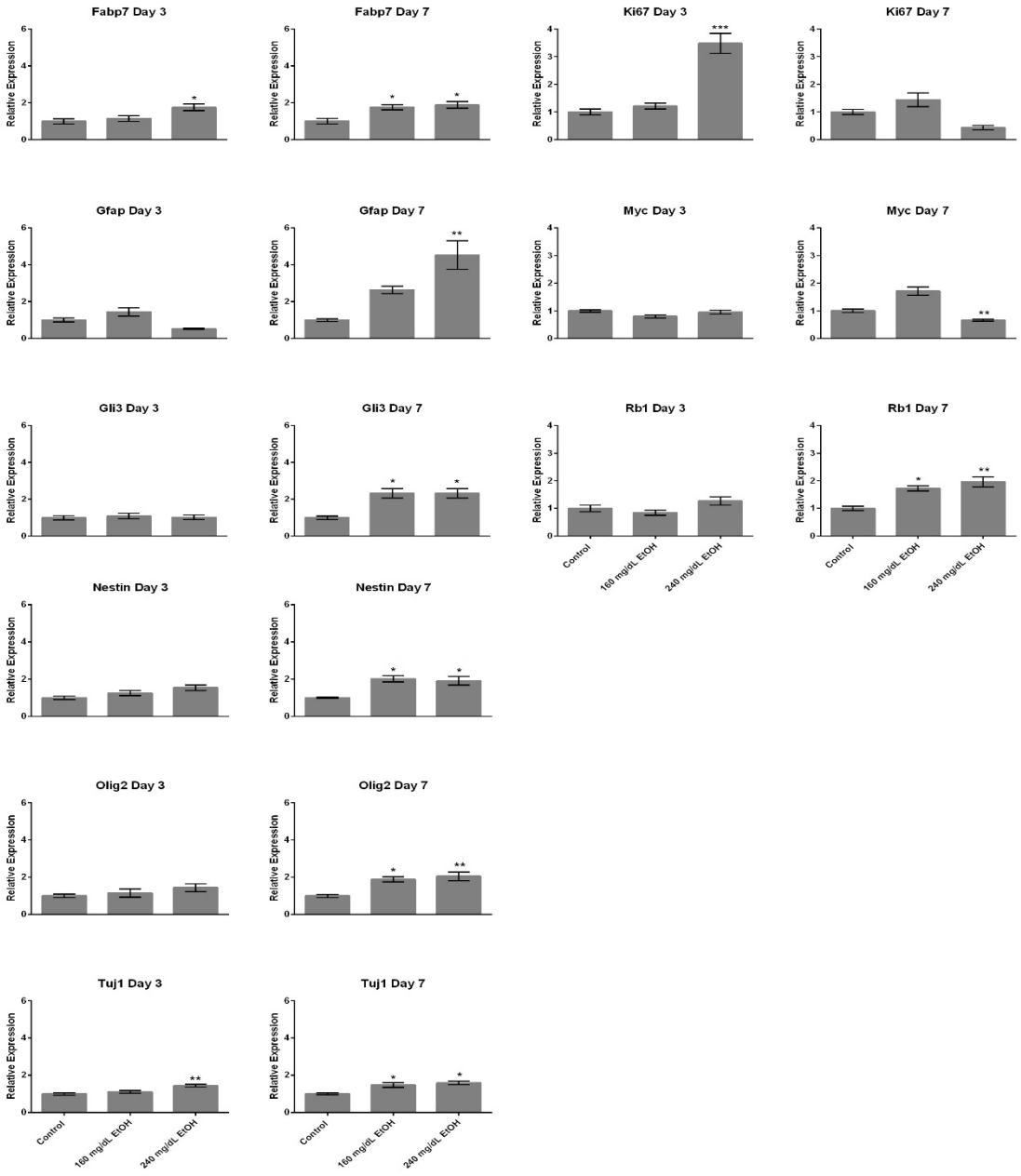

Figure 20: Alterations in transcripts encoding proteins regulating neural stem cell identity and proliferation predominantly arise after the window of EtOH exposure.
Neural stem cells were cultured in the presence of 160 mg/dL or 240 mg/dL EtOH for 3 days, followed by a 4 day recovery in media lacking EtOH. Cells were harvested at days-3 and 7, and transcript levels measured using RT-qPCR. Graphs represent 3 independent replicates, (N = 3) with 2 independent RT reactions and 3 qPCR measurements for each RT. Differences were measured using a one-way ANOVA, error bars represent SEM. *p<0.05; **p<0.01; ***p<0.001.

resulting from acute early gestational ethanol exposures. An acute binge-like ethanol treatment on gestational day seven (GD7) (equivalent to the early third week of human development - gastrulation) results in a range of grossly observable fetal anomalies such as holoprosencephaly and classic FAS facial characteristics (Sulik et al., 1981; Godin et al., 2010). Importantly, both the craniofacial and midline brain anomalies can be consistently scored and their degree of severity correlated with concurrently developing defects within the CNS (Parnell et al., 2006; Godin et al., 2010). We therefore examined the prevalence of altered chromatin structure within the cortex of mouse pups exposed to an early, binge-like gestational exposure.

On GD7, pregnant dams were intraperitoneally administered 2 injections of either vehicle or 2.9 g/kg EtOH 4 hours apart, yielding peak maternal blood alcohol concentrations averaging 440 mg/dL (Godin et al., 2010). These blood alcohol concentrations are much higher than those utilized in our *in vitro* studies, however in mouse models of FAS, lower concentrations do not consistently produce holoprosencephaly and classic FAS facial characteristics (Parnell et al., 2006). We therefore elected to use a treatment paradigm that would produce a low, but consistent frequency of alcohol induced birth defects, yet that was not overtly toxic. On GD17, stage-matched control and EtOH-exposed fetuses were dissected, and scored for ocular defects as described previously (Parnell et al., 2006). Using this model, 12% of the EtOH exposed pups displayed holoprosencephaly and FAS facial characteristics, whereas the remaining animals were morphologically normal. Mice were then sorted into groups by treatment and morphological appearance. In total, 25 mice from 6 different litters were selected for analysis; 10 control, 8 EtOH exposed - morphologically normal, and 7 EtOH exposed - malformed. To examine the impact of EtOH exposure upon the epigenetic program of the developing central nervous system, the fetal cortex was dissected out, and using chromatin immunoprecipitation, we assayed cellular extracts for alterations in the chromatin marks examined above (Figure 7).

In samples derived from EtOH exposed - malformed pups, we observed a pattern of change that largely correlated with the *in vitro* post-recovery signature

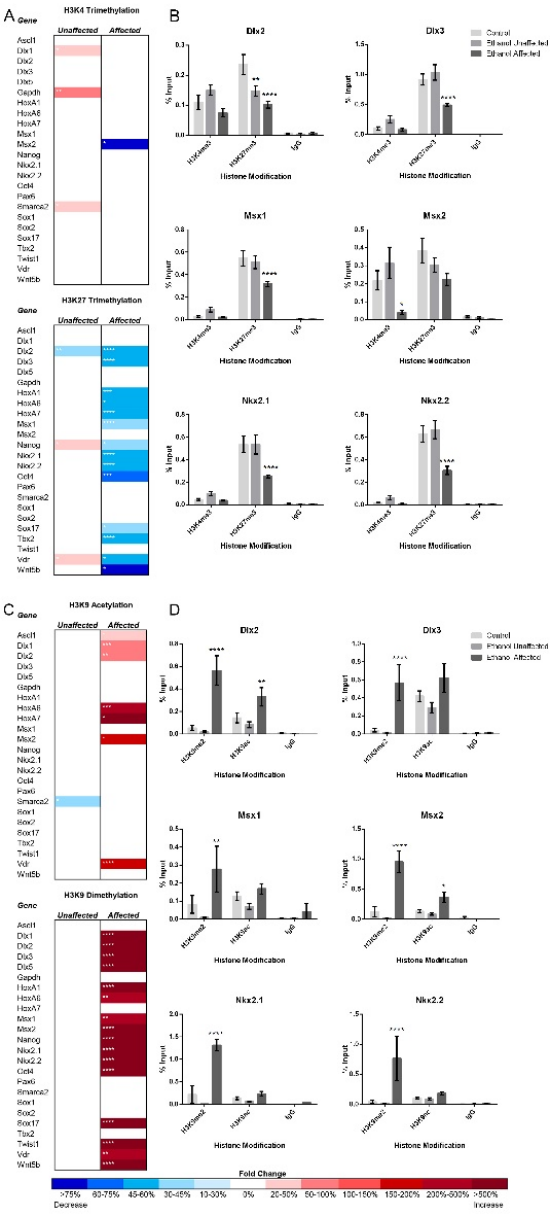

Figure 21: Lasting alcohol-induced alterations in H3K4 me3, H3K9 ac, H3K9 me2, and H3K27 me3 within the prenatal cortex arising from an early gestational exposure.
Pregnant dams were injected with 2.9g/kg EtOH at GD7 and embryos harvested at GD17. Embryos were scored for ocular and cortical patterning defects, and sorted into 3 groups - control, EtOH exposed - morphologically normal, and EtOH exposed - malformed. After dissection of the fetal cortex, ChIP-qPCR analysis was performed on cellular extracts using antibodies recognizing H3K4 me3, H3K9 ac, H3K9 me2, and H3K27me3. A & C) Heat maps representing fold change in the levels of the indicated post-translational modifications relative to samples derived from saline exposed controls. In the experiments examining H3K4 me3 and H3K27 me3, four ChIP experiments were performed on a total of 15 brains across 5 different litters. For analysis of H3K9 ac and H3K9 me2, three ChIP experiments were performed on a total of 10 brains across 5 different litters. Two replicates of qPCR were performed on each ChIP. Significance was determined using a two-way ANOVA. Error bars represent SEM.*p<0.05; **p<0.01; ***p<0.001; ****p<0.0001. B & D) Representative graphs depicting alcohol-induced alterations in chromatin structure. A complete analysis of individual genes may be viewed in Additional file 2.

observed in the 160mg/dL treatment group in Figure 1. Fetal mice exhibiting craniofacial dysmorphology and midline brain defects displayed loss of H3K27 me3 in 14 of the 24 (58%) candidates examined, a modest enrichment of H3K9 ac in 7 / 24 candidate genes (29%), and a dramatic increase in H3K9 me2 in 17/24 (70%) of the candidate regulatory regions examined. The hypermethylated state of H3K9 in particular was robust and very consistent. With the exception of a modest change within the promoter region of *Msx2*, no alterations of H3K4 me3 were observed in the EtOH exposed - malformed tissue samples. It is interesting to note that across at least three of the four post-translational modifications examined, *Dlx2*, *HoxA6*, *HoxA7*, *Msx2*, and *Vdr* consistently displayed alterations in chromatin structure, suggesting certain genes may be more susceptible to epigenetic errors than others. In our analysis, we noticed that post-translational modifications associated with repressive chromatin structure are profoundly impacted as compared to those associated with transcriptionally active, yet these changes move in opposite directions; H3K27 me3 is lost while H3K9 me2 is gained. This was surprising given EHMT2 (G9a) and the *Polycomb* group have been observed as part of a common complex, and on at least a subset of genes in ES cells, increased H3K9 me2 enhanced EZH2 activity (Mozzetta et al., 2014). In contrast, EtOH exposed - morphologically normal pups displayed modest changes in H3K4 me3 and H3K27 me3, while levels of H3K9 me2 were identical to those measured in the controls. Collectively, these observations indicate that an epigenetic signature of EtOH exposure persists beyond the window of exposure, and is largely linked to alterations in repressive chromatin structure; H3K9 me2 in particular. Importantly, these observed alterations strongly correlate with the development of FASD-associated congenital malformations.

Discussion

Epidemiologic studies have shown that alcohol is the most prevalent teratogen to which humans are exposed, and in the United States, 6-9 infants per 1000 live births are diagnosed with some degree of fetal alcohol spectrum disorder (Fox et al., 2015). Despite years of intense study, determining the developmental

basis for the enormous variation in both the severity and range of birth defects linked to prenatal alcohol exposure remains a formidable challenge. We and others have demonstrated multiple alterations in chromatin structure arising as a consequence of EtOH exposure, but linking these epigenetic changes to alterations in the developmental program, and ultimately to the acquisition of congenital abnormalities, has yet to be achieved (Mead and Sarkar, 2014; Resendiz et al., 2014). Our observation that the two concentrations of EtOH tested *in vitro* were able to elicit distinct changes in chromatin structure suggest some of the variation in FAS clinical cases may be attributable to dose dependent alterations in the epigenetic program. It is noteworthy that the direction of change arising from the 160mg/dL exposure for H3K4 me3, H3K27 me3, and H3K9 ac are opposite to those induced by the 240mg/dL treatments. Only H3K9 me2 was uniformly affected. The mechanisms underlying the observed non-linear dose responses in fetal alcohol exposure are unclear. However, such data emphasize that the teratogenic potential of ethanol is not diminished with lower doses.

Alterations in H3K9 me2 are consistently induced by EtOH exposure, persist beyond the window of exposure, and have a strong association with the development of congenital abnormalities. Previous studies of acute EtOH-induced liver injury, neuroplasticity, neurodegeneration, and neuroadaptation have also observed gene-specific changes in H3K9 methylation indicating alterations to this post-translational mark may be a core aspect of EtOH teratogenicity (Pal-Bhadra et al., 2007; Qiang et al., 2011; Moonat et al., 2013; Subbanna et al., 2014). The correlative shifts in transcript abundance of the major genes regulating the dynamics of H3K9 methylation support this assertion. Recently, two independent studies in yeast have reported a potential reader-writer mechanism of epigenetic inheritance for H3K9 methyl-marks (Ragunathan et al., 2014; Audergon et al., 2015). These observations suggest disruptions in H3K9 methylation may be heritable through development and therefore represent a plausible mechanism of transmitting a lasting signature of EtOH exposure. If alterations at this residue are indeed linked to gestational EtOH exposures causing birth defects, we speculate this signature may be identifiable in clinical samples such as cord blood, and thus potentially serve as a

biomarker of exposures linked to patterning defects. If true, this could yield the potential to identify FASD cases that do not present with overt craniofacial abnormalities, but yet have associated neurological deficits (Fox et al., 2015). The predictive value of epigenomic markers over genetic ones is starting to gain wider acceptance (Clarke-Harris et al., 2014), thus this strategy may be helpful in the delivery of FASD educational interventions at the earliest possible points.

Researchers have speculated that some of the teratogenicity associated with EtOH exposure is linked to oxidative stress, and inhibition of aspects of one carbon metabolism (Brocardo et al., 2011; Zeisel, 2011). Our data both *in vitro* and *in vivo*, suggest that some loci gain methylation while others exhibit a decrease. Specifically, the dramatic increases in H3K9 me3 observed within our candidate gene regulatory regions does not support the notion that a shortage of methyl groups underlies the observed changes in chromatin structure. However, our analysis is focused on select regulatory sequences and does not examine global changes in any of these post-translational histone marks, nor does it examine alterations in global levels of DNA methylation, which previous reports have found to be significantly reduced in EtOH exposed animals (Garro et al., 1991; Zhou et al., 2011). Additionally, we did not observe a correlation between epigenetic alterations brought on by *in vitro* EtOH exposure and changes in the examined markers of cell death, cell stress or oxidative stress. Although we did observe alterations in *Tet1* transcript levels, these were not associated with measurable changes in 5hmC. Thus, we were unable to find evidence supporting the notion that epigenetic modifications induced by alcohol are associated with genes downstream of the oxidative stress pathways, at least at the concentrations examined here.

Current research suggests epigenetic changes to the chromatin template begin at conception and continue as an iterative process enabling a progressive ‘‘memory’’ of prior developmental fate decisions. However, the biochemical nature of this memory is the subject of some debate. In the case of the H3K27 me3 mark, work by two independent laboratories has suggested that established H3K27 me3 attracts the *EED* component of the *Polycomb Repressive Complex 2 (PRC2)*, and is

required to stimulate the enzymatic activity necessary to maintain this mark on the daughter strands during incorporation of newly synthesized histones (Hansen et al., 2008; Margueron et al., 2009). In contrast, another study has suggested that only binding of the *Polycomb* complex through S-phase is required to propagate this post-translational modification (Petruk et al., 2012). We have previously observed depletion of H3K27 me3 at multiple loci in response to EtOH exposure, however ChIP analysis of EZH2 binding failed to identify significant changes in *PRC2* localization (Veazey et al., 2013). The persisting reductions of this mark observed 10 days after an acute *in vivo* exposure, but not within *in vitro* neurosphere cultures maintained in the stem cell state, suggest recovery of this mark may be dependent upon cells being in a stem cell versus a differentiating state.

In our *in vitro* studies, we did not observe a consistent correlation between alcohol-induced alterations in histone post-translational modifications and changes in gene transcription. The large majority of alterations in chromatin structure we observed indicate an increase in marks associated with transcriptional repression at Day-7, yet our candidate genes demonstrated an increase in expression at this time. These *in vitro* observations add one more piece of data to suggest histone post-translational modifications, in isolation, are not likely causal in regulating transcription (Henikoff and Shilatifard, 2011). Therefore, the established lexicon of 'activating' and 'repressive' chromatin modifications is an over-simplification that should be curtailed. Basic principles of teratogenesis state that a teratogen must cause malformations through a specific mechanism during a period in which the conceptus is susceptible to said mechanism (KARNOFSKY, 1965). Embryonic stem cells have been derived with genetic deletions of the major enzymes controlling DNA methylation (*Dnmt1*$^{-/-}$*Dnmt3a*$^{-/-}$*Dnmt3b*$^{-/-}$triple knockout), H3K27 me3 (Suz12 $^{-/-}$) and H3K9 me2 / me3 [(*G9a*$^{-/-}$*GLP*$^{-/-}$ double knockout) (*Suv39h1*$^{-/-}$ */ Suv39h2*$^{-/-}$double knockout) ESET/Setdb1 knockout $^{-/-}$] (Peters et al., 2003; Tachibana et al., 2005; Tsumura et al., 2006; Pasini et al., 2007; Matsui et al., 2010). In most cases, these cells continue to grow and demonstrate subtle changes in gene transcription. However, once induced to begin the process of differentiation, these cultures uniformly undergo apoptosis. Thus, perhaps the stem cell state is tolerant of major

shifts in chromatin structure without associated perturbation of transcriptional control, while in contrast, differentiating cells become ‘locked in’ and are more reliant upon chromatin states to control gene expression. In animal models, correlation of acute EtOH exposures with major periods of organ growth indicate that different tissues are largely susceptible to alcohol-induced teratogenesis during specific developmental windows. It is thus tempting to speculate that differences in chromatin biology between pluripotent, differentiating and differentiated cells underlie some aspects of susceptibility to alcohol teratogenesis.

Our analysis of mouse cortices derived from EtOH exposed - malformed pups clearly indicate alterations in chromatin structure are heritable and persist beyond the window of exposure. Importantly, these alcohol-induced changes in chromatin structure can be found within the regulatory regions of genes with clear links to the development of FASD clinical phenotypes (Figure 6B & D) (Rifas et al., 1997; Godin et al., 2011). Thus, our data strongly suggest acute alcohol exposures have the capacity to perturb the developmental program and contribute to EtOH induced birth defects. As approximately 50% of pregnancies in the United States are unplanned, many women inadvertently subject their children to acute prenatal EtOH exposures (Henshaw, 1998). Therefore a better understanding of the role of alcohol-induced epigenetic errors in the development program play in the etiology of FASDs will enhance our ability to develop clinical interventions and better diagnostics in the treatment of this condition.

Materials and Methods

Neural Stem Cell Culture and EtOH Exposure

All animal procedures were approved and conducted in accordance with the Institutional Animal Care and Use Committee at the Texas A&M College of Veterinary Medicine (protocol number 2014-0087), and the University of North Carolina. Derivation of primary mouse fetal cerebral cortical neuroepithelial stem cells have been described in detail previously (Miranda et al., 2008). Cells were cultured as free floating neurospheres in T75 flasks containing a 50%/50% mixture

of Neurobasal media (Cat# 21103-049; Invitrogen) and DMEM F-12 (Cat# 11320-033; Invitrogen). This medium was supplemented with the N2-supplement (Cat# 17502-048; Invitrogen), B27 supplement (Cat# 17504-044; Invitrogen), 0.05% TC grade BSA in PBS (Cat# A1933 Sigma), 2mM L-glutamine (Cat# 25030-081; Invitrogen), 1 x Penicillin/Streptomycin (Cat# 15140-122; Invitrogen), 20 µg/ml FGF basic (Cat# PMG0034; Invitrogen), 20 µg/ml EGF (Cat# PHG0311; Invitrogen), and 0.85 units/ml heparin (Cat# H3149; Sigma). Neurospheres were incubated at 37 °C, in a 5% CO_2 humidified environment. Medium was changed every 2 or 3 days depending on the level of confluence. Alcohol treatment groups were cultured in medium containing either 80 mg/dL, 120 mg/dL, 160 mg/dL, 240 mg/dL, or control cultures containing no EtOH. Cells were grown in flasks sealed with parafilm to prevent evaporation. Medium treatments were replaced every 48 hours and samples collected for ChIP and RNA analysis at the indicated time points.

Chromatin Immunoprecipitation Analysis

Cells were grown to 80% confluence, washed twice in warm PBS, dissociated using Accutase (Cat# SCR005; Millipore), and re-suspended in warm medium (DMEM F-12 Cat# 11320-033; Invitrogen) containing 0.1 volume crosslinking solution (Kondo et al., 2004). ChIP reactions were performed as described previously (Golding et al., 2010) followed by DNA purification using a Qiaquick PCR Cleanup kit (Cat# 28106; QIAGEN). Antibodies used include: anti-H3K4me3 (Cat# 04-745; Millipore), anti-H3K27me3 (Cat# 39155; Active Motif), anti-H3K9ac (Cat# 07-352; Millipore), and anti-H3K9me2 (Cat# 39239; Active Motif). Antibodies for modified histones were used at 1 µg/ChIP reaction. The concentration of IgG (Cat# SC-2027; Santa Cruz) was also used at 1µg / ChIP. For analysis of candidate loci, real-time PCR was performed using the Dynamo Flash supermix (Cat# F-415XL; Thermo Scientific) according to the recommended protocol. Reactions were performed on a Bio-Rad CFX384 Touch PCR system. Primer sequences are listed in Additional file 3.

Murine Fetal Forebrain Chromatin Immunoprecipitation Analysis

IP injections of EtOH (2.9g/kg) were administered to pregnant dams at GD7 as described previously (Godin et al., 2010). Control dams were injected with a comparable volume of lactated Ringer's solution. Embryos were harvested at GD17, and fetal mice scored for ocular and cortical patterning defects (Parnell et al., 2006; Godin et al., 2010). After assessment, the left and right cortices were dissected and flash frozen. Cortices of a single brain were thawed and filtered into a single-cell suspension using gentle mechanical dissociation in a 100 um cell strainer (Cat# 352360; Corning Life Sciences). Cells were washed twice with PBS containing protease inhibitor cocktail (Cat# 78437; Thermo Scientific) and re-suspended in medium (DMEM F-12 Cat# 11320-033; Invitrogen) containing 0.1 volume crosslinking solution (Kondo et al., 2004). ChIP reactions were performed as described above.

RNA Analysis

Cultured cells were grown to 80% confluence, washed twice in warm PBS, and dissociated with 1X trypsin (Accutase Cat# SCR005; Millipore). Cells were spun down, washed once in cold PBS, and RNA isolated using Trizol (Cat# 15596026; Invitrogen) according to the manufacturer's protocol. One microgram of purified total RNA was treated with amplification grade DNase I (Cat# AMPD1; Sigma) according to the manufacturer's recommendations, and 250 ng RNA seeded into a reverse transcription reaction using the SuperScriptII system (Cat# 18064-071; Invitrogen) by combining 1 µl random hexamer oligonucleotides (Cat# 48190011; Invitrogen), 1 µl 10 mM dNTP (Cat# 18427-013; Invitrogen), and 11 µl RNA plus water. This mixture was brought to 70°C for 5 minutes and then cooled to room temperature. SuperScriptII reaction buffer, DTT, and SuperScriptII were then added according to manufacturer's protocol, and the mixture brought to 25°C for 5 minutes, 42°C for 50 minutes, 45°C for 20 minutes, 50°C for 15 minutes, and then 70°C for 5 minutes. Relative levels of candidate gene transcripts were analyzed using the Dynamo Flash

mastermix according to the recommended protocol. Reactions were performed on a Bio-Rad CFX38. Primer sequences are listed in Additional file 3.

Histone Methyltransferase Activity Assay

Cells were dissociated, washed twice in PBS, pelleted, and nuclear extracts prepared. Briefly, cell pellets were initially resuspended in 200 µL of Buffer A (10 mM HEPES, 10 mM KCl, 0.1 mM EDTA). Following a 10 minute incubation, samples were centrifuged at 20,000 x g for 3 minutes at 4°C. The supernatants were removed and nuclei resuspended in 30 µL Buffer B (20mM HEPES, 0.4 M NaCl, 1 mM EDTA, 10% glycerol). Samples were shaken at 1,000 RPM for 2 hours followed by centrifugation at 20,000 x g for 5 minutes. H3K27 Methyltransferase activity was assayed using the EpiQuik HMT Activity Assay Kit (Cat# P-3005; Epigentek), according to the manufacturer's instructions. Absorbance was measured on a Cary Eclipse microplate reader (Agilent Technologies) at a wavelength of 450nm. Activity was calculated according to the manufacturer's instructions.

Analysis of Cellular Stress and Apoptosis

Intracellular Glutathione Assay – One million cells were prepared in 1 mL warm DMEM F-12 (Cat# 11320-033; Invitrogen), and glutathione measured using an Intracellular GSH detection assay (Cat# ab112132; Abcam) following the manufacturer's recommendations. Fluorescence was monitored using an Accuri C6 flow cytometer (BD Biosciences).

Lactate Dehydrogenase Assay – One million cells were collected and LDH levels quantified using a Lactate Dehydrogenase Activity Assay Kit (Cat# MAK066; Sigma), according to the recommended protocol. Measurements were taken using a Cary Eclipse microplate reader (Agilent Technologies) at a wavelength of 450nm.

Annexin V Apoptosis Assay – Cells were examined using the Annexin V Apoptosis Detection Kit (APC; Cat# 88-8007; eBioscience). Five million cells were washed once in PBS and resuspended in Binding Buffer. 5 µL of Annexin V was added to

100uL of cell suspension and incubated for 15 minutes at room temperature. Cells were then washed in PBS and resuspended in 200 µL of Binding Buffer. 5 µL of Propidium Iodide solution was added, and cells analyzed using an Accuri C6 flow cytometer (BD Biosciences).

TUNEL Assay – Using a APO-BrdU TUNEL Assay Kit (Cat# A35127; Invitrogen), one million cells were fixed using paraformaldehyde and resuspended in 50 µL DNA labeling solution according to the manufacturer's protocols. 500 µL of propidium iodide/RNase A staining buffer was added to each sample and incubated for an additional 30 minutes at room temperature in the dark. Samples were analyzed using an Accuri C6 flow cytometer (BD Biosciences).

Analysis of DNA Methylation and DNA Hydroxymethylation

Genomic DNA was isolated from treated neurospheres using the DNeasy Blood and Tissue kit (Cat# 69506; QIAGEN) according to the recommended protocol. We utilized glucosylation of genomic DNA followed by methylation-sensitive qPCR (glucMS-qPCR) to quantify levels of 5-methyl-cytosine and 5-hydroxy-methyl-cytosine. Here, 30 µg of genomic DNA was treated with 30 units of T4 phage β-glucosyltransferase (T4 BGT, Cat# M0357S; NEB) at 37°C overnight. Glycosylated genomic DNA was then digested with 100 units of MspI (Cat# R0106M; NEB) or 50 units of HpaII (Cat# R0171L; NEB), or no enzyme at 37°C overnight. Reactions were inactivated by treatment with proteinase K (Cat# 19133; QIAGEN) at 40°C for 30 minutes. The proteinase K was inactivated by incubation at 95°C for 10 minutes. The HpaII- or MspI-resistant fractions were quantified by qPCR using primers designed around a single HpaII/MspI site. Primers listed in Table S1 - Primer Sequences. Levels of 5-methyl-cytosine were determined by calculating differences in HpaII- vs. MspI- digested samples using the following formula: **[*% methylation = (2*$^{(\text{Uncut T4BGT treated} - \text{HpaII cut T4BGT treated})}$ *– 2*$^{(\text{Uncut T4BGT treated} - \text{MspI cut T4BGT treated})}$*) x 100*]**. Levels of 5-hydroxy-methyl-cytosine were determined by calculating the difference between glucosylated samples and genomic DNA digested with MspI

using the following formula: **[*% hydroxymethylation = (2*$^{(Uncut\ T4BGT\ treated\ -\ MspI\ cut\ T4BGT\ treated)}$ *– 2*$^{(Uncut\ -\ MspI\ cut)}$*) x 100*]**.

Statistical Analysis

For all experiments, statistical significance was set at alpha = 0.05.

For analysis of gene expression, the replicate cycle threshold (CT) values for each transcript were compiled and normalized to the geometric mean of the reference genes phosphoglycerate kinase 1 (Pgk1—NM_008828), glyceraldehyde 3-phosphate dehydrogenase (Gapdh—NM_008084), and hypoxanthine-phosphoribosyl transferase (Hprt—NM_013556). From our previous studies of 14 candidate reference genes in EtOH-exposed cultures, *Pgk1*, *Gapdh*, and *Hprt* have been validated as stable across the range of alcohol treatments utilized in this study (Carnahan et al., 2013). Normalized expression levels were calculated using the DDCT method described previously (Schmittgen and Livak, 2008). Values from each biological replicate were transferred into the statistical analysis program GraphPad (GraphPad Software, Inc., La Jolla, CA), verified for normality, and an analysis of variance (ANOVA) run to assay differences between experimental treatments. For samples with p-values < 0.05, we applied Tukey's HSD analysis for multiple comparisons, and have marked statistically significant differences with an asterisk.

For quantitative analysis of candidate gene regulatory region enrichment in primary fetal cerebral cortical neuroepithelial stem cells, ChIP samples were first normalized to 1% input, using the formula previously described by Mukhopadhyay et al., 2008 (Mukhopadhyay et al., 2008). To independently examine alterations in each post-translational modification, the means from each independent sample were normalized to the control. The results of 3 independent experiments were then tabulated, cumulative means calculated and standard error of the mean derived. The statistical analysis package GraphPad was used to first measure the normality of samples using the D'Agostino-Pearson test. As several of the candidate genes did not exhibit a normal distribution, we quantified differences between control and

EtOH-treated samples using the Wilcoxon Signed Rank Test. This non-parametric test is applied when the population has unequal variances and cannot be assumed to be normally distributed. Importantly, this test has been widely employed in genome wide studies of histone variants, histone post-translational marks and transcription factor binding (Liu et al., 2013; Nakato et al., 2013).

For quantitative analysis of candidate gene regulatory region enrichment in fetal forebrains, ChIP samples were normalized to 1% input, using the formula previously described (Mukhopadhyay et al., 2008). The cumulative mean from each of the 3 independent experiments calculated and the standard error of the mean derived. The statistical analysis package GraphPad was used to verify normality, and assay differences between each of the control, EtOH exposed - morphologically normal, and EtOH exposed - malformed samples using a two-way analysis of variance (ANOVA).

For quantitative analysis of DNA methylation, percentages of DNA 5-methylcytosine and 5-hydroxymethylcytosine derived from the formulas listed above were transferred into the statistical analysis package GraphPad, verified for normality, and an analysis of variance (ANOVA) run to assay differences between experimental treatments. A Student's t-test was run to assay differences between Days 3 and 7 among all samples tested.

CHAPTER VI

UNIQUE, DOSE-DEPENDENT ALTERATIONS IN CHROMATIN STRUCTURE BEHAVE INDEPENDENTLY OF TRANSCRIPTIONAL RESPONSE IN A MURINE EMBRYONIC STEM CELL MODEL OF ACUTE ETHANOL EXPOSURE

Introduction

The preimplantation blastocyst is made up of the trophectoderm, extraembryonic endoderm, and the inner cell mass, which become the placenta, the yolk sac, and the embryo, respectively. The inner cell mass is made up of pluripotent embryonic stem cells (ESCs), which have the capacity to become any differentiated cell type within the embryo proper. The differentiation of these cells along specific lineages requires the coordinated recruitment of chromatin modifying enzymes at precise time points during development. The recruitment of these chromatin modifiers establish epigenetic marks that are associated with patterns of lineage-specific gene expression, which guide the cell through the transcriptional states required to transition from pluripotency towards a terminal state that performs a specific function required within the body. Recent evidence suggest this phase of development sets the stage for life-long health and is extremely susceptible to environmental factors that the embryo is exposed to during development. Environment-induced alterations in developmental programming can have long term impacts on adult health and disease.

Chromatin structure is regulated through interactions with chromatin modifying enzymes and is associated with the establishment of epigenetic signatures of gene expression. Epigenetics is defined as heritable influences in gene expression that are not caused by the DNA sequence itself, including DNA methylation and histone modifications. These signatures represent a cellular memory of gene expression, in which the information contained within the chromatin structure can last through many cell divisions and allow the cell to both establish and maintain its identity. Cellular memory and heritability of chromatin structure are essential as cells divide along the multitude of developmental pathways required

during mammalian gestation. Through heritable chromatin structure, daughter cells are able to retain their identity as differentiation progresses. Chromatin structure is plastic, therefore developmentally sensitive time periods occur as cellular identity is being established. Epigenetic signatures and their associated chromatin structure are highly dynamic, and can be altered by exposure to external or environmental factors. Changes in these signatures during an environmental insult can be associated with aberrations in development, and possibly a halt in cellular differentiation altogether.

Many teratogens are suspected of impacting the epigenome, however, given an acute exposure, the question remains of whether the observed changes in chromatin structure persists after the environmental exposure. For example, alcohol has been shown to alter development and has been associated with acute changes in both DNA methylation and histone modifications, but to date there have not been studies examining the heritability of changes in chromatin structure after the removal of alcohol.

Alcohol has been shown to affect both DNA methylation and histone modifications (Veazey et al., 2013; Zakhari, 2013). Work to date suggests the effects of alcohol can be attributed to depletion of methyl groups and oxidative stress caused by alcohol metabolism, which in turn effect the availability of metabolites to contribute to DNA and histone methylation. While this mechanism seems plausible, and alcohol-induced changes to chromatin structure have been reported, no specific mechanism of alcohol-chromatin interaction has been elucidated. Although several models have examined epigenetic alterations in stem cells in response to alcohol exposure, many utilize chronic models of exposure or endpoint studies, and fail to examine whether stem cells have the capacity to resolve alcohol-induced epigenetic alterations after ethanol is removed from the system. If FASD phenotypes are linked to alcohol, then changes to chromatin structure would persist after exposure and correlate with alteration in gene expression. It is important to decipher the heritability of ethanol-induced changes in chromatin structure post-exposure because controversy remains over the concept that histone modifications are a true

epigenetic mark, i.e. heritable and causal in the case of environmentally-affected phenotypes (Henikoff and Shilatifard, 2011).

In our previous study, we tested the heritability of ethanol-induced changes in chromatin structure using a murine neural stem cell model (Veazey et al., 2015). After acute exposure to ethanol, histone marks displayed lasting alterations at promoters of genes regulating core aspects of neural differentiation. Changes in expression of these genes persisted after a 4-day recovery period in which no ethanol was present. In light of this evidence, we were curious as to whether ethanol-induced changes in chromatin structure are tied to the differentiation state of the cell. In order to test the question of whether alcohol-induced changes persist past the window of exposure in a higher stem cell state, we employed a murine embryonic stem cell model of acute alcohol exposure, followed by an extended recovery period. Embryonic stem cells are a particularly well-suited cell type for examining changes to chromatin structure as large parts of their genome are in a poised chromatin configuration that can be accessed by transcription machinery (reviewed in Chen and Dent, 2013). We monitored changes in histone modifications at promoters of genes regulating pluripotency and core aspects of neural differentiation and their dynamics during a period of exposure and during a recovery period. Changes in the expression of these genes, as well as select epigenetic modifiers and genes regulating oxidative stress pathways were monitored throughout the exposure and recovery periods. Similar to our previous study in neural stem cells, we find that changes in post-translational histone modifications are dose-dependent as well as histone-mark-dependent. The extent and “direction” of the changes in histone marks also differ between the exposure period and the recovery period. The changes in marks persist up to 10 days after ethanol exposure, but the fluctuations in marks slowly begin to return to near control levels. Unlike our findings in neural stem cells, these changes occur despite few changes in the expression of the genes tested, and minimal changes in the expression of key genes involved in oxidative stress response pathways and chromatin modification.

Materials and Methods

Embryonic Stem Cell Culture

Primary embryonic stem cells (ESCs) were derived from B6XCAST F_1 embryos (Golding et al., 2010). This genotype allows the examination of allele specific expression and epigenetic modifications in a parent of origin specific fashion. ESCs were maintained in ESC media under 3i conditions (Yamaji et al., 2013) containing DMEM (Cat# D5671; Sigma) supplemented with 50µg/ml penicillin/streptomycin (Cat# P4333; Sigma), 100 µM B-mercaptoethanol (Cat# M3148; Sigma) , 1x LIF (Cat# L5158;Sigma), 1x MBIO (Cat# B1686; Sigma), 2 mM L-Glutamine (Cat# G3126; Sigma), 1x MEM nonessential amino acids (Cat# M7145; Sigma), and 15% hyclone ESC grade fetal bovine serum (Cat# SH30080.03E; GE Healthcare). ESCs were maintained on mitomycin C (Cat# M4287; Sigma)-treated feeder fibroblast layer, and media was changed every 48 hours. When passaging, cells were washed twice with 1x PBS, then disassociated with 1x Accutase (Cat# SF006; Millipore) and split 1:20 onto a new feeder layer. To prevent contamination from underlying feeder layers, ESCs were expanded into feeder-free flasks in preparation for treatments.

Ethanol Exposure

The concentrations of alcohol utilized in this study are meant to mimic those obtained from a casual and a binge drinker. For the casual drinker we selected the legal limit for operating a motor vehicle, 80mg/dL. For a binge drinker we utilized projected concentrations based on observations by White et al. which demonstrated that out of 7,356 college age females surveyed, 33.7% reported typical consumption rates at 1 x binge alcohol levels (four or more drinks at a time) and 8.2% reported consumption at 2 x binge levels (eight or more drinks at a time) (White et al., 2006). Based on average height and weight, these rates of consumption would yield blood alcohol levels in the range of 160mg/dL and 240 mg/dL respectively (Wisconsin Department of Transportation, Division of State Patrol). The alcohol

treatment groups were cultured in ESC medium containing no ethanol, 80 mg/dL, 160 mg/dL or 240 mg/dL ethanol and the lid was sealed with parafilm to prevent evaporation. The medium and treatment were replaced every 48 hours. Cellular extracts were taken for chromatin immunoprecipitation and RNA analysis at day 4 (ethanol exposure time period), day 8 (4 days post ethanol exposure), and day 14 (10 days post ethanol exposure).

Neural Differentiation of Ethanol-Exposed ESCs

ESCs were exposed to ethanol and allowed to recover in 3i medium maintaining a base level of stemness as described above. Following recovery, ESCs were split into flasks containing 50% ESC media (described above), and 50% Neural stem cell (NSC) media containing a 50%/50% mixture of Neurobasal media (Cat# 21103-049; Invitrogen) and DMEM F-12 (Cat# 11320-033; Invitrogen) supplemented with the N2-supplement (Cat# 17502-048; Invitrogen), B27 supplement (Cat# 17504-044; Invitrogen), 0.05% TC grade BSA in PBS (Cat# A1933 Sigma), 2mM L-glutamine (Cat# 25030-081; Invitrogen), 1 x Penicillin/Streptomycin (Cat# 15140-122; Invitrogen), 20 µg/ml FGF basic (Cat# PMG0034; Invitrogen), 20 µg/ml EGF (Cat# PHG0311; Invitrogen), and 0.85 units/ml heparin (Cat# H3149; Sigma). After 5 days, cells were moved into laminin-coated flasks containing 25% ESC media and 75% NSC media for final differentiation. At 10 days, cells were split into laminin-coated flasks with NSC media only. Samples were taken for flow cytometry at Day 4 (EtOH-exposed), Day 14 (recovery –ESC media), and Day 19 (5-day differentiation).

Chromatin Immunoprecipitation Analysis

Cells were grown to 80% confluence, washed twice in warm PBS, trypsinized, and re-suspended in warm medium (DMEM F-12 Cat# 11320-033; Invitrogen) containing 0.1 volume crosslinking solution (Kondo et al., 2004). ChIP reactions were performed as described previously (Martens et al., 2005) followed by DNA purification with a Qiaquick PCR Cleanup kit (Cat# 28106; QIAGEN). Antibodies used include: anti-H3K4me3 (Cat# 04-745; Millipore), anti-H3K27me3 (Cat# 39155;

Active Motif), anti-H3K9ac (Cat# 07-352; Millipore), anti-H3K9me2 (Cat# 39239; Active Motif), and anti-Ezh2 (Cat# 17-662; Millipore). Antibodies for modified histones were used at 1 µg/ChIP reaction. The concentration of IgG (Cat# SC-2027; Santa Cruz) was also used at 1 ug/ChIP reaction. For analysis of candidate loci, real-time PCR was performed with the Dynamo Flash supermix (Cat# F-415XL; Thermo Scientific) according to the recommended protocol. Reactions were performed on a Bio-Rad CFX384 Touch PCR system. Data was analyzed using the formula previously described (Mukhopadhyay et al., 2008). Primer sequences are listed in Table S1- Primer Sequences.

RNA Analysis

Cultured cells were grown to 80% confluence, washed twice in warm PBS, and dissociated with 0.5x Accutase (Cat# SCR005; Millipore). Cells were spun down, washed once in cold PBS, and RNA isolated using Trizol (Cat# 15596026; Invitrogen) according to the manufacturer's protocol. One microgram of purified total RNA was treated with amplification grade DNase I (Cat# AMPD1; Sigma) according to the manufacturer's recommendations, and 250 ng RNA seeded into a reverse transcription reaction using the SuperScriptII system (Cat# 18064-071; Invitrogen) by combining 1 µl random hexamer oligonucleotides (Cat# 48190011; Invitrogen), 1 µl 10 mM dNTP (Cat# 18427-013; Invitrogen), and 11 µl RNA plus water. This mixture was brought to 70°C for 5 minutes and then cooled to room temperature. SuperScriptII reaction buffer, DTT, and SuperScriptII were then added according to manufacturer's protocol, and the mixture brought to 25°C for 5 minutes, 42°C for 50 minutes, 45°C for 20 minutes, 50°C for 15 minutes, and then 70°C for 5 minutes. Relative levels of candidate gene transcripts were analyzed using the Dynamo Flash mastermix according to the recommended protocol. Reactions were performed on a Bio-Rad CFX38. Primers are listed in Table S1 - Primer Sequences.

Flow Cytometry

Flow cytometry was performed using conjugated antibodies to CD90.2 (Cat#; BD Biosciences) and CD24a (Cat#; BD Biosciences). About 5 million cells were

washed in 1ml PBS + 0.1% BSA and incubated with 0.3 ul of each antibody in 100ul PBS +BSA for 20 minutes at 4 C. Cells were then washed again in 1ml PBS + BSA, then resuspended in 300 ul PBS+BSA and analyzed using a Beckman Coulter Gallios Flow Cytometer. Populations were visualized using the Kaluza Flow Analysis Software.

Statistical Analysis

For all experiments, statistical significance was set at alpha = 0.05. This value is widely accepted as a level of significance in biomedical research, and has been established by statisticians as an adequate cutoff to denote that the changes observed are not occurring by chance ([NO STYLE for: Fisher 1992]; Bross, 1971). For this study, we chose alpha = 0.05 as a statistical cutoff because we believe that in a panel of 25 genes, which is a relatively small study compared to genome-wide approaches, alterations that occur by chance would likely not be included.

For analysis of gene expression, the replicate cycle threshold (CT) values for each transcript were compiled and normalized to the geometric mean of the reference genes peptidylprolyl isomerase A (Ppia—NM_008907), glyceraldehyde 3-phosphate dehydrogenase (Gapdh—NM_008084), and hypoxanthine-phosphoribosyl transferase (Hprt—NM_013556). From our previous studies of 14 candidate reference genes in EtOH-exposed cultures, Ppia, Gapdh, and Hprt have been validated as stable across the range of alcohol treatments utilized in this study (Carnahan et al., 2013). Normalized expression levels were calculated using the DDCT method described previously (Schmittgen and Livak, 2008). Relative fold change values from each biological replicate were transferred into the statistical analysis program GraphPad (GraphPad Software, Inc., La Jolla, CA), verified for normality using the Brown-Forsythe test, and an analysis of variance (ANOVA) utilized to assay differences between experimental treatments. For comparisons with p-values < 0.05, we applied Tukey's HSD analysis for multiple comparisons, and have marked statistically significant differences with an asterisk.

For quantitative analysis of candidate gene regulatory region enrichment in ESCs, ChIP samples were first normalized to 1% input, using the formula previously described (Mukhopadhyay et al., 2008). To independently examine alterations in each post-translational modification, the means from each independent sample were normalized to the control. The results of 3 independent experiments were then tabulated, cumulative means calculated and standard error of the mean derived. Values from each biological replicate were transferred into the statistical analysis program GraphPad (GraphPad Software, Inc., La Jolla, CA), verified for normality using the Brown-Forsythe test, and an analysis of variance (ANOVA) run to assay differences between experimental treatments. For samples with p-values < 0.05, we applied Tukey's HSD analysis for multiple comparisons, and have marked statistically significant differences with an asterisk.

Results

Effects of Ethanol on Chromatin Structure During Exposure and After Recovery are Dose-Dependent and Signature-Specific

In order to analyze the heritability of changes in chromatin structure induced upon ethanol exposure at a higher state of stemness than neural stem cells, we employed a murine embryonic stem cell (ESC) model in which we treated cells for four days with physiologically relevant concentrations of ethanol (80 mg/dL, 160 mg/dL, and 240 mg/dL). After the four-day exposure period, ethanol was removed from the media and ESCs were allowed to recover for a 10-day period (Fig. 1A). Samples were taken at days 4, 8, and 14, which represent acute response, 4 day recovery, and 10 day recovery, respectively. These samples were analyzed for histone post-translational modifications associated with permissive chromatin structure (histone 3 lysine 4 trimethylation and histone 3 lysine 9 acetylation) and repressive chromatin structure (histone 3 lysine 27 trimethylation and histone 3 lysine 9 dimethylation) via chromatin immunoprecipitation. These post-translational modifications can be found at promoters of genes regulating lineage commitment in ESCs, and provide good representation of marks commonly associated with

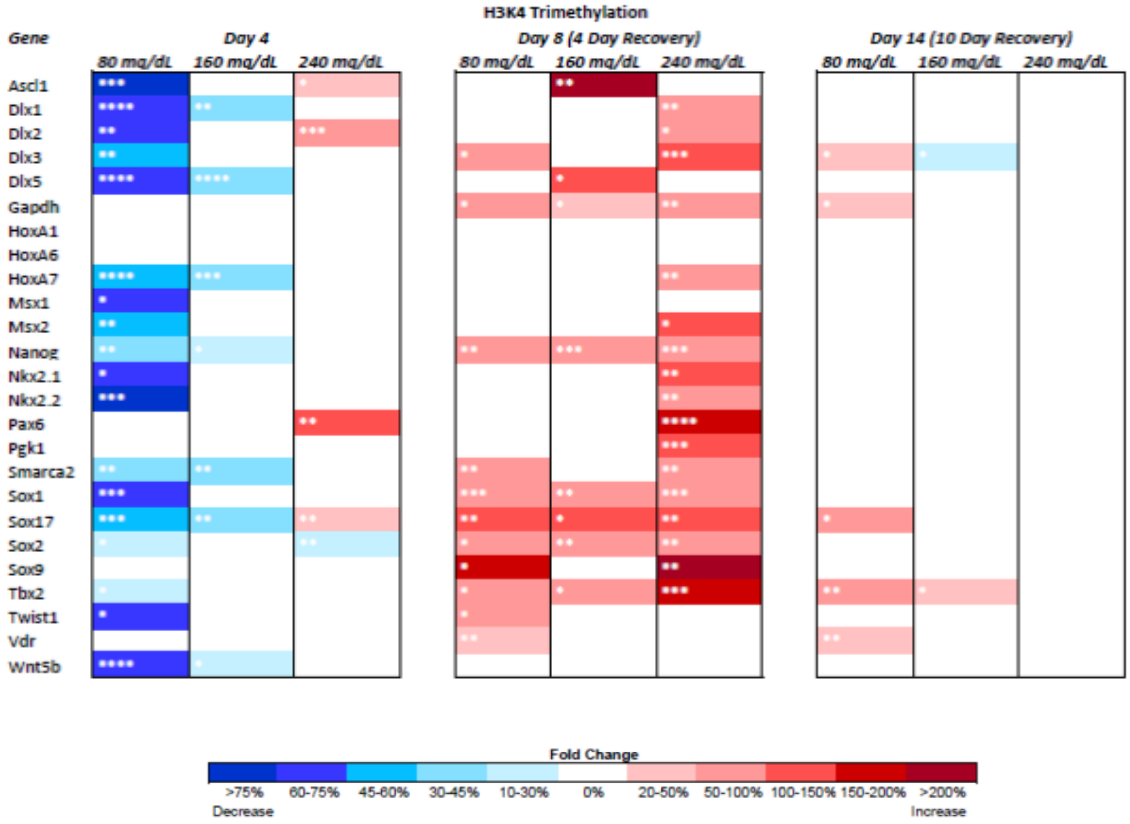

Figure 22: Dose-dependent and histone modification-specific changes in chromatin structure upon exposure to ethanol. Murine embryonic stem cells were cultured in varying concentrations of ethanol (80mg/dL, 160 mg/dL, or 240 mg/dL) for four days, followed by a no-ethanol recovery period for ten days. Samples were taken at days 4, 8, and 14 for chromatin immunoprecipitation with antibodies for H3K4me3, H3K9ac, H3K27me3, and H3K9me2. Levels of histone marks were then analyzed via qPCR with primers to the promoters of known regulatory genes in neural development. Samples were normalized to % Input and analyzed relative to control levels. The heat map represents significant fold changes compared to the control group. N=3. * p<0.05, ** p<0.01, *** p<0.001, **** p<0.0001.

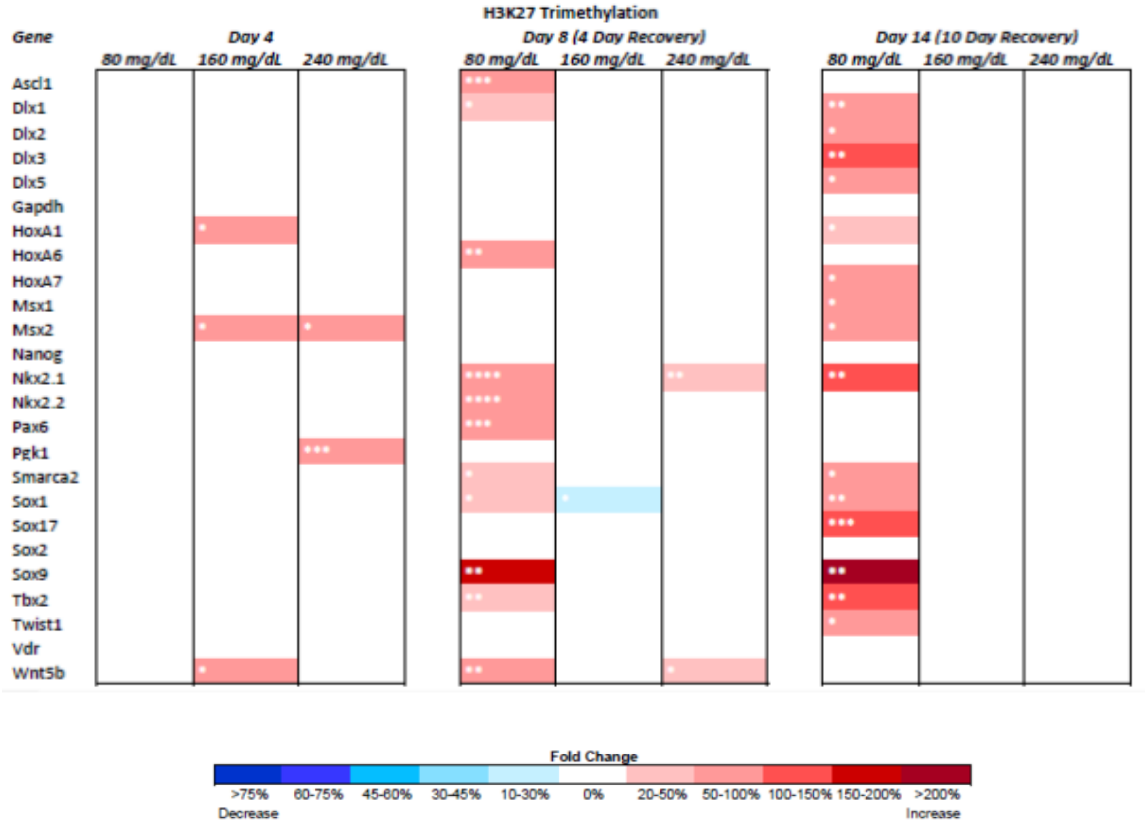

Figure 22 Continued

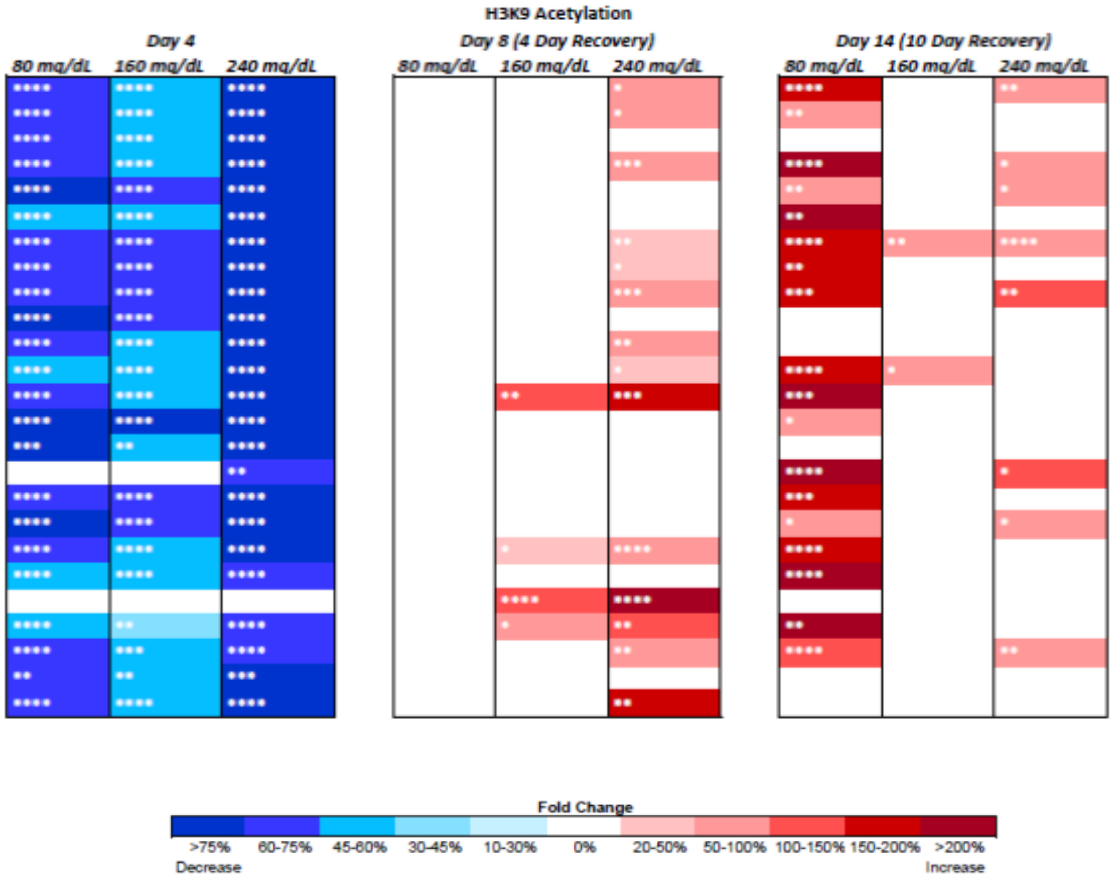

Figure 22 Continued

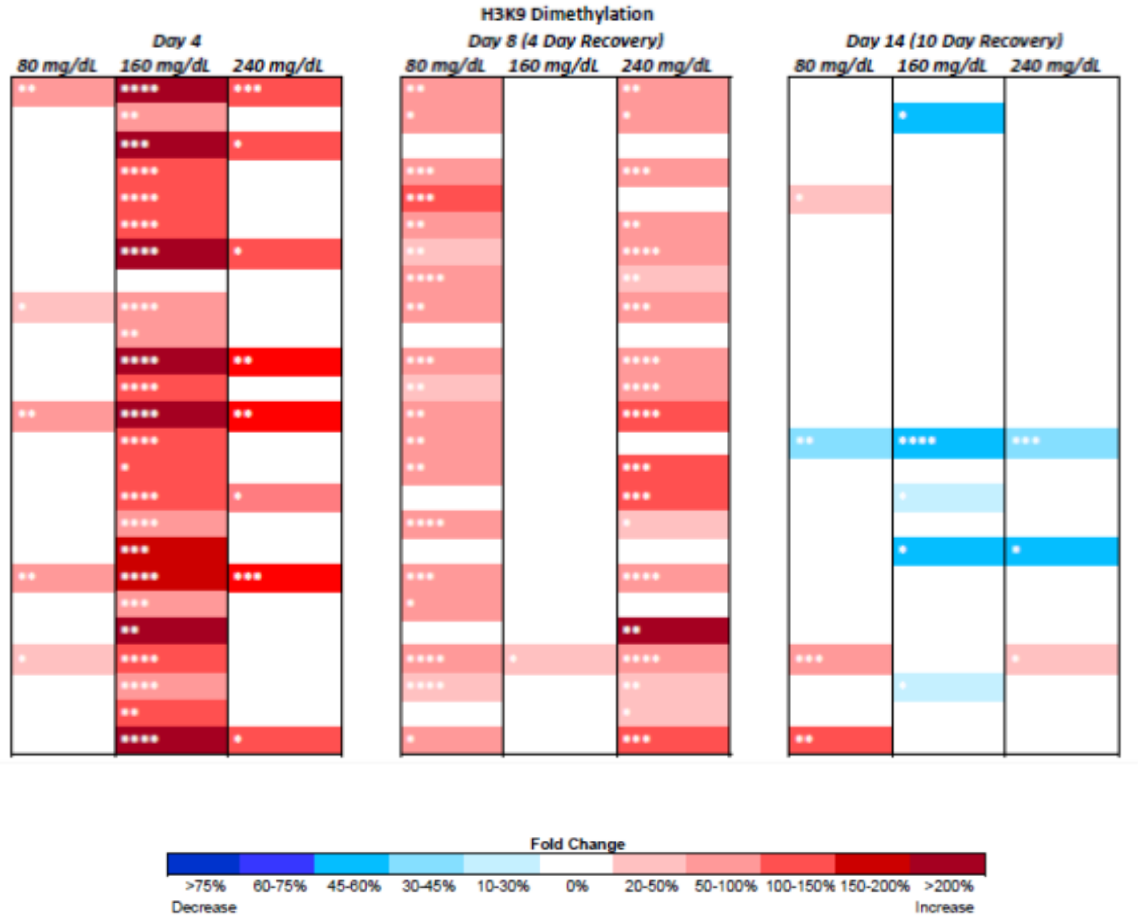

Figure 22 Continued

repressive chromatin and permissive chromatin throughout development. qPCR was employed to examine extracts for the enrichment or loss these modifications on a panel of 25 genes. These genes were chosen given their roles in neural development and their involvement with the establishment of functions characteristically impaired in FASD children (Rugg-Gunn et al., 2010; Kuegler et al., 2010; Zhou et al., 2011).

A comprehensive map of the effects observed upon ethanol exposure and after recovery are presented in Figure 1B. Each post-translational modification examined behaves differently upon insult by alcohol exposure. After four days of ethanol exposure, especially in low dose groups (80 mg/dL) marks associated with open chromatin configuration are decreased compared to control levels. At higher doses, each mark behaves differently, with H3K4 me3 becoming high at Day-8 in many genes but leveling off toward levels comparable to control by Day-14, and H3K9 ac becoming high by Day-8 in 240 mg/dL, and high by day 14 at 80 mg/dL. It is important to note that H3K9 acetylation is widely reduced upon ethanol exposure in all concentrations tested, but this reduction reverses after ethanol is removed from the system.

Marks associated with repressive chromatin states are also uniquely affected, and do not follow an inverse relationship with marks associated with a permissive chromatin state. H3K9 me2 is at significantly high levels at day 4 in the 160 mg/dL treatment group, but returns to control levels after a 4 day recovery, and levels at least 45% lower than control in the neural regulators *Nkx2.2*, *Dlx1*, and *Sox1* by Day-14. Despite these changes, H3K9ac was inversely affected by ethanol at day 4 compared to changes in H3K9me2, but did not display this inverse relationship after recovery. At day 8, when samples exposed to 80 mg/dL and 240 mg/dL doses of showed high levels of H3K9me2, no inverse relationship was apparent in H3K9ac. H3K27me3 showed fewer changes in levels than the other marks tested, as this mark was only increased in the 80 mg/dL group at day 8 and day 14. These observations suggest that epigenetic changes upon EtOH exposure and after recovery are variable and dependent on dose of EtOH, gene of interest, and histone

mark of interest. As the penetrance of FASDs is also highly variable, these observations may be relevant to the molecular basis underlying the disorder.

Changes in Chromatin Structure at Homeobox Gene Promoters Do Not Correlate with Transcriptional Status During or After the Period of EtOH Exposure

The current widely-accepted belief in the field epigenetics is that changes in the post-translational histone modifications are reflective of alterations in chromatin structure at a gene promoter that directly effect the level of expression of the associated gene. We and others have previously challenged this notion using various models of ethanol exposure (Veazey et al., 2015; Zhou et al., 2011; Ponomarev et al., 2012). Furthermore, others have called into question the true significance of histone marks as a heritable epigenetic mark, and cast doubt as to if they have a causal role in transcriptional regulation rather than a correlative one – id est cause or consequence (Henikoff and Shilatifard, 2011). To determine whether this phenomenon was present in a pluripotent cell type, where chromatin is generally hypothesized to be in a more open configuration than in differentiated cell types (Chen and Dent, 2013). To determine if the genes displaying alterations in chromatin marks during or after EtOH exposure also display alterations in gene expression, RNA was isolated from all treatment groups utilized in our ChIP experiments and gene expression was analyzed using reverse transcriptase polymerase chain reaction (RT-qPCR). Of our 25 candidate genes involved in neural differentiation, we were able to detect *Ascl1*, *Msx2*, *Nanog*, *Oct4*, *Smarca2*, and *Sox2* transcripts in embryonic stem cells (Figure 2). Only *Nanog* displayed an increase in expression at day 4 and day 8 in the 160 mg/dL EtOH-exposed ESCs. The only other gene that displayed a significant change was *Sox2*, which increased in expression at day 8 in the 160 mg/dL EtOH-exposed cells. Interestingly, these changes in pluripotency-associated transcription factors agree with previous work stating that ethanol exposure alters the balance of Sox2 and Nanog in ESCs (Ogony et al., 2013).

Exposure to EtOH is Not Associated with Lasting Changes in the Expression of DNA Methyltransferases, Histone Methyltransferases, or Histone Demethylases

Using primary neural stem cells, we have previously shown that transcripts encoding the H3K27 and H3K9 methyltransferases, as well as H3K9 demethylases and DNA methyltransferases are altered upon acute exposure to EtOH, and that these alterations can persist days after the initial period of exposure in (Veazey et al., 2015). We therefore sought to examine whether the same alterations in expression of chromatin modifiers occur in pluripotent stem cells, or if this phenomenon is cell type-specific. We examined transcript levels of the DNA methyltransferases and their associated proteins (*Dnmt1*, *Dnmt3b*, *Uhrf1*, Polycomb Repressive Complex 2 (PRC2) members (*Eed*, *Ezh2*), and the H3K9 methyltransferases (*Ehmt2*, *Setdb1*) (Figure 3a). Upon 4 days of exposure, only *Dnmt1* and *Uhrf1* displayed dose-dependent decreases in expression relative to the control. In the 160 mg/dL dose, transcription levels of *Uhrf1* showed an opposite trend after 4 days of recovery, with increased expression compared to the control group. By 10 days post-exposure, no significant differences were observed in any transcript.

Transcription of the histone methyltransferases were not significantly altered at any concentration of EtOH at day 4. However, after four days of recovery, both members of PRC2 displayed increased expression in the 160 mg/dL exposed ESCs. This increase did not correlate with changes in H3K27me3 at day 8. Interestingly, despite a widespread increase in H3K9me2 at day 4 and day 8, No changes in the expression of *Ehmt2* were detected. These discrepancies between HMT transcript levels and their corresponding histone marks suggest that EtOH may be interfering with the transcription of histone demethylases. In order to test this idea, we measured the relative levels of transcription of two H3K9 demethylases, *Kdm3a* and *Kdm4c* (Figure 3b). Surprisingly, no alterations in transcripts of either enzyme were detected. These observations suggest that lasting changes to the transcriptional regulation of enzymes responsible for imparting chromatin structure are not likely responsible for the observed changes in chromatin structure of ESCs.

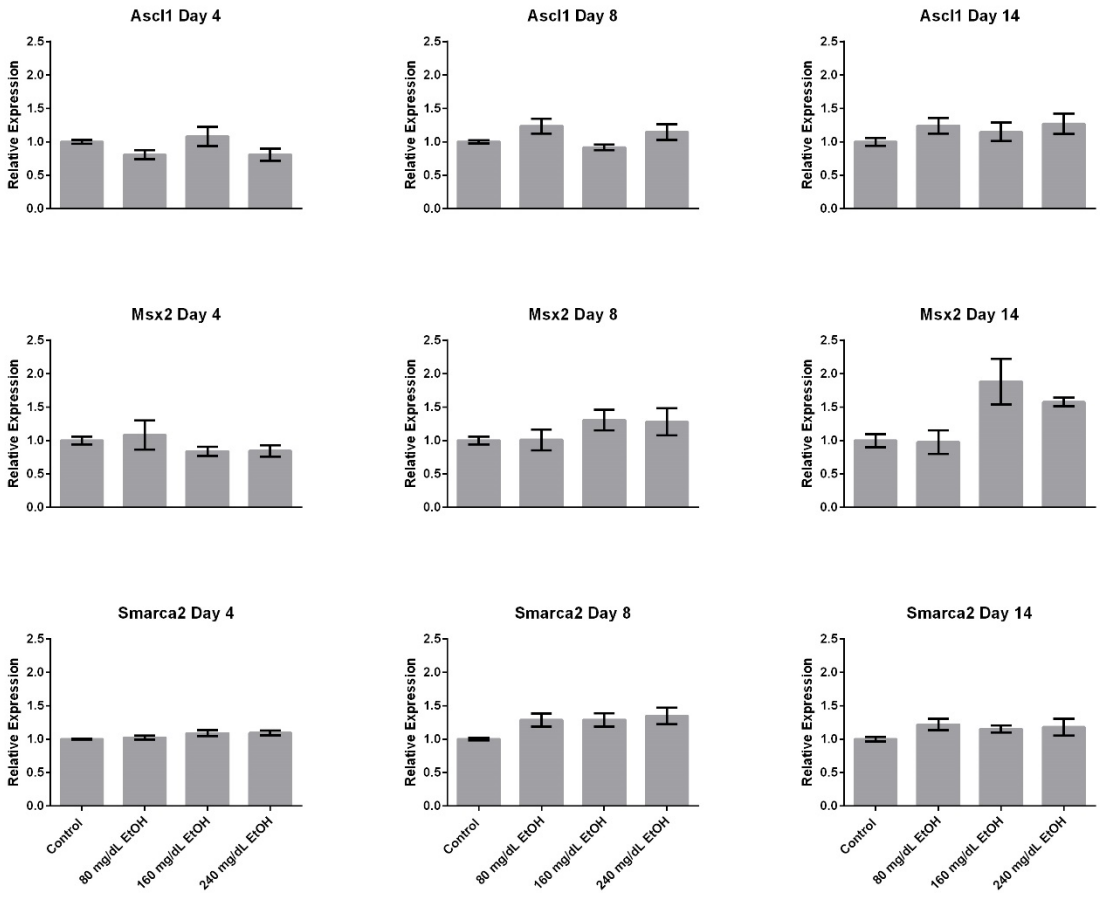

Figure 23: Gene expression of neural developmental genes upon ethanol exposure and recovery. Murine embryonic stem cells were cultured in varying concentrations of ethanol (80mg/dL, 160 mg/dL, or 240 mg/dL) for four days, followed by a no-ethanol recovery period for ten days. Samples were taken at days 4, 8, and 14 for RT-qPCR analysis of expression of genes known to be regulators of neural development. Ct values were graphed relative to control expression, and normalized to the geometric mean of Gapdh, Hprt, and Ppia. N=3. * $p<0.05$, ** $p<0.01$, *** $p<0.001$, **** $p<0.0001$.

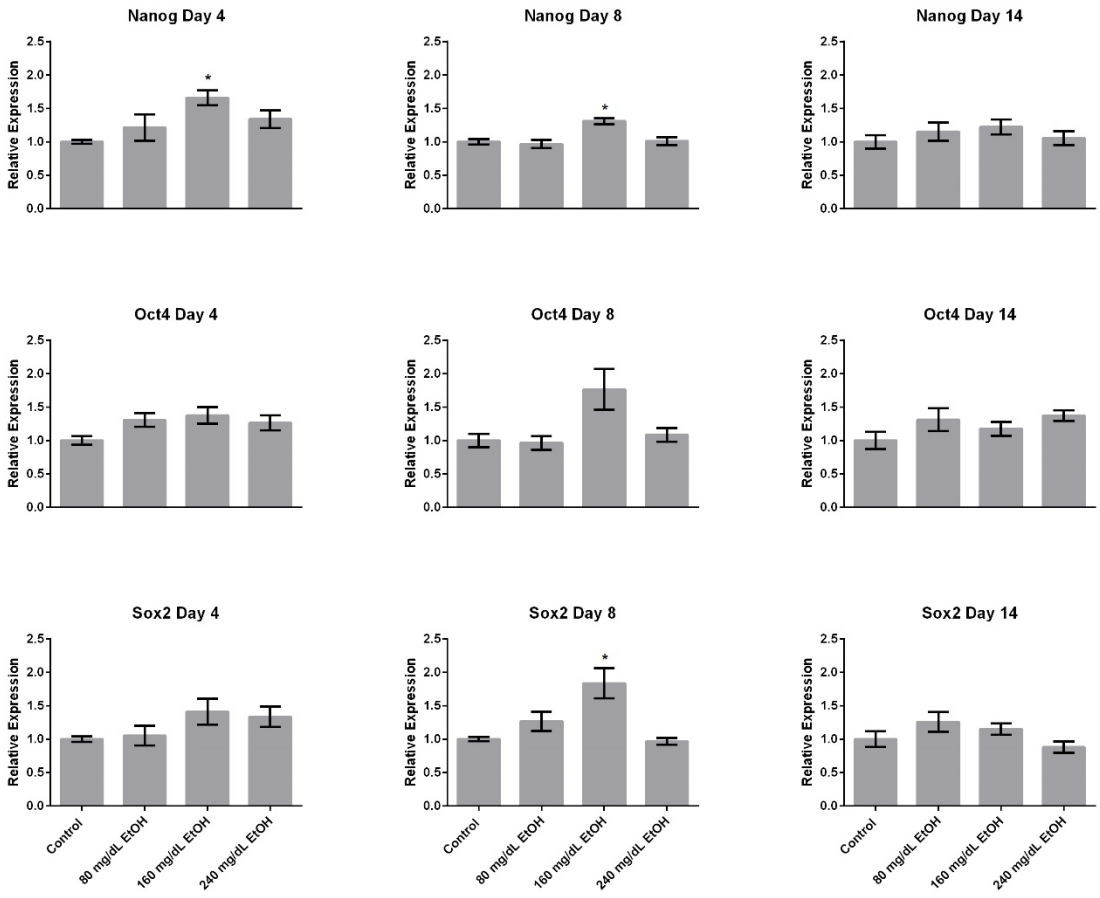

Figure 23 Continued

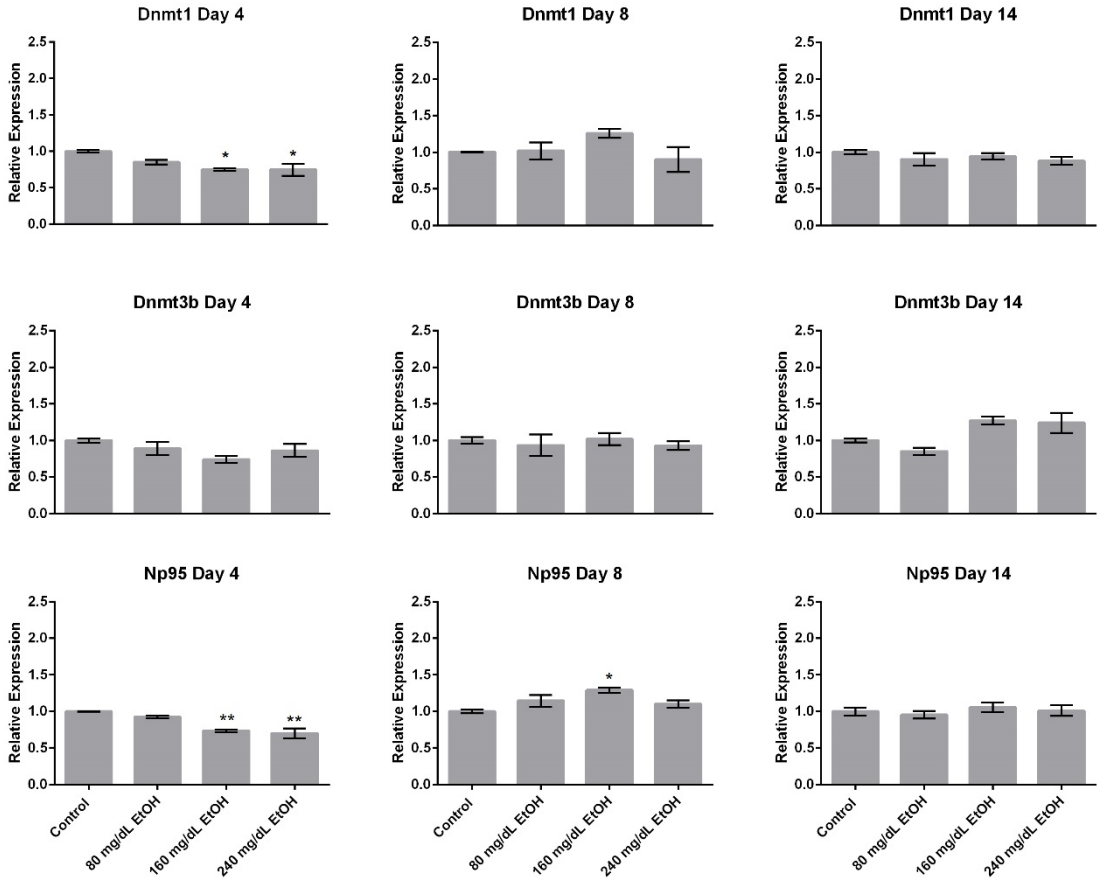

Figure 24: Gene expression of chromatin modifiers and DNA methyltransferases upon ethanol exposure and recovery. Murine embryonic stem cells were cultured in varying concentrations of ethanol (80mg/dL, 160 mg/dL, or 240 mg/dL) for four days, followed by a no-ethanol recovery period for ten days. Samples were taken at days 4, 8, and 14 for RT-qPCR analysis of expression of chromatin remodelers including the enzymes responsible for DNA methylation, H3K27 trimethylation, and H3K9 di- and trimethylation as well as H3K9 demethylases. Ct values were graphed relative to control expression, and normalized to the geometric mean of Gapdh, Hprt, and Ppia. N=3. * $p<0.05$, ** $p<0.01$, *** $p<0.001$, **** $p<0.0001$.

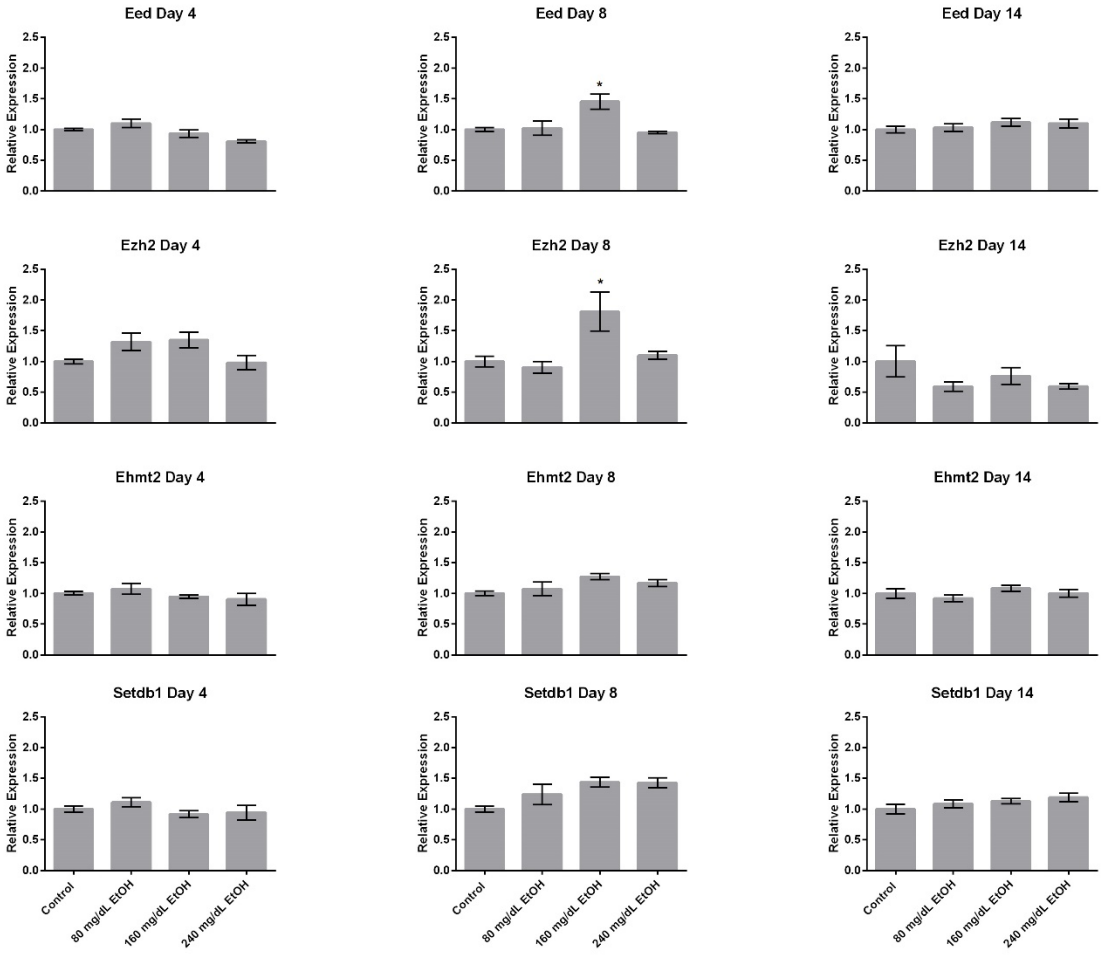

Figure 24 Continued

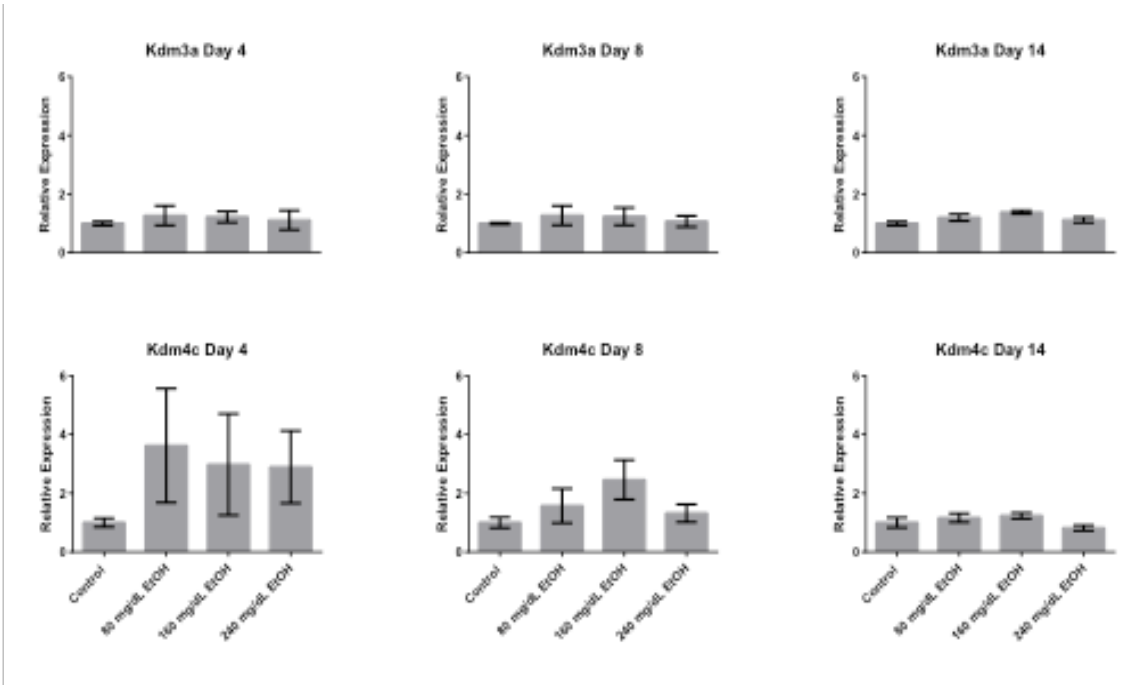

Figure 24 Continued

Exposure to EtOH is Associated with Changes in Expression of Alcohol Metabolism and Tet Genes, but Does Not Cause Significant Alterations in the Oxidative Stress Transcriptional Response

Alcohol metabolism is known to increase reactive oxygen species (ROS), which has been suggested to contribute to the phenotypic effects of EtOH exposure during development (Dong et al., 2008; Brocardo et al., 2011). We therefore sought to examine the link between alcohol metabolism, oxidative stress, and alterations in chromatin structure by monitoring the effects of EtOH on transcription of 20 genes involved in either alcohol processing and/or the oxidative stress response pathways (Figure 4). Of the genes regulating alcohol metabolism, only *Adh* and *Catalase* were expressed in our ESCs. Both displayed increases upon exposure to higher doses of EtOH, *Adh* at only 160 mg/dL, and *Catalase* at both 160 and 240 mg/dL. The only enzyme involved in the oxidative stress pathway that showed altered expression was *Gstm3*, a glutathione S-transferase that functions in the detoxification of electrophilic compounds, whose transcriptional level was increased in the 240 mg/dL-exposed group. Interestingly, all three *Tet* genes displayed changes in expression upon ethanol exposure. The TET family are Fe(II) and a-KG-dependent dioxygenases that utilize oxygen to convert 5-methyl-cytosine (5mC) to 5-hydroxymethyl-cytosine (5hmC), which is an abundant mark in the brain and is considered an intermediate in the DNA demethylation cycle (Tahiliani et al., 2009; Kriaucionis and Heintz, 2009). This DNA demethylation cycle can also influence histone marks including H3K4me3, H3K9me2, and H3K27me3 (Viré et al., 2006; Ciccone et al., 2009; Rothbart et al., 2012). Both *Tet1* and *Tet2* displayed increases in expression (*Tet1* only in 160 mg/dL, and *Tet2* in all EtOH- exposed groups). *Tet3* displayed a reduction in expression in the 240 mg/dL group. These results suggest that changes in histone marks are not likely tied to an oxidative stress response, but may be correlated with changes in 5hmC arising from altered expression of TET family genes.

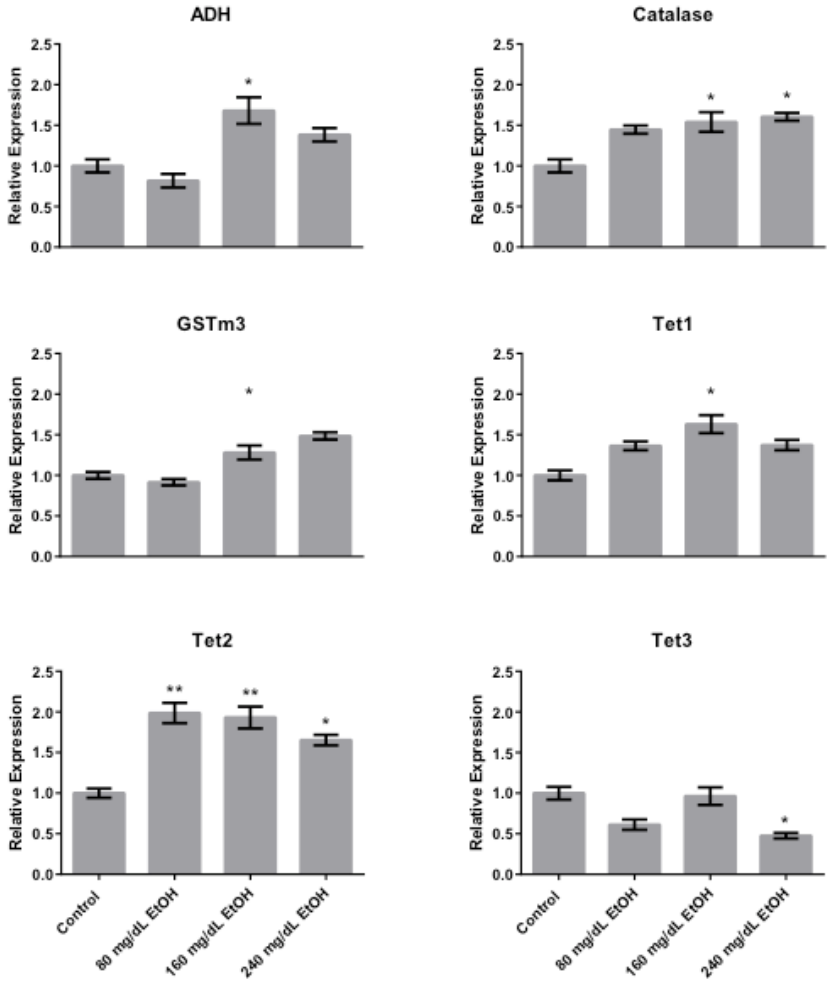

Figure 25: Ethanol exposure does not alter the oxidative stress transcriptional response. Murine embryonic stem cells were cultured in varying concentrations of ethanol (80mg/dL, 160 mg/dL, or 240 mg/dL) for four days and analyzed via RT-qPCR for expression of 20 genes with known roles in the cellular oxidative stress response and alcohol metabolism. Ct values were graphed relative to control expression, and normalized to the geometric mean of Gapdh, Hprt, and Ppia. N=3. * $p<0.05$, ** $p<0.01$.

Acute Exposure to EtOH Does Not Disrupt the Ability of ESCs to Differentiate into Neural Stem Cells

It is important to determine whether acute EtOH exposure and the observed changes in chromatin structure hinder the capacity of *in vitro* cultured ESCs to differentiate along the neural lineage. Resolution of chromatin structure and maintenance of the correct transcriptional program in pluripotent cells after acute ethanol exposure would allow ESCs to maintain their ability to differentiate into neural cells. To determine if this is the case, we exposed ESCs to EtOH for 4 days, followed by a 10 day recovery. After the 10 day recovery, ESCs were allowed to differentiate into neural stem cells (NSCs) for 5 days. We compared the ability of the recovered ESCs to differentiate with cells differentiated entirely in the presence of ethanol. Samples were taken at Days 4 (EtOH-exposed), 8 (4 day recovery, maintaining stemness), and 19 (after 10 day recovery and 5 day differentiation). Recovered ESCs were analyzed via flow cytometry for the expression of neural-specific markers CD90.2 and CD24a (Figure 5). Differentiated cells were found to have increased expression of CD24a, and decreased expression of CD90.2 compared to undifferentiated ESCs. Ethanol exposure was not a factor in the ability of cells to express CD24a, or the loss of CD90.2. Cell morphology was monitored throughout the experiment, and cells with axonal growths were observed in all groups that were allowed to recover before differentiation (Fig. 26). These observations suggest that the restoration of chromatin structure in the pluripotent state allows cells to regain their capacity to differentiate into neural stem cells after environmental insult.

Discussion

Our previous studies have defined changes in chromatin structure as a result of ethanol insult that persist beyond the window of exposure in neural stem cells (Veazey et al., 2013; Veazey et al., 2015). In this study we sought to examine whether ethanol-induced alterations in chromatin structure are tied to the differentiation state of the cell. We accomplished this by examining epigenetic

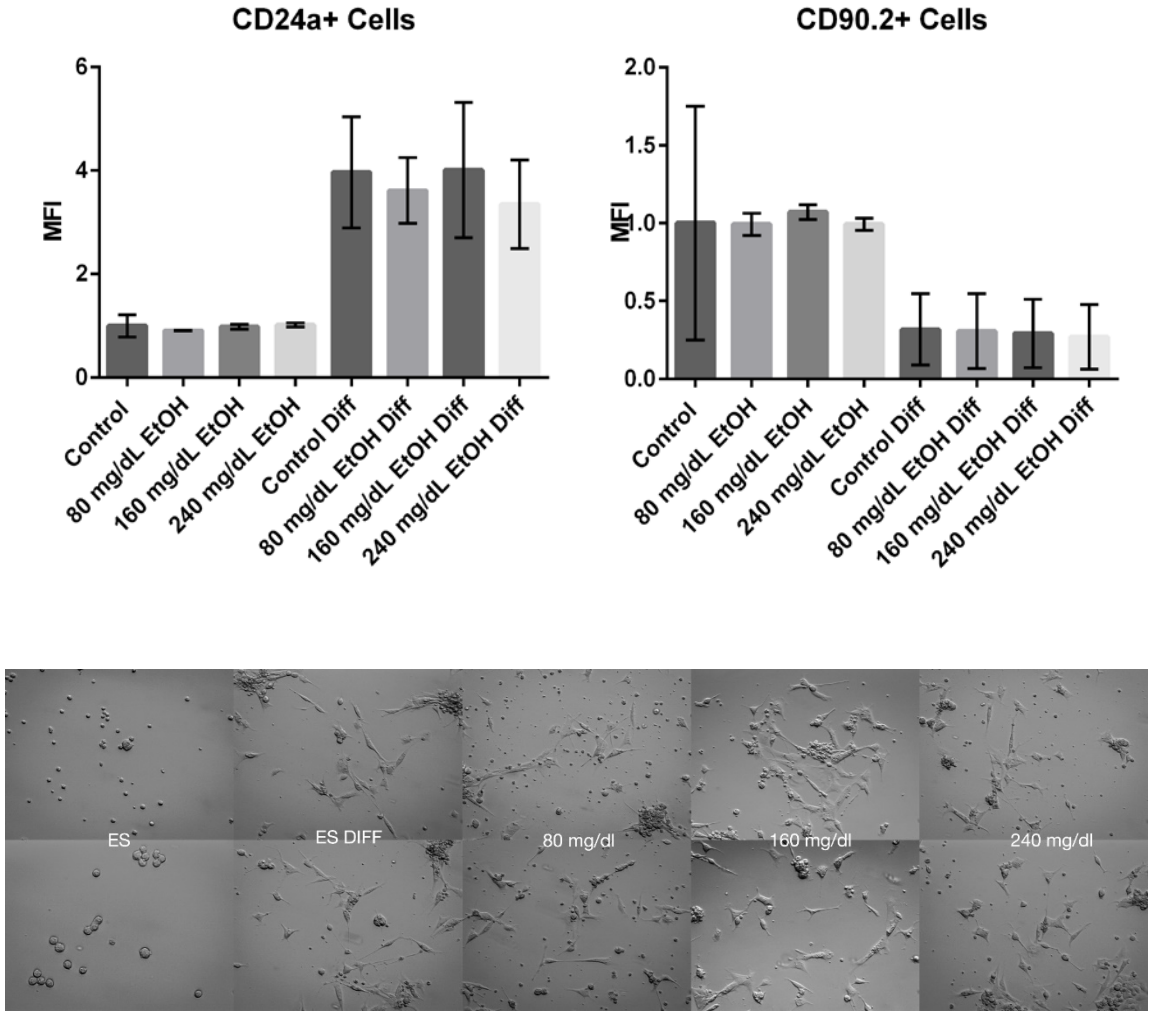

Figure 26: Approximately 500,000 murine embryonic stem cells were seeded into flasks and exposed to varying concentrations of ethanol (0mg/dL, 80mg/dL, 160 mg/dL, or 240 mg/dL) for four days, followed by a no-ethanol recovery period for ten days, then allowed to differentiate along a neural lineage in neural stem cell media. Cells were monitored for changes in morphology and analyzed via flow cytometry for neural surface markers CD90.2 and CD24a.

changes induced by acute ethanol exposure in a pluripotent stem cell type derived from the preimplantation blastocyst. Specifically, we sought to determine if epigenetic alterations persist beyond the window of exposure in ESCs, and if these changes in the histone marks examined correspond with transcriptional alterations in the expression of our candidate genes. Furthermore, we sought to determine whether changes in the histone marks examined correlate with transcription of chromatin modifiers, oxidative stress and alcohol metabolism genes, or diminished stem cell potency. Our results indicate that ESCs maintained as stem cells are susceptible to acute ethanol-induced chromatin disruption, and that this disruption seems to oscillate as far as 10 days post-acute ethanol exposure. Despite these fluctuating changes in chromatin structure, expression of the candidate genes examined does not significantly differ from control levels. Additionally, expression of H3K9 methyltransferases and demethylases and oxidative stress genes are not altered during or after ethanol exposure. These data highlight the complexity of the relationship between epigenetic programming and transcription after an acute exposure to ethanol, and call into question the role of histone post-translational modifications as a regulator of gene expression.

H3K9ac and H3K9me2 are the two histone modifications most impacted by ethanol in this study, and alterations in these marks persist at least 10 days beyond the window of exposure. During ethanol exposure, these marks segregate, which agrees with the established idea that they are mutually exclusive marks (reviewed in Zhang, 2001). However, during the recovery phase this dichotomy disappears and the marks both display increased levels 4 days post-exposure. The increase in H3K9ac at the 10-day recovery phase of this experiment correlates with a gradual return of H3K9me2 to near-control levels or reduced levels. The return of these marks to near control levels may indicate a protective mechanism at work to maintain the integrity of chromatin structure after an environmental insult. In fact, H3K9me2 has been shown to be associated with heterochromatin formation and protection of DNA from Tet-mediated demethylation during genome-wide erasure of DNA methylation after fertilization (Nakamura et al., 2012; reviewed in Rose and Klose, 2014). Furthermore, alcohol exposure is associated with an abnormal burst in

cellular proliferation of neural stem cells (Santillano et al., 2005), and studies have shown that retinoblastoma protein (Rb) interacts with H3K9 methylation to control cell cycle gene silencing and suppress proliferation (Nielsen et al., 2001; Sdek et al., 2011). Our previous studies have shown an increase in *Rb* after exposure to alcohol concordant with an increase in H3K9me2 in neural stem cells (Veazey et al., 2015), suggesting these may play a role in a protective cellular mechanism to prevent aberrant proliferation and gene expression.

The association between H3K9me2-associated protection and the observed changes in *Tet* gene expression are of particular interest in this study. In addition to their role as DNA hydroxymethyltransferases, TET proteins interact indirectly with the enzyme complexes responsible for H3K4 methylation, share target genes with PRC2, and are involved in the regulation of homeobox genes (Wu and Zhang, 2011). TET1 colocalizes with H3K4me3 at transcriptionally active or poised genes, but has been shown to interact with histone deacetylases, promoting transcriptional repression (Williams et al., 2011). *TET2*-mutated diffuse large B-cell lymphomas are associated with DNA hypermethylation on gene promoters that are bivalent in human ES cells (Asmar et al., 2013). In our study, *Tet1* and *Tet2* are increased in alcohol-exposed cells, indicating that this may coincide with alcohol's pro-proliferative effects by increasing hypomethylation and availability of gene promoters. A direct relationship between H3K9 methylation and TET proteins has not been defined, however DNA hydroxymethylation and H3K9 dimethylation are not correlated with similar forms of gene expression in embryonic development. H3K9 dimethylation is generally associated with repressive chromatin and DNA methylation while DNA hydroxymethylation is generally associated with a transition from a repressive chromatin state to a permissive state (Liu et al., 2013).

According to these findings and in comparison to our previous studies (Veazey et al., 2015), the persistence of alterations in chromatin structure are cell-type-specific and display unique patterns depending on the cell type present during the window of exposure. Furthermore, the alterations in histone marks imparted by ethanol do not likely have a causal role in epigenetic regulation of transcription, as

reported previously (Henikoff and Shilatifard, 2011). Interestingly, the transcriptional program in less differentiated stem cell types seems to be more able to recover from ethanol insult than in more differentiated cell types. This suggests that pluripotent cells harbor a protective mechanism that may be lost throughout development, and cells that have begun the path to differentiation and are undergoing changes in transcription may be more susceptible to teratogens such as ethanol. The results of this study narrow down the search for the developmental window in which susceptibility to ethanol is highest, and suggest that the specific time point of exposure during development can be more dangerous than the amount of ethanol encountered by the developing embryo.

CHAPTER VII
CONCLUSIONS AND FUTURE DIRECTIONS

Alcohol exposure during early development results in a range of phenotypes that may be linked to alterations in epigenetic programming. Chromatin structure is affected by many different environmental factors, and each factor can affect chromatin in many different ways, resulting in a broad range of phenotypes. The aims of this dissertation were to examine the impact of alcohol exposure on chromatin structure, determine the heritability of these effects both *in vitro* and *in vivo*, and determine whether the severity of these alterations could be tied to the differentiation state of the cell. This dissertation has demonstrated that acute ethanol exposure has the capacity to disrupt chromatin structure in multiple cell types, that the severity of change is associated with stem cell identity, and importantly, that the observed changes in chromatin structure arising acutely are distinct from those observed past the window of exposure. Furthermore, we observe that changes in the levels of histone post-translational modifications linked to active and inactive chromatin states do not correlate with changes in expression of the genes under investigation, or the localization of associated chromatin modifiers. These results highlight the complexity of epigenetic effects of ethanol and challenge current assumptions made about chromatin structure and transcription in the field of epigenetics.

The first major focus of this study was to identify stable reference genes in populations of embryonic stem cells as well as those from the fetal neural epithelium. qPCR is a reliable, widely-used technique employed in the measurement of gene expression. However, the accuracy of this technique is predicated on the use of stable reference genes to normalize measurements against. The Minimum Information for Publication of Quantitative qPCR Experiments (MIQE) guidelines state that use of the geometric mean of three stable reference genes is essential to conducting accurate qPCR (Vandesompele et al., 2002). Our initial experiments identified stable reference genes for use in embryonic, extraembryonic, and neural

stem cell studies of alcohol exposure. Reference genes were identified for cells exposed to concentrations of alcohol ranging from 60 mg/dL to 320 mg/dL.

The second major focus of this study was to determine if alcohol could disrupt chromatin structure using a neural stem cell model of development. Exposing neural stem cells to physiologically relevant doses of ethanol for 5 days resulted in the loss of both the H3K4me3 and H3K27me3 histone marks at the promoters of several key genes regulating neural stemness and differentiation. Surprisingly, many of the genes examined did not exhibit the anticipated alterations in gene expression. Furthermore, chromatin modifiers involved with H3K4me3 showed mixed changes in expression upon acute alcohol exposure, and members of Polycomb Repressive Complex 2 showed no significant changes in expression or localization compared to control levels.

The third major experimental series sought to determine if the observed alcohol-induced disturbances are heritable through cell division after removal of ethanol from the system. Using a novel approach of a 3-day ethanol exposure followed by a 4-day recovery period allowed for observation of histone marks immediately after an acute exposure as well as after a recovery period consisting of at least three population doublings without ethanol. We found that the effects of ethanol on chromatin structure were unique to the histone post-translational modification under investigation. Interestingly, despite published observations indicating that marks associated with similar and or opposite chromatin states would correlate (Binda et al., 2010), we find that each histone mark behaves independently of other marks, and no two marks display a correlative pattern. The changes in these marks were also dose-specific, but did not show a linear dose-response profile. Each histone mark displayed varying levels of susceptibility to ethanol, with H3K9me2 being particularly affected. In our in vitro studies, after a recovery period, we observed almost every gene examined had significantly higher levels than control. This was also the case *in vivo*, as ethanol affected fetal brains showed a significant increase in H3K9me2 in the majority of genes examined. In fact, changes in gene expression appeared to be latent, and did not predominantly

manifest until after the recovery period. Similar to our findings in chapter IV, gene expression did not correlate with changes in histone modifications upon ethanol exposure Again, these changes did not correlate with the histone signatures we examined.

The final major topic of this dissertation focused on whether alcohol's capacity to cause epigenetic alterations is tied to the differentiation state of the cell. Utilizing an experiment similar to the neural stem cell recovery approach, we determined the capacity of alcohol to cause lasting changes in chromatin structure in embryonic stem cells, which we infer to exhibit a lower state of differentiation than neuroepithelial stem cells. To this point, embryonic stem cells are pluripotent, and are therefore are assumed to have a much more open chromatin state and greater vulnerability to environmental insults than more differentiated cell types. Embryonic stem cells were exposed to ethanol for 4 days, then allowed to recover for 10 days, with samples taken for ChIP-qPCR and RNA analysis at days 4, 8, and 14 of the experiment. Like neural stem cells, the alcohol-induced alterations in each histone modification was distinct and dose-dependent. Interestingly, post-translational modification of H3K9 were again the most severely affected.

This work helps to develop an association between alcohol-induced changes in chromatin structure and FASD phenotypes. The errors in chromatin structure are dose-dependent, but do not follow a linear dose-response curve. This suggests that the epigenetic effects of ethanol may be tied to the cell type present at the time of exposure, rather than the amount of ethanol that comes into contact with the cell. Furthermore, alterations in chromatin structure vary depending on the mark under investigation, and no two marks display a distinct coordination of changes. These observations call into question the current dogma of the histone code, and disputes whether histone post-translational modifications are themselves are causal in gene activation or silencing. A particulary interesting finding is that H3K9me2 seems to be the key post-translational modification impacted by acute ethanol exposure. This could be a sign of an underlying protective mechanism imparted by less differentiated cell types to maintain the integrity of chromatin structure. For example,

H3K9me2 is associated with heterochromatin formation and the protection of maternal DNA from Tet-mediated DNA demethylation in embryonic development (Nakamura et al., 2012). Furthermore, H3K9 methylation is associated with retinoblastoma protein (Rb1)-mediated control of cell cycle gene silencing and suppression of proliferation. The correlation of an increase in Rb and H3K9me2 could be an indicator of a cell-cycle mechanism activated to protect transcriptional integrity by forming a temporary repressive chromatin state. This is a compelling idea as less differentiated stem cells have a relatively open chromatin conformation compared to terminal cell types, which may make them more flexible and refractory to environmental effects on chromatin structure.

It is of particular importance to note that these changes in histone marks did not correlate with changes in the transcription of the genes whose promoters were examined, oxidative stress genes, or chromatin modifiers. These unique findings as a whole do not lead to a mechanistic conclusion, but rather bring into question the significance of histone marks and their true roles in response to a teratogen. For example, in brains, FASD phenotypic effects correlate exclusively with an increase in H3K9me2, but this mark is not significantly altered in mice exposed to ethanol that do not display phenotypic effects, suggesting its potential utility as a marker for FASD (Veazey et al., 2015). However, many more studies are needed to establish a bonafide association and mechanistic explanation as to how, if at all, changes in chromatin structure are associated with FASDs.

One particularly enticing theory is that, rather than perturbing an established chromatin signature, ethanol alters the period or the amplitude of oscillation of histone marks present at gene promoters. Previous studies have shown that histone marks are dynamic and fluctuate depending on cell cycle progression, and are not precisely maintained at the mononucleosome level (Alabert et al., 2015; Huang et al., 2012). Normal dynamics of histone marks at gene promoters have a specific magnitude of fluctuation that associates with proper maintenance of gene expression throughout the cell cycle (reviewed in Zentner and Henikoff, 2013; Barth and Imhof, 2010). However, upon teratogenic insult, the “wave” of oscillation may

change in various ways. For example, on one hand, a teratogen my alter the amplitude of the fluctuations in marks, causing the marks to be at much higher or much lower levels at a given point in time. On the other hand, a teratogen may alter the period of the fluctuation in marks, causing the marks to be at an abnormal level for longer periods of time than the normal cycle. Rather than trying to pinpoint the presence of histone marks with a single snapshot, perhaps more understanding could be gained by observing the changes in these marks over time.

In light of the data presented in this dissertation, it is of great interest to begin genome-wide recovery studies of changes in chromatin interactions upon exposure to alcohol. This will allow us to determine if changes in chromatin structure are genome-wide, or localized to genes involved in specific pathways. To accomplish this, we can incorporate a novel low-input ChIP-seq approach to analyze genome-wide epigenetic signatures in ethanol-exposed murine fetal brains. This will give us a genome-wide view of ethanol-induced alterations in epigenetic signatures and determine if they correlate with forebrain and ocular defects in mice subjected to acute alcohol exposure. For example, the specificity of increased H3K9me2 to only ethanol-affected brains shows that it may be a potential marker for FASD development in the future, and we can determine if changes to this mark persist genome-wide.

Furthermore, the answer to the histone-mark/gene expression discrepancy may lie in enhancer-promoter interactions and the association of chromatin with areas of active transcription within the nucleus. Chromatin is compartmentalized within the nucleus into areas of active transcription and areas that are not heavily transcribed. The location of genes within these compartments may determine their susceptibility to insult by exposure to teratogens. For example, genes localized in areas of heavy transcription may acquire more teratogen-induced alterations in chromatin structure because they are highly accessible at the time of insult. Chromatin interaction analyses with paired-end tag sequencing (ChIA-PET) can identify higher-order chromatin structures that involve interactions between gene promoters and regulatory elements such as enhancers. The binding of transcription

factors to these specific sequences makes up a network of transcriptional regulation and coordination. We can contrast developmental programming within regions of the brain that display overt morphological patterning errors and those that do not display structural abnormalities. This will allow us to determine whether ethanol disrupts chromatin interactions and nuclear architecture in these areas and help to gain a better understanding of the true consequences of the observed alterations in histone post-translational modifications in teratogenicity.

In conclusion, this dissertation has produced one of the first analyses of histone structure within a model of ethanol-induced teratogenesis that has suggested an epigenetic basis to a syndrome prevalent in our society. Furthermore, it has contributed to the field of epigenetics by calling into question the correlation/causality roles of histone marks and chromatin structure of gene promoters in the context of environmental exposures. These data pave the way for new hypotheses in fetal alcohol epigenetics and possibly the establishment of a mechanism of alcohol's effects on chromatin structure.

REFERENCES

Alabert, C., Barth, T.K., Reverón-Gómez, N., Sidoli, S., Schmidt, A., Jensen, O.N., Imhof, A., and Groth, A. (2015). Two distinct modes for propagation of histone PTMs across the cell cycle. Genes Dev *29*, 585-590.

Allen, T.A., Von Kaenel, S., Goodrich, J.A., and Kugel, J.F. (2004). The SINE-encoded mouse B2 RNA represses mRNA transcription in response to heat shock. Nat Struct Mol Biol *11*, 816-821.

Andersen, C.L., Jensen, J.L., and Ørntoft, T.F. (2004). Normalization of real-time quantitative reverse transcription-PCR data: a model-based variance estimation approach to identify genes suited for normalization, applied to bladder and colon cancer data sets. Cancer Res *64*, 5245-250.

Arzumnayan, A., Arzumanyan, A., Anni, H., Rubin, R., and Rubin, E. (2009). Effects of ethanol on mouse embryonic stem cells. Alcohol Clin Exp Res *33*, 2172-79.

Asmar, F., Punj, V., Christensen, J., Pedersen, M.T., Pedersen, A., Nielsen, A.B., Hother, C., Ralfkiaer, U., Brown, P., et al. (2013). Genome-wide profiling identifies a DNA methylation signature that associates with TET2 mutations in diffuse large B-cell lymphoma. Haematologica *98*, 1912-920.

Audergon, P.N., Catania, S., Kagansky, A., Tong, P., Shukla, M., Pidoux, A.L., and Allshire, R.C. (2015). Restricted epigenetic inheritance of H3K9 methylation. Science *348*, 132-35.

Bain, G., Kitchens, D., Yao, M., Huettner, J.E., and Gottlieb, D.I. (1995). Embryonic stem cells express neuronal properties in vitro. Developmental biology *168*, 342-357.

Bannister, A.J., Zegerman, P., Partridge, J.F., Miska, E.A., Thomas, J.O., Allshire, R.C., and Kouzarides, T. (2001). Selective recognition of methylated lysine 9 on histone H3 by the HP1 chromo domain. Nature *410*, 120-24.

Barrero, M.J., Boué, S., and Izpisúa Belmonte, J.C. (2010). Epigenetic Mechanisms that Regulate Cell Identity. Cell Stem Cell *7*, 565-570.

Barski, A., Cuddapah, S., Cui, K., Roh, T.-Y., Schones, D.E., Wang, Z., Wei, G., Chepelev, I., and Zhao, K. (2007). High-Resolution Profiling of Histone Methylations in the Human Genome. Cell *129*, 823-837.

Barth, T.K., and Imhof, A. (2010). Fast signals and slow marks: the dynamics of histone modifications. Trends in Biochemical Sciences *35*, 618-626.

Becker, H.C., Diaz-Granados, J.L., and Randall, C.L. (1996). Teratogenic actions of ethanol in the mouse: a minireview. Pharmacol Biochem Behav *55*, 501-513.

Bekdash, R.A., Zhang, C., and Sarkar, D.K. (2013). Gestational choline supplementation normalized fetal alcohol-induced alterations in histone modifications, DNA methylation, and proopiomelanocortin (POMC) gene expression in β-endorphin-producing POMC neurons of the hypothalamus. Alcohol Clin Exp Res *37*, 1133-142.

Bernstein, B.E., Mikkelsen, T.S., Xie, X., Kamal, M., Huebert, D.J., Cuff, J., Fry, B., Meissner, A., Wernig, M., et al. (2006). A Bivalent Chromatin Structure Marks Key Developmental Genes in Embryonic Stem Cells. Cell *125*, 315-326.

Bielawski, D.M., Zaher, F.M., Svinarich, D.M., and Abel, E.L. (2002). Paternal alcohol exposure affects sperm cytosine methyltransferase messenger RNA levels. Alcohol Clin Exp Res *26*, 347-351.

Binda, O., LeRoy, G., Bua, D.J., Garcia, B.A., Gozani, O., and Richard, S. (2010). Trimethylation of histone H3 lysine 4 impairs methylation of histone H3 lysine 9. Epigenetics *5*, 767-775.

Boda, E., Pini, A., Hoxha, E., Parolisi, R., and Tempia, F. (2008). Selection of Reference Genes for Quantitative Real-time RT-PCR Studies in Mouse Brain. Journal of Molecular Neuroscience *37*, 238-253.

Bosch-Presegué, L., Raurell-Vila, H., Marazuela-Duque, A., Kane-Goldsmith, N., Valle, A., Oliver, J., Serrano, L., and Vaquero, A. (2011). Stabilization of Suv39H1 by SirT1 is part of oxidative stress response and ensures genome protection. Mol Cell *42*, 210-223.

Bostick, M., Kim, J.K., Estève, P.O., Clark, A., Pradhan, S., and Jacobsen, S.E. (2007). UHRF1 plays a role in maintaining DNA methylation in mammalian cells. Science *317*, 1760-64.

Boujedidi, H., Bouchet-Delbos, L., Cassard-Doulcier, A., Njiké-Nakseu, M., Maitre, S., Prévot, S., Dagher, I., Agostini, H., Voican, C.S., et al. (2011). Housekeeping Gene Variability in the Liver of Alcoholic Patients. Alcohol Clin Exp Res *36*, 258-266.

Boyer, L.A., Plath, K., Zeitlinger, J., Brambrink, T., Medeiros, L.A., Lee, T.I., Levine, S.S., Wernig, M., Tajonar, A., et al. (2006). Polycomb complexes repress developmental regulators in murine embryonic stem cells. Nature *441*, 349-353.

Böhlenius H., Eriksson S., Parcy F., & Nilsson O. (2007). *Retraction.* Science *316*, 367.

Brien, J.F., Loomis, C.W., Tranmer, J., and McGrath, M. (1983). Disposition of ethanol in human maternal venous blood and amniotic fluid. Am J Obstet Gynecol *146*, 181-86.

Brocardo, P.S., Gil-Mohapel, J., and Christie, B.R. (2011). The role of oxidative stress in fetal alcohol spectrum disorders. Brain Res Rev *67*, 209-225.

Bross, I.D. (1971). Critical levels, statistical language and scientific inference. Foundations of statistical inference, 500-513.

Brzezinski, M.R., Boutelet-Bochan, H., Person, R.E., Fantel, A.G., and Juchau, M.R. (1999). Catalytic activity and quantitation of cytochrome P-450 2E1 in prenatal human brain. J Pharmacol Exp Ther *289*, 1648-653.

Bustin, A., Benes, V., Garson, A., Hellemans, J., Huggett, J., Kubista, M., Mueller, R., Nolan, T., Pfaffl, .W., et al. (2009). The MIQE Guidelines: Minimum Information for Publication of Quantitative Real-Time PCR Experiments. Clinical Chemistry *55*, 611-622.

Bustin, S.A., and Nolan, T. (2004). Pitfalls of quantitative real-time reverse-transcription polymerase chain reaction. J Biomol Tech *15*, 155-166.

Camarillo, C., and Miranda, R.C. (2008). Ethanol exposure during neurogenesis induces persistent effects on neural maturation: evidence from an ex vivo model of fetal cerebral cortical neuroepithelial progenitor maturation. Gene Expr *14*, 159-171.

Campos, L.S. (2004). Neurospheres: Insights into neural stem cell biology. J. Neurosci. Res. *78*, 761-69.

Cao, R., Wang, L., Wang, H., Xia, L., Erdjument-Bromage, H., Tempst, P., Jones, R.S., and Zhang, Y. (2002). Role of histone H3 lysine 27 methylation in Polycomb-group silencing. Science *298*, 1039-043.

Carnahan, M.N., Veazey, K.J., Muller, D., Tingling, J.D., Miranda, R.C., and Golding, M.C. (2013). Identification of cell-specific patterns of reference gene stability in quantitative reverse-transcriptase polymerase chain reaction studies of embryonic,

placental and neural stem models of prenatal ethanol exposure. Alcohol *47*, 109-120.

Centers for Disease Control and Prevention (CDC) (2004). Alcohol consumption among women who are pregnant or who might become pregnant--United States, 2002. MMWR Morb Mortal Wkly Rep *53*, 1178-181.

Chen, T., and Dent, S.Y.R. (2013). Chromatin modifiers and remodellers: regulators of cellular differentiation. Nat Rev Genet *15*, 93-106.

Chen, Z.F., and Behringer, R.R. (1995). Twist is required in head mesenchyme for cranial neural tube morphogenesis. Genes Dev *9*, 686-699.

Cherry, S.R., Biniszkiewicz, D., Van Parijs, L., Baltimore, D., and Jaenisch, R. (2000). Retroviral expression in embryonic stem cells and hematopoietic stem cells. Mol Cell Biol *20*, 7419-426.

Chia, N., Wang, L., Lu, X., Senut, M.C., Brenner, C., and Ruden, D.M. (2011). Hypothesis: environmental regulation of 5-hydroxymethylcytosine by oxidative stress. Epigenetics *6*, 853-56.

Choudhury, M., Park, P.-H., Jackson, D., and Shukla, S.D. (2010). Evidence for the role of oxidative stress in the acetylation of histone H3 by ethanol in rat hepatocytes. Alcohol *44*, 531-540.

Ciccone, D.N., Su, H., Hevi, S., Gay, F., Lei, H., Bajko, J., Xu, G., Li, E., and Chen, T. (2009). KDM1B is a histone H3K4 demethylase required to establish maternal genomic imprints. Nature *461*, 415-18.

Clarke-Harris, R., Wilkin, T.J., Hosking, J., Pinkney, J., Jeffery, A.N., Metcalf, B.S., Godfrey, K.M., Voss, L.D., Lillycrop, K.A., and Burdge, G.C. (2014). PGC1α

promoter methylation in blood at 5-7 years predicts adiposity from 9 to 14 years (EarlyBird 50). Diabetes *63*, 2528-537.

Conti, L., and Cattaneo, E. (2010). Neural stem cell systems: physiological players or in vitro entities? Nature Reviews Neuroscience

Crabb, D.W., Zeng, Y., Liangpunsakul, S., Jones, R., and Considine, R. (2011). Ethanol Impairs Differentiation of Human Adipocyte Stromal Cells in Culture. Alcohol Clin Exp Res *35*, 1584-592.

Crews, T., Mdzinarishvili, A., Kim, D., He, J., and Nixon, K. (2006). Neurogenesis in adolescent brain is potently inhibited by ethanol. Neuroscience *137*, 437-445.

Czermin, B., Melfi, R., McCabe, D., Seitz, V., Imhof, A., and Pirrotta, V. (2002). Drosophila enhancer of Zeste/ESC complexes have a histone H3 methyltransferase activity that marks chromosomal Polycomb sites. Cell *111*, 185-196.

Dheda, K., Huggett, J.F., Chang, J.S., Kim, L.U., Bustin, S.A., Johnson, M.A., Rook, G.A.W., and Zumla, A. (2005). The implications of using an inappropriate reference gene for real-time reverse transcription PCR data normalization. Analytical Biochemistry *344*, 141-43.

Dong, J., Sulik, K.K., and Chen, S.Y. (2008). Nrf2-mediated transcriptional induction of antioxidant response in mouse embryos exposed to ethanol in vivo: implications for the prevention of fetal alcohol spectrum disorders. Antioxid Redox Signal *10*, 2023-033.

Dong, K.B., Maksakova, I.A., Mohn, F., Leung, D., Appanah, R., Lee, S., Yang, H.W., Lam, L.L., Mager, D.L., et al. (2008). DNA methylation in ES cells requires the lysine methyltransferase G9a but not its catalytic activity. EMBO J *27*, 2691-2701.

Downing, C., Johnson, T.E., Larson, C., Leakey, T.I., Siegfried, R.N., Rafferty, T.M., and Cooney, C.A. (2011). Subtle decreases in DNA methylation and gene expression at the mouse Igf2 locus following prenatal alcohol exposure: effects of a methyl-supplemented diet. Alcohol *45*, 65-71.

Espinoza, C.A., Allen, T.A., Hieb, A.R., Kugel, J.F., and Goodrich, J.A. (2004). B2 RNA binds directly to RNA polymerase II to repress transcript synthesis. Nat Struct Mol Biol *11*, 822-29.

Fan, J.Y., Rangasamy, D., Luger, K., and Tremethick, D.J. (2004). H2A. Z alters the nucleosome surface to promote HP1α-mediated chromatin fiber folding. Mol Cell *16*, 655-661.

Feil, R., and Fraga, M.F. (2011). Epigenetics and the environment: emerging patterns and implications. Nat Rev Genet *13*, 97-109.

Fisher, C.L., and Fisher, A.G. (2011). Chromatin states in pluripotent, differentiated, and reprogrammed cells. Curr Opin Genet Dev *21*, 140-46.

Floyd, R.L., and Sidhu, J.S. (2004). Monitoring prenatal alcohol exposure. American Journal of Medical Genetics *127C*, 3-9.

Floyd, R.L., Weber, M.K., Denny, C., and O'Connor, M.J. (2009). Prevention of fetal alcohol spectrum disorders. Developmental Disabilities Research Reviews *15*, 193-99.

Fortier, A.L., Lopes, F.L., Darricarrere, N., Martel, J., and Trasler, J.M. (2008). Superovulation alters the expression of imprinted genes in the midgestation mouse placenta. Hum Mol Genet *17*, 1653-665.

Fox, D.J., Pettygrove, S., Cunniff, C., O'Leary, L.A., Gilboa, S.M., Bertrand, J., Druschel, C.M., Breen, A., Robinson, L., et al. (2015). Fetal alcohol syndrome

among children aged 7-9 years - Arizona, Colorado, and New York, 2010. MMWR Morb Mortal Wkly Rep *64*, 54-57.

Frederiksen, K., Jat, P.S., Valtz, N., Levy, D., and McKay, R. (1988). Immortalization of precursor cells from the mammalian CNS. Neuron *1*, 439-448.

Galiveti, C.R., Rozhdestvensky, T.S., Brosius, J., Lehrach, H., and Konthur, Z. (2009). Application of housekeeping npcRNAs for quantitative expression analysis of human transcriptome by real-time PCR. RNA *16*, 450-461.

Garro, A.J., Espina, N., McBeth, D., Wang, S.L., and Wu-Wang, C.Y. (1992). Effects of alcohol consumption on DNA methylation reactions and gene expression: implications for increased cancer risk. Eur J Cancer Prev *1 Suppl 3*, 19-23.

Garro, A.J., McBeth, D.L., Lima, V., and Lieber, C.S. (1991). Ethanol consumption inhibits fetal DNA methylation in mice: implications for the fetal alcohol syndrome. Alcohol Clin Exp Res *15*, 395-98.

Gilsbach, R., Kouta, M., Bönisch, H., and Brüss, M. (2006). Comparison of in vitro and in vivo reference genes for internal standardization of real-time PCR data. BioTechniques *40*, 173-77.

Godin, E.A., Dehart, D.B., Parnell, S.E., O'Leary-Moore, S.K., and Sulik, K.K. (2011). Ventromedian forebrain dysgenesis follows early prenatal ethanol exposure in mice. Neurotoxicol Teratol *33*, 231-39.

Godin, E.A., OâLeary-Moore, S.K., Khan, A.A., Parnell, S.E., Ament, J.J., Dehart, D.B., Johnson, B.W., Allan Johnson, G., Styner, M.A., and Sulik, K.K. (2010). Magnetic Resonance Microscopy Defines Ethanol-Induced Brain Abnormalities in Prenatal Mice: Effects of Acute Insult on Gestational Day 7. Alcohol Clin Exp Res *34*, 98-111.

Golding, M.C., and Mann, M.R. (2011). A bidirectional promoter architecture enhances lentiviral transgenesis in embryonic and extraembryonic stem cells. Gene Ther *18*, 817-826.

Golding, M.C., Zhang, L., and Mann, M.R. (2010). Multiple epigenetic modifiers induce aggressive viral extinction in extraembryonic endoderm stem cells. Cell Stem Cell *6*, 457-467.

Golebiewska, A., Atkinson, S.P., Lako, M., and Armstrong, L. (2009). Epigenetic Landscaping During hESC Differentiation to Neural Cells. Stem Cells *27*, 1298-1308.

Gong, Z., and Wezeman, F.H. (2004). Inhibitory Effect of Alcohol on Osteogenic Differentiation in Human Bone Marrow Derived Mesenchymal Stem Cells. Alcohol Clin Exp Res *28*, 468-479.

Goossens, K., Van Poucke, M., Van Soom, A., Vandesompele, J., Van Zeveren, A., and Peelman, L.J. (2005). Selection of reference genes for quantitative real-time PCR in bovine preimplantation embryos. BMC Dev Biol *5*, 27.

Greaves, I.K., Rangasamy, D., Ridgway, P., and Tremethick, D.J. (2007). H2A. Z contributes to the unique 3D structure of the centromere. Proc Natl Acad Sci U S A *104*, 525-530.

Guillemot, F., Lo, L.C., Johnson, J.E., Auerbach, A., Anderson, D.J., and Joyner, A.L. (1993). Mammalian achaete-scute homolog 1 is required for the early development of olfactory and autonomic neurons. Cell *75*, 463-476.

Gutierrez, L., Mauriat, M., Gunin, S., Pelloux, J., Lefebvre, J., Louvet, R., Rusterucci, C., Moritz, T., Guerineau, F., et al. (2008). The lack of a systematic validation of reference genes: a serious pitfall undervalued in reverse transcription-polymerase chain reaction (RT-PCR) analysis in plants. Plant Biotechnology Journal *6*, 609-618.

Guttman, M., Donaghey, J., Carey, B.W., Garber, M., Grenier, J.K., Munson, G., Young, G., Lucas, A.B., Ach, R., et al. (2011). lincRNAs act in the circuitry controlling pluripotency and differentiation. Nature *477*, 295-300.

Halsted, C.H., Villanueva, J.A., Devlin, A.M., Niemelä, O., Parkkila, S., Garrow, T.A., Wallock, L.M., Shigenaga, M.K., Melnyk, S., and James, S.J. (2002). Folate deficiency disturbs hepatic methionine metabolism and promotes liver injury in the ethanol-fed micropig. Proc Natl Acad Sci U S A *99*, 10072-77.

Hansen, K.H., Bracken, A.P., Pasini, D., Dietrich, N., Gehani, S.S., Monrad, A., Rappsilber, J., Lerdrup, M., and Helin, K. (2008). A model for transmission of the H3K27me3 epigenetic mark. Nat Cell Biol *10*, 1291-1300.

Hashimoto-Torii, K., Kawasawa, Y.I., Kuhn, A., and Rakic, P. (2011). Combined transcriptome analysis of fetal human and mouse cerebral cortex exposed to alcohol. Proc Natl Acad Sci U S A *108*, 4212-17.

Haycock, P.C. (2009). Fetal Alcohol Spectrum Disorders: The Epigenetic Perspective. Biol Reprod *81*, 607-617.

Haycock, P.C., and Ramsay, M. (2009). Exposure of mouse embryos to ethanol during preimplantation development: effect on DNA methylation in the h19 imprinting control region. Biol Reprod *81*, 618-627.

Hellemans, J., Mortier, G., De Paepe, A., Speleman, F., and Vandesompele, J. (2007). Genome Biol *8*, R19.

Hemberger, M., Dean, W., and Reik, W. (2009). Epigenetic dynamics of stem cells and cell lineage commitment: digging Waddington's canal. Nat Rev Mol Cell Biol *10*, 526-537.

Henikoff, S., and Shilatifard, A. (2011). Histone modification: cause or cog? Trends Genet *27*, 389-396.

Henshaw, S.K. (1998). Unintended pregnancy in the United States. Fam Plann Perspect *30*, 24-9, 46.

Hernandez, L., Kozlov, S., Piras, G., and Stewart, C.L. (2003). Paternal and maternal genomes confer opposite effects on proliferation, cell-cycle length, senescence, and tumor formation. Proc Natl Acad Sci U S A *100*, 13344-49.

Hicks, S.D., Middleton, F.A., and Miller, M.W. (2010). Ethanol-induced methylation of cell cycle genes in neural stem cells. Journal of Neurochemistry *114*, 1767-780.

Hipp, J.A., Hipp, J.D., Atala, A., and Soker, S. (2010). Ethanol Alters the Osteogenic Differentiation of Amniotic Fluid-Derived Stem Cells. Alcohol Clin Exp Res *34*, 1714-722.

Hirabayashi, Y., and Gotoh, Y. (2010). Epigenetic control of neural precursor cell fate during development. Nature Reviews Neuroscience *11*, 377-388.

Hoyme, H.E., May, P.A., Kalberg, W.O., Kodituwakku, P., Gossage, J.P., Trujillo, P.M., Buckley, D.G., Miller, J.H., Aragon, A.S., and Khaole, N. (2005). A practical clinical approach to diagnosis of fetal alcohol spectrum disorders: clarification of the 1996 institute of medicine criteria. Pediatrics *115*, 39-47.

Huang, L., Pu, Y., Hepps, D., Danielpour, D., and Prins, G.S. (2007). Posterior Hox gene expression and differential androgen regulation in the developing and adult rat prostate lobes. Endocrinology *148*, 1235-245.

Hwang, H.W., Wentzel, E.A., and Mendell, J.T. (2007). A hexanucleotide element directs microRNA nuclear import. Science *315*, 97-100.

Huang, H.S., Allen, J.A., Mabb, A.M., King, I.F., Miriyala, J., Taylor-Blake, B., Sciaky, N., Dutton, J.W., Lee, H.M., et al. (2012). Topoisomerase inhibitors unsilence the dormant allele of Ube3a in neurons. Nature *481*, 185-89.

Ieraci, A., and Herrera, D.G. (2007). Single alcohol exposure in early life damages hippocampal stem/progenitor cells and reduces adult neurogenesis. Neurobiology of Disease *26*, 597-605.

Irwin, R.E., Thakur, A., O' Neill, K.M., and Walsh, C.P. (2014). 5-Hydroxymethylation marks a class of neuronal gene regulated by intragenic methylcytosine levels. Genomics *104*, 383-392.

J.M. Coffin, S.H. Hughes, and H.E. Varmus, eds. (1997). Retroviruses, (Cold Spring Harbor (NY): Cold Spring Harbor Laboratory Press).

Jiang, H., Shukla, A., Wang, X., Chen, W., Bernstein, B.E., and Roeder, R.G. (2011). Role for Dpy-30 in ES Cell-Fate Specification by Regulation of H3K4 Methylation within Bivalent Domains. Cell *144*, 513-525.

Johansson, S., Fuchs, A., Ökvist, A., Karimi, M., Harper, C., Garrick, T., Sheedy, D., Hurd, Y., Bakalkin, G., and Ekström, T.J. (2007). Validation of endogenous controls for quantitative gene expression analysis: Application on brain cortices of human chronic alcoholics. Brain Research *1132*, 20-28.

Jones, K.L., and Smith, D.W. (1975). The fetal alcohol syndrome. Teratology *12*, 1-10.

Kaminen-Ahola, N., Ahola, A., Maga, M., Mallitt, K.A., Fahey, P., Cox, T.C., Whitelaw, E., and Chong, S. (2010). Maternal ethanol consumption alters the epigenotype and the phenotype of offspring in a mouse model. PLoS Genet *6*, e1000811.

Karnofsky, D.A. (1965). Drugs as teratogens in animals and man. Annu Rev Pharmacol *10*, 447-472.

Kim, S. (2005). Histone H3 modifications in rat hepatic stellate cells by ethanol. Alcohol and Alcoholism *40*, 367-372.

Knezovich, J.G., and Ramsay, M. (2012). The Effect of Preconception Paternal Alcohol Exposure on Epigenetic Remodeling of the H19 and Rasgrf1 Imprinting Control Regions in Mouse Offspring. Front. Gene. *3*

Koch, .M., Andrews, .M., Flicek, P., Dillon, .C., Karaoz, U., Clelland, .K., Wilcox, S., Beare, .M., Fowler, .C., et al. (2007). The landscape of histone modifications across 1% of the human genome in five human cell lines. Genome Research *17*, 691-707.

Kondo, Y., Shen, L., Yan, P.S., Huang, T.H., and Issa, J.P. (2004). Chromatin immunoprecipitation microarrays for identification of genes silenced by histone H3 lysine 9 methylation. Proc Natl Acad Sci U S A *101*, 7398-7403.

Kornberg, R.D. (2007). The molecular basis of eukaryotic transcription. Proc Natl Acad Sci U S A *104*, 12955-961.

Kriaucionis, S., and Heintz, N. (2009). The nuclear DNA base 5-hydroxymethylcytosine is present in Purkinje neurons and the brain. Science *324*, 929-930.

Ku, M., van Steensel, B., Koche, R.P., Rheinbay, E., Mendenhall, E.M., Endoh, M., Mikkelsen, T.S., Presser, A., Nusbaum, C., et al. (2008). Genomewide Analysis of PRC1 and PRC2 Occupancy Identifies Two Classes of Bivalent Domains. PLoS Genet *4*, e1000242.

Kuegler, P.B., Zimmer, B., Waldmann, T., Baudis, B., Ilmjärv, S., Hescheler, J., Gaughwin, P., Brundin, P., Mundy, W., et al. (2010). Markers of murine embryonic and neural stem cells, neurons and astrocytes: reference points for developmental neurotoxicity testing. ALTEX *27*, 17-42.

Kunath, T. (2005). Imprinted X-inactivation in extra-embryonic endoderm cell lines from mouse blastocysts. Development *132*, 1649-661.

Lachner, M., O'Carroll, D., Rea, S., Mechtler, K., and Jenuwein, T. (2001). Methylation of histone H3 lysine 9 creates a binding site for HP1 proteins. Nature *410*, 116-120.

Landeira, D., Sauer, S., Poot, R., Dvorkina, M., Mazzarella, L., Jørgensen, H.F., Pereira, C.F., Leleu, M., Piccolo, F.M., et al. (2010). Jarid2 is a PRC2 component in embryonic stem cells required for multi-lineage differentiation and recruitment of PRC1 and RNA Polymerase II to developmental regulators. Nat Cell Biol *12*, 618-624.

Lanoix, D., Lacasse, A., St-Pierre, J., Taylor, S.C., Ethier-Chiasson, M., Lafond, J., and Vaillancourt, C. (2012). Quantitative PCR Pitfalls: The Case of the Human Placenta. Molecular Biotechnology *52*, 234-243.

Laurent, B., Ruitu, L., Murn, J., Hempel, K., Ferrao, R., Xiang, Y., Liu, S., Garcia, B., Wu, H., et al. (2015). A Specific LSD1/KDM1A Isoform Regulates Neuronal Differentiation through H3K9 Demethylation. Mol Cell *57*, 957-970.

Lee, C.H., Shah, B., Moioli, E.K., and Mao, J.J. (2010). CTGF directs fibroblast differentiation from human mesenchymal stem/stromal cells and defines connective tissue healing in a rodent injury model. Journal of Clinical Investigation *120*, 3340-49.

Leeb, M., Pasini, D., Novatchkova, M., Jaritz, M., Helin, K., and Wutz, A. (2010). Polycomb complexes act redundantly to repress genomic repeats and genes. Genes Dev *24*, 265-276.

Lewis, E.B. (1978). A gene complex controlling segmentation in Drosophila. Nature *276*, 565-570.

Li, E., Bestor, T.H., and Jaenisch, R. (1992). Targeted mutation of the DNA methyltransferase gene results in embryonic lethality. Cell *69*, 915-926.

Li, G., Margueron, R., Ku, M., Chambon, P., Bernstein, B.E., and Reinberg, D. (2010). Jarid2 and PRC2, partners in regulating gene expression. Genes Dev *24*, 368-380.

Liang, G., Lin, J.C., Wei, V., Yoo, C., Cheng, J.C., Nguyen, C.T., Weisenberger, D.J., Egger, G., Takai, D., et al. (2004). Distinct localization of histone H3 acetylation and H3-K4 methylation to the transcription start sites in the human genome. Proc Natl Acad Sci U S A *101*, 7357-362.

Lim, D.A., Huang, Y., Swigut, T., Mirick, A.L., Garcia-Verdugo, J.M., Wysocka, J., Ernst, P., and Alvarez-Buylla, A. (2009). Chromatin remodelling factor Mll1 is essential for neurogenesis from postnatal neural stem cells. Nature *458*, 529-533.

Liu, B., Yi, J., Sv, A., Lan, X., Ma, Y., Huang, T.H., Leone, G., and Jin, V.X. (2013). QChIPat: a quantitative method to identify distinct binding patterns for two biological ChIP-seq samples in different experimental conditions. BMC Genomics *14 Suppl 8*, S3.

Liu, Y., Balaraman, Y., Wang, G., Nephew, K.P., and Zhou, F.C. (2009). Alcohol exposure alters DNA methylation profiles in mouse embryos at early neurulation. Epigenetics *4*, 500-511.

Livak, K.J., and Schmittgen, T.D. (2001). Analysis of relative gene expression data using real-time quantitative PCR and the 2(-Delta Delta C(T)) Method. Methods *25*, 402-08.

Lubitz, S., Glaser, S., Schaft, J., Stewart, A.F., and Anastassiadis, K. (2007). Increased apoptosis and skewed differentiation in mouse embryonic stem cells lacking the histone methyltransferase Mll2. Mol Biol Cell *18*, 2356-366.

Macfarlan, T.S., Gifford, W.D., Agarwal, S., Driscoll, S., Lettieri, K., Wang, J., Andrews, S.E., Franco, L., Rosenfeld, M.G., et al. (2011). Endogenous retroviruses and neighboring genes are coordinately repressed by LSD1/KDM1A. Genes Dev *25*, 594-607.

Mamo, S., Gal, A.B., Bodo, S., and Dinnyes, A. (2007). Quantitative evaluation and selection of reference genes in mouse oocytes and embryos cultured in vivo and in vitro. BMC Dev Biol *7*, 14.

Mandal, P.K., and Kazazian, H.H. (2008). SnapShot: Vertebrate Transposons. Cell *135*, 192-192.e1.

Mann, M.R., Lee, S.S., Doherty, A.S., Verona, R.I., Nolen, L.D., Schultz, R.M., and Bartolomei, M.S. (2004). Selective loss of imprinting in the placenta following preimplantation development in culture. Development *131*, 3727-735.

Margueron, R., Justin, N., Ohno, K., Sharpe, M.L., Son, J., Drury III, W.J., Voigt, P., Martin, S.R., Taylor, W.R., et al. (2009). Role of the polycomb protein EED in the propagation of repressive histone marks. Nature *461*, 762-67.

Market-Velker, B.A., Zhang, L., Magri, L.S., Bonvissuto, A.C., and Mann, M.R. (2009). Dual effects of superovulation: loss of maternal and paternal imprinted methylation in a dose-dependent manner. Hum Mol Genet *19*, 36-51.

Martens, J.H.A., O'Sullivan, R.J., Braunschweig, U., Opravil, S., Radolf, M., Steinlein, P., and Jenuwein, T. (2005). The profile of repeat-associated histone lysine methylation states in the mouse epigenome. EMBO J *24*, 800-812.

Martin, G.R. (1981). Isolation of a pluripotent cell line from early mouse embryos cultured in medium conditioned by teratocarcinoma stem cells. Proc Natl Acad Sci U S A *78*, 7634-38.

Matsui, T., Leung, D., Miyashita, H., Maksakova, I.A., Miyachi, H., Kimura, H., Tachibana, M., Lorincz, M.C., and Shinkai, Y. (2010). Proviral silencing in embryonic stem cells requires the histone methyltransferase ESET. Nature *464*, 927-931.

McKay, R. (1997). Stem Cells in the Central Nervous System. Science *276*, 66-71.

Mead, E.A., and Sarkar, D.K. (2014). Fetal alcohol spectrum disorders and their transmission through genetic and epigenetic mechanisms. Front Genet *5*, 154.

Meissner, A., Mikkelsen, T.S., Gu, H., Wernig, M., Hanna, J., Sivachenko, A., Zhang, X., Bernstein, B.E., Nusbaum, C., et al. (2008). Genome-scale DNA methylation maps of pluripotent and differentiated cells. Nature *454*, 766-770.

Mejetta, S., Morey, L., Pascual, G., Kuebler, B., Mysliwiec, M.R., Lee, Y., Shiekhattar, R., Di Croce, L., and Benitah, S.A. (2011). Jarid2 regulates mouse epidermal stem cell activation and differentiation. EMBO J *30*, 3635-646.

Mikkelsen, T.S., Ku, M., Jaffe, D.B., Issac, B., Lieberman, E., Giannoukos, G., Alvarez, P., Brockman, W., Kim, T.K., et al. (2007). Genome-wide maps of chromatin state in pluripotent and lineage-committed cells. Nature *448*, 553-560.

Miranda, R.C., Santillano, D.R., Camarillo, C., and Dohrman, D. (2008). Modeling the impact of alcohol on cortical development in a dish: strategies from mapping neural stem cell fate. Methods Mol Biol *447*, 151-168.

Mo, Z., Milivojevic, V., and Zecevic, N. (2012). Enforced Pax6 Expression Rescues Alcohol-Induced Defects of Neuronal Differentiation in Cultures of Human Cortical Progenitor Cells. Alcohol Clin Exp Res *36*, 1374-1384.

Moonat, S., Sakharkar, A.J., Zhang, H., Tang, L., and Pandey, S.C. (2013). Aberrant histone deacetylase2-mediated histone modifications and synaptic plasticity in the amygdala predisposes to anxiety and alcoholism. Biol Psychiatry *73*, 763-773.

Mozzetta, C., Pontis, J., Fritsch, L., Robin, P., Portoso, M., Proux, C., Margueron, R., and Ait-Si-Ali, S. (2014). The histone H3 lysine 9 methyltransferases G9a and GLP regulate polycomb repressive complex 2-mediated gene silencing. Mol Cell *53*, 277-289.

Mukhopadhyay, A., Deplancke, B., Walhout, A.J.M., and Tissenbaum, H.A. (2008). Chromatin immunoprecipitation (ChIP) coupled to detection by quantitative real-time PCR to study transcription factor binding to DNA in Caenorhabditis elegans. Nature Protocols *3*, 698-709.

Muotri, A.R., Chu, V.T., Marchetto, M.C., Deng, W., Moran, J.V., and Gage, F.H. (2005). Somatic mosaicism in neuronal precursor cells mediated by L1 retrotransposition. Nature *435*, 903-910.

Nagy, A., Gocza, E., Diaz, E.M., Prideaux, V., Ivanyi, E., Markkula, M., and Rossant, J. (1990). Embryonic stem cells alone are able to support fetal development in the mouse. Development *110*, 815-821.

Nagy, A., Rossant, J., Nagy, R., Abramow-Newerly, W., and Roder, J.C. (1993). Derivation of completely cell culture-derived mice from early-passage embryonic stem cells. Proc Natl Acad Sci U S A *90*, 8424-28.

Nakamura, T., Liu, Y.J., Nakashima, H., Umehara, H., Inoue, K., Matoba, S., Tachibana, M., Ogura, A., Shinkai, Y., and Nakano, T. (2012). PGC7 binds histone

H3K9me2 to protect against conversion of 5mC to 5hmC in early embryos. Nature *486*, 415-19.

Nakato, R., Itoh, T., and Shirahige, K. (2013). DROMPA: easy-to-handle peak calling and visualization software for the computational analysis and validation of ChIP-seq data. Genes Cells *18*, 589-601.

Nestler, E.J. (2014). Epigenetic mechanisms of drug addiction. Neuropharmacology *76 Pt B*, 259-268.

Nielsen, S.J., Schneider, R., Bauer, U.M., Bannister, A.J., Morrison, A., O'Carroll, D., Firestein, R., Cleary, M., Jenuwein, T., et al. (2001). Rb targets histone H3 methylation and HP1 to promoters. Nature *412*, 561-65.

Niwa, H., Burdon, T., Chambers, I., and Smith, A. (1998). Self-renewal of pluripotent embryonic stem cells is mediated via activation of STAT3. Genes Dev *12*, 2048-060.

Niwa, H., Miyazaki, J., and Smith, A.G. (2000). Quantitative expression of Oct-3/4 defines differentiation, dedifferentiation or self-renewal of ES cells. Nat Genet *24*, 372-76.

O'Carroll, D., Scherthan, H., Peters, A.H., Opravil, S., Haynes, A.R., Laible, G., Rea, S., Schmid, M., Lebersorger, A., et al. (2000). Isolation and characterization of Suv39h2, a second histone H3 methyltransferase gene that displays testis-specific expression. Mol Cell Biol *20*, 9423-433.

Ogony, J.W., Malahias, E., Vadigepalli, R., and Anni, H. (2013). Ethanol Alters the Balance of Sox2, Oct4, and Nanog Expression in Distinct Subpopulations During Differentiation of Embryonic Stem Cells. Stem Cells Dev *22*, 2196-2210.

Okano, M., Bell, D.W., Haber, D.A., and Li, E. (1999). DNA methyltransferases Dnmt3a and Dnmt3b are essential for de novo methylation and mammalian development. Cell *99*, 247-257.

Okashita, N., Kumaki, Y., Ebi, K., Nishi, M., Okamoto, Y., Nakayama, M., Hashimoto, S., Nakamura, T., Sugasawa, K., et al. (2014). PRDM14 promotes active DNA demethylation through the ten-eleven translocation (TET)-mediated base excision repair pathway in embryonic stem cells. Development *141*, 269-280.

Ouko, L.A., Shantikumar, K., Knezovich, J., Haycock, P., Schnugh, D.J., and Ramsay, M. (2009). Effect of Alcohol Consumption on CpG Methylation in the Differentially Methylated Regions of H19 and IG-DMR in Male Gametes-Implications for Fetal Alcohol Spectrum Disorders. Alcohol Clin Exp Res *33*, 1615-627.

Oyedotun, K.S., and Lemire, B.D. (2003). The Quaternary Structure of the Saccharomyces cerevisiae Succinate Dehydrogenase: homology modeling, cofactor docking, and molecular dynamics simulation studies. Journal of Biological Chemistry *279*, 9424-431.

Pal-Bhadra, M., Bhadra, U., Jackson, D.E., Mamatha, L., Park, P.H., and Shukla, S.D. (2007). Distinct methylation patterns in histone H3 at Lys-4 and Lys-9 correlate with up- & down-regulation of genes by ethanol in hepatocytes. Life Sci *81*, 979-987.

Pan, B., Zhu, J., Lv, T., Sun, H., Huang, X., and Tian, J. (2014). Alcohol consumption during gestation causes histone3 lysine9 hyperacetylation and an alternation of expression of heart development-related genes in mice. Alcohol Clin Exp Res *38*, 2396-2402.

Pan, G., Tian, S., Nie, J., Yang, C., Ruotti, V., Wei, H., Jonsdottir, G.A., Stewart, R., and Thomson, J.A. (2007). Whole-Genome Analysis of Histone H3 Lysine 4 and Lysine 27 Methylation in Human Embryonic Stem Cells. Cell Stem Cell *1*, 299-312.

Park, -H. (2005). Involvement of histone acetyltransferase (HAT) in ethanol-induced acetylation of histone H3 in hepatocytes: potential mechanism for gene expression. AJP: Gastrointestinal and Liver Physiology *289*, G1124-136.

Parnell, S.E., Dehart, D.B., Wills, T.A., Chen, S.Y., Hodge, C.W., Besheer, J., Waage-Baudet, H.G., Charness, M.E., and Sulik, K.K. (2006). Maternal oral intake mouse model for fetal alcohol spectrum disorders: ocular defects as a measure of effect. Alcohol Clin Exp Res *30*, 1791-98.

Parnell, S.E., O'Leary-Moore, S.K., Godin, E.A., Dehart, D.B., Johnson, B.W., Allan Johnson, G., Styner, M.A., and Sulik, K.K. (2009). Magnetic resonance microscopy defines ethanol-induced brain abnormalities in prenatal mice: effects of acute insult on gestational day 8. Alcohol Clin Exp Res *33*, 1001-011.

Pasini, D., Bracken, A.P., Hansen, J.B., Capillo, M., and Helin, K. (2007). The polycomb group protein Suz12 is required for embryonic stem cell differentiation. Mol Cell Biol *27*, 3769-779.

Pereira, J.D., Sansom, S.N., Smith, J., Dobenecker, M.W., Tarakhovsky, A., and Livesey, F.J. (2010). Ezh2, the histone methyltransferase of PRC2, regulates the balance between self-renewal and differentiation in the cerebral cortex. Proc Natl Acad Sci U S A *107*, 15957-962.

Peters, A.H., Kubicek, S., Mechtler, K., O'Sullivan, R.J., Derijck, A.A., Perez-Burgos, L., Kohlmaier, A., Opravil, S., Tachibana, M., et al. (2003). Partitioning and plasticity of repressive histone methylation states in mammalian chromatin. Mol Cell *12*, 1577-589.

Petruk, S., Sedkov, Y., Johnston, D., Hodgson, J., Black, K., Kovermann, S., Beck, S., Canaani, E., Brock, H., and Mazo, A. (2012). TrxG and PcG Proteins but Not Methylated Histones Remain Associated with DNA through Replication. Cell *150*, 922-933.

Pfaffl, M.W., Tichopad, A., Prgomet, C., and Neuvians, T.P. (2004). Determination of stable housekeeping genes, differentially regulated target genes and sample integrity: BestKeeper--Excel-based tool using pair-wise correlations. Biotechnol Lett *26*, 509-515.

Pikkarainen, P.H. (1971). Metabolism of ethanol and acetaldehyde in perfused human fetal liver. Life Sci II *10*, 1359-364.

Ponomarev, I., Wang, S., Zhang, L., Harris, R.A., and Mayfield, R.D. (2012). Gene Coexpression Networks in Human Brain Identify Epigenetic Modifications in Alcohol Dependence. Journal of Neuroscience *32*, 1884-897.

Poux, S., Horard, B., Sigrist, C.J., and Pirrotta, V. (2002). The Drosophila trithorax protein is a coactivator required to prevent re-establishment of polycomb silencing. Development *129*, 2483-493.

Qiang, M., Denny, A., Lieu, M., Carreon, S., and Li, J. (2011). Histone H3K9 modifications are a local chromatin event involved in ethanol-induced neuroadaptation of the NR2B gene. Epigenetics *6*, 1095-1104.

Radonić, A., Thulke, S., Mackay, I.M., Landt, O., Siegert, W., and Nitsche, A. (2004). Guideline to reference gene selection for quantitative real-time PCR. Biochem Biophys Res Commun *313*, 856-862.

Ragunathan, K., Jih, G., and Moazed, D. (2014). Epigenetic inheritance uncoupled from sequence-specific recruitment. Science *348*, 1258699-9.

Rangasamy, D., Greaves, I., and Tremethick, D.J. (2004). RNA interference demonstrates a novel role for H2A.Z in chromosome segregation. Nat Struct Mol Biol *11*, 650-55.

Rea, S., Eisenhaber, F., O'Carroll, D., Strahl, B.D., Sun, Z.W., Schmid, M., Opravil, S., Mechtler, K., Ponting, C.P., et al. (2000). Regulation of chromatin structure by site-specific histone H3 methyltransferases. Nature *406*, 593-99.

Resendiz, M., Mason, S., Lo, C.L., and Zhou, F.C. (2014). Epigenetic regulation of the neural transcriptome and alcohol interference during development. Front Genet *5*, 285.

Retraction--Ileal-lymphoid-nodular hyperplasia, non-specific colitis, and pervasive developmental disorder in children. (2010). Lancet *351*. 637-641.

Rifas, L., Towler, D.A., and Avioli, L.V. (1997). Gestational exposure to ethanol suppresses msx2 expression in developing mouse embryos. Proc Natl Acad Sci U S A *94*, 7549-554.

Riley, E.P., Infante, M.A., and Warren, K.R. (2011). Fetal Alcohol Spectrum Disorders: An Overview. Neuropsychol Rev *21*, 73-80.

Rinn, J.L., Kertesz, M., Wang, J.K., Squazzo, S.L., Xu, X., Brugmann, S.A., Goodnough, L.H., Helms, J.A., Farnham, P.J., et al. (2007). Functional demarcation of active and silent chromatin domains in human HOX loci by noncoding RNAs. Cell *129*, 1311-323.

Roh, -Y. (2005). Active chromatin domains are defined by acetylation islands revealed by genome-wide mapping. Genes Dev *19*, 542-552.

Roitbak, T., Thomas, K., Martin, A., Allan, A., and Cunningham, L.A. (2011). Moderate fetal alcohol exposure impairs neurogenic capacity of murine neural stem cells isolated from the adult subventricular zone. Experimental Neurology *229*, 522-25.

Romero, A.M., Esteban-Pretel, G., Marín, M.P., Ponsoda, X., Ballestín, R., Canales, J.J., and Renau-Piqueras, J. (2010). Chronic ethanol exposure alters the levels, assembly, and cellular organization of the actin cytoskeleton and microtubules in hippocampal neurons in primary culture. Toxicol Sci *118*, 602-612.

Rose, N.R., and Klose, R.J. (2014). Understanding the relationship between DNA methylation and histone lysine methylation. Biochim Biophys Acta *1839*, 1362-372.

Rosenfeld, J.A., Wang, Z., Schones, D.E., Zhao, K., DeSalle, R., and Zhang, M.Q. (2009). Determination of enriched histone modifications in non-genic portions of the human genome. BMC Genomics *10*, 143.

Rossant, J. (1975). Investigation of the determinative state of the mouse inner cell mass. II. The fate of isolated inner cell masses transferred to the oviduct. J Embryol Exp Morphol *33*, 991-1001.

Rossant, J., and Tam, P.P. (2004). Emerging asymmetry and embryonic patterning in early mouse development. Dev Cell *7*, 155-164.

Rossant, J., and Tam, P.P.L. (2009). Blastocyst lineage formation, early embryonic asymmetries and axis patterning in the mouse. Development *136*, 701-713.

Rothbart, S.B., Krajewski, K., Nady, N., Tempel, W., Xue, S., Badeaux, A.I., Barsyte-Lovejoy, D., Martinez, J.Y., Bedford, M.T., et al. (2012). Association of UHRF1 with methylated H3K9 directs the maintenance of DNA methylation. Nat Struct Mol Biol *19*, 1155-160.

Rugg-Gunn, J., Cox, .J., Ralston, A., and Rossant, J. (2010). Inaugural Article: Distinct histone modifications in stem cell lines and tissue lineages from the early mouse embryo. Proc Natl Acad Sci U S A *107*, 10783-790.

Sakharkar, A.J., Tang, L., Zhang, H., Chen, Y., Grayson, D.R., and Pandey, S.C. (2014). Effects of acute ethanol exposure on anxiety measures and epigenetic modifiers in the extended amygdala of adolescent rats. Int J Neuropsychopharmacol *17*, 2057-067.

Santillano, D.R., Kumar, L.S., Prock, T.L., Camarillo, C., Tingling, J.D., and Miranda, R.C. (2005). Ethanol induces cell-cycle activity and reduces stem cell diversity to alter both regenerative capacity and differentiation potential of cerebral cortical neuroepithelial precursors. BMC Neurosci *6*, 59.

Schmittgen, T.D., and Livak, K.J. (2008). Analyzing real-time PCR data by the comparative C(T) method. Nat Protoc *3*, 1101-08.

Schuettengruber, B., Chourrout, D., Vervoort, M., Leblanc, B., and Cavalli, G. (2007). Genome Regulation by Polycomb and Trithorax Proteins. Cell *128*, 735-745.

Schultz, D.C., Ayyanathan, K., Negorev, D., Maul, G.G., and Rauscher, F.J. (2002). SETDB1: a novel KAP-1-associated histone H3, lysine 9-specific methyltransferase that contributes to HP1-mediated silencing of euchromatic genes by KRAB zinc-finger proteins. Genes Dev *16*, 919-932.

Sdek, P., Zhao, P., Wang, Y., Huang, C.J., Ko, C.Y., Butler, P.C., Weiss, J.N., and Maclellan, W.R. (2011). Rb and p130 control cell cycle gene silencing to maintain the postmitotic phenotype in cardiac myocytes. J Cell Biol *194*, 407-423.

Sharif, J., Muto, M., Takebayashi, S., Suetake, I., Iwamatsu, A., Endo, T.A., Shinga, J., Mizutani-Koseki, Y., Toyoda, T., et al. (2007). The SRA protein Np95 mediates epigenetic inheritance by recruiting Dnmt1 to methylated DNA. Nature *450*, 908-912.

Steward, M.M., Lee, J., O'Donovan, A., Wyatt, M., Bernstein, B.E., and Shilatifard, A. (2006). Molecular regulation of H3K4 trimethylation by ASH2L, a shared subunit of MLL complexes. Nat Struct Mol Biol *13*, 852-54.

Strahl, B.D., Ohba, R., Cook, R.G., and Allis, C.D. (1999). Methylation of histone H3 at lysine 4 is highly conserved and correlates with transcriptionally active nuclei in Tetrahymena. Proc Natl Acad Sci U S A *96*, 14967-972.

Strumpf, D. (2005). Cdx2 is required for correct cell fate specification and differentiation of trophectoderm in the mouse blastocyst. Development *132*, 2093-2102.

Strutz, F., Okada, H., Lo, C.W., Danoff, T., Carone, R.L., Tomaszewski, J.E., and Neilson, E.G. (1995). Identification and characterization of a fibroblast marker: FSP1. J Cell Biol *130*, 393-405.

Subbanna, S., Nagre, N.N., Shivakumar, M., Umapathy, N.S., Psychoyos, D., and Basavarajappa, B.S. (2014). Ethanol induced acetylation of histone at G9a exon1 and G9a-mediated histone H3 dimethylation leads to neurodegeneration in neonatal mice. Neuroscience *258*, 422-432.

Sulik, K.K., Johnston, M.C., and Webb, M.A. (1981). Fetal alcohol syndrome: embryogenesis in a mouse model. Science *214*, 936-38.

Suter, M.A., and Aagaard-Tillery, K.M. (2009). Environmental influences on epigenetic profiles. Semin Reprod Med *27*, 380-390.

Swayze, V.W., Johnson, V.P., Hanson, J.W., Piven, J., Sato, Y., Giedd, J.N., Mosnik, D., and Andreasen, N.C. (1997). Magnetic resonance imaging of brain anomalies in fetal alcohol syndrome. Pediatrics *99*, 232-240.

Syndrome, C.T.S.F.A., and Medicine, I.O. (1996). Fetal Alcohol Syndrome: Diagnosis, Epidemiology, Prevention, and Treatment, K. Stratton, C. Howe, and F.C. Battaglia, eds. (National Academies Press).

Tachibana, M., Sugimoto, K., Nozaki, M., Ueda, J., Ohta, T., Ohki, M., Fukuda, M., Takeda, N., Niida, H., et al. (2002). G9a histone methyltransferase plays a dominant role in euchromatic histone H3 lysine 9 methylation and is essential for early embryogenesis. Genes Dev *16*, 1779-791.

Tachibana, M., Ueda, J., Fukuda, M., Takeda, N., Ohta, T., Iwanari, H., Sakihama, T., Kodama, T., Hamakubo, T., and Shinkai, Y. (2005). Histone methyltransferases G9a and GLP form heteromeric complexes and are both crucial for methylation of euchromatin at H3-K9. Genes Dev *19*, 815-826.

Tahiliani, M., Koh, K.P., Shen, Y., Pastor, W.A., Bandukwala, H., Brudno, Y., Agarwal, S., Iyer, L.M., Liu, D.R., et al. (2009). Conversion of 5-methylcytosine to 5-hydroxymethylcytosine in mammalian DNA by MLL partner TET1. Science *324*, 930-35.

Taléns-Visconti, R., Sanchez-Vera, I., Kostic, J., Perez-Arago, M.A., Erceg, S., Stojkovic, M., and Guerri, C. (2011). Neural differentiation from human embryonic stem cells as a tool to study early brain development and the neuroteratogenic effects of ethanol. Stem Cells Dev *20*, 327-339.

Tan, L., Xiong, L., Xu, W., Wu, F., Huang, N., Xu, Y., Kong, L., Zheng, L., Schwartz, L., et al. (2013). Genome-wide comparison of DNA hydroxymethylation in mouse embryonic stem cells and neural progenitor cells by a new comparative hMeDIP-seq method. Nucleic Acids Res *41*, e84.

Tanaka, S. (1998). Promotion of Trophoblast Stem Cell Proliferation by FGF4. Science *282*, 2072-75.

Tatsumi, K., Ohashi, K., Taminishi, S., Okano, T., Yoshioka, A., and Shima, M. (2008). Reference gene selection for real-time RT-PCR in regenerating mouse livers. Biochem Biophys Res Commun *374*, 106-110.

Tsumura, A., Hayakawa, T., Kumaki, Y., Takebayashi, S., Sakaue, M., Matsuoka, C., Shimotohno, K., Ishikawa, F., Li, E., et al. (2006). Maintenance of self-renewal ability of mouse embryonic stem cells in the absence of DNA methyltransferases Dnmt1, Dnmt3a and Dnmt3b. Genes Cells *11*, 805-814.

Ungerer, M., Knezovich, J., and Ramsay, M. (2013). In utero alcohol exposure, epigenetic changes, and their consequences. Alcohol Res *35*, 37-46.

Vakoc, C.R., Mandat, S.A., Olenchock, B.A., and Blobel, G.A. (2005). Histone H3 Lysine 9 Methylation and HP1γ Are Associated with Transcription Elongation through Mammalian Chromatin. Mol Cell *19*, 381-391.

van den Bergen, J.A., Miles, D.C., Sinclair, A.H., and Western, P.S. (2009). Normalizing Gene Expression Levels in Mouse Fetal Germ Cells. Biol Reprod *81*, 362-370.

Vandesompele, J., De Preter, K., Pattyn, F., Poppe, B., Van Roy, N., De Paepe, A., and Speleman, F. (2002). Accurate normalization of real-time quantitative RT-PCR data by geometric averaging of multiple internal control genes. Genome Biol *3*, RESEARCH0034.

Vangipuram, S.D., and Lyman, W.D. (2010). Ethanol Alters Cell Fate of Fetal Human Brain-Derived Stem and Progenitor Cells. Alcohol Clin Exp Res *34*, 1574-583.

Vangipuram, S.D., and Lyman, W.D. (2012). Ethanol Affects Differentiation-Related Pathways and Suppresses Wnt Signaling Protein Expression in Human Neural Stem Cells. Alcohol Clin Exp Res *36*, 788-797.

Varambally, S., Dhanasekaran, S.M., Zhou, M., Barrette, T.R., Kumar-Sinha, C., Sanda, M.G., Ghosh, D., Pienta, K.J., Sewalt, R.G., and Otte, A.P. (2002). The

polycomb group protein EZH2 is involved in progression of prostate cancer. Nature *419*, 624-29.

Veazey, K.J., and Golding, M.C. (2011). Selection of stable reference genes for quantitative rt-PCR comparisons of mouse embryonic and extra-embryonic stem cells. PLoS One *6*, e27592.

Veazey, K.J., Carnahan, M.N., Muller, D., Miranda, R.C., and Golding, M.C. (2013). Alcohol-induced epigenetic alterations to developmentally crucial genes regulating neural stemness and differentiation. Alcohol Clin Exp Res *37*, 1111-122.

Veazey, K.J., Parnell, S.E., Miranda, R.C., and Golding, M.C. (2015). Dose-dependent alcohol-induced alterations in chromatin structure persist beyond the window of exposure and correlate with fetal alcohol syndrome birth defects. Epigenetics Chromatin *8*.

VEMURI, M., and CHETTY, C. (2005). Alcohol impairs astrogliogenesis by stem cells in rodent neurospheres. Neurochemistry International *47*, 129-135.

Viré, E., Brenner, C., Deplus, R., Blanchon, L., Fraga, M., Didelot, C., Morey, L., Van Eynde, A., Bernard, D., et al. (2006). The Polycomb group protein EZH2 directly controls DNA methylation. Nature *439*, 871-74.

Viré, E., Brenner, C., Deplus, R., Blanchon, L., Fraga, M., Didelot, C., Morey, L., Van Eynde, A., Bernard, D., et al. (2006). The Polycomb group protein EZH2 directly controls DNA methylation. Nature *439*, 871-74.

Vong, Q.P., Liu, Z., Yoo, J.G., Chen, R., Xie, W., Sharov, A.A., Fan, C., Liu, C., Ko, M.S., and Zheng, Y. (2010). A Role for Borg5 During Trophectoderm Differentiation. Stem Cells *28*, 1030-38.

Waltman, R., and Iniquez, E.S. (1972). Placental transfer of ethanol and its elimination at term. Obstet Gynecol *40*, 180-85.

Wang, H., Wang, L., Erdjument-Bromage, H., Vidal, M., Tempst, P., Jones, R.S., and Zhang, Y. (2004). Role of histone H2A ubiquitination in Polycomb silencing. Nature *431*, 873-78.

Wentzel, P., and Eriksson, U.J. (2009). Altered gene expression in neural crest cells exposed to ethanol in vitro. Brain Res *1305 Suppl*, S50-S60.

Whetstine, J.R., Nottke, A., Lan, F., Huarte, M., Smolikov, S., Chen, Z., Spooner, E., Li, E., Zhang, G., et al. (2006). Reversal of Histone Lysine Trimethylation by the JMJD2 Family of Histone Demethylases. Cell *125*, 467-481.

White, A.M., Kraus, C.L., and Swartzwelder, H.S. (2006). Many College Freshmen Drink at Levels Far Beyond the Binge Threshold. Alcohol Clin Exp Res *30*, 1006-010.

Willems, E., Mateizel, I., Kemp, C., Cauffman, G., Sermon, K., and Leyns, L. (2006). Selection of reference genes in mouse embryos and in differentiating human and mouse ES cells. Int. J. Dev. Biol. *50*, 627-635.

Williams, K., Christensen, J., and Helin, K. (2011). DNA methylation: TET proteins—guardians of CpG islands? EMBO Rep *13*, 28-35.

Williams, R.L., Hilton, D.J., Pease, S., Willson, T.A., Stewart, C.L., Gearing, D.P., Wagner, E.F., Metcalf, D., Nicola, N.A., and Gough, N.M. (1988). Myeloid leukaemia inhibitory factor maintains the developmental potential of embryonic stem cells. Nature *336*, 684-87.

Wissmann, M., Yin, N., Müller, J.M., Greschik, H., Fodor, B.D., Jenuwein, T., Vogler, C., Schneider, R., Günther, T., et al. (2007). Cooperative demethylation by JMJD2C

and LSD1 promotes androgen receptor-dependent gene expression. Nat Cell Biol *9*, 347-353.

Wu, H., and Zhang, Y. (2011). Mechanisms and functions of Tet protein-mediated 5-methylcytosine oxidation. Genes Dev *25*, 2436-452.

Wysocka, J., Swigut, T., Milne, T.A., Dou, Y., Zhang, X., Burlingame, A.L., Roeder, R.G., Brivanlou, A.H., and Allis, C.D. (2005). WDR5 Associates with Histone H3 Methylated at K4 and Is Essential for H3 K4 Methylation and Vertebrate Development. Cell *121*, 859-872.

Yamaji, M., Ueda, J., Hayashi, K., Ohta, H., Yabuta, Y., Kurimoto, K., Nakato, R., Yamada, Y., Shirahige, K., and Saitou, M. (2013). PRDM14 Ensures Naive Pluripotency through Dual Regulation of Signaling and Epigenetic Pathways in Mouse Embryonic Stem Cells. Cell Stem Cell *12*, 368-382.

Yamane, K., Toumazou, C., Tsukada, Y., Erdjument-Bromage, H., Tempst, P., Wong, J., and Zhang, Y. (2006). JHDM2A, a JmjC-Containing H3K9 Demethylase, Facilitates Transcription Activation by Androgen Receptor. Cell *125*, 483-495.

Yoder, J.A., Walsh, C.P., and Bestor, T.H. (1997). Cytosine methylation and the ecology of intragenomic parasites. Trends in genetics *13*, 335-340.

Yoshida, A., and Tani, K. (1983). Phosphoglycerate kinase abnormalities: functional, structural and genomic aspects. Biomed Biochim Acta *42*, S263-67.

Yu, B.D., Hess, J.L., Horning, S.E., Brown, G.A., and Korsmeyer, S.J. (1995). Altered Hox expression and segmental identity in Mll-mutant mice. Nature *378*, 505-08.

Zakhari, S. (2013). Alcohol metabolism and epigenetics changes. Alcohol Res *35*, 6-16.

Zeisel, S.H. (2011). What Choline Metabolism Can Tell Us About the Underlying Mechanisms of Fetal Alcohol Spectrum Disorders. Molecular Neurobiology *44*, 185-191.

Zentner, G.E., and Henikoff, S. (2013). Regulation of nucleosome dynamics by histone modifications. Nat Struct Mol Biol *20*, 259-266.

Zhang, Y. (2001). Transcription regulation by histone methylation: interplay between different covalent modifications of the core histone tails. Genes Dev *15*, 2343-360.

Zhou, F.C., Balaraman, Y., Teng, M., Liu, Y., Singh, R.P., and Nephew, K.P. (2011). Alcohol Alters DNA Methylation Patterns and Inhibits Neural Stem Cell Differentiation. Alcohol Clin Exp Res *35*, 735-746.

Zhou, F.C., Chen, Y., and Love, A. (2011). Cellular DNA methylation program during neurulation and its alteration by alcohol exposure. Birth Defects Res A Clin Mol Teratol *91*, 703-715.

Zhou, F.C., Zhao, Q., Liu, Y., Goodlett, C.R., Liang, T., McClintick, J.N., Edenberg, H.J., and Li, L. (2011). Alteration of gene expression by alcohol exposure at early neurulation. BMC Genomics *12*, 124.

Zhou, Z., Yuan, Q., Mash, D.C., and Goldman, D. (2011). Substance-specific and shared transcription and epigenetic changes in the human hippocampus chronically exposed to cocaine and alcohol. Proc Natl Acad Sci U S A *108*, 6626-631.

Zorn, A.M., and Wells, J.M. (2009). Vertebrate Endoderm Development and Organ Formation. Annual Review of Cell and Developmental Biology *25*, 221-251.

APPENDIX

Primer Name	Sequence	Tm	Amplicon Size	Reference
mH2afz Sen	GCGCAGCCATCCTGGAGTA	60		Mamo et al. 2007
m2afz Asen	CCGATCAGCGATTTGTGGA	60	202	
mGAPDH Sen	TGACGTGCCGCCTGGAGAAA	60		Mamo et al. 2007
mGAPDH Asen	AGTGTAGCCCAAGATGCCCTTCAG	60	98	
mHPRT1 Sen	CTGGTGAAAAGGACCTCTCGAA	60		Mamo et al. 2007
mHPRT1 Asen	CTGAAGTACTCATTATAGTCAAGGG CAT	60	117	
mPPIA Sen	CGCGTCTCCTTCGAGCTGTTTG	60		Mamo et al. 2007
mPPIA Asen	TGTAAAGTCACCACCCTGGCACAT	60	150	
mYWHAZ Sen	TTGATCCCCAATGCTTCGC	60		This study
mYWHAZ Asen	CAGCAACCTCGGCCAAGTAA	60	88	
mSDHA Sen 2	GCTCCTGCCTCTGTGGTTGA	60		This study
mSDHA Asen 2	AGCAACACCGATGAGCCTG	60	134	
mB2M Sen	CCGCCTCACATTGAAATCCA	60		This study
mB2M Asen	TCGATCCCAGTAGACGGTCTTG	60	199	
mGUSB Sen 2	GGCTGGTGACCTACTGGATTT	60		This study
mGUSB Asen 2	TTGGCACTGGGAACCTGAAGT	60	134	
mTBP Sen	GAAGAACAATCCAGACTAGCAGCA	60		This study
mTBP Asen	CCTTATAGGGAACTTCACATCACAG	60	127	
mPGK1 Sen	CTGACTTTGGACAAGCTGGACG	60		This study
mPGK1 Asen	GCAGCCTTGATCCTTTGGTTG	60	110	
mHexokinase II Fwd	CCCTGTGAAGATGTTGCCCAC	60		Allen et al.,2004
mHexocinase II Rev	TGCCCATGTACTCAAGGAAGT	60	251	
mActb Fwd	TGGTGGGTATGGGTCAGAAG	57		Allen et al.,2004
mActb Rev	GGTCATCTTTTCACGGTTGG	57	269	
mhsp70 Fwd	ACGTGGCCTTCACCGACACC	57		Allen et al.,2004
mhsp70 Rev	CGATCTCCTTCATCTTCGTC	57	270	
mRn7sk Fwd	ATTGATCGCCAGGGTTGATT	60		Allen et al.,2004
mRn7sk Rev	CGGGGAAGGTCGTCCTCTTC	60	123	
mOct4 Fwd	ATGGCTGGACACCTGGCTTC	60		Golding et al., 2010
mOct4 Rev	GGTCGGCACAGGGCTCAGA	60	337	

mCDX2 Fwd	GCAGTCCCTAGGAAGCCAAGTGA	60		Strumpf et al., 2005
mCDX2 Rev	CTCTCGGAGAGCCCAAGTGTG	60	162	
mGATA4 Fwd	CCTCTATCACAAGATGAACGGC	60		Golding et al., 2010
mGATA4 Rev	CACTGCTGCTGCTGCTGCTA	60	356	
mNanog Fwd	GCACTCAAGGACAGGTTTCAGA	60		Golding et al., 2010
mNanog Rev	GGTGGAGTCACAGAGTAGTTCAGG	60	578	
mSox7 Fwd	CGCCGCCCGCCGTCCCCCGA	60		Golding et al., 2010
mSox7 Rev	CACCCCTGTCCTCCTTCTCC	60	399	
mHand 1 Fwd	GATGCTGCCCCAGATTTCCCT	60		Golding et al., 2010
mHand 1 Rev	CCCTTTTCCGCTTGCTTTCG	60	388	
mFSP1 Fwd	GGCAAGACCCTTGGAGGAG	60		This study
mFSP1 Rev	CCTTTTCCCCAGGAAGCTAG	60	212	

Table S1. Description and sequences of the primers used in the in the analysis of both the candidate reference genes and lineage specific transcription factors for Chapter III.

Primer Name	Sequence	Experiment	Reference
mGAPDH Sen1	TGACGTGCCGCCTGGAGAAA	Reference Gene	Mamo et al.2007
mGAPDH Asen1	AGTGTAGCCCAAGATGCCCTTCAG	Reference Gene	
mHPRT1 Sen 1	CTG GTG AAA AGG ACC TCT CGA A	Reference Gene	Mamo et al.2007
mHPRT1 Asen 1	CTGAAGTACTCATTATAGTCAAGGGCAT	Reference Gene	
mPGK1 Sen1	CTG ACT TTG GAC AAG CTG GAC G	Reference Gene	Veazey and Golding 2011
mPGK1 Asen1	GCA GCC TTG ATC CTT TGG TTG	Reference Gene	
IAP1 F	ACAAGAAAAGAAGCCCGTGA	Expression Endogenous Retroviral Elements	Watanabe et al., 2006
IAP1 R	GCCAGAACATGTGTCAATGG	Expression Endogenous Retroviral Elements	
IAP LTR Fwd	GCACATGCGCAGATTATTTGTT	Expression Endogenous Retroviral Elements	Carmell et al., 2007
IAP LTR Rev	CCACATTCGCCGTTACAAGAT	Expression Endogenous Retroviral Elements	
IAP Gag Fwd	AACCAATGCTAATTTCACCTTGGT	Expression Endogenous Retroviral Elements	Carmell et al., 2007

IAP Gag Rev	GCCAATCAGCAGGCGTTAGT	Expression Endogenous Retroviral Elements	
L1 Md Fwd	GAGACATAACAACAGATCCTGA	Expression Endogenous Retroviral Elements	Watanabe et al., 2006
L1 Md Rev	GAACTTTGGTACCTGGTATCTG	Expression Endogenous Retroviral Elements	
L1 5 UTR Fwd	GGCGAAAGGCAAACGTAAGA	Expression Endogenous Retroviral Elements	Carmell et al., 2007
L1 5UTR Rev	GGAGTGCTGCGTTCTGATGA	Expression Endogenous Retroviral Elements	
L1 ORF2 Fwd	GGAGGGACATTTCATTCTCATCA	Expression Endogenous Retroviral Elements	Carmell et al., 2007
L1 ORF2 Rev	GCTGCTCTTGTATTTGGAGCATAGA	Expression Endogenous Retroviral Elements	
Etn Set 1 Fwd	CACCGCTTGGTGCAGAGATAC	Expression Endogenous Retroviral Elements	This study
Etn Set 1 Rev	GCGAGGTAGAGCCGGAGAATA	Expression Endogenous	

		Retroviral Elements	
Etn Set 2 Fwd	TAAGAGGAACGCTGCATTGGA	Expression Endogenous Retroviral Elements	This study
Etn Set 2 Rev	TATCCTACCGCATCCTCAGCA	Expression Endogenous Retroviral Elements	
MusD1 Set 1 Fwd	GGATTCTGAATGGCGAGACG	Expression Endogenous Retroviral Elements	This study
MusD1 Set 1 Rev	GCGTACACTGCAACGGGAA	Expression Endogenous Retroviral Elements	
TRIM 33 Set 1 Fwd	TGATATCACAGGCCTCTCCC	Expression Analysis	This study
TRIM 33 Set 1 Rev	GGTGGGATCACAATGGAAAC	Expression Analysis	
NP95 Set 1 Sen	GGATGACAAGACTGTGTGGGAG	Expression Analysis	This study
Np95 Set 1 Asen	GCTCGTCCTCAGATAGGGCTCT	Expression Analysis	
NP95 Set2 Sen	GGTGCGGAGGCTGAAGACT	Expression Analysis	This study
NP95 Set2 Asen	CAGGAGCGTACTTGCTGTGTTT	Expression Analysis	
ZFP809 Set1 Sen	CTTGGAGGAGTGGCAGGACC	Expression Analysis	This study
ZFP809 Set 1 Asen	CAACTTAGGTTTGGCAATGCAG	Expression Analysis	

ZFP809 Set 2 Sen	TTGGAGCGTGGATTTGGG	Expression Analysis	This study
ZFP809 Set2 Asen	TGCTTCAATCGTGTCTTCA CTTG	Expression Analysis	
ZFP57 Set 1 Sen	GTGGCTAGAAGCAGTCTG GAATAG	Expression Analysis	This study
ZFP57 Set 1 Asen	CTGGATGGCTGGGAAGAC TGT	Expression Analysis	
ZFP57 Set 2 Sen	CGTTCATGCCCTGAGTGT GG	Expression Analysis	This study
ZFP57 Set 2 Asen	CGCTTGGGATCTAGGTGT TGTA	Expression Analysis	
Gtsf1L Set 1 Sen	GCTACTTGTCCCTTCAAT GCTCG	Expression Analysis	This study
Gtsf1L Set 1 Asen	TGTGCTCTCAGCCAGAGT CTCTT	Expression Analysis	
Mael Set 1 Sen	CCTCCCTTGTGAAATTGG CTG	Expression Analysis	This study
Mael Set 1 Asen	AATGGAATCGAAATCCTC GTGG	Expression Analysis	
HDAC1 Set1 Sen	GAGTTCTGTCAGTTGTCC ACGG	Expression Analysis	This study
HDAC1 Set1 Asen	CTCTTCCACGCCATCGCC	Expression Analysis	
Suv420H1 Set1 Sen	GGCAAGTTGTCTAATGAC CATCA	Expression Analysis	This study
Suv420H1 Set1 Asen	CCGAGTTACCATGACATC TGCT	Expression Analysis	
Suv420H1 Set2 Sen	CCACACAGTACGCTCTCT CTCAA	Expression Analysis	This study
Suv420H1 Set2 Asen	TACCCTGTTCTTTAAGTAG CTCTGC	Expression Analysis	
Suv420H2 Set1 Sen	CCCACTCCTGATTTCATC CCT	Expression Analysis	This study

Suv420H2 Set1 Asen	TCCATTCCGCTCCCTGTAAG	Expression Analysis	
Suv420H2 Set2 Sen	CAGAGCTGCGTGAAGAGGATG	Expression Analysis	This study
Suv420H2 Set2 Asen	CAGTCATGGTTGATGAAGGCAG	Expression Analysis	
Trim28 Set 1 Sen	CGGCGCTATGGTGGATTGT	Expression Analysis	This study
Trim28 Set 1 Asen	GGTTAGCATCCTGGGAATCAGAA	Expression Analysis	
Trim28 Set 2 Sen	GTGGCTGAGCGTCCTGGTAC	Expression Analysis	This study
Trim28 Set 2 Asen	CGGCTCTGCACTTGAATAGGG	Expression Analysis	
SetDB1 Set1 Sen	TCAGGTCTGGCTTTATGCTGG	Expression Analysis	This study
SetDB1 Set1 Asen	CTCTATGAAGTCTCGGCAGGAGC	Expression Analysis	
SetDB1 Set 2 Sen	AGCTGGAGACGTGGGTACTACAG	Expression Analysis	This study
SetDB1 Set 2 Asen	GGAATCTCAATGATCTCTGTGGG	Expression Analysis	
Ehmt1 Set 1 Sen	ATGCTGGTTCAGGCGGGT	Expression Analysis	This study
Ehmt1 Set 1 Asen	AGCCCTCTGCGTCCTTCG	Expression Analysis	
Ehmt1 Set 2 Sen	GGAGCAGCTCGGGTTCG	Expression Analysis	This study
Ehmt1 Set 2 Asen	CACTGGCTTGCCTCTGGG	Expression Analysis	
G9a Set 1 Sen	GACAGGGGCAGGAAAGTCG	Expression Analysis	This study
G9a Set 1 Asen	CCTGGGCGGCAGTTGTTG	Expression Analysis	

G9a Set 2 Sen	CGCTGATGGTGCTCTGTGAG	Expression Analysis	This study
Smarca1 Set 1 Fwd	AGTGTGTACGGAATGCTCCC	Expression Analysis	
Smarca1 Set 1 Rev	TCAGTCTTCACACCATCCCA	Expression Analysis	This study
Smarca1 Set 2 Fwd	GGTAAAATGGTCGCTCTGGA	Expression Analysis	
Smarca1 Set 2 Rev	TGCTGCTATTTGGAGCATTG	Expression Analysis	This study
Smarcc2 Set 1 Fwd	GTCTGGAGAGTAGCGGCATC	Expression Analysis	
Smarcc2 Set 1 Rev	AGGTTGCCTTCACCAATGTC	Expression Analysis	This study
Smarcd1 Set 1 Fwd	ACTGGTCCCAGAATCACAGG	Expression Analysis	
Smarcd1 Set 1 Rev	TGGTAGTCCAGCATCAGCAG	Expression Analysis	This study
Smacad1 Set 1 Fwd	ATAACAGAACTCCGGCCCTT	Expression Analysis	
Smarcad1 Set 1 Rev	GTGGAGGCTGGAACAACAAT	Expression Analysis	This study
Actl6b Set 1 Fwd	TACAGCAAGGCATCGTCAAG	Expression Analysis	
Actl6b Set 1 Rev	GGCGAATGTCAATGTCACAC	Expression Analysis	This study
Smarca5 Set 1 Fwd	GCTCTCCGTGTTAGTGAGCC	Expression Analysis	
Smarca5 Set 1 Rev	CATCGCAGTTCTGGACTTGA	Expression Analysis	This study
Smarca5 Set 2 Fwd	GCTCTCCGTGTTAGTGAGCC	Expression Analysis	

Smarca5 Set 2 Rev	GCTGTTCCTCTTTCTGTGCC	Expression Analysis	This study
Hdac2 Set 1 Fwd	CCGGTGTTTGATGGACTCTT	Expression Analysis	
Hdac2 Set 1 Rev	GCGCTAGGCTGGTACATCTC	Expression Analysis	This study
Pcgf6 Set 1 Fwd	TCCACCAGACTCAGCCTCTT	Expression Analysis	
Pcgf6 Set 1 Rev	GAAGAACAAGCAGACCGTCC	Expression Analysis	This study
Phc2 Set 1 Fwd	CATTGTGAAACCCCAAATCC	Expression Analysis	
Phc2 Set 1 Rev	AAAGTCCCACTCGTTTGGTG	Expression Analysis	This study
Suv39H1 Set 1 Fwd	ACTGCCCAAACCGTGTAGTC	Expression Analysis	
Suv39H1 Set 1 Rev	TTCGGGTACTCTCCATGTCC	Expression Analysis	This study
Suv39H1 Set 2 Fwd	ACTGCCCAAACCGTGTAGTC	Expression Analysis	
Suv39H1 Set 2 Rev	GTCCATTCGGGTACTCTCCA	Expression Analysis	This study
Phc3 Set 1 Fwd	TACCTGCAGCAGATGTACGC	Expression Analysis	
Phc3 Set 1 Rev	TGCAGACTGACAGGAAGGTG	Expression Analysis	This study
Dnmt3a Set 1 Fwd	GCTGTGGAAGTGCAGAACAA	Expression Analysis	
Dnmt3a Set 1 Rev	CATGTAGCAGTTCCAGGGGT	Expression Analysis	This study
Dnmt3a Set 2 Fwd	GCTGTGGAAGTGCAGAACA	Expression Analysis	
Dnmt3a Set 2 Rev	ACATGTAGCAGTTCCAGGG	Expression Analysis	This study

Eed Set 1 Fwd	GAGAGGGAAGTGTCGACTGC	Expression Analysis	
Eed Set 1 Rev	ATAGAGGGTGGCTGGTGTTG	Expression Analysis	This study
SirT1 Set 1 Fwd	TTGTGAAGCTGTTCGTGGA	Expression Analysis	
SirT1 Set 1 rev	GGCGTGGAGGTTTTTCAGA	Expression Analysis	This study
SirT1 Set 2 Fwd	TACTGAAAAACCTCCACGCC	Expression Analysis	
SirT1 Set 2 Rev	TCCGTATCATCTTCCAAGCC	Expression Analysis	This study
Dnmt1 Set 1 Fwd	AAGAGAACCCTGTACCCAGAGA	Expression Analysis	
Dnmt1 Set 1 Rev	ATGGTTTGGTGGGTCTTCA	Expression Analysis	This study
EzH2 Set 1 Fwd	CCTGTTCCCACTGAGGATGT	Expression Analysis	
EzH2 Set 1 Rev	TTTGATAAAGATGCCCCAGC	Expression Analysis	This study
Hdac9 Set 1 Fwd	CTCAGAGCCCAACTTGAAGG	Expression Analysis	
Hdac9 Set 1 Rev	CCATTGCTACATGAACGTGG	Expression Analysis	This study
Hdac7 Set 1 Fwd	TGGAGACAACAGCAAGCATC	Expression Analysis	
Hdac7 Set 1 rev	CACTGGGGTCCTGGTAGAAA	Expression Analysis	This study
mGfap Fwd	TGCTGGAGGGCGAAGAAAA	Expression Analysis	
mGfap Rev	TTGGTGCTTTTGCCCCCT	Expression Analysis	This study
mNeuN Fwd	AGTTTCCCCTACCCCACCAC	Expression Analysis	

mNeuN Rev	GTTTGCTCCAGTGCCGCTC	Expression Analysis	This study
Nestin Fwd	CTTTCCTGACCCCAAGCTGA	Expression Analysis	
Nestin Rev	GGCCAAGGTGGGGGTTC	Expression Analysis	This study
mS100a4 Fwd	GGCAAGACCCTTGGAGGAG	Expression Analysis	
mS100a4 Rev	CCTTTTCCCCAGGAAGCTAG	Expression Analysis	This study
mIGF1 Pro Fwd	CGGGAAACAGTGTGTGCCT	Expression Analysis	
mIGF1 Pro Rev	AGTGGGCTGGCTCCTGTC	Expression Analysis	This study
Oct4 F	TCAGGTTGGACTGGGCCTA	Expression Analysis	
Oct4 R	CCTCGAAGCGACAGATGGT	Expression Analysis	This study
Math1 Fwd	GGAGAAGCTTCGTTGCACG	Expression Analysis	
Math1 Rev	GGGACATCGCACTGCAAT	Expression Analysis	This study
Nkx2.2 F	GCAGAGCCTGCCCCTTAA	Expression Analysis	
Nkx2.2 R	GCCCTGGGTCTCCTTGTCA	Expression Analysis	This study
Msx1 F	CCTCTCGGCCATTTCTCAG	Expression Analysis	
Msx1 R	GGTTGGTCTTGTGCTTGCG	Expression Analysis	This study
Nkx2.9 F	CCACCTCTGGACGCCTCG	Expression Analysis	
Nkx2.9 R	CCAGCTGCGACGAGTCTGC	Expression Analysis	This study

Mash1 F	TGGAGACGCTGCGCTCG GC	Expression Analysis	
Mash1 R	GTTGCTTCAATGGAGGCA AAT	Expression Analysis	This study
HoxA7 F	AAGCCAGTTTCCGCATCT ACC	Expression Analysis	
HoxA7 R	GTAGCGGTTGAAATGGAA TTCC	Expression Analysis	This study
Gata4 F	GAGGCTCAGCCGCAGTTG CAG	Expression Analysis	
Gata4 R	CGGCTAAAGAAGCCTAGT CCTTGCTT	Expression Analysis	This study
Gata1 F	GTCCTCACCATCAGATTC CACAG	Expression Analysis	
Gata1 R	AGTGGATACACCTGAAAG ACTGGG	Expression Analysis	This study
mMll1 Fwd Set 1	CCCTGAGTACAACCCTAA CGATG	Expression Analysis	
mMll1 Rev Set 1	GAGACCTGTAGACACCAA CCGC	Expression Analysis	This study
mMll1 Few Set 2	TAGACAAGGGGAGCGGC AA	Expression Analysis	
mMll1 Rev Set 2	ACACTCCTTCTGCGATGG CT	Expression Analysis	This study
mAsh2l1 Fwd Set 1	GCTCTGTGGATGAGGAGA ATGG	Expression Analysis	
mAsh2l1 Rev Set 1	GAAGCTGTAGTTGGTCAT AAAAGGC	Expression Analysis	This study
mAsh2l1 Fwd Set 2	TGGCAAGCACTATTCGTC TGG	Expression Analysis	
mAsh2l1 Rev Set 2	CCACACCCTGATTGACAC CAT	Expression Analysis	This study
mWdr5 Fwd Set 1	GGGAATATCTGATGTAGC GTGG	Expression Analysis	

mWdr5 Rev Set 1	CAGCAGAAGACGTAGTTACTGTGG	Expression Analysis	This study
mWdr5 Fwd Set 2	AATCCTCCAGTGTCCTTCGTGA	Expression Analysis	
mWdr5 Rev Set 2	CAGACACAATCCACTTCCCG	Expression Analysis	This study
mJmjd3 Fwd Set 1	GAGCGATATGAGTGGAACGAGG	Expression Analysis	
mJmjd3 Rev Set 1	CCATTCTCACTTGTAACGAACAGG	Expression Analysis	This study
mJmjd3 Fwd Set 2	CTCATCAAGGTGGAAAGTGGG	Expression Analysis	
mJmjd3 Rev Set 2	GGCAGCTTCTCCTCAGTGTTG	Expression Analysis	This study
mKdm1b Fwd Set 1	CACACGGTGGAGCACAGAGC	Expression Analysis	
mKdm1b Rev Set 1	CTCGTACACCACTTAAATATGCCC	Expression Analysis	This study
mKdm1b Fwd Set 2	GCAAACATCTCAATGGATACAGG	Expression Analysis	
mKdm1b Rev Set 2	CAGTGGACCTGCCTATGGGA	Expression Analysis	This study
mUtx Fwd Set 1	ACTGGAGAGACACCTAACAGCACT	Expression Analysis	
mUtx Rev Set 1	GGACAGTTGGGTGGATGTTATTG	Expression Analysis	This study
mUtx Fwd Set 2	TGTAGCACATCAAGAACACTGGG	Expression Analysis	
mUtx Rev Set 2	CCTGCCAAATGTGAACTCGG	Expression Analysis	This study
mMll2 Fwd Set 1	CTACATTGAGCGGGACGAGG	Expression Analysis	
mMll2 Rev Set 1	GGAGACGCATCGGTGAAGAC	Expression Analysis	This study

mMll2 Fwd Set 2	CCGCATCATTGAGCCTGTG	Expression Analysis	
mMll2 Rev Set 2	GTGAAGGTGCTCTGATACGCC	Expression Analysis	This study
Sox2 RlTm Sen	ATGAACGGCTGGAGCAACG	Expression Analysis	
Sox2 RlTm Asen	GCTGCGAGTAGGACATGCTGTAG	Expression Analysis	This study
mDlx2 Fwd 1	CACGCACCATCTACTCCAGTTT	Expression Analysis	
mDlx2 Rev 1	TGCTGCTCGGTGGGTATCTC	Expression Analysis	This study
mDlx2 Fwd 2	CTCAGGGTCCTTGGTCTCTTCA	Expression Analysis	
mDlx2 Rev 2	GGTAGGTGATAGGGTGGAGTAGGA	Expression Analysis	This study
mMsx2 RNA Fwd 1	CGAAGGGCTAAGGCGAAAAG	Expression Analysis	
mMsx2 RNA Rev 1	GGAGCACAGGTCTATGGAAGG	Expression Analysis	This study
mMsx2 RNA Fwd 2	GGTGATTGGAAGAGGACATGGTA	Expression Analysis	
mMsx2 RNA Rev 2	GGGAAGAGATGGACAGGAAGG	Expression Analysis	This study
mPax6 Fwd RlTm	GGGACTTCAGTACCAGGGCA	Expression Analysis	
mPax6 Rev RlTm	TTCATCCGAGTCTTCTCCGTTAG	Expression Analysis	This study
mPax6 Fwd 2 RlTm	GAGTTCTTCGCAACCTGGCTA	Expression Analysis	
mFabp7 Fwd RlTm	CCCGAGTTCCTCCAGTTCC	Expression Analysis	This study
mFabp7 Rev RlTm	ATCACCACTTTGCCACCTTCC	Expression Analysis	

mSox2 Fwd RlTm	GGCGGCAACCAGAAGAACA	Expression Analysis	This study
mSox2 Rev RlTm	TTCTCGGTCTCGGACAAAAGTT	Expression Analysis	
mGli3 Fwd RlTm	CACTGGGGAGAAGCCTCACA	Expression Analysis	This study
mGli3 Rev RlTm	GTTCTGTTTTGGTGCTTGGC	Expression Analysis	
mGli3 Fwd 2 RlTm	CCTCCCATTCCCATCCCTAT	Expression Analysis	This study
mGli3 Rev 2 RlTm	CCCAAGTCATTTCAGTCTTTGTG	Expression Analysis	
mOlig2 Fwd RlTm	GCGGTGGCTTCAAGTCATCT	Expression Analysis	This study
mOlig2 Rev RlTm	CGAGTTGGTGAGCATGAGGAT	Expression Analysis	
mTuJ1 Fwd RlTm	CCATCCAGAGTAAGAACAGCAGC	Expression Analysis	This study
mTuJ1 Rev RlTm	CTCCGAGATGCGTTTGAACA	Expression Analysis	
mNkx2.1 Fwd	GAAAACTGCGGGGATCTGAG	Expression Analysis	This study
mNxi2.1 Rev	CGGAGTCGTGTGCTTTGGA	Expression Analysis	
mNkx2.1 Fwd 2	TCGCAGCGTACAGACAGGG	Expression Analysis	This study
mNkx2.1 Rev 2	ATGAAGCGGGAGATGGCG	Expression Analysis	
Ezh1 F	CGAGTCTTCCACGGCACCTA	Expression Analysis	This study
Ezh1 R	GCAAACTGAAAGACCTGCTTGC	Expression Analysis	
Ezh2 F	CCTTCCATGCAACACCCAAC	Expression Analysis	This study

Ezh2 R	GCTCCCTCCAGATGCTGG TAA	Expression Analysis	
Major Satellite Exp F	GACGACTTGAAAAATGAC GAAATC	Expression Analysis	Rugg-Gunn
Major Satellite Exp R	CATATTCCAGGTCCTTCA GTGTGC	Expression Analysis	
Vdr Exp F	AGCTGAACCTCCATGAGG AAGAAC	Expression Analysis	Rugg-Gunn
Vdr Exp R	TCAACCAGCTTAGCATCC TGTACC	Expression Analysis	
Dlx3 Exp F	GCTGGGCCTCACACAAAC AC	Expression Analysis	Rugg-Gunn
Dlx3 Exp R	TGTTGTTGGGGCTGTGTT CC	Expression Analysis	
Dlx5 Exp F	AGCCAGCCAGAGAAAGAA GTGG	Expression Analysis	Rugg-Gunn
Dlx5 Exp R	GTCCTGGGTTTACGAACT TTCTTTG	Expression Analysis	
mHOTAIR Fwd 1	CAGTGGCAGGATAGGCAC AGT	Expression Analysis	This study
mHOTAIR Rev 1	GCAGACATATTGTTTATGA GTCCACA	Expression Analysis	
mHOTAIR Fwd 2	GCTGACATACATGGCTAT TTCAAAG	Expression Analysis	This study
mHOTAIR Rev 2	CAGAGCTGAAGGTATGGG AAGGTAGAC	Expression Analysis	
mLinc1471 Fwd 1	TCTCTCAACAAACACTCCT CATCTG	Expression Analysis	This study
mLinc1471 Rev 1	TCCAAGTCAAACATGAAA CCCA	Expression Analysis	
mLinc1471 Fwd 2	TCTCCCCATTCCATACAG CC	Expression Analysis	This study
mLinc1471 Rev 2	CTCTGTGTCCCTCTGTCT GCC	Expression Analysis	

mLinc1230 Fwd 1	AGGCTCTGCTGGAGAACACC	Expression Analysis	This study
mLinc1230 Rev 1	CTGCCAGTGGAGAGTGTGTGTG	Expression Analysis	
mLinc1230 Fwd 2	ACAGAGCCTGGAACTCCCG	Expression Analysis	This study
mLinc1230 Rev 2	CCTAGTTTTACCCGATCCATGAA	Expression Analysis	
mLinc1354 Fwd 1	AAGGCTGAGATGACTGGTGCTC	Expression Analysis	This study
mLinc1354 Rev 1	GGGGACTGCTAGTGGAGTGTC	Expression Analysis	
mLinc1354 Fwd 2	GACTGCTCCGCTGTCCTCAT	Expression Analysis	This study
mLinc1354 Rev 2	CATCTTCCAACGTCACGCAT	Expression Analysis	
mLinc1281 Fwd 1	GGCTCCCATACCGTCTTCTG	Expression Analysis	This study
mLinc1281 Rev 1	CTGTTGAAAATCCAACTACTCCTCC	Expression Analysis	
mLinc1281 Fwd 2	GCACTGGTTAGAGTCTACTGTCTGGT	Expression Analysis	This study
mLinc1281 Rev 2	GCAGTACAGCTCACAGGAATCG	Expression Analysis	
mMistral Fwd 1	GACCTTGATGCTTCTAACTGATAGTCT	Expression Analysis	This study
mMistral Rev 1	GAGAGGACAGTGAGTCTGGGAAC	Expression Analysis	
mMistral Fwd 2	TCCCAGACTCACTGTCCTCTCC	Expression Analysis	This study
mMistral Rev 2	CAGAATTAGTTCAATACAACACACCAT	Expression Analysis	
mLinc1418 Fwd 1	TACTCAGAGGGGATTGGGGTC	Expression Analysis	This study

mLinc1418 Rev 1	GAGAGAGGCTCAGGAGGGCA	Expression Analysis	
mLinc1418 Fwd 2	GACTGTTGACTCTAGGATTAGCAGC	Expression Analysis	This study
mLinc1418 Rev 2	CCTGTCAGTCTGTCCGCTTTC	Expression Analysis	
mLinc1456 Fwd 1	AAAGAATGTGAACGGATCTCCC	Expression Analysis	This study
mLinc1456 Rev 1	CCATGCCCAGTGCGTACAAG	Expression Analysis	
mLinc1456 Fwd 2	CCGTGTCACTGATGAGGTCCC	Expression Analysis	This study
mLinc1456 Rev 2	CCTCTACCTAGCCCAGCTTTGA	Expression Analysis	
Smarca2 Pro Fwd	GCTGCTATTCGCCTCCC	ChIP	This study
Smarca2 Pro Rev	CCATCCCAGACTACTACCGC	ChIP	
Smarca2 Pro Fwd2	ACCAAAACAAACAGGCGG	ChIP	This study
Smarca2 Pro Rev2	GGGAGCTGTGGTTAGAGCATT	ChIP	
ApoC2-F	CCATGCGTAGGGCATTAGAAGA	ChIP	Rugg-Gunn et al., 2010
ApoC2-R	GGCCCATCCTGTAACAGAGCTT	ChIP	
Cdx2-F	CCAGGTTGGAAGGAGGAAGC	ChIP	Rugg-Gunn et al., 2010
Cdx2-R	ACCACCCCCAGAAACACGAT	ChIP	
Dlx3-F	ACAGCGCTCCTCAGCATGAC	ChIP	Rugg-Gunn et al., 2010
Dlx3-R	CTGCGAGCCCATTGAGATTG	ChIP	

Dlx5-F	GCTTCGCTGGCTAATCCAGACT	ChIP	Rugg-Gunn et al., 2010
Dlx5-R	CAGCCCTAGTGGTGTTTGCGTA	ChIP	
Eomes-F	CCTCTGGGACCTGCCAAACT	ChIP	Rugg-Gunn et al., 2010
Eomes-R	CTCTATGGCGCCGGAGAAAC	ChIP	
Epas1-F	CTCGGACCTGCGAGCACTAA	ChIP	Rugg-Gunn et al., 2010
Epas1-R	CGGAGCACCTGGGTTCCTTA	ChIP	
Esrrb-F	CAGCCAGCCCAACCATGTAA	ChIP	Rugg-Gunn et al., 2010
Esrrb-R	AGGAGGATGTGTCGGGAGGA	ChIP	
FoxA2-F	TCCTCCTGAAGTCATCCCACAA	ChIP	Rugg-Gunn et al., 2010
FoxA2-R	TAAATCCAAGGTGCCCAAAGC	ChIP	
Gapdh-F	TCCTATCCTGGGAACCATCACC	ChIP	Rugg-Gunn et al., 2010
Gapdh-R	TCTTTGGACCCGCCTCATTT	ChIP	
Gata1-F	TGCCCCAACTTCTTCCCATT	ChIP	Rugg-Gunn et al., 2010
Gata1-R	CAGGCCTGGGAGGATGAAGA	ChIP	
Gata6-F	CTGGGTGGCGGGTATGACTT	ChIP	Rugg-Gunn et al., 2010
Gata6-R	CGCCCAGCTAAAGGACACCA	ChIP	
Gbx1-F	CAAGCCCTTCTGAACTATCCCAAT	ChIP	Rugg-Gunn et al., 2010

Gbx1-R	AGCTCCCAGAGTTAGGAG ACAGGA	ChIP	
Hoxa7-F	GAGAGGTGGGCAAAGAG TGG	ChIP	Tanaka et al., 1998
Hoxa7-R	CCGACAACCTCATACCTA TTCCTG	ChIP	
Hoxa9-F	GGAGGGAGGGGAGTAAC AAA	ChIP	Kunath et al., 2005
Hoxa9-R	TCACCTCGCCTAGTTTCT GG	ChIP	
Intergenic-F	GGAGAGAAGTGGAGTGG CCAAG	ChIP	Rugg-Gunn et al., 2010
Intergenic-R	TTGCCAGCCTAATCATGA GGAA	ChIP	
Irx1-F	CGGTCACCTCGGTGCTAG G	ChIP	Rugg-Gunn et al., 2010
Irx1-R	ATAGGGCAAGAAGGCGCT GT	ChIP	
Kcnq1ot1-F	CAAAGCACACTGAGGATG GCTAGT	ChIP	Rugg-Gunn et al., 2010
Kcnq1ot1-R	GCCTCAGCATATTTGTCC ACAGTT	ChIP	
Lhx2-F	GATGCACTGGGCCGGTTA	ChIP	Rugg-Gunn et al., 2010
Lhx2-R	GCCCGACAGACTGTGGAA CA	ChIP	
Major Satellite-F	GACGACTTGAAAAATGAC GAAATC	ChIP	Umlauf et al., 2004
Major Satellite-R	CATATTCCAGGTCCTTCA GTGTGC	ChIP	
Msx1-F	ACAGAAAGAAATAGCACA GACCATAAGA	ChIP	Tanaka et al., 1998
Msx1-R	TTCTACCAAGTTCCAGAG GGACTTT	ChIP	

Nanog-F	CAGACTGGGAGGGAGGGAAA	ChIP	Rugg-Gunn et al., 2010
Nanog-R	GAGGTGCAGCCGTGGTTAAA	ChIP	
Nostrin-F	TGCTTGATGAGGTGCCAACA	ChIP	Rugg-Gunn et al., 2010
Nostrin-R	GTGTGGAGGGGAGGCAAATC	ChIP	
Npas2-F	TTGTGTCACTACGTTCCTGGGTCT	ChIP	Rugg-Gunn et al., 2010
Npas2-R	GAGCGCAGAGCTGTCTAAGCAC	ChIP	
Phf21b-F	GCCCCTCCTTACTTGTTTGTCG	ChIP	Rugg-Gunn et al., 2010
Phf21b-R	CCCGCTCCTCTGTGTCTTCATA	ChIP	
Pik3r3-F	TTCCCTTTGTGGCGATTCCT	ChIP	Rugg-Gunn et al., 2010
Pik3r3-R	TGAGAGAAGCACGGAGTCTCAAA	ChIP	
Pou5f1-F	TGGCTGAGTGGGCTGTAAGG	ChIP	Rugg-Gunn et al., 2010
Pou5f1-R	CAAACCAGTTGCTCGGATGC	ChIP	
Prdm1-F	GGGTGGACATGAGAGAGGCTTA	ChIP	Rugg-Gunn et al., 2010
Prdm1-R	GGTTCCTTACCAAGGTCGTACCC	ChIP	
Prdm8-F	GGAGGATCTGCGAAGGAAGAGA	ChIP	Rugg-Gunn et al., 2010
Prdm8-R	CAGGACCCCGGGCTTTATAGTA	ChIP	
Prl3b1-F	GGAGGGCTTTCGTTACCACCT	ChIP	Rugg-Gunn et al., 2010

Prl3b1-R	GGTTCCATAGTGACGCAGACCA	ChIP	
Prtg-F	GGCCGCACGTGGTTTTATTT	ChIP	Rugg-Gunn et al., 2010
Prtg-R	GAGGAACCCCACTGCAAACC	ChIP	
Sox17-F	CACCAACCCGCTTGCTACAG	ChIP	Rugg-Gunn et al., 2010
Sox17-R	TAAGCCACATCCCCAAAGCA	ChIP	
Sox2-F	CCATCCACCCTTATGTATCCAAG	ChIP	Tanaka, S. et al (1998)
Sox2-R	CGAAGGAAGTGGGTAAACAGCAC	ChIP	
Sox7-F	TGCCAGTTTAGGGAAGTCAGT	ChIP	Rugg-Gunn et al., 2010
Sox7-R	GTCATCTCGCCCCAGTAAAC	ChIP	
Tbx2-F	CTTACTGCTGAGGCTTCCGACAC	ChIP	Rugg-Gunn et al., 2010
Tbx2-R	TTTGGACCAATTGTGGGTCTCC	ChIP	
Tcfap2a-F	ACAGGGGAGACGCTGGAGAT	ChIP	Rugg-Gunn et al., 2010
Tcfap2a-R	GGGGAAAGAGTGGAACACGA	ChIP	
Twist1-F	GGGAATCCCTTGGGACTAGAGGTT	ChIP	Rugg-Gunn et al., 2010
Twist1-R	AAAGTTTCAACAACCGAGTCCATC	ChIP	
Vdr-F	CTCCCTTCTTACTCCTCCACTCCA	ChIP	Rugg-Gunn et al., 2010
Vdr-R	AGTCCTTAGCTAGGAGGGTGCTCA	ChIP	

Wnt5b-F	GATGTCTGTCACAGCCGCTCAT	ChIP	Rugg-Gunn et al., 2010
Wnt5b-R	TCATAAGATGTTGAAGGGCAGGTG	ChIP	
mUntr6 Fwd	CAGGCATGAACCACCATACC	ChIP	Sofronescu et al., 2010
mUntr6 Rev	CAACATCCACACGTCCAGTG	ChIP	
Pax6 Fwd	AGAGGGAGCATCCAATCGG	ChIP	This study
Pax6 Rev	CTCCTCACTGGCCCATTAGC	ChIP	
Pax6 Fwd 2	GTCGGGGGAGGAGCAAGAA	ChIP	This study
Pax6 Rev 2	CCTGGAGGGGCGGGAGACT	ChIP	
mHoxB1 Fwd 1	ACGTAGGTGGTGACTTGGAACT	ChIP	This study
mHoxB1 Rev 1	AGAGATGGCCTATGTGCTGTG	ChIP	
mHoxB1 Fwd Set 2	TGGGGTGCAGCGATGAGGAA	ChIP	This study
mHoxB1 Rev Set 2	GCCCTAACCACTGTCCCGCCCT	ChIP	
mHoxB2 Fwd	GATCCCCACTTAACACCCAA	ChIP	This study
mHoxB2 Rev	CTTGGGAAACTGCTCTTAACTAG	ChIP	
mHoxA1 Set 2 Fwd	GGCTGCTAACAACAAACTGC	ChIP	This study
mHoxA1 Set 2 Rev	GATAAACTGCTGGGACTCATTC	ChIP	
mNkx2.2 Pro Set 2 Fwd	CCAACAGGAGCGGGACATT	ChIP	This study

mNkx2.2 Pro set 2 Rev	CAAACACAAATACAAACC GATTGC	ChIP	
mAscl1 Pro Set1 Fwd	TCAAGCCCAGGCTGGAGC AAG	ChIP	This study
mAscl1 Pro Set1 Rev	GGCGATCGTCTTCCCTCT GCG	ChIP	
mAscl1 Pro Set2 Fwd	TCTTTCTCTGTCGCCATTC A	ChIP	This study
mAscl1 Pro Set2 Rev	GGACGCTCCGGTTTGTAT AG	ChIP	
mDlx2 Pro Fwd 1	CGTAATATCTCTGTGGGT AGTTTGG	ChIP	This study
mDlx2 Pro Rev 1	ACATCTCTTGTCCAACTTC GCC	ChIP	
mDlx2 Pro Fwd 2	GCTCAGATGTGCGTCATT ACTAGA	ChIP	This study
mDlx2 Pro Rev 2	GCCTGGCTCGCACTACTC TT	ChIP	
mMsx2 Pro Fwd 1	CTCCGCAGATTTCCAACA TTC	ChIP	This study
mMsx2 Pro Rev 1	CAGGAGCAGTCAGCAGA GTTGT	ChIP	
mMSx2 Pro Fwd 2	CCTAATAACAACTCTGCT GACTGCT	ChIP	This study
mMsx2 Pro Rev 2	AAGTGGGAGACTCGGCTC AAC	ChIP	
mMsx2 Pro Fwd 3	CAGTGGGGTAGCAAGTTC AGG	ChIP	This study
mMsx2 Pro Rev 3	GATGAGAAAGGCTGAGAG GTGG	ChIP	
mNkx2.1 Pro 1 Fwd	GAACAGCAGACAAGCAAA GC	ChIP	This study
mNkx2.1 Pro 1 Rev	GGTTACCCAGCCAAGCCC T	ChIP	

mNkx2.1 TSS Fwd	CCACTTAGCTGCTGATCCTGAC	ChIP	This study
mNkx2.1 TSS Rev	TTTCCTGTCTGAGCGTTCC	ChIP	
mNkx2.1 Exon 1 Fwd	GAAAACTGCGGGGATCTGAG	ChIP	This study
mNkx2.1 Exon 1 Rev	CTACGAGGCTAAGGGTGCG	ChIP	
MusD LTR Fwd	CAGCCTGAAACCTGCTTGCT	ChIP	This study
MusD LTR Rev	ATAAAGGAAGGGGGAGGGGA	ChIP	

Table S2. Description and sequences of the primers used in the in the analysis of candidate reference genes, lineage specific transcription factors, expression analysis, and ChIP experiments for Chapter IV.

ChIP Primers			
Primer name	Fwd/Rev	Sequence	Reference
Ascl1 Pro set 2	Fwd	TCTTTCTCTGTCGCCATTCA	Veazey et al., 2013
	Rev	GGACGCTCCGGTTTGTATAG	
Dlx1	Fwd	GGTGAGGAAGAGATCGGGC	Veazey et al., 2013
	Rev	GAGTACTTGGGGTTTGGGAGTC	
Dlx2 Pro 2	Fwd	GCTCAGATGTGCGTCATTACTAGA	Veazey et al., 2013
	Rev	GCCTGGCTCGCACTACTCTT	
Dlx3	Fwd	ACAGCGCTCCTCAGCATGAC	Rugg-Gunn et al., 2010
	Rev	CTGCGAGCCCATTGAGATTG	
Dlx5	Fwd	GCTTCGCTGGCTAATCCAGACT	Rugg-Gunn et al., 2010
	Rev	CAGCCCTAGTGGTGTTTGCGTA	
Gapdh	Fwd	TCCTATCCTGGGAACCATCACC	Rugg-Gunn et al., 2010
	Rev	TCTTTGGACCCGCCTCATTT	
Gata1	Fwd	TGCCCCAACTTCTTCCCATT	Veazey et al., 2013
	Rev	CAGGCCTGGGAGGATGAAGA	
Hoxa1	Fwd	GGCTGCTAACAACAAACTGC	Veazey et al., 2013
	Rev	GATAAACTGCTGGGACTCATTC	
Hoxa6	Fwd	GGGCTGTTTGTAACTTTGCTGC	Veazey et al., 2013
	Rev	CATCTGGCTATAACTATTAGTAGTCATCG	
Hoxa7	Fwd	GAGAGGTGGGCAAAGAGTGG	Tanaka et al., 1998
	Rev	CCGACAACCTCATACCTATTCCTG	

Intergenic	Fwd	GGAGAGAAGTGGAGTGGCCAAG	Rugg-Gunn et al., 2010
	Rev	TTGCCAGCCTAATCATGAGGAA	
Msx1	Fwd	ACAGAAAGAAATAGCACAGACCATAAGA	Tanaka et al., 1998
	Rev	TTCTACCAAGTTCCAGAGGGACTTT	
Msx2 Pro 2	Fwd	CCTAATAACAACTCTGCTGACTGCT	Veazey et al., 2013
	Rev	AAGTGGGAGACTCGGCTCAAC	
Nanog	Fwd	CAGACTGGGAGGGAGGGAAA	Rugg-Gunn et al., 2010
	Rev	GAGGTGCAGCCGTGGTTAAA	
Nkx2.1 Pro	Fwd	GAACAGCAGACAAGCAAAGC	Veazey et al., 2013
	Rev	GGTTACCCAGCCAAGCCCT	
Nkx2.2 Pro	Fwd	CCAACAGGAGCGGGACATT	Veazey et al., 2013
	Rev	CAAACACAAATACAAACCGATTGC	
Pax6	Fwd	AGAGGGAGCATCCAATCGG	Veazey et al., 2013
	Rev	CTCCTCACTGGCCCATTAGC	
Pou5f1	Fwd	TGGCTGAGTGGGCTGTAAGG	Rugg-Gunn et al., 2010
	Rev	CAAACCAGTTGCTCGGATGC	
Smarca 2 Pro 2	Fwd	ACCAAAACAAACAGGCGG	Veazey et al., 2013
	Rev	GGGAGCTGTGGTTAGAGCATT	
Sox1	Fwd	CACAAACTTCTTTTTACTGTCGGAG	Veazey et al., 2013
	Rev	TAATCTACCCCGAACTTTCTTGG	
Sox2	Fwd	CCATCCACCCTTATGTATCCAAG	Tanaka et al., 1998
	Rev	CGAAGGAAGTGGGTAAACAGCAC	

Sox17	Fwd	CACCAACCCGCTTGCTACAG	Rugg-Gunn et al., 2010
	Rev	TAAGCCACATCCCCAAAGCA	
Tbx2	Fwd	CTTACTGCTGAGGCTTCCGACAC	Rugg-Gunn et al., 2010
	Rev	TTTGGACCAATTGTGGGTCTCC	
Twist1	Fwd	GGGAATCCCTTGGGACTAGAGGTT	Rugg-Gunn et al., 2010
	Rev	AAAGTTTCAACAACCGAGTCCATC	
Untr6	Fwd	CAGGCATGAACCACCATACC	Sofronescu et al., 2010
	Rev	CAACATCCACACGTCCAGTG	
Vdr	Fwd	CTCCCTTCTTACTCCTCCACTCCA	Rugg-Gunn et al., 2010
	Rev	AGTCCTTAGCTAGGAGGGTGCTCA	
Wnt5b	Fwd	GATGTCTGTCACAGCCGCTCAT	Rugg-Gunn et al., 2010
	Rev	TCATAAGATGTTGAAGGGCAGGTG	

Oxidative Stress Expression Analysis Primers

Primer name	Fwd/Rev	Sequence	Reference
Catalase	Fwd	CCAGCGACCAGATGAAGCAG	Veazey et al., 2013
	Rev	TATCGTGGGTGACCTCAAAGTATCC	
Catalase set 2	Fwd	GAACGAGGAGGAGAGGAAACG	Veazey et al., 2013
	Rev	CAGGAAACGGCATCAAAAGC	
Adh1	Fwd	CCACTGGTGTCTGCCGCTC	Veazey et al., 2013
	Rev	ACACAAGTCACCCCTTCTCCAA	
Adh1 Set 2	Fwd	GCACCAGCACCTTCTCCCA	Veazey et al., 2013
	Rev	GACTTTGACGGCAGAGCCATAG	

Aldh1	Fwd	GTGGAAGAAGGGGACAAGGC	Veazey et al., 2013
	Rev	CCACACACTCCAATAGGTTCACG	
Aldh1 Set 2	Fwd	CTCCTCTCACGGCTCTTCACC	Veazey et al., 2013
	Rev	CAACAGCAATGTCCAAGTCGG	
Cyp2e1	Fwd	GGCCAGCCTTTTGACCCTACC	Veazey et al., 2013
	Rev	CTGTGTTTTTCCTTCTCCATCTCTAT	
Cyp2e1 Set 2	Fwd	CAGGAACAGAGACCACCAGCAC	Veazey et al., 2013
	Rev	TGGAAGGGACGAGGTTGATG	
Gpx1	Fwd	GAAGAACTTGGGCCATTTGG	Dong et al., 2008
	Rev	TCTCGCCTGGCTCCTGTTT	
Gpx3	Fwd	ACAATTGTCCCAGTGTGTGCAT	Dong et al., 2008
	Rev	TGGACCATCCCTGGGTTTC	
Gsr	Fwd	GCTATGCAACATTCGCAGATG	Dong et al., 2008
	Rev	AGCGGTAAACTTTTTCCCATTG	
Gstm2	Fwd	GCTCTTACCACGTGCAGCTT	Dong et al., 2008
	Rev	GGCTGGGAAGAGGAAATGGA	
Gstm3	Fwd	CACCCGCATACAGCTCATGAT	Dong et al., 2008
	Rev	TTCTCAGGGATGGCCTTCAA	
Gstp1	Fwd	TGGGCATCTGAAGCCTTTTG	Dong et al., 2008
	Rev	GATCTGGTCACCCACGATGAA	
Hif1a	Fwd	CCTCACCAGACAGAGCAGGAA	This study
	Rev	TCAGGAACAGTATTTCTTTGATTCA	
Nrf2	Fwd	CGAGATATACGCAGGAGAGGTAAGA	Dong et al., 2008

	Rev	GCTCGACAATGTTCTCCAGCTT	
Nqo1	Fwd	TATCCTTCCGAGTCATCTCTAGCA	Dong et al., 2008
	Rev	TCTGCAGCTTCCAGCTTCTTG	
Prx1	Fwd	GATCCCAAGCGCACCATT	Dong et al., 2008
	Rev	TAATAAAAAGGCCCCTGAAAGAGAT	
Sod1	Fwd	GTGATTGGGATTGCGCAGTA	Dong et al., 2008
	Rev	TGGTTTGAGGGTAGCAGATGAGT	
Sod2	Fwd	TTAACGCGCAGATCATGCA	Dong et al., 2008
	Rev	GGTGGCGTTGAGATTGTTCA	
Sod3	Fwd	CATGCAATCTGCAGGGTACAA	Dong et al., 2008
	Rev	AGAACCAAGCCGGTGATCTG	
Tet1	Fwd	GAGCCTGTTCCTCGATGTGG	Ko et al., 2010
	Rev	CAAACCCACCTGAGGCTGTT	
Tet2	Fwd	AACCTGGCTACTGTCATTGCTC	Ko et al., 2010
	Rev	TGTTCTGCTGGTCTCTGTGGG	
Tet3	Fwd	TCCGGATTGAGAAGGTCATC	Ko et al., 2010
	Rev	CCAGGCCAGGATCAAGATAA	
Trx	Fwd	CCGCGGGAGACAAGCTT	Dong et al., 2008
	Rev	GGAATGGAAGAAGGGCTTGATC	

Gluc-MS-qPCR Primers

Primer name	Fwd/Rev	Sequence	Reference
Adcy6	Fwd	GTGAGGCTGCTCTGGTTCAT	Irwin et al., Genomics 2014
	Rev	GGGTTTGACGACACTGAGGT	

Ankrd23	Fwd	TAGTCCCGGAGCTTTCTCCT	Tan et al., 2013 NAR
	Rev	CCCACAGAAGCCAGGATCTA	
Dpep3	Fwd	GTCACTGGTCACACCTGACG	Irwin et al., Genomics 2014
	Rev	CTGCTGGGGGTGTTACTTCT	
Gf 5UTR	Fwd	TAAGCCACAGCAGCAGCGG	Okashita et al., 2014
	Rev	CCCAGGTGGTACAGACTCTC	
Hist1h2aa	Fwd	CCAAGGTCAAGTCTCGCTCT	Tan et al., 2013 NAR
	Rev	GAGGAGTAATGCGCGTCTTC	
Peg3	Fwd	AATCTACCTGCTTGCTCTCCTC	
	Rev	TGACTGTCTGCATAGCGAAAC	
Rhox6	Fwd	AGCGTCGGATCCAGAGATTC	
	Rev	ACCAGGCTGTTCTTCCTTGTC	
Rhox13	Fwd	GTCTGGACTGGACCGGTAAC	Irwin et al., Genomics 2014
	Rev	CGTGGGCCATGACTAGAAC	
Snrpn	Fwd	GGACAGAGACCCCTGCATT	Irwin et al., Genomics 2014
	Rev	CGTTGCAAATCACTCCTCAG	
Snrpn exp	Fwd	TCTGTGATTGTGATGAGTTCAGG	Irwin et al., Genomics 2014
	Rev	CAATGCCAGTATCTTTAGGAGGT	
Sycp3	Fwd	GGGGCTATACGTAAGCGTGT	Irwin et al., Genomics 2014
	Rev	CTCCCCCATCTCCTTACCTC	

Epigenetic Factor Expression Primers

Primer name	Fwd/Rev	Sequence	Reference
Dnmt1 Set 2	Fwd	ATGCGGCACATCCCACTG	Veazey et al., 2013
	Rev	CAGACTCCACGCAGGGCAC	
Dnmt3b	Fwd	GCAGACAATAACCACCAAGTCG	Veazey et al., 2013
	Rev	GCACCACAAAACGTCGTCCT	
NP95 Set 1	Fwd	GGATGACAAGACTGTGTGGGAG	Veazey et al., 2013
	Rev	GCTCGTCCTCAGATAGGGCTCT	
NP95 Set2	Fwd	GGTGCGGAGGCTGAAGACT	Veazey et al., 2013
	Rev	CAGGAGCGTACTTGCTGTGTTT	
EED	Fwd	GAGATACGGTTATTGCAGTCCTATG	Veazey et al., 2013
	Rev	AGAAGGTTTGGGTCTCGTGG	
Ezh2	Fwd	CCTTCCATGCAACACCCAAC	Veazey et al., 2013
	Rev	GCTCCCTCCAGATGCTGGTAA	
G9a Set 1	Fwd	GACAGGGGCAGGAAAGTCG	Veazey et al., 2013
	Rev	CCTGGGCGGCAGTTGTTG	
SetDB1 Set1	Fwd	TCAGGTCTGGCTTTATGCTGG	Veazey et al., 2013
	Rev	CTCTATGAAGTCTCGGCAGGAGC	
SetDB1 Set 2	Fwd	AGCTGGAGACGTGGGTACTACAG	Veazey et al., 2013
	Rev	GGAATCTCAATGATCTCTGTGGG	

Homeobox Gene Expression Analysis Primers

Primer name	Fwd/Rev	Sequence	Reference

Dlx2	Fwd	CACGCACCATCTACTCCAGTTT	Veazey et al., 2013
	Rev	TGCTGCTCGGTGGGTATCTC	
Nkx2.2	Fwd	GCAGAGCCTGCCCCTTAA	Veazey et al., 2013
	Rev	GCCCTGGGTCTCCTTGTCA	
Pax6	Fwd	GAGTTCTTCGCAACCTGGCTA	Veazey et al., 2013
	Rev	TTCATCCGAGTCTTCTCCGTTAG	
Smarca2	Fwd	CTGACAAAAGACATGGATGAGCC	Veazey et al., 2013
	Rev	GGATGATGATGTGGTGGGTCTG	
Sox1	Fwd	CTCGGATCTCTGGTCAAGTC	Veazey et al., 2013
	Rev	GGTACATGCTGATCATCTCG	
Sox2	Fwd	GGCGGCAACCAGAAGAACA	Veazey et al., 2013
	Rev	TTCTCGGTCTCGGACAAAAGTT	
Tbx2	Fwd	GAAGCTGACCAACAACATTTCTG	Veazey et al., 2013
	Rev	CGGTCTCTGGGAAGACATAGG	
Vdr	Fwd	AGCTGAACCTCCATGAGGAAGAAC	Veazey et al., 2013
	Rev	TCAACCAGCTTAGCATCCTGTACC	
mAscl1	Fwd	GTCCTGTCGCCCACCATCT	Veazey et al., 2013
	Rev	CCACCCCTGTTTGCTGAGAA	
Dlx3	Fwd	GCTGGGCCTCACACAAACAC	Rugg-Gunn et al., 2010
	Rev	TGTTGTTGGGGCTGTGTTCC	
mSox17	Fwd	GAACCTCCAGTAAGCCAGATTTG	Veazey et al., 2013
	Rev	CTCTCCAGACCGACCCCGA	

mSox17	Fwd	CACAACGCAGAGCTAAGCAAG	Veazey et al., 2013
	Rev	CGGTACTTGTAGTTGGGGTGG	

Reference primers

Primer name	Fwd/Rev	Sequence	Reference
Gapdh	Fwd	TGACGTGCCGCCTGGAGAAA	Carnahan et al., 2013
	Rev	AGTGTAGCCCAAGATGCCCTTCAG	
Hprt	Fwd	CTGGTGAAAAGGACCTCTCGAA	Carnahan et al., 2013
	Rev	CTGAAGTACTCATTATAGTCAAGGGCAT	
Pgk1	Fwd	CTGACTTTGGACAAGCTGGACG	Carnahan et al., 2013
	Rev	GCAGCCTTGATCCTTTGGTTG	

Table S3. Description and sequences of the primers used in the in the analysis of candidate reference genes, lineage specific transcription factors, expression analysis, and ChIP experiments for Chapter V.